The role of fog in the ecohydrology and biogeochemistry of the Namib Desert

Keir Stephen Soderberg
Germantown, MD

MSc, University of Cape Town, 2003
BSE, Princeton University, 2000

A Dissertation presented to the Graduate Faculty
of the University of Virginia in Candidacy for the Degree of
Doctor of Philosophy

Department of Environmental Sciences

University of Virginia
May, 2010

Dr. Stephen A. Macko

Dr. Robert J. Swap

Dr. Paolo D'Odorico

Dr. P. Paxton Marshall Paxton Marshall

Abstract

The Namib Desert on the west coast of southern Africa is hyper-arid in terms of rainfall, but receives up to 100 days of fog each year. This project adds to the understanding of the occurrence of fog in the Namib, the importance of fog as a water source for this ecosystem, and the role of fog in carbon, nitrogen and sulfur cycles. Stable isotopes (δ^{2}H, δ^{18}O, δ^{34}S) of fog, groundwater, plant water and soil water (collected from 2007 to 2009) indicate that plants growing in or near the ephemeral Kuiseb River have a distinctly depleted water isotope signal, similar to groundwater in the alluvial aquifer. In contrast, shrubs and grasses growing on the dunes and gravel plains tend to have an enriched signal, representing a minimum of 5 to 40% fog water usage in these plants. Notably, the very long-lived gymnosperm *Welwitschia mirabilis*, has a depleted water isotope signal, statistically similar to the trees growing in the Kuiseb River. This finding is consistent with long-term observations associating growth with annual rainfall. Together these studies can dispel the popular perception that *W. mirabilis* survives in the desert via fog water uptake, which is significant because this plant is important as a national symbol and potentially threatened by proposed uranium and copper mines. The δ^{34}S of plant material tends to be more enriched in plants that use more fog water, providing a first-order corroboration of the water isotope results. *W. mirabilis* has significantly more enriched δ^{13}C values in lower rainfall areas, but also exhibits high variability in δ^{13}C (range of 4 ‰) within a single community, suggesting the influence of microhabitat on photosynthesis. The δ^{15}N of C3 plants becomes more depleted closer to the coast in an apparent reversal of the trend found across the Kalahari.

Table of Contents

Figures

Tables

Acknowledgements

I would first like to thank my PhD committee – Stephen Macko, Robert Swap, and Paolo D'Odorico – for their enthusiastic support and guidance of the research presented here. This project developed from discussions with Mary Seely, Joh Henschel, and other colleagues in Namibia from 2005 to 2007. I also had substantial early input from discussions with Frank Eckardt, John Compton, Ed February and Klaudia Schachtschneider at the University of Cape Town. I sincerely thank them for introducing me to this endlessly interesting living desert. Gobabeb staff (Hiskia, Myck, Veronica, Calvin, Taimi, Emily, John-Aris, Elsita, Jaime, John, Alex and James) and undergraduates at the University of Namibia assisted with fieldwork and ongoing equipment monitoring. Thanks as well to Shaamielah Davids at the University of Cape Town, Abi Bhattachan at the University of Virginia, Kaycie Billmark at the University of Minnesota and S. Leigh McCallister at Virginia Commonwealth University for providing laboratory services, and to Kathleen Weathers at the Cary Institute of Ecosystem Studies for use of a Teflon fog collector. Tim Smalley provided borehole access and construction. Discussions with John Maben and Bill Keene were invaluable for setting up the aerosol sampling campaign. Several undergraduates at the University of Virginia also helped with sample preparation: Alice Wang, Karen Lee, and Dana Doggrell. Funding came from the Fulbright U.S. Student Program, Rufford Small Grants for Nature Conservation, Decagon Devices Inc., Explorers Club Washington Group, and the University of Virginia Department of Environmental Sciences (Moore and Garstang Research Awards). Lastly, thanks to the Macko Lab Group and my two girls for their patience.

Chapter 1 : Introduction

1.1 Water in the Namib Desert

The Namib Desert on the west coast of southern Africa supports diverse flora and fauna while receiving extremely little water as rainfall. Although rainfall pulses are important for many arid ecosystem processes (Seely, 1978; Jacobson and Jacobson, 1998; Huxman *et al*., 2004), the ability to survive between these pulses can be linked in the Namib to much more frequent fog events. Significant work has been done to show the utilization of fog water by Namib biota (Louw, 1972; Hamilton and Seely, 1976; Seely and Hamilton, 1976; Henschel and Seely, 2008), the general occurrence and characteristics of fog events (Lancaster *et al*., 1984; Pietruszka and Seely, 1985; Olivier, 1995; Henschel *et al*., 1998; Hachfeld and Jurgens, 2000), as well as geochemical aspects of Namib ecosystem relating to fog deposition (Eckardt and Schemenauer, 1998; Goudie and Parker, 1998; Viles, 2005). However, several questions remain about the role of fog water in the ecohydrology and nutrient cycling of these ecosystems. In particular, the amount of fog water used by the unique plants of the Namib is virtually unknown. The main goals of this study are to (1) estimate the relative utilization of fog water by several Namib plants and (2) infer effects of fog on C, N and S cycling.

Two early studies used tritiated water to demonstrate the ability, *in situ*, to take up simulated fog water via surficial roots in a common dune grass, *Stipagrostis sabulicola* (Louw and Seely, 1980), and via leaves in a dune shrub, *Trianthema hereroensis* (Seely *et al*., 1977). Investigators have also suggested that the long-lived and floristically enigmatic *Welwitschia mirabilis* absorbs fog water through its leaves (Bornman *et al*., 1973), leading to the widespread view that this species survives on fog and dew deposition (McGough *et al*., 2004; Curtis and Mannheimer, 2005). However, this pathway has not been proven and long-term observations link growth to rainfall rather than fog (Walter and Breckle, 1986; Henschel and Seely, 2000). Other studies have relied on correlating species distribution (*Zygophyllum stapffii, Arthraerua leubnitziae*) with fog occurrence (Hachfeld and Jurgens, 2000), or studying plant-scale water relations (Ebert, 2000; Loris, 2004).

Fog in the Namib most commonly occurs through advection of a low stratus cloud that forms over the cool Benguela Current that upwells along the southwestern coast of Africa. When advected inland, this cloud intersects the land at elevations of 100-500 mamsl, which translates to 10-60km from the coast (Figure 2). Occasionally very low elevation fog occurs within 10 km of the coast. Radiation fog, which occurs much less frequently, results from warm moist air cooling rapidly at night in low-lying areas. Winter frontal systems from the southwest infrequntly bring light drizzle. Rain accumulations range between 20 and 80mm/yr, increasing to the east. Whereas, fog deposition has been measured at 20-180mm/yr within 60km of the coast (Lancaster *et al*., 1984; Henschel *et al*., 1998; Hachfeld and Jurgens, 2000; Shanyengana *et al*., 2002). A simplified version of these patterns gives a sense of the overall atmospheric moisture regime active in the Namib (Figure 1-2), but sampling at higher resolution for 1 year indicates the spatial heterogeneity of the system (Figure 1-3).

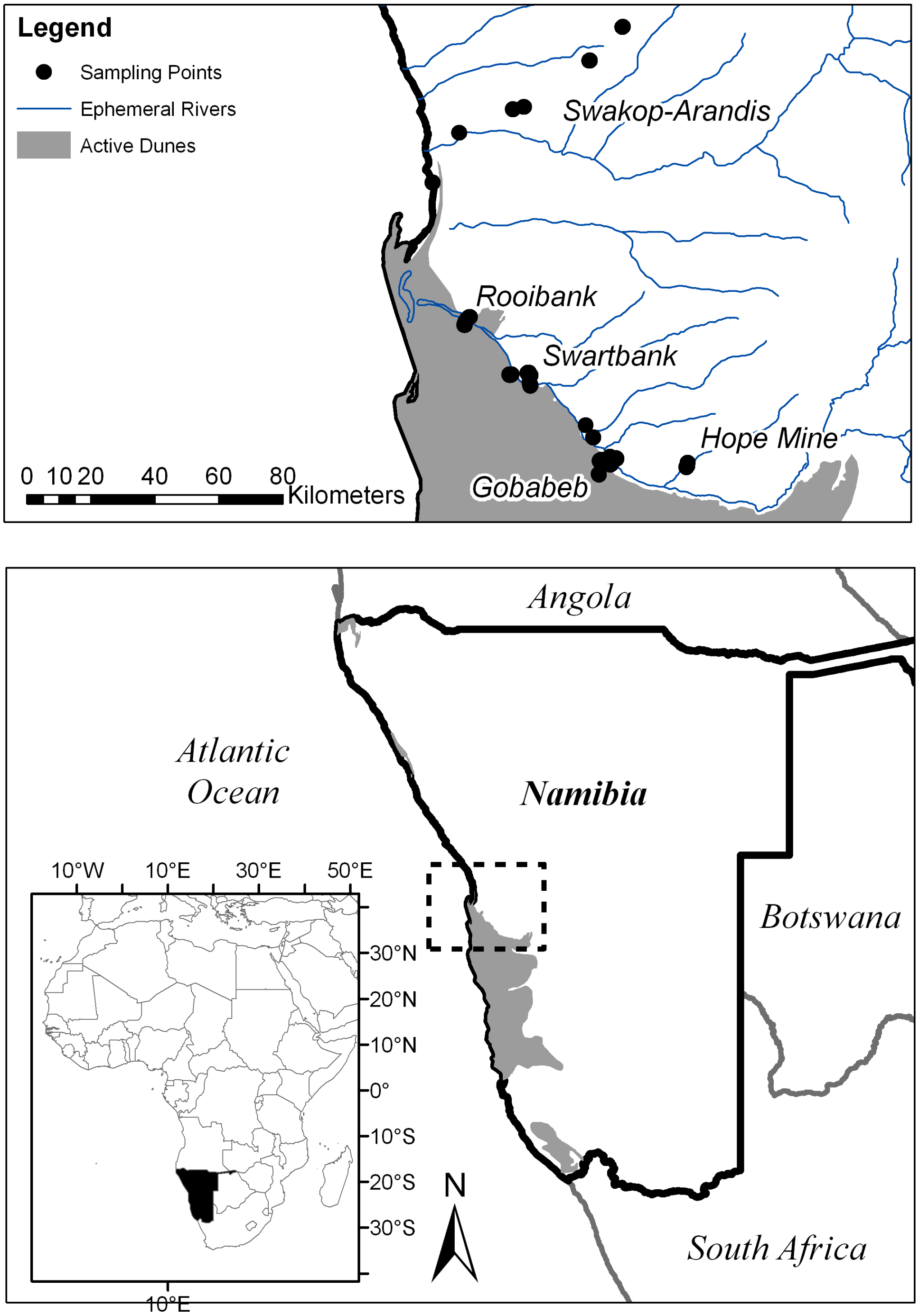

Figure 1-1: Site location map.

The fog and rain deposition pattern affect the distribution of vegetation across the Namib, with large trees generally confined to the eastern edge of the desert and along ephemeral watercourses (Walter and Breckle, 1986; Burke, 2003; Curtis and Mannheimer, 2005; Burke, 2006). Here the trees have access to the relatively shallow alluvial aquifers, which are recharged by seasonal floods that have high interannual variability and can be absent for several years (Jacobson *et al*., 1995; Lange, 2005). Common trees in the riverbeds include *Acacia erioloba*, *Faidherbia albida*, and *Tamarix usneoides*. The Kuiseb River marks the boundary between the great dune sea to the south and the gravel plains to the north. Perennial vegetation in the dunes is dominated by *S. sabulicola,* with *T. hereroensis* co-dominating towards the coast. And the gravel plains comprise various species of perennial shrubs (e.g., *A. leubnitziae, Z. stapffii, Calicorema capitata*) notably including the gymnosperm *W. mirabilis*.

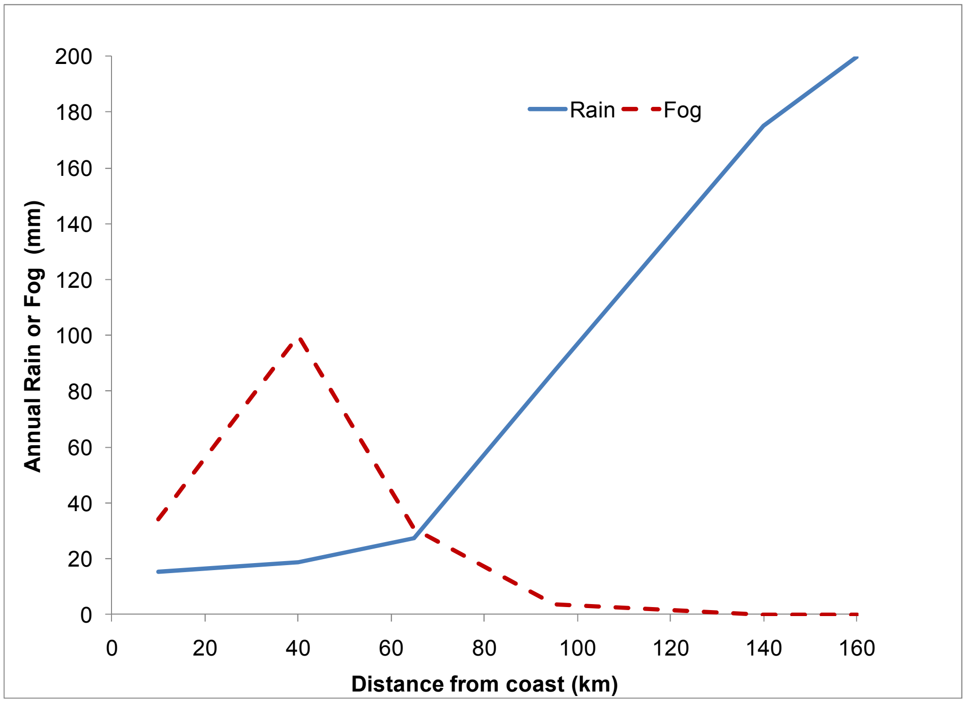

Figure 1-2: Simplified rain and fog annual totals across the Namib Desert (after Lancaster *et al.* (1984)).

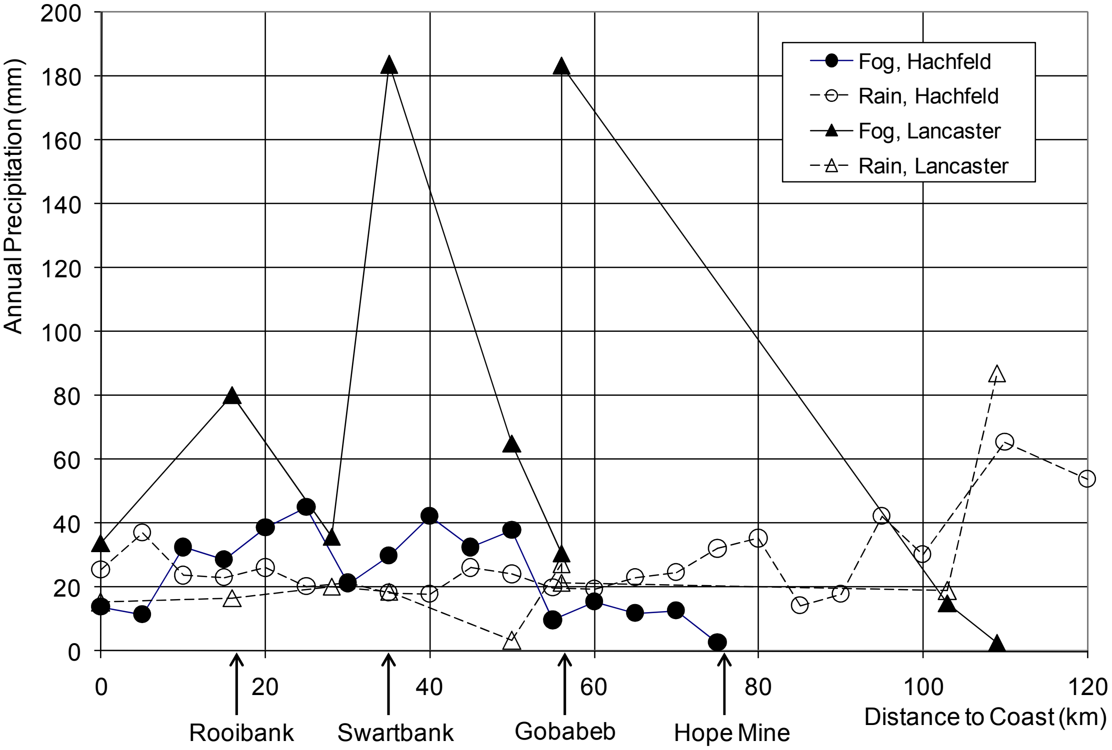

Figure 1-3: Fog and rain annual totals for two transects from the coast inland.
The "Lancaster" transect includes 9 stations with up to 16 years of monthly data (Lancaster *et al.*, 1984), and the "Hachfeld" transect includes 23 stations with one year of weekly data (Hachfeld and Jurgens, 2000). Rain was collected in open buckets in both studies, whereas fog was collected with cylindrical wire mesh in the "Lancaster" transect and bunches of vertical wires in the "Hachfeld" transect.

Although the age of the Namib is still debated (Lancaster, 2002) it has seen at least semi-arid conditions since the breakup of the Gondwana supercontinent in the Late Cretaceous (about 80 million years before present, Ma) and arid to hyper-arid conditions since the intensification of the cold Benguela current upwelling about 10 Ma in the Late Miocene (Siesser, 1980; Wilkinson, 1990; Goudie and Eckardt, 1999). The cold water upwelling enhances the overall stable atmosphere. Storms originating in the Indian Ocean have lost most of their moisture by the time they reach the western edge of the inland plateau (the

Great Escarpment), which forms the eastern border of the Namib about 150 km from the Atlantic coast (Jacobson *et al*., 1995).

This persistent aridity has kept the Namib quite geomorphologically stable, one of several characteristics the Namib shares with the Atacama Desert in Chile (Bierman and Caffee, 2001). The Namib and the Atacama are also climatologically similar with extremely low rainfall, frequent fog events, and proximity to a cold upwelling coastal current. Geochemically, both deserts also have extensive pedogenic gypsum crusts (Eckardt *et al*., 2001; Rech *et al*., 2003) as well as more unusual evaporites (Eckardt personal communication). Heavy fog events occur in the Atacama (up to 189 fog days per year), adding significantly to the total wet deposition (Rech *et al*., 2003; Michalski *et al*., 2004). Other areas of the world with significant hydrologic input from fog include parts of Kenya, New Zealand, Hawaii, Oman, China and the Canary Islands (Ingraham and Matthews, 1988; Ingraham and Mark, 2000; Scholl *et al*., 2002; Stock *et al*., 2003; Garcia-Santos *et al*., 2004; Liu *et al*., 2005; Hildebrandt and Eltahir, 2006).

1.2 Water demands in the Namib

Despite its general lack of water and inhospitable appearance, the Namib is critical to the Namibian economy. The desert lies on the Atlantic coast where the upwelling of the cold Benguela current just offshore supplies abundant nutrients (e.g. N, P, S) to one of the richest fisheries in the world (Siesser, 1980; Jacobson *et al*., 1995). The coastal communities of Walvis Bay and Swakopmund support this industry as well as the shipping and tourism industries in Namibia. Other parts of the Namib are tourist hotspots as well, with private and communal tourist operations continuing to increase (Bethune and Schachtschneider, 2004). The capacity to supply water to a growing population in the Namib is clearly important for the economy. Collection of fog water has been suggested and tested as one potential source of supplementary water for the coastal region (Shanyengana *et al*., 2002).

Namibia also has great mineral wealth and is among the leading global producers of uranium and diamonds, with significant production of other metals including copper. The recent rise in prices has seen increased uranium exploration and mine development in Namibia, including within its national parks. Namibia contributed 7.5%, 7.7%, and 9.1% of global uranium production during 2005, 2006 and 2007, respectively (Kwasny *et al*., 2007). Although there is currently a moratorium on issuing uranium prospecting licenses in Namibia, more than 60 licenses exist (Weidlich, 2008) – most are in the Namib, many within national parks. Demands on local water sources and potential impacts by future mines are currently being evaluated; however, studies of ecosystem water requirements in the mining areas are difficult, expensive, and can require long-term monitoring. While the demand for water increases, the requirements of the Namib's natural ecosystem need to be met as well.

1.3 Quantifying fog input

Three basic pieces of information are needed to begin quantifying the importance of fog in an ecosystem. First, the frequency of fog incidence needs to be consistently recorded. Second, the volume of fog deposition needs to be estimated. And third, the potential pathways for fog uptake need to be identified for the vegetation and habitats present in the ecosystem. Each of these should be considered with respect to other potential sources of water.

Fog is typically defined by a drop in horizontal visibility below 1 km. This criterion, however, is dependent on sampling frequency and does not give a nighttime measure unless a specialized system is set up. The visibility criterion has been used historically because it is relatively simple and because most concern about fog came from the transportation industry (Jiusto, 1981). When considering fog as a water source, the wetting of soil and plant surfaces by fog is more directly important than visibility. As noted above, biological soil crusts can make use of fog and dew water in addition to the direct uptake by some vascular plants. In recognition of the importance of surface wetting, a new measure of fog and dew occurrence is being used – Leaf Wetness – which is measured through changes in resistance or capacitance across a grid of electrodes that is painted to mimic a leaf surface (Campbell Scientific, 2006; Decagon Devices, 2007). Leaf Wetness Sensors (LWS's) record the amount of time that a surface has been wet, or "hours of wetness", which can be divided into daytime and nighttime wetness hours.

In areas of significant fog occurrence, and with reference to certain parts of the ecosystem that can benefit from fog and dew, annual hours of wetness can be a better measure of aridity than mean annual rainfall (MAR). For example, in a study of hypolithic cyanobacterial crusts in the Atacama Desert, Leaf Wetness was recorded for four sites along an "aridity gradient" defined by MAR. The study found an increase in crust occurrence along the gradient, but it did not correlate well with MAR (Warren-

Rhodes *et al*., 2006). However, if the crust occurrence is plotted against total annual hours of wetness, an extremely significant log-log relationship is observed (see Chapter 3).

Leaf Wetness Sensors were designed to measure the duration of fog over a given time period. In order to estimate the volume of fog deposited in an ecosystem, typically an artificial structure is used to collect fog droplets and deposit them into a sample container. For estimates of natural deposition rates, this collection is done passively, relying on the ambient wind to draw fog-laden air across the collecting surface. Early techniques involved placing a wire mesh cylinder on top of a standard rainfall collector or tipping bucket (Nagel, 1956; Lancaster *et al*., 1984). The cylindrical shape allows fog from any direction to be collected, and thus larger, more recently designed collectors are also omni-directional (Goodman, 1985; Fischer and Still, 2007). In an effort to provide comparable volume measurements to assess the ability to collect water for human use, a Standard Fog Collector was designed (Schemenauer and Cereceda, 1994). The SFC is a 1 m^2 plastic mesh screen on a vertical, flat square frame standing 1.5 m above the ground, and is oriented orthogonal to the typical prevailing wind direction during fog events in a given area. However, if the wind direction changes the fog collecting efficiency is altered. Another technique that is common in forested areas is to collect fog drip with an array of rainfall collectors under the canopy, which can be compared to above-canopy or open field collectors to differentiate between fog and rain (Kerfoot, 1968; Dawson, 1998; Hildebrandt *et al*., 2007). These fog drip volumes may be more representative of the amount of fog water available for infiltration and uptake by roots than the volumes collected by artificial surfaces. It should be noted, however, that when fog water collects on trees, a significant volume of water could be transported to the soil via stemflow rather than dripping onto the soil (Hildebrandt *et al*., 2007), with a third pathway being direct foliar absorption of deposited water (Seely *et al*., 1977; Burgess and Dawson, 2004). In Chapter 3, a new method is described for estimating fog and dew deposition amounts using Leaf Wetness Sensors.

Fog input can also be estimated with experimental addition of isotopically labeled water. As mentioned above, uptake through the above-ground portions of the Namib dune shrub *T. hereroensis* was shown by spraying tritiated water onto several individuals surrounded by plastic sheeting to prevent sprayed water from reaching the roots directly. After two hours the tritiated water was found in the root tips (Seely *et al*., 1977). Similarly, tritiated water was sprayed onto the sand surrounding two large stands of the dune grass *S. sabulicola* with plastic placed around the above-ground portions of each individual to prevent sprayed water from reaching the grass blades directly. In addition to a significant vertical root system, this grass has very shallow lateral roots that extend up to 20 m away from the plant. The tritiated water was found in the grass blades, vertical roots, and lateral roots after one day. The highest concentration was in the lateral roots. Seven weeks later tritiated water remained in all parts of the plants, although only very little remained in the grass blades (Louw and Seely, 1980). Such experiments are quite useful for identifying the fate of deposited fog as well as uptake pathways. However, in order to identify the overall importance of fog to an ecosystem, an integrated measure of the uptake of water from all available sources is needed.

The stable isotopes of oxygen and hydrogen can provide this integrated measure in ecosystems with isotopically distinct water sources to link the three aspects discussed above: occurrence, volume and uptake. Isotopes are measured as ratios of the heavy isotope to the light isotope ($^{18}O/^{16}O$, $^{2}H/^{1}H$), and reported relative to a standard in "per mil" (‰) notation by convention (Equation 1-1 gives the example of $\delta^{18}O$).

$$\delta^{18}O = (R_{sample}/R_{VSMOW} - 1) \times 1000 \qquad (1\text{-}1)$$

Where, R = the abundance ratio of ^{18}O to ^{16}O
VSMOW = Vienna Standard Mean Ocean Water, the international reference standard for water isotopes.

The movement of water in the environment leads to changes in isotopic composition due to fractionations that occur primarily during evaporation and condensation. Consistent variations in $\delta^{2}H$ and $\delta^{18}O$ in meteoric water globally were first reported almost 50 years ago (Craig, 1961), establishing the Global Meteoric Water Line (GMWL; Equation 1-2).

$$\delta^{2}H = 8 \times \delta^{18}O + 10 \qquad (1\text{-}2)$$

Processes dominated by kinetic fractionation lead to deviations from the GMWL, as in evaporation from soil (Barnes and Allison, 1988) and evapotranspiration in leaves (Twining *et al*., 2006; Gat *et al*., 2007). If the $\delta^{18}O$ and $\delta^{2}H$ values of the potential water sources for an ecosystem are significantly different, they can be used as end members in a mixing equation that describes their relative contribution to a given population of plant or soil water samples (White *et al*., 1985; Dawson and Ehleringer, 1991; Dawson *et al*., 2002). This situation is commonly the case for studying contributions from fog and rain because fog condenses from humid air at relatively low altitudes, resulting in relatively little fractionation of stable isotopes. Whereas, rain is often depleted due to condensation at higher altitudes than fog, as well as rainout of the heavy isotopes from a given cloud as it moves across land (Ingraham and Mark, 2000).

For example, the California redwoods receive summer fog that is isotopically enriched relative to the winter rainfall by about 60 ‰ in δ^2H (Table 1-1). Water extracted from redwoods and undergrowth had δ^2H values between the fog and rain endmembers, showing an annual contribution of 34% from fog (Dawson, 1998). Several other studies have been able to use the isotopic difference between fog and rain to determine the hydrologic importance of fog water in, for example, arid northern Kenya, grass fields of New Zealand, and the Atacama Desert of Chile (Table 1-1). No integrated isotopic study of plant water sources has been performed for the Namib, but sufficient isotopic discrimination between fog and rain in the Namib is suggested by separate studies of fog (Eckardt, 1996), rain (Rozanski *et al*., 1993) and groundwater (Schmitz, 2004).

The use of extracted plant water for source identification is possible because water in non-photosynthetic parts of plants (e.g. xylem) is not significantly different than its source water (White *et al*., 1985), although isotopic exchange can occur xylem water and enriched leaf water involved in transpiration (Shu *et al*., 2005). This evaporative enrichement is important in studying desert plant water isotopes, but still allows for the determination of original source water isotope signatures due to the relative stability of evaporative fractionation for a given plant at a given location (Kuells, 2000; Gat *et al*., 2007). Soil water extraction and interpretation is more complex, especially in very dry soils, due to the presence of mineral bound water that is isotopically different from the water available for uptake by plant roots (Walker *et al*., 1994). However, if the complications can be controlled for, soil water isotopes can be a powerful and sometimes necessary component of this type of study (Corbin *et al*., 2005; Gat *et al*., 2007).

Table 1-1:Ecosystem studies that make use of an isotopic difference between fog and other water sources.

Location	Description	δ^2H§				$\delta^{18}O$§			
		Fog	Rain	Ground water	Surface Water	Fog	Rain	Ground water	Surface Water
California Redwoods[1]	Coastal fog, prominent in summer	0.0†	-59†	NA	NA	NA	NA	NA	NA
Kenya[2]	Cloud condensation in hill rising from the Chalbi Desert; heavy enrichment in fog thought to be from rainfall that evaporated and recondensed	10.9	NA	-16.6	-20.5	-1	NA	-3.6	-4.3
New Zealand[3]	Upland snow tussocklands	-47	-66	-58	NA	-7.4	-9.7	-8.7	NA
Atacama Desert, Chile[4]	Coastal fog, northern Chile	-11	-28	-81	NA	-2.3	-4.8	-10.5	NA
Atacama Desert, Chile[5]	Coastal fog, northern Chile	-2.9	-39.7	-30	-29.5	-1.8	-5.8	-5.1	-4.3
Namib Desert[6]	Coastal Atlantic fog, rain and subsequent groundwater recharge from Indian Ocean storms	-0.7	-24.5†	-38.3	-73.7	2.1	-5.0	-6.1	-11.2

Note that the Namib Desert example is from three separate studies, without a synthesis relating to ecohydrology of the Namib ecosystem.
NA – Not Analyzed
References: 1, (Dawson, 1998); 2, (Ingraham and Matthews, 1988); 3, (Ingraham and Mark, 2000); 4, (Squeo *et al*., 2006); 5, (Aravena *et al*., 1989); 6, (Rozanski *et al*., 1993; Eckardt, 1996; Schmitz, 2004)
§ - Per mil relative to VSMOW; arithmetic mean except where noted
† - Volume weighted mean; Note that the Namib Desert rain value is from Windhoek, about 150km east of the desert.

Evaporation is a non-equilibrium process leading to Rayleigh isotope fractionation, where the lighter isotope preferentially enters the vapor phase and this phase is continually removed from the system. This process leads to isotopic enrichment in the remaining water. The plots of δ^2H vs $\delta^{18}O$ for water that remains after evaporation are “Evaporation Lines”. The slopes of these lines, always less than 8 (Dansgaard, 1964), reflect the relative fractionation of ^{2}H and ^{18}O in the evaporation process. The pattern of evaporative enrichment in soil water is mainly controlled by the humidity of the air (Sofer and Gat, 1975) and the soil physical properties that affect diffusion rates (Zimmerman *et al*., 1967; Allison and Barnes, 1983; Shurbaji and Phillips, 1995). Saturated soil Evaporation Lines have slopes similar to those of free water, 4 to 6, whereas unsaturated soils have slopes in the range of 2 to 5 with lower slopes associated with drier soils (Barnes and Allison, 1988). Transpiration losses via stomata lead to similar fractionation patterns (Aravena *et al*., 1989; Twining *et al*., 2006; Gat *et al*., 2007), which can sometimes be helpful in determining water sources (Figure 1-4). Using evapotranspiration lines such as this will allow for source water apportionment between fog and groundwater. Relationships among Fog Contribution, species and plant size can then be investigated, as in the California redwoods where larger plants used less fog as their roots were able to reach deeper soil water (Figure 5).

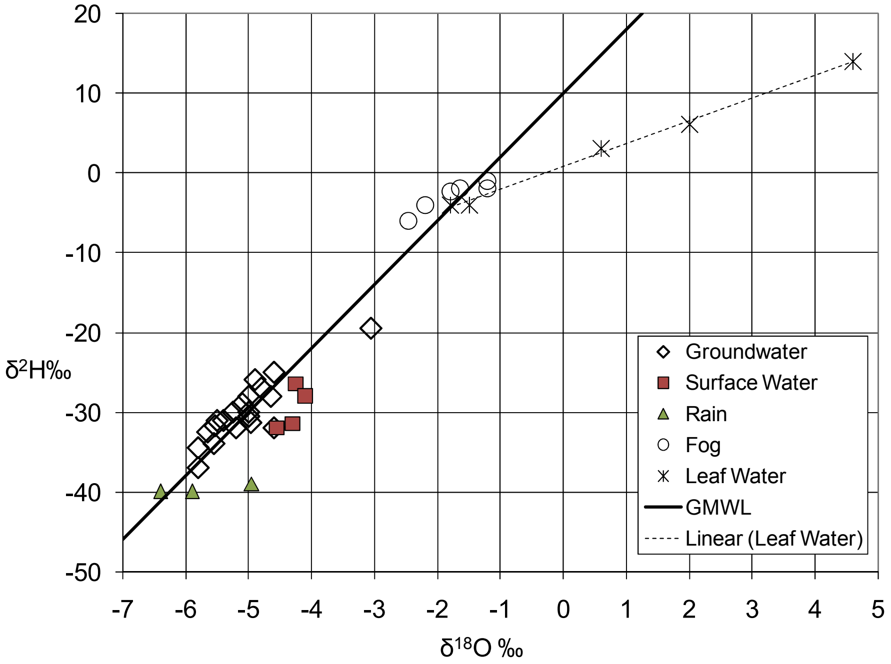

Figure 1-4: Atacama Desert eucalyptus leaf water is enriched through transpiration losses, but tracking this enrichment indicates that the source water is fog rather than rain, groundwater, or surface water (after Aravena *et al.* (1989)).

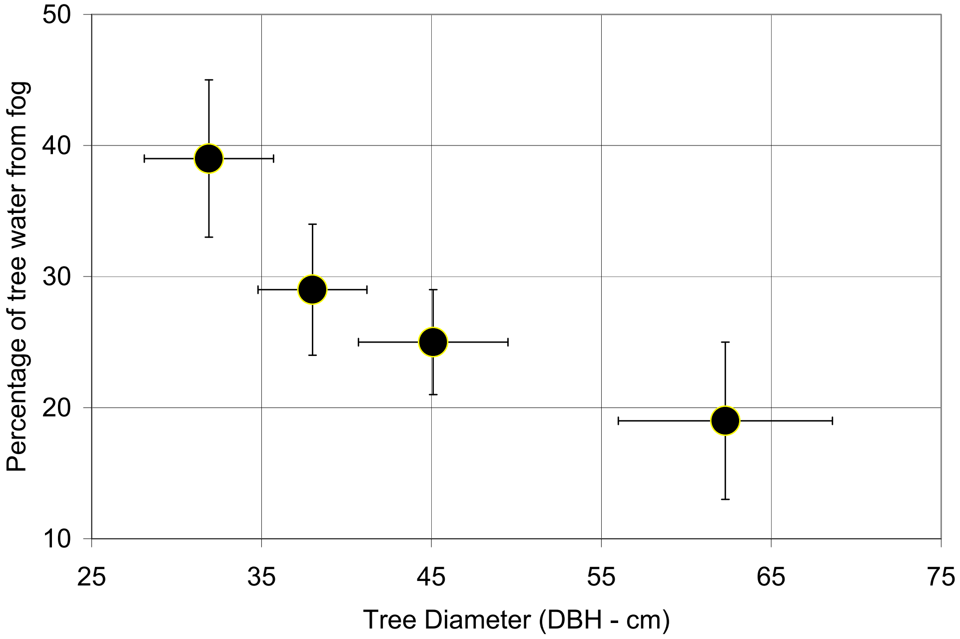

Figure 1-5: Use of fog water by California coastal redwood trees (after Dawson (1998)).

1.4 Microenvironmental controls on photosynthesis

Several studies have concluded that *W. mirabilis* makes use of both the C3 and CAM photosynthetic pathways (Schulze *et al*. 1976, von Willert *et al*. 2005), with apparently more CAM usage, and resultant higher $\delta^{13}C$, closer to the coast. One interpretation of this relationship is that the more water-efficient CAM adaptation is utilized to a greater extent in areas with lower rainfall, and therefore with less available soil and ground water. A study of microenvironmental control and $\delta^{13}C$ in C3 plants of the Sonoran Desert found enriched values in the more water-stressed habitats. This enrichment was attributed to water-use efficiency in water stressed plants (Ehleringer and Cooper, 1988). A similar study is presented in Chapter 6 for the *W. mirabilis* population at Hope Mine in the Namib Desert.

1.5 Fog and nutrient cycling

Lastly, fog may play a significant role in nutrient supply and cycling in the Central Namib. A relationship between $\delta^{15}N$ and rainfall was found in C3 plants growing on Kalahari sands in southern Africa, and indicates more nitrogen isotope discrimination in lower rainfall areas (Swap *et al*., 2004). The present study (Chapter 6) provides additional $\delta^{15}N$ data from several trees and shrubs to extend the Kalahari Mean Annual Rainfall gradient (200-1200 mm/yr) into the hyperarid Namib Desert (20-80 mm/yr).

There is also the potential for feedback mechanisms to exist between the occurrence of fog and dust in the Central Namib. The chemical composition of fog indicates that particles of dust have contributed elements such as sulfur and calcium by dissolving into the water droplets that make up fog, although there appears to be an additional source of Ca other than gypsum in some of the samples (Figure 1-6). The "Enrichment" of sulfur and calcium means that more of the element is present relative to chloride when compared to the composition of seawater. Seawater is the primary source of fog and rain water in the Namib. Dust that mixes with clouds in India has been shown to deter the formation of rain droplets in clouds due to the high abundance of condensation nuclei (Rosenfeld *et al*. 2001). Dust can also help to "seed" clouds because water may condense out of the atmosphere onto the dust particles, depending on the type of dust (Noone *et al*. 2000). Dust may also suppress cloud formation on larger scales by helping to cool the sea surface (Lau and Kim 2007). It is unclear what the interactions are between Namib dust and fog, but the initial chemistry data indicates that they do interact in some way. Here, stable isotope ratios of sulfur ($\delta^{34}S$) in size-segregated aerosols are used to evaluate the marine influence on background aerosol composition in the Namib Desert (Chapter 7).

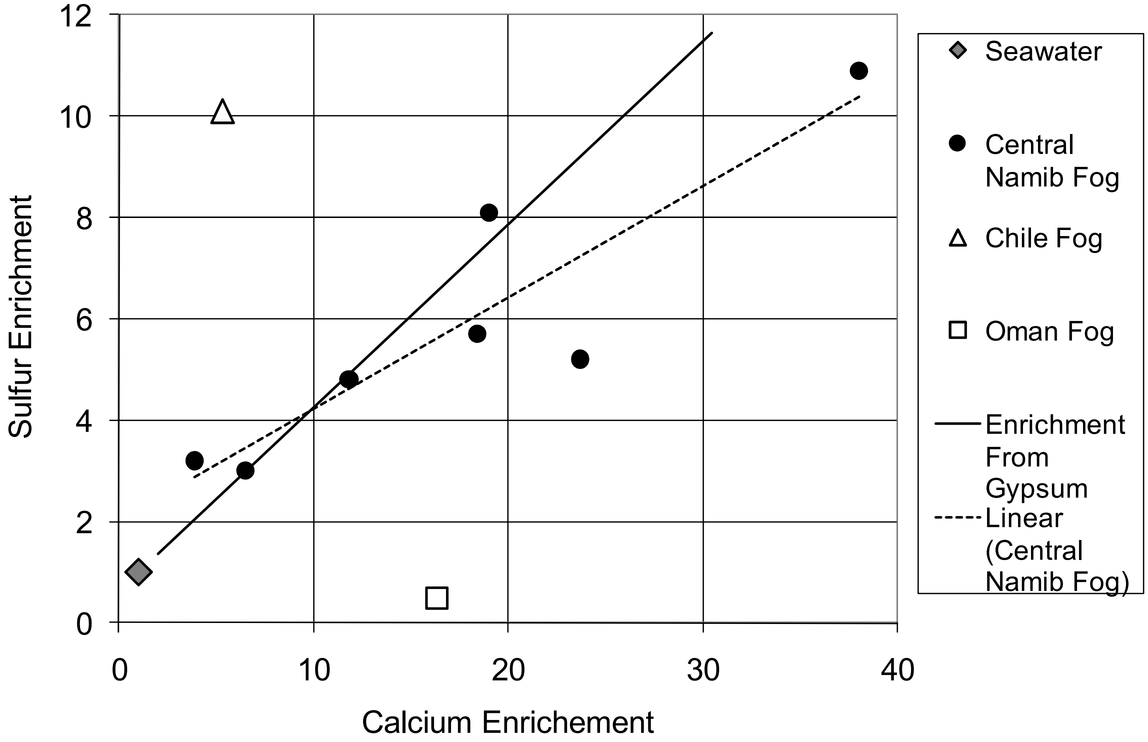

Figure 1-6: Sulfur and calcium enrichment in fog from the Namib, Chile, and Oman (after Eckardt and Schemenauer 1998).

1.5 Hypotheses

(1) Fog is a significant source of water for several common plant species within 60 km of the coast, and is variably less important for deeply-rooted trees and shrubs.

(2) Fog utilization increases with increased fog deposition. Thus, for a given species, highest fog utilization is expected on the upper slopes of dunes or inselbergs, especially on west-facing slopes. The coast-inland fog gradient is non-linear, and fog utilization by a given species is expected to follow this gradient.

(3) *Welwitschia mirabilis* makes use of the CAM photosynthetic pathway more often in more water-limited microenvironments, which are defined both by access to subsurface water and fog occurrence.

(4) Nitrogen isotopes of plants and soils in the coastal Namib do not follow the rainfall trend found in the Kalahari due to the influence of fog and dew.

(5) The sulfur isotopes of plants will correlate with fog deposition. That is, the patterns of $\delta^{34}S$ of plant material will be similar to that in fog water uptake.

1.6 Objectives

The primary objective in evaluating these hypotheses is to characterize the following end-members: $\delta^{2}H$ and $\delta^{18}O$ for fog, groundwater, soil water and plant water; $\delta^{13}C$ and $\delta^{15}N$ for plant tissue; $\delta^{34}S$ for fog water, rain, soils, groundwater and plant tissue. Ground-based climatological parameters specific to the microenvironments around the sampled plants and soils will aid in the interpretation of the isotope results. Long-term data from Gobabeb will help extrapolate the findings of this two-year study.

The impact of fog on a given species will be evident from inter-species differences at each location as well as intraspecies differences among locations that receive differing amounts of fog. The plants to be sampled are representative of common plants in the three habitats of the Central Namib – dune, river bed, gravel plains (Table 1-2). Results from co-occurring species (*A. leubnitziae* and *Z. stapffii* in the gravel plains, *S. sabulicola* and *T. hereroensis* in the dunes) will give insight into their relative fog utilization. Most of the species distributions extend from the coast (Rooibank) to the edge of the fog zone (Hope Mine). An exception is *A. leubnitziae*, which only occurs in areas of high fog frequency. *A. leubnitziae* is absent at Gobabeb and Hope, so *C. capitata* will be sampled where it is present at these locations for comparison with *Z. stapffii*. The shrubs *C. capitata* and *A. leubnitziae* are both in the Amaranthaceae family and co-occur with *Z. stapffii*. Their main difference is that *C. capitata* lacks the longitudinal grooves on its stems. A small set of samples will also be collected from the Swakop-Arandis transect, which was the subject of an intense study of fog influence on vegetation patterns (Hachfeld and Jurgens, 2000). In addition to this overall fog gradient, local gradients in elevation also separate areas of differing fog deposition. These local gradients will also be investigated (High Dune at Gobabeb and Swartbank Berg, both about 100 m high). Permission to sample *W. mirabilis* is difficult to obtain due to its extremely localized distribution, CITES protection, and importance as a national symbol for Namibia. Thus, *W. mirabilis* samples were only taken from Hope Mine. However, it is hoped that comparisons with *Z. stapffii* in this area will help elucidate connections with the fog gradient given that *Z. stapffii* occurs throughout the fog zone.

Sampling and observations occurred from August 2007 to June 2009, including continuous measurements at Gobabeb's Permanent Weather Stations and at least six months of data from Mini Stations as described in Chapter 3. Water, plant and soil samples were collected at Gobabeb and along the fog gradient during four field campaigns: August to December 2007, June to July 2008, January 2009, and June to July 2009.

Table 1-2: Summary of plants to be sampled.

Species	Habitat	Description	Photosynthetic pathway	Reported fog use	References	Occurrence			
						Rooibank	Swartbank	Gobabeb	Hope Mine
Stipagrostis sabulicola	Dune	Common dune grass	C4	Absorption via very shallow lateral roots	1,2,4	X	X	X	
Trianthema hereroensis		Succulent dune shrub	CAM	Foliar absorption	1,3,4,5,7	X	X	X	
Acanthosicyos horridus		Succulent, produces !nara melons	Unknown	Channels fog to roots via longitudinal grooves in stems	6,7,8,9	X	X	X	
Acacia erioloba	River bed	Large leguminous tree	C3	None reported	10,11,12	X	X	X	
Faidherbia albida		Large leguminous tree	C3	None reported	11,13,14,15	X	X	X	
Tamarix usneoides		Medium evergreen tree – salt tolerant	C3	None reported	14,16	X	X	X	
Zygophyllum stapffii	Gravel plains	Succulent shrub	Apparent C3	None reported	1,7,17,19,24	X	X	X	X
Arthraerua leubnitziae		Shrub – green stems	Apparent C3	Channels fog to roots via longitudinal grooves in stems	1,7,17,18,19,24	X	X		
Calicorema capitata		Shrub – green stems	Apparent C3	None reported	1,20			X	
Welwitschia mirabilis		Ancient shrub, two large wide leaves	C3/CAM	Foliar absorption (still debated)	1,7,21,22,23				X

References: 1 (Vogel and Seely, 1977), 2 (Louw and Seely, 1980), 3 (Seely *et al*., 1977), 4 (Southgate *et al*., 1996), 5 (Nott, 1985), 6 (Sandelowsky, 1990), 7 (Kutschera *et al*., 1997), 8 (Hebeler *et al*., 2004), 9 (Moser, 2004), 10 (Canadell *et al*., 1996), 11 (Schulze *et al*., 1991), 12 (Schulze *et al*., 1998), 13 (Ward and Breen, 1983), 14 (Bate and Walker, 1993), 15 (Roupsard *et al*., 1999), 16 (Horton and Clark, 2001), 17 (Ebert, 2000), 18 (Loris, 2004), 19 (Hachfeld and Jurgens, 2000), 20 (Burke, 2003), 21 (Bornman *et al*., 1973), 22 (Schulze *et al*., 1976), 23 (von Willert *et al*., 2005), 24 (Schulze and Schulze, 1976)

References

Allison, G.B., Barnes, C.J., 1983. Estimation of Evaporation from Non-Vegetated Surfaces Using Natural Deuterium. Nature 301, 143-145.

Aravena, R., Suzuki, O., Pollastri, A., 1989. Coastal Fog and Its Relation to Groundwater in the Iv-Region of Northern Chile. Chemical Geology 79, 83-91.

Barnes, C.J., Allison, G.B., 1988. Tracing of Water-Movement in the Unsaturated Zone Using Stable Isotopes of Hydrogen and Oxygen. Journal of Hydrology 100, 143-176.

Bate, G.C., Walker, B.H., 1993. Water relations of the vegetation along the Kuiseb River, Namibia. Madoqua 18, 85-91.

Bethune, S., Schachtschneider, K., 2004. How community action, science and common sense can work together to develop an alternative way to combat desertification. Environmental Monitoring and Assessment 99, 161-168.

Bierman, P.R., Caffee, M., 2001. Slow rates of rock surface erosion and sediment production across the Namib Desert and escarpment, southern Africa. American Journal of Science 301, 326-358.

Bornman, C.H., Botha, C.E.J., Nash, L.J., 1973. *Welwitschia mirabilis*: observations on movement of water and assimilates under föhn and fog conditions. Madoqua Series II 2, 25-31.

Burgess, S.S.O., Dawson, T.E., 2004. The contribution of fog to the water relations of Sequoia sempervirens (D. Don): foliar uptake and prevention of dehydration. Plant Cell and Environment 27, 1023-1034.

Burke, A., 2003. Wild flowers of the central Namib. Namibia Scientific Society, Windhoek.

Burke, A., 2006. Savanna trees in Namibia - Factors controlling their distribution at the arid end of the spectrum. Flora 201, 189-201.

Campbell Scientific, 2006. 237 and 237F Wetness Sensing Grids User Guide. Campbell Scientific, Ltd., Edmonton.

Canadell, J., Jackson, R.B., Ehleringer, J.R., Mooney, H.A., Sala, O.E., Schulze, E.D., 1996. Maximum rooting depth of vegetation types at the global scale. Oecologia 108, 583-595.

Corbin, J.D., Thomsen, M.A., Dawson, T.E., D'Antonio, C.M., 2005. Summer water use by California coastal prairie grasses: fog, drought, and community composition. Oecologia 145, 511-521.

Craig, H., 1961. Isotopic variations in meteoric waters. Science 133, 1702-1703.

Curtis, B., Mannheimer, C., 2005. Tree atlas of Namibia. National Botanical Research Institute, Ministry of Agriculture, Water and Forestry, Windhoek.

Dansgaard, W., 1964. Stable Isotopes in Precipitation. Tellus 16, 436-468.

Dawson, T.E., 1998. Fog in the redwood forest: ecosystem inputs and use by plants. Oecologia 117, 476-485.

Dawson, T.E., Ehleringer, J.R., 1991. Streamside trees that do not use stream water. Nature 350, 335-337.

Dawson, T.E., Mambelli, S., Plamboeck, A.H., Templer, P.H., Tu, K.P., 2002. Stable isotopes in plant ecology. Annual Review of Ecology and Systematics 33, 507-559.

Decagon Devices, 2007. Dielectric Leaf Wetness Sensor Operator's Manual: Version 2. Decagon Devices, Inc., Pullman, WA.

Ebert, O., 2000. Vergleichende Untersuchungen zum Wasserverbrauch von Sträuchern in der Namib-Wüste. Teaching Diploma. Universität Hohenheim Institut für Botanik, Stuttgart.

Eckardt, F., 1996. The distribution and origin of gypsum in the Central Namib Desert, Namibia. University of Oxford, Oxford.

Eckardt, F.D., Drake, N., Goudie, A.S., White, K., Viles, H., 2001. The role of playas in pedogenic gypsum crust formation in the Central Namib Desert: A theoretical model. Earth Surface Processes and Landforms 26, 1177-1193.

Eckardt, F.D., Schemenauer, R.S., 1998. Fog water chemistry in the Namib Desert Namibia. Atmospheric Environment 32, 2595-2599.

Ehleringer, J.R., Cooper, T.A., 1988. Correlations between Carbon Isotope Ratio and Microhabitat in Desert Plants. Oecologia 76, 562-566.

Fischer, D.T., Still, C., 2007. Evaluating patterns of fog water deposition and isotopic composition on the California Channel Islands. Water Resources Research 43, W04420.

Garcia-Santos, G., Marzol, M.V., Aschan, G., 2004. Water dynamics in a laurel montane cloud forest in the Garajonay National Park (Canary Islands, Spain). Hydrology and Earth System Sciences 8, 1065-1075.

Gat, J.R., Yakir, D., Goodfriend, G., Fritz, P., Trimborn, P., Lipp, J., Gev, I., Adar, E., Waisel, Y., 2007. Stable isotope composition of water in desert plants. Plant and Soil 298, 31-45.

Goodman, J., 1985. The Collection of Fog Drip. Water Resources Research 21, 392-394.

Goudie, A.S., Eckardt, F., 1999. The evolution of the morphological framework of the Central Namib Desert, Namibia, since the Early Cretaceous. Geografiska Annaler Series A-Physical Geography 81A, 443-458.

Goudie, A.S., Parker, A.G., 1998. Experimental simulation of rapid rock block disintegration by sodium chloride in a foggy coastal desert. Journal of Arid Environments 40, 347-355.

Hachfeld, B., Jurgens, N., 2000. Climate patterns and their impact on the vegetation in a fog driven desert: The Central Namib Desert in Namibia. Phytocoenologia 30, 567-589.

Hamilton, W.J., Seely, M.K., 1976. Fog basking by the Namib Desert beetle, *Onymacris unguicularis*. Nature 262, 284-285.

Hebeler, F., Botha, C., van Bel, A., 2004. Water, photosynthesis and transpiration of !nara. In: Henschel, J.R., Dausab, R., Moser, P., Pallett, J. (Eds.), !Nara: Fruit for development of the !Khuiseb Topnaar. Namibia Scientific Society, Windhoek, Namibia, pp. 93-106.

Henschel, J., Mtuleni, V., Gruntkowski, N., Seely, M., Shanyengana, S.E., 1998. NAMFOG: Namibian application of fog-collecting systems Desert Research Foundation of Namibia, Windhoek.

Henschel, J.R., Seely, M.K., 2000. Long-term growth patterns of *Welwitschia mirabilis*, a long-lived plant of the Namib Desert (including a bibliography). Plant Ecology 150, 7-26.

Henschel, J.R., Seely, M.K., 2008. Ecophysiology of atmospheric moisture in the Namib Desert. Atmospheric Research 87, 362-368.

Hildebrandt, A., Al Aufi, M., Amerjeed, M., Shammas, M., Eltahir, E.A.B., 2007. Ecohydrology of a seasonal cloud forest in Dhofar: 1. Field experiment. Water Resources Research 43, W10411.

Hildebrandt, A., Eltahir, E.A.B., 2006. Forest on the edge: Seasonal cloud forest in Oman creates its own ecological niche. Geophysical Research Letters 33, L11401.

Horton, J.L., Clark, J.L., 2001. Water table decline alters growth and survival of Salix gooddingii and Tamarix chinensis seedlings. Forest Ecology and Management 140, 239-247.

Huxman, T.E., Snyder, K.A., Tissue, D., Leffler, A.J., Ogle, K., Pockman, W.T., Sandquist, D.R., Potts, D.L., Schwinning, S., 2004. Precipitation pulses and carbon fluxes in semiarid and arid ecosystems. Oecologia 141, 254-268.

Ingraham, N.L., Mark, A.F., 2000. Isotopic assessment of the hydrologic importance of fog deposition on tall snow tussock grass on southern New Zealand uplands. Austral Ecology 25, 402-408.

Ingraham, N.L., Matthews, R.A., 1988. Fog-Drip as a Source of Groundwater Recharge in Northern Kenya. Water Resources Research 24, 1406-1410.

Jacobson, K.M., Jacobson, P.J., 1998. Rainfall regulates decomposition of buried cellulose in the Namib Desert. Journal of Arid Environments 38, 571-583.

Jacobson, P.J., Jacobson, K.M., Seely, M., 1995. Ephemeral rivers and their catchments : sustaining people and development in western Namibia. Desert Research Foundation of Namibia, Windhoek.

Jiusto, J.E., 1981. Fog Structure. In: Hobbs, P.V., Deepak, A. (Eds.), Clouds: Their formation, optical properties, and effects. Academic Press, New York, pp. 187-239.

Kerfoot, O., 1968. Mist precipitation on vegetation. Forestry Abstracts 29, 8-20.

Kuells, C., 2000. Groundwater of the North-Western Kalahari, Namibia: Estimation of Recharge and Quantification of the Flow Systems. Julius-Maximilian University of Würzburg, Würzburg, Germany.

Kutschera, L., Lichtenegger, E., Sobotik, M., Haas, D., 1997. Die Wurzel das neue Organ Ihre Bedeutung für das Leben von *Welwitschia mirabilis* und anderer Arten der Namib sowie von Arten angrenzender Gebiete mit Erklärung des geotropen Wachstums der Pflanzen. Eigenverlag: Pflanzensoziologisches Institut, Klagenfurt, Klagenfurt/Austria.

Kwasny, R., Aul, F., Lohrey, K., 2007. Recent activities and trends in the uranium market. Atw-International Journal for Nuclear Power 52, 696-710.

Lancaster, J., Lancaster, N., Seely, M.K., 1984. Climate of the central Namib Desert. Madoqua 14, 5-61.

Lancaster, N., 2002. How dry was dry? - Late Pleistocene palaeoclimates in the Namib Desert. Quaternary Science Reviews 21, 769-782.

Lange, J., 2005. Dynamics of transmission losses in a large and stream channel. Journal of Hydrology 306, 112-126.

Liu, W.H., Zhang, Y.P., Li, H.M., Liu, Y.H., 2005. Fog drip and its relation to groundwater in the tropical seasonal rain forest of Xishuangbanna, Southwest China: a preliminary study. Water Research 39, 787-794.

Loris, K., 2004. Nebel als Wasserressource für den Strauch Arthraerua leubnitziae. In: Walter, H., Breckle, S.-W. (Eds.), Ökologie der Erde: Spezielle Ökologie der tropischen und subtropischen Zonen. Spektrum-Verlag, pp. 485-489.

Louw, G.N., 1972. The role of advective fog in the water economy of certain Namib Desert animals. Symposia of the Zoological Society of London 31, 297-314.

Louw, G.N., Seely, M.K., 1980. Exploitation of fog water by a perennial Namib dune grass, *Stipagrostis sabulicola*. South African Journal of Science 76, 38-39.

McGough, H.N., Groves, M., Mustard, M., Brodie, C., 2004. CITES and Succulents: An introduction to succulent plants covered by the Convention on International Trade in Endangered Species. Royal Botanic Gardens, Kew, London.

Michalski, G., Bohlke, J.K., Thiemens, M., 2004. Long term atmospheric deposition as the source of nitrate and other salts in the Atacama Desert, Chile: New evidence from mass-independent oxygen isotopic compositions. Geochimica Et Cosmochimica Acta 68, 4023-4038.

Moser, P., 2004. Root and shoot development of !nara seedlings. In: Henschel, J., Dausab, R., Moser, P., Pallett, J. (Eds.), !NARA: Fruit for development of the !Khuiseb Topnaar. Namibia Scientific Society, Windhoek, pp. 85-91.

Nagel, J.F., 1956. Fog precipitation on Table Mountain. Quarterly Journal of the Royal Meteorological Society 82, 452-460.

Nott, K., 1985. An autecological study of a Namib dune succulent, Trianthema hereroensis. Department of Soil Science and Agrometeorology. University of Natal, Pietermaritzburg.

Olivier, J., 1995. Spatial-Distribution of Fog in the Namib. Journal of Arid Environments 29, 129-138.

Pietruszka, R.D., Seely, M.K., 1985. Predictability of two moisture sources in the Namib Desert. South African Journal of Science 81, 682-685.

Rech, J.A., Quade, J., Hart, W.S., 2003. Isotopic evidence for the source of Ca and S in soil gypsum, anhydrite and calcite in the Atacama Desert, Chile. Geochimica Et Cosmochimica Acta 67, 575-586.

Roupsard, O., Ferhi, A., Granier, A., Pallo, F., Depommier, D., Mallet, B., Joly, H.I., Dreyer, E., 1999. Reverse phenology and dry-season water uptake by Faidherbia albida (Del.) A. Chev. in an agroforestry parkland of Sudanese west Africa. Functional Ecology 13, 460-472.

Rozanski, K., Araguasaraguas, L., Gonfiantini, R., 1993. Isotopic Patterns in Modern Global Precipitation. In: Swart, P.K., Lohmann, K.C., McKenzie, J., Savin, S. (Eds.), Climate Change in Continental Isotopic Records. American Geophysical Union, Washington, DC.

Sandelowsky, B.H., 1990. *Acanthosicyos horridus*, a multipurpose plant of the Namib Desert in southwestern Africa. In: Bates, D.M., Robinson, R.W., Jeffrey, C. (Eds.), Biology & Utilization of the Cucurbitaeceae. Cornell University Press, Ithaca & London, pp. 349-355.

Schemenauer, R.S., Cereceda, P., 1994. A proposed standard fog collector for use in high-elevation regions. Journal of Applied Meteorology 33, 1313-1322.

Schmitz, A.U., 2004. Transmission losses and soil moisture dynamics in the alluvial fill of the Kuiseb river, Namibia. Albert-Ludwigs-Universität Freiburg i. Br., Freiburg i. Br.

Scholl, M.A., Gingerich, S.B., Tribble, G.W., 2002. The influence of microclimates and fog on stable isotope signatures used in interpretation of regional hydrology: East Maui, Hawaii. Journal of Hydrology 264, 170-184.

Schulze, E.-D., Schulze, I., 1976. Distribution and control of photosynthetic pathways in plants growing in the Namib Desert, with special regard to *Welwitschia mirabilis* Hook. fil. Madoqua 9, 5-13.

Schulze, E.-D., Ziegler, H., Stichler, W., 1976. Environmental control of crassulacean acid metabolism in *Welwitschia mirabilis* Hook. Fil. in its range of natural distribution in the Namib Desert. Oecologia 24, 323-334.

Schulze, E.D., Gebauer, G., Ziegler, H., Lange, O.L., 1991. Estimates of Nitrogen-Fixation by Trees on an Aridity Gradient in Namibia. Oecologia 88, 451-455.

Schulze, E.D., Williams, R.J., Farquhar, G.D., Schulze, W., Langridge, J., Miller, J.M., Walker, B.H., 1998. Carbon and nitrogen isotope discrimination and nitrogen nutrition of trees along a rainfall gradient in northern Australia. Australian Journal of Plant Physiology 25, 413-425.

Seely, M.K., 1978. Grassland productivity: the desert end of the curve. South African Journal of Science 74, 295-297.

Seely, M.K., de Vos, M.P., Louw, G.N., 1977. Fog imbibition, satellite fauna and unusual leaf structure in a Namib Desert dune plant *Trianthema hereroensis*. South African Journal of Science 73, 169-172.

Seely, M.K., Hamilton, W.J., 1976. Fog Catchment Sand Trenches Constructed by Tenebrionid Beetles, Lepidochora, from the Namib Desert. Science 193, 484-486.

Shanyengana, E.S., Henschel, J.R., Seely, M.K., Sanderson, R.D., 2002. Exploring fog as a supplementary water source in Namibia. Atmospheric Research 64, 251-259.

Shu, Y., Feng, X.H., Gazis, C., Anderson, D., Faiia, A.M., Tang, K.L., Etti, G.J., 2005. Relative humidity recorded in tree rings: A study along a precipitation gradient in the Olympic Mountains, Washington, USA. Geochimica Et Cosmochimica Acta 69, 791-799.

Shurbaji, A.R.M., Phillips, F.M., 1995. A Numerical-Model for the Movement of H2o, H-2 O-18, and (Hho)-H-2 in the Unsaturated Zone. Journal of Hydrology 171, 125-142.

Siesser, W.G., 1980. Late Miocene Origin of the Benguela Upswelling System off Northern Namibia. Science 208, 283-285.

Sofer, Z., Gat, J.R., 1975. Isotope Composition of Evaporating Brines - Effect of Isotopic Activity Ratio in Saline Solutions. Earth and Planetary Science Letters 26, 179-186.

Southgate, R.I., Masters, P., Seely, M.K., 1996. Precipitation and biomass changes in the Namib Desert dune ecosystem. Journal of Arid Environments 33, 267-280.

Squeo, F.A., Aravena, R., Aguirre, E., Pollastri, A., Jorquera, C.B., Ehleringer, J.R., 2006. Groundwater dynamics in a coastal aquifer in north-central Chile: Implications for groundwater recharge in an arid ecosystem. Journal of Arid Environments 67, 240-254.

Stock, J., Coil, J., Kirch, P.V., 2003. Paleohydrology of and southeastern Maui, Hawaiian Islands, and its implications for prehistoric human settlement. Quaternary Research 59, 12-24.

Swap, R.J., Aranibar, J.N., Dowty, P.R., Gilhooly, W.P., Macko, S.A., 2004. Natural abundance of C-13 and N-15 in C-3 and C-4 vegetation of southern Africa: patterns and implications. Global Change Biology 10, 350-358.

Twining, J., Stone, D., Tadros, C., Henderson-Sellers, A., Williams, A., 2006. Moisture Isotopes in the Biosphere and Atmosphere (MIBA) in Australia: A priori estimates and preliminary observations of stable water isotopes in soil, plant and vapour for the Tumbarumba Field Campaign. Global and Planetary Change 51, 59-72.

Viles, H.A., 2005. Microclimate and weathering in the central Namib Desert, Namibia. Geomorphology 67, 189-209.

Vogel, J.C., Seely, M.K., 1977. Occurrence of C-4 plants in the central Namib Desert. Madoqua 10, 75-78.

von Willert, D.J., Armbruster, N., Drees, T., Zaborowski, M., 2005. *Welwitschia mirabilis*: CAM or not CAM - what is the answer? Functional Plant Biology 32, 389-395.

Walker, G.R., Woods, P.H., Allison, G.B., 1994. Interlaboratory comparison of methods to determine the stable isotope composition of soil water. Chemical Geology 111, 297-306.

Walter, H., Breckle, S.W., 1986. Tropical and subtropical zonobiomes. Springer-Verlag, Berlin.

Ward, J.D., Breen, C.M., 1983. Drought stress and the demise of *Acacia albida* along the lower Kuiseb River, central Namib Desert: preliminary findings. South African Journal of Science 79, 444-447.

Warren-Rhodes, K.A., Rhodes, K.L., Pointing, S.B., Ewing, S.A., Lacap, D.C., Gomez-Silva, B., Amundson, R., Friedmann, E.I., McKay, C.P., 2006. Hypolithic cyanobacteria, dry limit of photosynthesis, and microbial ecology in the hyperarid Atacama Desert. Microbial Ecology 52, 389-398.

Weidlich, B., 2008. Govt grants 25-year uranium license to Canada's Forsys. The Namibian, Windhoek.

White, J.W.C., Cook, E.R., Lawrence, J.R., Broecker, W.S., 1985. The D/H ratios of sap in trees: Implications for water sources and tree ring D/H ratios. Geochimica Et Cosmochimica Acta 49, 237-246.

Wilkinson, M.J., 1990. Paleoenvironments in the Namib Desert : the lower Tumas Basin in the Late Cenozoic. University of Chicago, Committee on Geographical Studies, Chicago, Ill., USA.

Zimmerman, U., Ehhalt, D., Munnich, K.O., 1967. Soil-water movement and evapotranspiration: Changes in the isotopic composition of the water. In: IAEA (Ed.), Isotopes in hydrology; Proceedings of the symposium (1966: Vienna). International Atomic Energy Agency, Vienna, pp. 567-585.

Chapter 2 : Methods

2.1 Ground-based measurements

Fog and dew deposition amounts are measured daily at Gobabeb, and long-term observation efforts at varying temporal resolutions have been conducted since the 1960's at stations across the Namib with the data available at Gobabeb (Lancaster *et al*., 1984; Henschel and Seely, 2008). In addition to these data, this study adds discrete, event-scale fog deposition and soil moisture measurements as well as continuous measurements of leaf wetness, soil moisture, air temperature, and relative humidity. The fog was collected using four portable, modified harp style ("X-harp") collectors comprised of nylon fishing line strung vertically between stainless steel threaded rods from which the fog drips into PVC troughs, through about 30 cm of tygon tubing into a sealed, clean High Density Polyethylene collection bottle (Fischer and Still, 2007). The X-harp collectors were built with local materials in 2007, and have a mean cross-sectional area of 0.084 m^2 (Figure 2-1B). For a few fog events, X-harp collectors were placed adjacent to the Gobabeb daily collector (Standard Fog Collector "SFC", 1 m^2 of a double-layer of plastic shade netting on a square frame facing northwest 2m off the ground; Figure 2-1A) for comparison with the large data set at Gobabeb and other locations worldwide (Schemenauer and Cereceda, 1994). Several deployments of a teflon harp-style collector (Figure 2-1C) were also made adjacent to the SFC at Gobabeb in an attempt to collect clean samples for major ion chemistry. Other X-harp deployments coincide with plant and soil sampling events at Gobabeb, Swartbank and Hope.

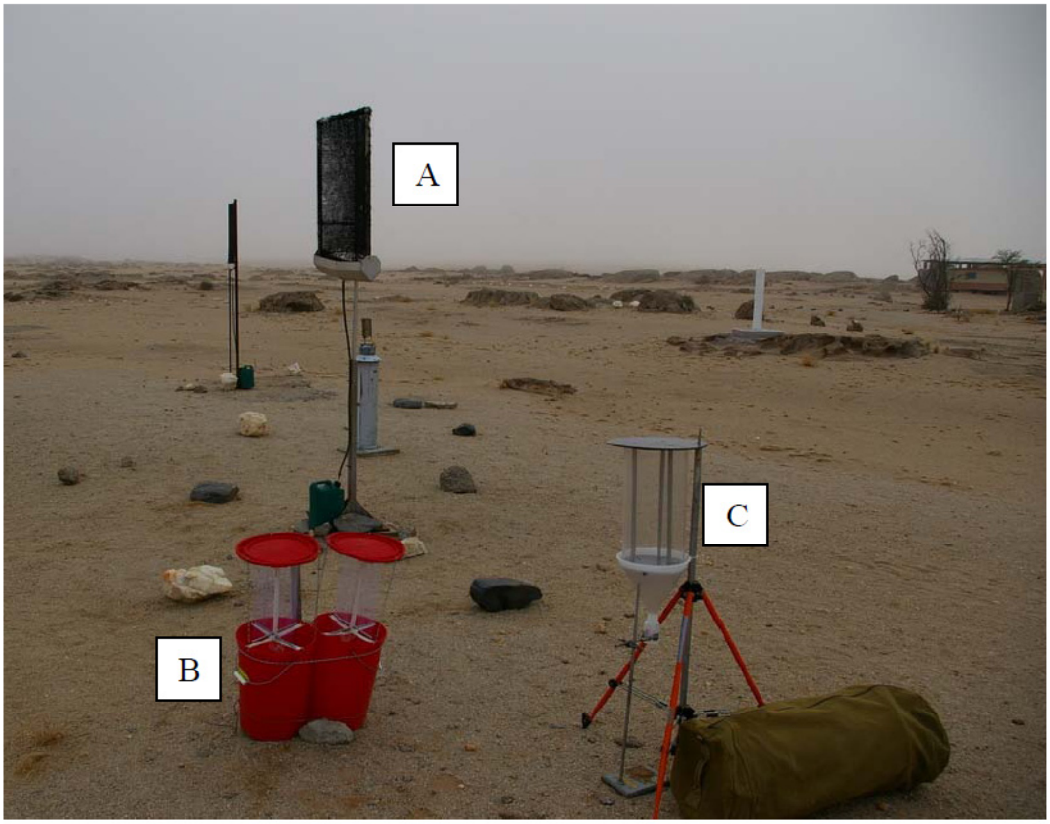

Figure 2-1: Fog collectors at Gobabeb.
Note: See text for descriptions and references.

Continuous measurements were made for at least six months in four locations across the Gobabeb-High Dune transect (“Mini Stations”), along with the permanent Gobabeb weather station (“Permanent Station”). As with the fog collection, short-term measurements adjacent to the Gobabeb weather station are used to connect with the larger Gobabeb data sets. The measurements comprise dielectric leaf wetness (Decagon Leaf Wetness Sensor “LWS”, or Campbell Scientific Sensor 237), dielectric soil moisture (volumetric moisture content, Decagon Sensor EC5 or 5TE), air temperature and relative humidity. Pyranometers and Water Activity sensors (Decagon Sensors PYR and MPS) were also used at several Mini Stations. Pyranometers can be used to estimate sky type

(Duchon and O'Malley, 1999) and water activity has been useful in characterizing soil moisture in other arid soils (Gee *et al*., 1992; Sandvig and Phillips, 2006). Leaf Wetness Sensors were placed within a plant's canopy, as well as just above the bare ground surface. Discrete soil moisture measurements were made gravimetrically by weighing wet soil collected in jars, drying at 70 °C and re-weighing. Measurements at the Mini Stations were made every 5 minutes, whereas the Permanent Station recorded every 15 minutes. In addition to the six months of data (June 2008 – January 2009) at Gobabeb, five permanent Mini Stations were placed at locations along the fog gradient in July 2009 (Appendix C). In order to characterize atmospheric moisture conditions, saturation vapor pressure is related to air temperature according to Equation 2-1 and relative humidity is related to vapor pressure and temperature using Equation 2-2.

$$e_s = 0.611 \times e^{\frac{17.502 \times T_a}{T_a + 240.97}} \qquad \text{2-1}$$

$$h = \frac{e_a}{e_s} \qquad \text{2-2}$$

with,
e_s = saturation vapor pressure (kPa)
T_a = air temperature (centigrade)
h = relative humidity (decimal form, not percentage)
e_a= ambient vapor pressure (kPa)

Leaf Wetness Sensors were designed to mimic the thermal properties and texture of leaves from food crops. Although an LWS typically gives a binary "wet" or "dry" response for a given time period based on a threshold electrical resistance value, the raw data allows for some quantification of the amount of water deposited. This quantification was performed using a separate calibration for each LWS (Figure 2-2) following the results of testing by the manufacturer (Decagon Devices, Inc. unpublished data 1999). With a 2500 mV excitation, the raw response of an LWS varied between around 100 and 1000 (mV), with a stable "dry" signal between 430 and 450 mV. Response above 450 mV indicates wetness, and range up to about 650 mV during heavy fog or rain. Values below 430 mV and equal to 1023 mV were indicators of poor sensor response. From field observations, the very low values could be due to the sensor touching the sand surface or plant material. And, the very high value of 1023 mV seems to correspond to times when a crust formed on the upper side of the sensor – possibly due to jackal or fox urine based on animal tracks nearby. Much of the data surrounding these high and low response events had to be discarded due to irregular response patterns. After this data quality check, "wet" events were identified as periods with a response greater than 450 mV which persisted for more than 1 hr, ending with the response staying below 450 mV for at least 1 hr. Each event was then categorized as rain, fog or dew through an objective comparison with both manual and continuous weather monitoring data at Gobabeb. The event was labeled as rain if rain was collected at Gobabeb (2 km Northeast of the High Dune LWS); fog if (1) fog was noted through manual observations, (2) if a fog sample was collected, or (3) if there were very low clouds observed at 8am; and the remaining events were considered to be dew.

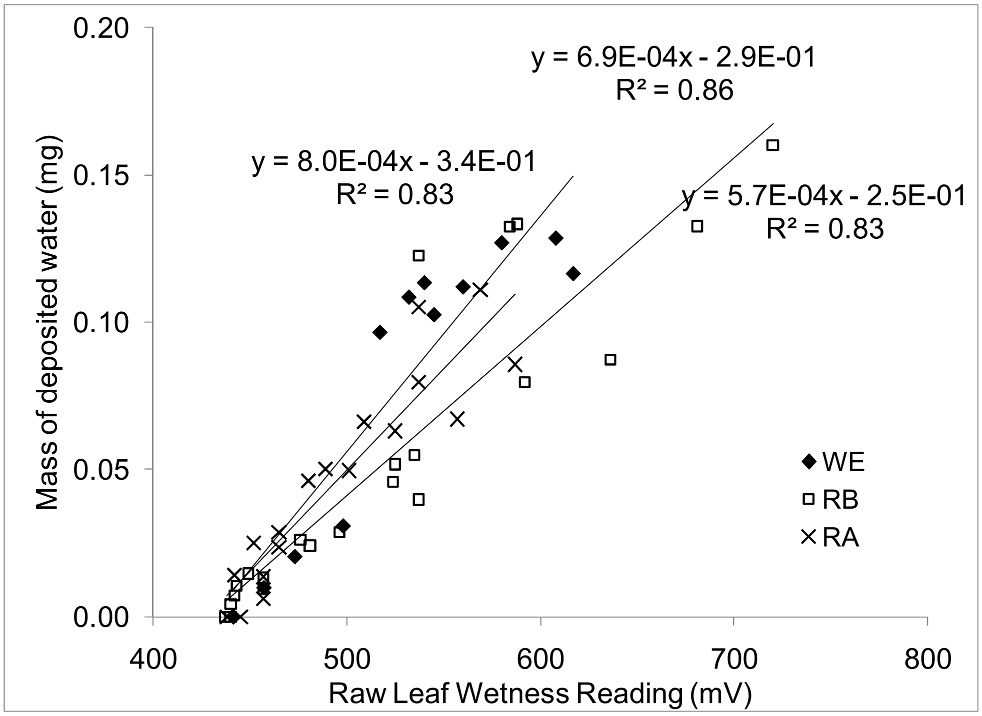

Figure 2-2: Example calibration data for converting raw data from Leaf Wetness Sensors to an amount of water deposited.

After converting the raw values to volume per area (ml/m^2) using separate calibrations for each sensor (Figure 2-2), the amount of water deposited was calculated as the sum of positive increments in the volume of water deposited. That is, if the volume per area increased from one 5-min average value to the next during a wetting event, this increment was interpreted as an addition of water to the surface of the sensor. An alternative interpretation would be to take the maximum value per event as the total amount deposited. However, the incremental procedure used allows for a more realistic description of wetting and drying of the sensor during a fog or dew event. There is minimal noise in the 5-min averaged data, but this aspect should be examined before applying the procedure elsewhere. It is possible that additional noise in, for example, 1-min averaged data would add an artificial amount of water to the total due to minor variations in the sensor response. Any such higher-frequency variations appear to be averaged out in the 5-min data.

2.2 Climate model predictions

Arid areas of southern Africa are generally predicted to become drier under the influence of climate change, and thus produce more dust (Hulme *et al*., 2001; Thomas *et al*., 2005; Giannini *et al*., 2008). However, the Namib "fog desert" is potentially less affected by decreased rainfall as long as the fog frequency does not decrease. The broad impacts of climate change on fog occurrence in the Namib will be examined using existing output from various models using the most recent IPCC climate scenarios (Intergovernmental Panel on Climate Change, 2007). Predictions for changes to relative humidity (RH, an output of some climate models) in the desert will be related to fog occurrence through a relationship between fog and RH from ground-based observations using data from 2007-2009.

2.3 Sampling – water

Fog samples were collected at Gobabeb by research station technicians during the 8am manual weather station duty from the Gobabeb SFC and stored at 4°C in 12 mL vacutainers sealed with Parafilm. Concomitant fog samples from X-harp collectors placed around Gobabeb, Swartbank and Hope were collected during field campaigns (Appendix C). Dew samples were also collected during field campaigns from the

Gobabeb Standard Dew Collector ("SDC"), a 1 m^2 teflon sheet sitting at 45° on a frame about 0.5 m off the ground. The SDC is checked for water and emptied every morning. Dew samples were collected on days when no fog was observed or collected in the vertical SFC. Correlations among SFC fog, X-harp fog, and dew samples collected during field campaigns serve to extend the more continuous SFC fog data.

Rain water was collected opportunistically during field campaigns. Groundwater and surface water has been analyzed extensively for $\delta^{34}S$, $\delta^{2}H$ and $\delta^{18}O$ in previous studies (Eckardt, 1996; Schmitz, 2004), and the $\delta^{2}H$ and $\delta^{18}O$ values from groundwater were regionally shown to have a well-defined signal. Groundwater from Gobabeb was be sampled periodically to confirm this apparently robust signal.

2.4 Sampling – plants and soils

Plants were sampled and stored according to the IAEA-MIBA (Moisture Isotopes in the Biosphere and Atmosphere) program protocol (Twining *et al*., 2006). In this protocol, the stem material is stripped of bark and any phloem material that may contain photosynthates. The exposed tissue is then stored in a glass vacutainer sealed with Parafilm, chilled in the field, and refrigerated in the laboratory. Due to long storage times (6-12 months) in the present study, the samples were stored frozen. Both exposed stem and leaf material from the same branch were collected in order to examine proximal and distal signals. For several individual plants, a series of stem samples was collected separately from various points along the stem. For grass samples (*S. sabulicola*), a non-green piece of stalk was collected in lieu of stem material. In order to obtain an integrated water sample from the branchless *W. mirabilis,* a 5mm diameter core (Haglof increment borer) was taken from 12 individuals (Appendix B). Soils were collected and stored frozen in glass mason jars. Several soil profiles were collected in sand dunes from areas where the sand is solid enough to allow an auger to penetrate 0.5-1m.

2.5 Sampling – aerosols

Aerosols were collected with a High Volume Cascade Impactor system (Turekian *et al*., 2001; Tisch Environmental Inc., 2004) at flow rates averaging about 1000 liters per minute (L min^{-1}). Glass Fiber filters on four impactor stages (7.6, 1.5, 1.0, and 0.5 µm) were used to collect aerosols for 11 hr sampling periods: "Day" (~7am to 6pm local time) and "Night" (~7pm to 6am). Flow rates were recorded continuously and calibrated with a NIST-traceable variable orifice calibration unit at the beginning and end of the sampling period. The aerodynamic diameter particle size cutoffs for each of stage vary up to 0.1 µm based on flow rate and atmospheric conditions. Flow rate and size cutoff calculations are given in Appendix A. Collection was performed at Gobabeb from 21 June to 2 July 2009 at 1.5 m above the ground in a location as far as possible from the daily activities of the research station (~500 m). Filters were pre-ashed at 550°C for 4 hours and no sulfur was detected in field or lab blanks of the slotted GF filters. The backing filter media contained a binder that retained a sulfur blank after ashing, and thus these results are not presented.

Additional aerosol samples were collected using a low flow cascade impactor (Sioutas, 2004) with four stages (2.5, 1.0, 0.5 and 0.25 µm) and a backing filter (Quartz

Fiber). This collector was placed at a height of 4 m above the ground and ran at a flow rate of 9 L min^{-1} from 19 June to 2 July 2009, resulting in 4 sets of day and night samples. Separate sets of day and night collection stages were used for up to four days to increase sample mass. The same backing filter was used for all four days. However, due to insufficient mass collected on each individual stage, the two coarse and two fine fraction stages were combined for each δ^{34}S analysis. Analytical grade tin was used as the collection substrate on the impactor stages. The tin material can be directly introduced to the Elemental Analyzer system described below , and is expected to have comparable aerosol collection efficiencies as Glass Fiber substrates (Sioutas, 2004). Three Total Suspended Particulate samples (Glass Fiber) were also collected at 6-8 L min^{-1} for a few hours each, but no sulfur was detected in these samples.

2.6 Analysis – plants and soils

Plant and soil samples were dried (60°C), homogenized, weighed into tin capsules and converted to CO_2, N_2 and SO_2 for isotope analysis using a Carlo Erba elemental analyzer (EA) which is coupled to an OPTIMA stable isotope ratio mass spectrometer (Micromass, Manchester, UK). Carbon and nitrogen isotopes were determined with a single combustion using a dual furnace system composed of an oxidation furnace at 1020^{o}C and a reduction furnace at 650^{o}C. Using the EA, the samples for sulfur were separately pyrolyzed at 1050^{o}C using a combination oxidation and reduction furnace system. The resulting gases are dried in a water trap ($MgClO_4$) and separated in a packed column gas chromatograph before flowing into the source of the mass spectrometer. The ratio of heavy to light isotope (e.g. $^{13}C/^{12}C$) in each sample is measured with respect to a reference peak of carbon dioxide, nitrogen or sulfur dioxide gases which have been calibrated against NBS 22, atmospheric N_2 and NBS 127, respectively. The stable isotopic ratio is reported as in Equation 1-1, using the following abundance ratios of the heavy to light isotopes: $^{13}C/^{12}C$, $^{15}N/^{14}N$ or $^{34}S/^{32}S$. The standard for carbon is the Peedee Belemnite limestone (PDB), for nitrogen the standard is atmospheric N_2 (Air) and for sulfur the standard is the Canyon Diablo Troilite (CDT) which are assigned values of 0.0‰ for $\delta^{13}C$, $\delta^{15}N$, and $\delta^{34}S$. For sulfur and carbon the isotope value is corrected for contribution from ^{18}O content. This correction involves multiplying by 1.09 for sulfur (Giesemann *et al*., 1994) after adjusting the value to an internal standard ($BaSO_4$). The reproducibility of the measurement is typically better than ±0.2‰ for these elements using the continuous flow interface on the OPTIMA. Sample aliquots ranged from 4-10 mg for plants and 40-80 mg for soils, depending on N and S concentrations.

In addition to $\delta^{13}C$, $\delta^{15}N$ and $\delta^{34}S$, soil grain size and water content were determined. Water content was calculated from pre and post weighing of about 50 wet grams of soil during the cryogenic vacuum distillation procedure described below. Discrete sampling for gravimetric soil moisture was also performed from August to December 2007 at various depths. Grain size was determined on composite dune, riverbed and gravel plains soils using a laser diffraction particle size analyzer (Beckman Coulter CS I3 320).

Soil and plant water was extracted by cryogenic vacuum distillation (West *et al*., 2006), and the extracted water analyzed for $\delta^{2}H$ and $\delta^{18}O$ as described below. In this procedure, sample vials are connected to an isolated vacuum loop with Swagelok Ultra-torr fittings. After freezing the sample with liquid nitrogen and evacuating the vacuum loop, the sample is heated while cooling the collection tube with liquid nitrogen until no additional vapor evolves, and the collection tube is sealed with a blow torch or immediately transferred to a glass autosampler vial. The vacuum in each closed sample loop is also recorded immediately after completing the distillation, allowing for the identification of any obvious significant residual gases. The scale of the vacuum gauge (Varian 801) is somewhat arbitrary, but typical values from before and after a distillation were 0.01 and 0.03 Torr, respectively.

Although stem water can give an authentic isotope signature of the source water (White *et al*., 1985) if at least 98% of the water is extracted (West *et al*., 2006), water involved in transpiration will become enriched along an evaporation line (Aravena *et al*., 1989; Shu *et al*., 2005; Twining *et al*., 2006). Leaf water involved in photosynthesis exchanges with xylem water in leaves and small branches, enriching the extracted branch water relative to the water source (Shu *et al*., 2008). In eastern Namibia, evaporation lines have been used to calculate the original water source for infiltrating soil water using Equation 2-3 (Kuells, 2000). Here, branch and leaf samples taken under similar moisture conditions at different times of the day (ie different transpiration rates) will be used to calculate evaporation lines for source water determination. The corresponding δ^2H and $\delta^{18}O$ values that fall on the meteoric water line will be calculated using Equation 2-3 for individual samples and this value will then be used to calculate the “Fog Contribution” from a linear interpolation between average groundwater and average fog, winter rainfall and dew (Equation 2-4).

$$\delta^{18}O_c = \frac{\delta^2 H_m - s_m \times \delta^{18}O_m - d_g}{s_g - s_m} \qquad \text{(Equation 2-3)}$$

with,
$\delta^{18}O_c$ = isotope value "corrected" to fall on the meteoric water line
d = intercept of the δ^2H vs. δ^{18}O relationship
s = slope of the δ^2H vs. δ^{18}O relationship
subscript m = measured
subscript g = meteoric water line

$$F_f = \frac{\delta^{18}O_c - \delta^{18}O_w}{\delta^{18}O_f - \delta^{18}O_w} \times 100 \qquad \text{(Equation 2-4)}$$

with,
F_f = contribution of water from fog, winter rainfall and dew
$\delta^{18}O_w$ = average isotope value of groundwater
$\delta^{18}O_f$ = average isotope value of fog, winter rainfall and dew

2.7 Analysis – water samples

Extracted plant and soil water as well as fog, rain, and groundwater were sent to an external laboratory for measurement of δ^2H and δ^{18}O (University of Minnesota). These analyses were performed using Laser-Absorption Spectroscopy (LAS). This method is comparable in precision and accuracy to the traditional Isotope Ratio Mass Spectrometry (Wang *et al.*, 2009) and can be performed with very little volume of sample (< 50 μL), which was important for some of the plant and soil samples in this study. Dissolved sulfates in water samples were analyzed by IRMS at the University of Virginia (OPTIMA as described below for aerosol samples) after precipitation as $BaSO_4$ by adding a solution saturated with respect to $BaCl_2$, and subsequent filtration of the precipitate onto Whatman No. 1 Cellulose filters in the field.

2.8 Analysis – aerosols

Sulfur isotope values ($\delta^{34}S$) were determined using Isotope Ratio Mass Spectrometry (VG/Elementar Optima) on slotted, pre-ashed glass fiber filters. Immediately following collection, glass fiber filters were folded in half to protect the collection surfaces, enclosed in pre-ashed aluminum foil, and kept frozen until analysis. The collection surface of each impaction stage comprised 10 strips of filter separated by slots. The mass loading on each strip was not determined, but they were visually similar. One day prior to analysis, a scalpel was used to scrape the sample from a representative selection of 3 to 7 strips. The scrapings (10-20 mg of GF plus sample) were placed into a tin capsule. Even on heavily-loaded filters, the sample was concentrated along a thin line in the center (Figure 2-3).

Figure 2-3: Example glass fiber filter showing 3 strips scraped for analysis and 2 strips untouched.

The glass fiber filter samples contained very low levels of S, requiring correspondingly low-level standards and detailed post-processing of the data. This data processing involved three steps after allowing the software (GV Instruments, 1995) to find the sample and reference peaks. First, the peak zero lines were adjusted to include as much of the sample peak as possible. Second, the peak definitions were adjusted for consistency among samples and standards. And third, the sensitivity of the isotope ratio to changes in peak definition was checked and categorized. The peak end was changed by 50 to 100 s, and if the δ^{34}S changed by 1 to 5 ‰, the sample was assigned a large error bar (+/- 2 ‰); a 5 to 10 ‰ change was flagged as "Trace" and anything greater was flagged as "Non-detect."

In addition to δ^{34}S, elemental abundances of S, C and N were determined from δ^{34}S runs. S mass was determined through a calibration with mass 32 peak areas (Figure 2-4). And C and N masses were determined through TCD peak area calibration, although there is less separation between C and N peaks than during a typical C/N run with lower pressure on the He carrier gas. Given that there is a limited amount of sample for each aerosol filter, any C and N data available from a single δ^{34}S run is useful. Orchard Leaves (NBS 1571) were used as a standard for C and N elemental composition, giving a consistent calibration for November and December 2009.

$$N_{aliquot} = 34.6 * (A_{TCD} - A_{TCD,\,zero}) \qquad (2\text{-}5)$$
$$C_{aliquot} = 8.06 * (A_{TCD} - A_{TCD,\,zero}) \qquad (2\text{-}6)$$

with,
$N_{aliquot}$ and $C_{aliquot}$ in µg
A_{TCD} as the area of the identified TCD peak
$A_{TCD,zero}$ as the area of the TCD peak below the baseline

Elemental abundances of 45.6% and 2.71% were use for C and N, respectively, in Orchard Leaves (NBS 1571). Limits of detection were estimated by evaluating the variability in Orchard Leaves, which became quite high (+/- 50%) for masses lower than 10 µg for C and 2 µg for N. Field and laboratory blanks yielded values around 2 µg for both C and N. This blank mass was subtracted from the calculated values from Equations (2-5) and (2-6). If the original calculated mass was less than 10 µg for C and or 2 µg for N, the value was flagged as "Trace". If no TCD peak was found, the sample was flagged as "Non-detect". Finally, for many of the aerosol filters, only a portion of the full sample was analyzed as described above. The results for these aliquots were scaled up to the full sample size to give an estimate of the total C and N mass collected for each sampling period. Given this procedure and the low abundance of C and N in most of the aerosol samples, uncertainty is fairly high (+/- 10%), which is confirmed by two replicates taken through all sample preparation steps separately.

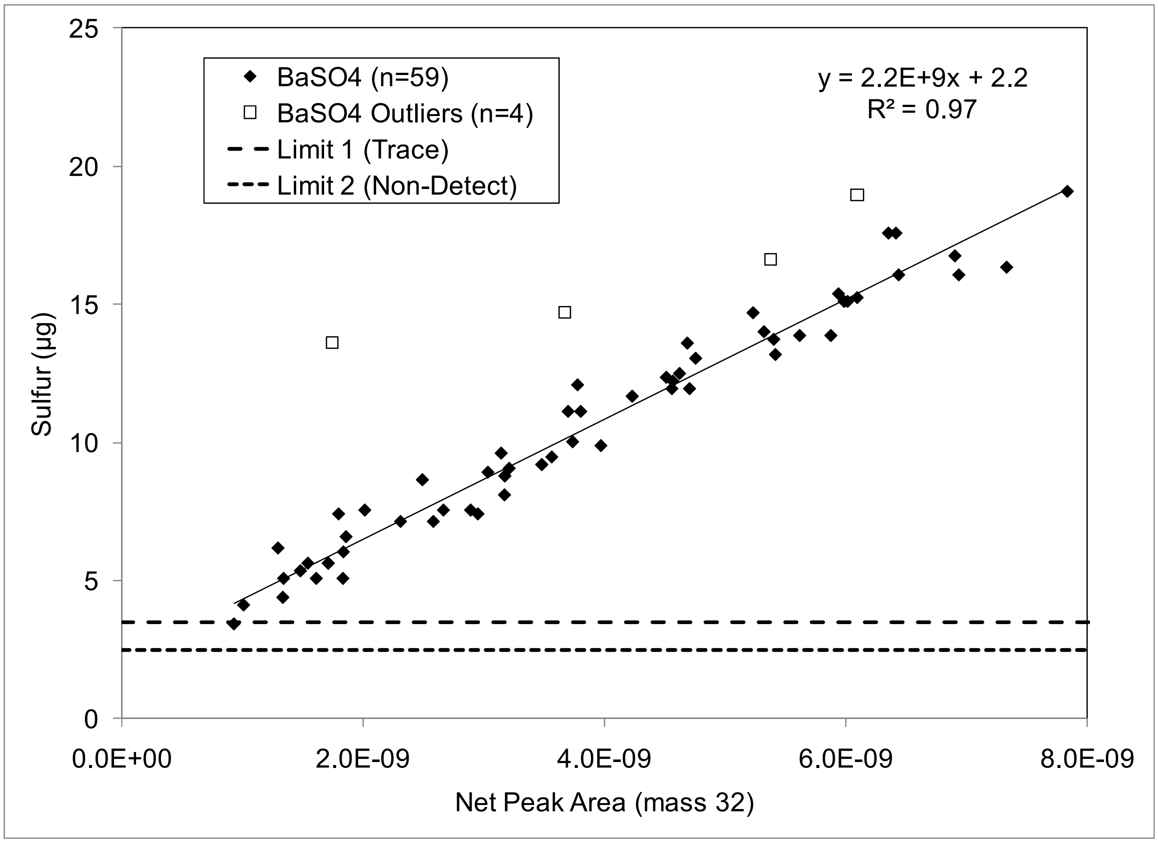

Figure 2-4: Sulfur abundance calibration.

References

Aravena, R., Suzuki, O., Pollastri, A., 1989. Coastal Fog and Its Relation to Groundwater in the Iv-Region of Northern Chile. Chemical Geology 79, 83-91.

Duchon, C.E., O'Malley, M.S., 1999. Estimating cloud type from pyranometer observations. Journal of Applied Meteorology 38, 132-141.

Eckardt, F., 1996. The distribution and origin of gypsum in the Central Namib Desert, Namibia. University of Oxford, Oxford.

Fischer, D.T., Still, C., 2007. Evaluating patterns of fog water deposition and isotopic composition on the California Channel Islands. Water Resources Research 43, W04420.

Gee, G.W., Campbell, M.D., Campbell, G.S., Campbell, J.H., 1992. Rapid mearurement of low soil-water potential using a water activity meter. Soil Science Society of America Journal 56, 1068-1070.

Giannini, A., Biasutti, M., Held, I.M., Sobel, A.H., 2008. A global perspective on African climate. Climatic Change 90, 359-383.

Giesemann, A., Jager, H.J., Norman, A.L., Krouse, H.P., Brand, W.A., 1994. Online sulfur isotope determination using an elemental analyzer coupled to a mass spectrometer. Analytical Chemistry 66, 2816-2819.

GV Instruments, 1995. Optima EA 1.4. Manchester, UK.

Henschel, J.R., Seely, M.K., 2008. Ecophysiology of atmospheric moisture in the Namib Desert. Atmospheric Research 87, 362-368.

Hulme, M., Doherty, R., Ngara, T., New, M., Lister, D., 2001. African climate change: 1900-2100. Climate Research 17, 145-168.

Intergovernmental Panel on Climate Change (Ed.), 2007. Climate change 2007 : The Physical Science Basis. IPCC Secretariat, Geneva.

Kuells, C., 2000. Groundwater of the North-Western Kalahari, Namibia: Estimation of Recharge and Quantification of the Flow Systems. Julius-Maximilian University of Würzburg, Würzburg, Germany.

Lancaster, J., Lancaster, N., Seely, M.K., 1984. Climate of the central Namib Desert. Madoqua 14, 5-61.

Sandvig, R.M., Phillips, F.M., 2006. Ecohydrological controls on soil moisture fluxes in arid to semiarid vadose zones. Water Resources Research 42, W08422.

Schemenauer, R.S., Cereceda, P., 1994. A proposed standard fog collector for use in high-elevation regions. Journal of Applied Meteorology 33, 1313-1322.

Schmitz, A.U., 2004. Transmission losses and soil moisture dynamics in the alluvial fill of the Kuiseb river, Namibia. Albert-Ludwigs-Universität Freiburg i. Br., Freiburg i. Br.

Shu, Y., Feng, X.H., Gazis, C., Anderson, D., Faiia, A.M., Tang, K.L., Etti, G.J., 2005. Relative humidity recorded in tree rings: A study along a precipitation gradient in the Olympic Mountains, Washington, USA. Geochimica Et Cosmochimica Acta 69, 791-799.

Shu, Y., Feng, X.H., Posmentier, E.S., Sonder, L.J., Faiia, A.M., Yakir, D., 2008. Isotopic studies of leaf water. Part 1: A physically based two-dimensional model for pine needles. Geochimica Et Cosmochimica Acta 72, 5175-5188.

Sioutas, C., 2004. Development of New Generation Personal Monitors for Fine Particulate Matter (PM) and its Metal Content. Research Report. NUATRC.

Thomas, D.S.G., Knight, M., Wiggs, G.F.S., 2005. Remobilization of southern African desert dune systems by twenty-first century global warming. Nature 435, 1218-1221.

Tisch Environmental Inc., 2004. Series 230 High Volume Cascade Impactors Multi-Stage Particulate Size Fractionator: Operations Manual. Village of Cleves, OH.

Turekian, V.C., Macko, S.A., Keene, W.C., 2001. Application of stable sulfur isotopes to differentiate sources of size-resolved particulate sulfate in polluted marine air at Bermuda during spring. Geophysical Research Letters 28, 1491-1494.

Twining, J., Stone, D., Tadros, C., Henderson-Sellers, A., Williams, A., 2006. Moisture Isotopes in the Biosphere and Atmosphere (MIBA) in Australia: A priori estimates and preliminary observations of stable water isotopes in soil, plant and vapour for the Tumbarumba Field Campaign. Global and Planetary Change 51, 59-72.

Wang, L.X., Caylor, K.K., Dragoni, D., 2009. On the calibration of continuous, high-precision delta O-18 and delta H-2 measurements using an off-axis integrated cavity output spectrometer. Rapid Communications in Mass Spectrometry 23, 530-536.

West, A.G., Partrickson, S.J., Ehleringer, J.R., 2006. Water extraction times for plant and soil materials used in stable isotope analysis. Rapid Communications in Mass Spectrometry 20, 1317-1321.

White, J.W.C., Cook, E.R., Lawrence, J.R., Broecker, W.S., 1985. The D/H ratios of sap in trees: Implications for water sources and tree ring D/H ratios. Geochimica Et Cosmochimica Acta 49, 237-246.

Chapter 3 : Precipitation, soil moisture and climate change in the Namib Desert

Abstract

Frequent fog events apparently play a major role in the ecophysiology of certain organisms in the hyperarid Namib Desert ecosystem. This study estimates the deposition of fog, dew and rainfall for 2007-2009 using various measurement techniques. Leaf wetness sensors were used to estimate both duration of wetness and amount of deposited water. Using ground-based observations to distinguish between fog and dew events, it is revealed that these two moisture sources are of the same order of magnitude in terms of annual hours of wetness (522 and 1172 hours, respectively) and precipitation depth (4.7 and 12.3 mm). These values are comparable to rainfall in this wet year (July 2008 to June 2009) in which rain events accounted for 233 hours of wetness and 57 mm of precipitation. Soil moisture is also reported, indicating no substantial contribution from fog or dew to soil moisture below the top 3 cm, and this wetted surface layer dries in a few hours after a fog or dew event. Lastly, arid areas of the world are generally predicted to become drier under the influence of climate change, and thus produce more dust. However, the Namib "fog desert" is potentially less affected by decreased rainfall. Current predictions for changes to relative humidity in the Namib are evaluated using 30-year monthly averages for two climate models, showing 0 and 1.5-3% decline in relative humidity over the coming century. To look at the potential impact of these findings on

fog deposition, a scaling-up of ground-based observations of fog occurrence is attempted through a correlation with relative humidity.

3.1 Introduction

The Namib Desert on the southwestern coast of Africa is hyperarid in terms of rainfall, but receives frequent coastal fog events that are thought to play a major role in the Namib ecosystem. Fog in the Namib most commonly occurs through advection of a low stratus cloud that forms over the cool Benguela Current that upwells along west coasts of South Africa, Namibia and southern Angola. When advected inland, this cloud intersects the land at elevations of 100-500 mamsl, which translates to 10-60km from the coast (Figure 1-2). Occasionally very low elevation fog occurs within 10 km of the coast. Radiation fog, which occurs much less frequently, results from warm moist air cooling rapidly at night in low-lying areas. Winter frontal systems from the southwest infrequntly bring light drizzle. Total rain accumulations range between 20 and 80mm/yr, increasing to the east. Fog deposition, although highly dependent on by the collection method, has been measured at 20-180 mm/yr within 60 km of the coast (Lancaster *et al*., 1984; Henschel *et al*., 1998; Hachfeld and Jurgens, 2000; Shanyengana *et al*., 2002). A simplified version of these patterns gives a sense of the overall atmospheric moisture regime active in the Namib, and the annual rainfall totals experienced during the present study describe the typically dramatic interannual variability in rainfall (Figure 1-2).

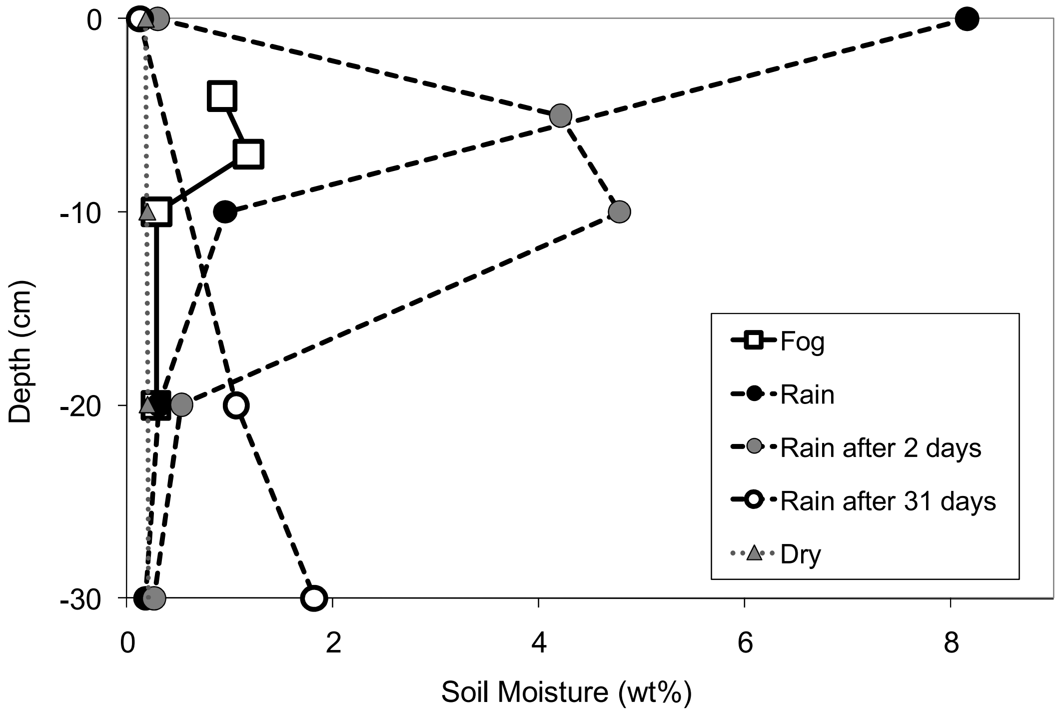

Figure 3-1: Soil moisture for fog and rain events on a Namib dune (after Gut (1988).

Fog and dew in ecosystems

In certain ecosystems fog and dew can be important stable water sources even though individual fog and dew events are low in terms of the amount of water delivered to a soil or plant surface (Weathers, 1999). The redwoods of California experience seasonal fog, and obtain up to 34% of their transpired water from fog. Most of the utilized fog water is from water that drips onto the soil and is taken up by roots of redwoods and undergrowth (Dawson, 1998), but about 6% of the transpired water may come from foliar absorption (Burgess and Dawson, 2004). This fog input to redwoods is lower in magnitude on an annual basis than water from the winter rains, but fog occurs in the summer which is when transpiration demand is highest. Thus, without fog the redwood water balance would be impacted more than is indicated by the annual fog uptake (Dawson, 1998). Fog occurrence in the redwoods has decreased 33% since the early 1900's due to warming of the sea surface and atmosphere (Johnstone and Dawson, 2010). Fog is also a controlling factor in moist tropical forest ecosystems such as in Monteverde, Costa Rica, where changes in species composition ecosystem productivity are expected due to effects on cloud height from changing global temperatures (Foster, 2001).

In areas that receive frequent fog the utilization of fog water by plants is somewhat expected, whereas the contribution of fog to subsurface water is more difficult to envision. Typically, fog deposited on soil is quickly evaporated after the fog lifts (Louw and Seely, 1982). However, significant infiltration of fog has been shown to occur in areas where fog is deposited with high frequency. For example, in broad-leaved forests of coastal Oman, seasonal dense fog helps contribute to stemflow, which was found to be 30 % of total precipitation (Hildebrandt *et al*., 2007) – quite high compared to the typical estimate of <10 % in arid lands (MartinezMeza and Whitford, 1996). This, along with the reduction in transpiration during the summer months leads to a doubling of the growing season relative to surrounding desert or deforested land (Hildebrandt *et al*., 2007). In another study, fog drip occurring in mountains of northern Kenya was found to contribute isotopically to the groundwater of a neighboring valley. The study was not long enough for the authors to calculate a percentage contribution from fog (Ingraham and Matthews, 1988), but it appears to be on the order of 30%.

Hydrologic input from fog is not limited to forest systems -- significant contribution (about 50%) from fog to deep drainage was found for a grassland in New

Zealand (Ingraham and Mark, 2000). The Atacama Desert in Chile, a climatological analog of the Namib, has been studied extensively for fog water harvesting (Schemenauer and Cereceda, 1991) and nutrient cycling (Weathers *et al*., 2000; Rech *et al*., 2003). Recent studies have found significant use of fog and dew by biological crusts in the Atacama (Warren-Rhodes *et al*., 2006), but comparisons with fog and groundwater have found no connection (Aravena *et al*., 1989; Squeo *et al*., 2006).

Fog and climate change

Predictions of extensive drying in southern Africa over the next 50 years (Hulme *et al*., 2001; Thomas *et al*., 2005; Giannini *et al*., 2008) (Thomas *et al*., 2005) raise the question of how climate change will affect the Namib "fog desert". From studies of cloud forests, where the mechanism of water delivery is the same as with fog, the cloud base height is expected to increase with rising atmospheric temperatures, essentially removing this water source from plants at lower elevations (Still *et al*., 1999; Foster, 2001). If a similar increase in cloud base height were to occur in the hyper-arid Namib, the impact on perennial vegetation and associated fauna could be significant.The present study looks at the temperature and humidity predictions for the Namib as a first step towards assessing the potential impacts on fog deposition in these ecosystems.

The Namib has an extremely stable atmosphere driven by (1) the cold Benguela current offshore, and (2) its position in the descending limb of the Hadley cell, which combine to dampen any atmospheric convection. This system, along with the continental rain shadow, has led to arid or hyperarid conditions since at least the mid-Miocene. The cold Benguela current is a highly productive upwelling that follows the southwestern coast of Africa, and has been established for millions of years (Siesser, 1980). Although it is not clear how the scarce water resources of the region will be affected by the predicted climate change scenarios, the fact that the overall stability and fog occurrence is driven partly by ocean currents could indicate a de-coupling of the Namib from the overall drying across southern Africa. However, increased air temperature will increase the saturation vapor pressure at a given specific humidity level. Thus, climate warming could have the effect of decreasing the frequency of condensation events at a given altitude, thereby reducing the supply of atmospheric water in the form of dew or canopy condensation. This study combines ground-based observations of fog occurrence, deposition amounts, leaf wetness, temperature and relative humidity in the Central Namib Desert with climate model predictions of temperature and specific humidity. Relationships between humidity and fog occurrence are obtained, which can be used for a qualitative prediction of the occurrence of fog under various climate scenarios.

3.2 Methods

Fog observation and monitoring

Fog and dew deposition amounts are manually measured daily at Gobabeb, and long-term observation efforts have been conducted since the 1960's at stations across the Namib with the data available at Gobabeb (Lancaster *et al.*, 1984; Henschel and Seely, 2008). The present study adds discrete, event-scale fog deposition and soil moisture measurements as well as continuous measurements of leaf wetness, soil moisture, air temperature, and relative humidity. Soil moisture data presented here includes: (1) gravimetric (drying at 70 ºC), (2) sequential weighing of a soil-filled plastic container in the field (Mettler BD202, 0.01g accuracy), and (3) continuous monitoring at a depth of 5-10 cm using dielectric probes (5TE and MPS-1 sensors, Decagon Devices, Inc.).

Leaf Wetness Sensors (LWS; Decagon Devices, Inc.) record a decrease in resistivity across a coated grid of wires when the surface is wetted, giving a duration of wetness. Although an LWS typically gives a binary “wet” or “dry” response for a given time period based on a threshold electrical resistance value, the raw data allows for some quantification of the amount of water deposited. This quantification was performed using a separate calibration for each LWS following the results of testing by the manufacturer (Decagon Devices, Inc. unpublished data 1999). Calibrations were performed in the laboratory by spraying a sensor with water and recording changes in weight and the corresponding sensor readings as the water evaporated. Correlation coefficients of the calibration curves averaged 0.90 (r^2) and ranged from 0.83 to 0.96 for the seven LWS’s investigated. The raw response of an LWS varied between around 100 and 1000 (unspecified units), with a stable “dry” signal between 430 and 450. Response above 450 indicates wetness. Values below 430 and equal to 1023 were indicators of poor sensor response. From field observations, the very low values could be due to the sensor touching the sand surface or plant material. And, the very high value of 1023 seems to correspond to times when a crust formed on the upper side of the sensor – possibly due to jackal or fox urine based on animal tracks nearby. Much of the data surrounding these high and low response events had to be discarded due to irregular response patterns. After this manual data quality check, “wet” events were identified as periods with a response greater than 450 which persisted for more than 1 hr, ending with the response staying below 450 for at least 1 hr. Each event was then categorized as rain, fog or dew through an objective comparison with both manual and continuous weather monitoring data at Gobabeb. The event was labeled as rain if rain was collected at Gobabeb; fog if (1) fog was noted through manual observations, (2) if a fog sample was collected, (3) if there were very low clouds observed at 8am; and the remaining events were considered to be dew.

After converting the raw values to volume per area (ml/m^2) using separate calibrations for each sensor, the amount of water deposited was calculated as the sum of positive increments in the volume of water deposited. That is, if the volume per area increased from one 5-min average value to the next, this increment was interpreted as an addition of water to the surface of the sensor. An alternative interpretation would be to take the maximum value per event as the total amount deposited. However, the incremental procedure used allows for a more realistic description of wetting and drying of the sensor during a fog or dew event. There is minimal noise in the 5-min averaged data, but this aspect should be examined before applying the procedure elsewhere. It is possible that additional noise in, for example, 1-min averaged data would add an artificial amount of water to the total due to minor variations in the sensor response. Any such higher-frequency variations appear to be averaged out in the 5-min data.

Climate model data

The Global Climate Model (GCM) data evaluated here comprises monthly averages for the 30-year composite summary data from the most recent work of the Intergovernmental Panel on Climate Change (IPCC, 2007). Two model outputs for the emissions scenario “SRESA1B” are evaluated. The models are MIROC 3.2 High-Resolution (“MIHR”; 0.28 x 0.19 degree resolution; 160x320 global grid) and BCM Version 2 (“BCM2”; 1.5 x 1.0 degree resolution; 64x128 global grid). The data are freely available from The IPCC Data Distribution Centre (http://www.ipcc-data.org). The SRESA1B emissions scenario is described this way: “In this world, people pursue personal wealth rather than environmental quality” (IPCC, 2007). This scenario was selected for this first order evaluation in order to get a somewhat “worst case” view of relative humidity changes in the Namib.

The ideal evaluation of GCM data for evidence of changes to fog frequency in the Namib would be to have high temporal (3hr) and spatial (<0.5 degree) resolution. Unfortunately, no humidity data is available at the 3hr temporal resolution. The spatial resolution is available in several models including MIHR, and this will be compared with the lower spatial resolution BCM2 model. To gain a first-order understanding of the predictions for relative humidity in the Namib, 30-year composite data are compiled for one pixel from BCM2 and two corresponding pixels from MIHR that cover the areas around Walvis Bay and Conception Bay to the south. The variables include air temperature, specific humidity, and atmospheric pressure, and they are combined via Equations (2-1) and (2-2) to generate the relative humidity values presented.

3.3 Results

Rain, fog and dew deposition

During the three years of sampling, rainfall varied considerably from a relatively dry year in 2007 to wet years in 2008 and 2009 (Figure 1-2). In fact, March 2008 saw unprecedented extreme rainfall and wind storms, with an estimated 14 mm in the first 30 minutes of storm activity leading to a total of around 81 mm for the month. Prior to the first plant and soil sampling in October 2007, just 13.5 mm of rain fell in the previous 16 months (1 mm May 2006, 7 mm October 2006, 5.5 mm March 2007). Rainfall exhibited typical seasonality, with the main storms occurring in the austral summer months. However, 2.3 mm and 1.8 mm did fall between May and September in 2008 and 2009, respectively. The winter rainfall totals are potentially important here as a supplemental dry season water source and because they typically arise from the over the Atlantic Ocean, and thus have a similar isotopic signature to fog (see Chapter 4). No winter rainfall was observed in 2007, so comparing these samples to 2008/9 should reveal any major additional contribution from winter rainfall relative to fog.

Fog and dew, as estimated by LWS's from July 2008 to June 2009, exhibited much less seasonality than rainfall (Figure 3-2). Wetness events (n=242 on 200 days) were characterized as rain (n=30 on 18 days) or fog (n=69 on 65 days) based on manual and continuous observations at the Gobabeb weather station and the remaining events were labeled as dew (n=143 on 117 days). Interestingly, the volume of water deposited by dew events (12.3 mm) exceeded that of fog events (4.7 mm) for the 12 months evaluated by a factor of 2.6 (Figure 3-3). However, when a vertical structure such as an

X-harp collector is placed near a LWS, it receives about 7 times the amount of water per cross-sectional area than an LWS (Figure 3-4). In terms of surface wetness, events lasted around 8 hours with fog events slightly shorter than dew and rain events. Fog events occurred mostly at night, but contributed 23% of the annual hours of daylight wetness compared to 15% from rain events and 63% from dew.

Table 3-1: Rain, fog and dew totals (July 2008 to June 2009) from the Gobabeb weather station (for rain volume) and a Leaf Wetness Sensor placed near the sand surface on the westward-facing plinth of High Dune 2 km SW of Gobabeb.

Event (n)	Total (mm)	Average (mm)	Average Rate (mm/hr)	Total Wetness Exposure (L^*Hr/m^2)	Average Wetness Exposure (L^*Hr/m^2)	Average Hours of Wetness	Average Daylight Hours of Wetness	Annual Hours of Wetness	Annual Daylight Hours of Wetness	Contribution to Annual Daylight Wetness
Fog (69)	4.7	0.07	0.011	41	0.6	7.6	3.5	522	224	23%
Dew (143)	12.3	0.09	0.014	150	1.0	8.2	4.3	1172	618	63%
Rain (30)	57	1.9	0.245			7.8	4.8	233	144	15%
Total (242)	74	0.31	0.038			8.0	4.1	1927	986	

A comparable set of Leaf Wetness measurements is available for sensors placed at the bottom and top of High Dune (2 km SW of Gobabeb; data available July 1st-October 20th 2009) and in Welwitschia Wash (14 km east of Gobabeb; data available July 1st-September 10th, 2009). Paired daily Hours of Wetness show consistently longer durations of wetness at the top of High Dune (overall mean of 2 Hours of Wetness per day, 120 Hours of Wetness total 1 July to 10 September) than at the bottom of High Dune or in Welwitschia Wash (Figure 3-5), which saw similar duration of fog and dew events (0.51 and 0.54 Hours of Wetness per day, 39 and 40 Hours of Wetness total 1 July to 10 September). In fact, of 50 days with some fog or dew at the top of High Dune, 28 saw no wetness at the bottom of High Dune. This local elevation difference was observed in fog collection on High Dune and Swartbank Berg – both with about 80 m elevation difference between bottom and top sampling locations – where X-harp collectors at the top saw about 3 times the amount of collected deposition than collectors at the bottom. This finding is also consistent with the dominance of moisture being advected inland from the Atlantic Ocean. The advection would be expected to deposit more moisture at higher elevations where the stratus would tend to be thicker at a given distance from the coast. Radiation fog would lead to more moisture, or longer durations of wetting events, in lower lying areas, which may explain the one event that recorded more Hours of Wetness at the bottom of High Dune than at the top (Figure 3-5).

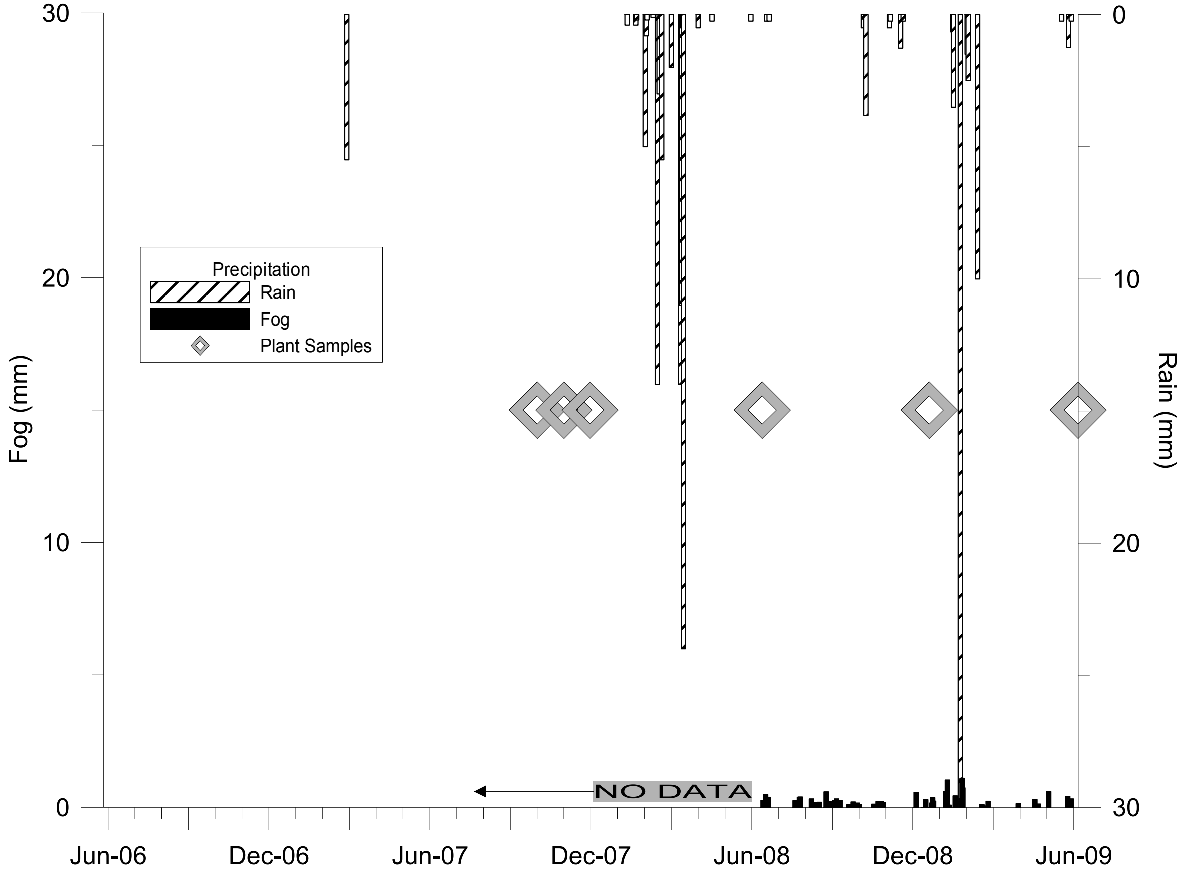

Figure 3-2: Daily rain and fog at Gobabeb (rain) and High Dune (fog).

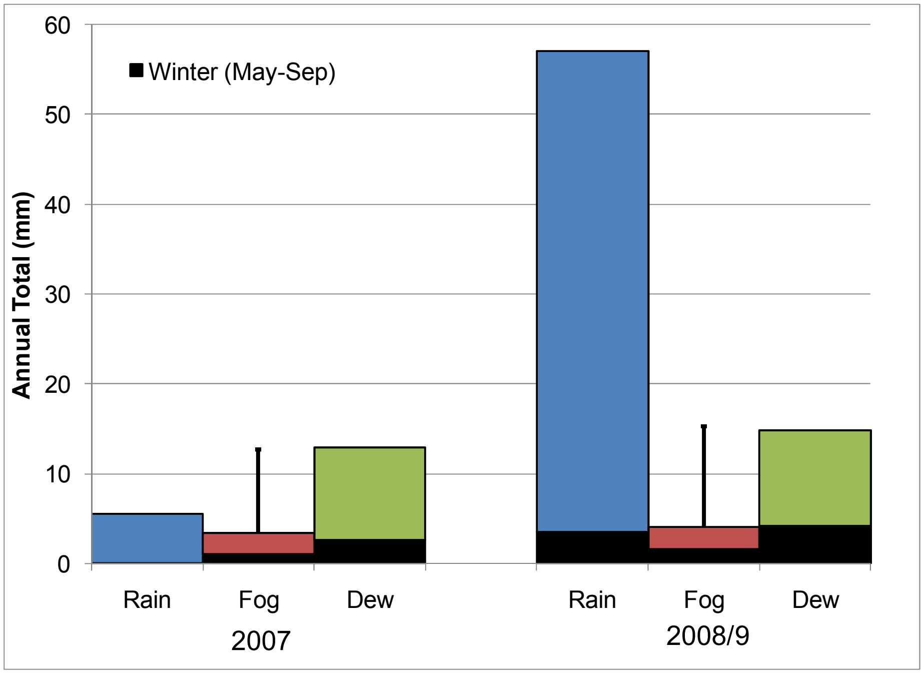

Figure 3-3: Rain, fog and dew totals for 2007 and the July 2008 to June 2009 study period.
Note: Black portions of the columns represent the deposition between May and September.

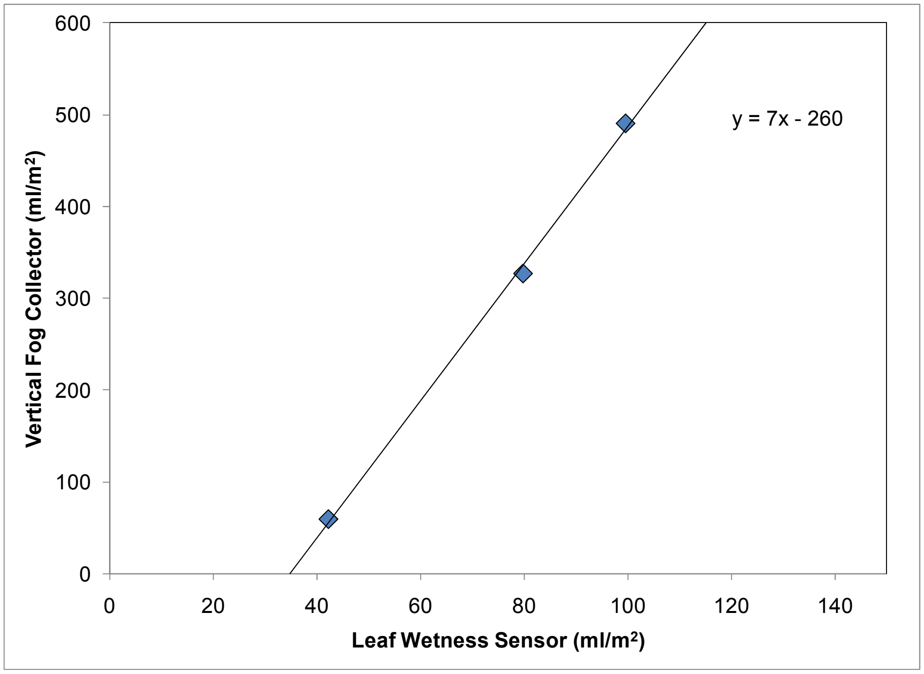

Figure 3-4: Volume of water deposited for three fog events on a vertical collector (X-harp) and a Leaf Wetness Sensor.

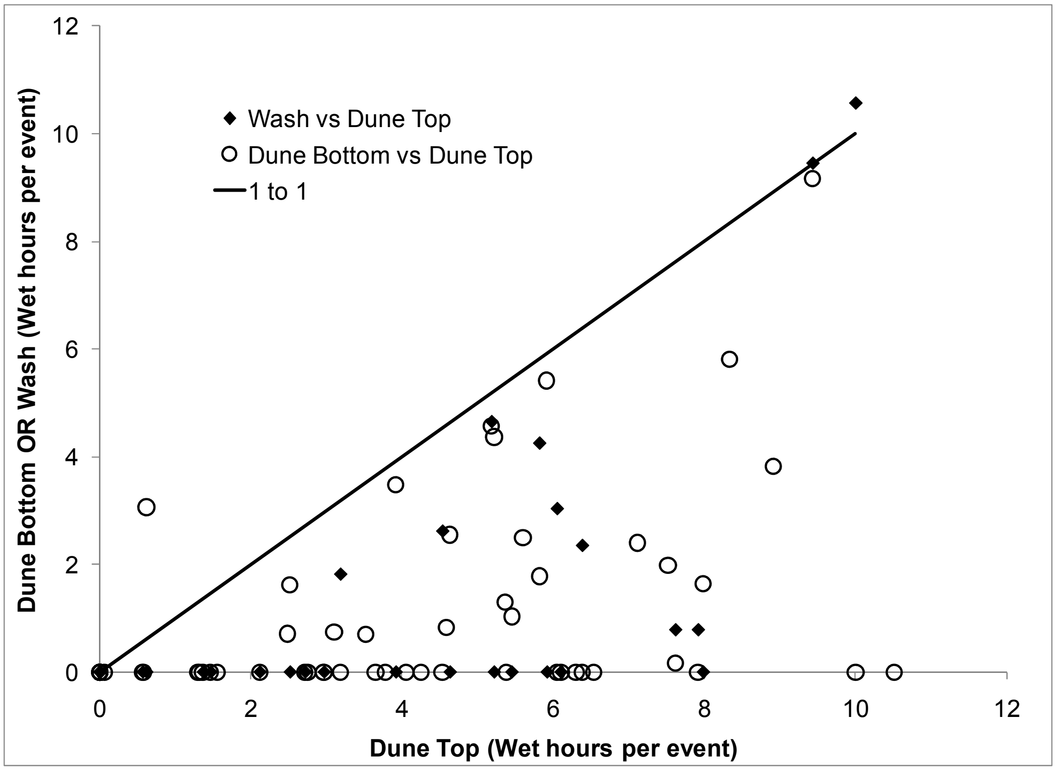

Figure 3-5: Daily hours of wetness at the top and bottom of Gobabeb High Dune as well as Welwitschia Wash.
Note: July to October 2009 for High Dune, July to September for Welwitschia Wash.

Soil moisture

Continuous monitoring data for soil moisture at Gobabeb and Welwitschia Wash (14 km east of Gobabeb) is currently available for July to October 2009, during which time no rain events were recorded. Volumetric soil moisture was relatively constant at each site, with the highest average daily value (0.06 m^3/m^3) near the top of High Dune at Gobabeb and lowest (0.03) at Welwitschia Wash (Figure 3-6). The soil water potential followed the same pattern, with daily mean values of -690, -850, and -960 kPa at Dune Top, Dune Bottom and Welwtischia Wash, respectively. However, soil water potential had greater variability -- Coefficient of Variation of 4-6% compared to 1.5-2.5% for volumetric soil moisture -- most likely due to temperature dependence of the dielectric measurement. The volumetric soil moisture is corrected for temperature dependence of the dielectric sensor automatically with soil temperature measured by a sensor in the same probe as the soil moisture (5TE, Decagon Devices, Inc.). Interestingly, soil moisture was highest at the top of high dune (Figure 3-6), where fog frequency and duration is highest: 120 hours of wetness compared to 39 and 40 hours at the bottom of high dune and Welwitschia Wash, respectively (July to mid-September 2009). However, there was no trend observed in volumetric soil moisture with the daily Hours of Wetness, indicating that fog and dew had no significant effect on the daily average soil moisture.

Gravimetric soil moisture in Namib soils was consistently about 0.2 to 0.3 wt% for soil that felt dry to the touch. In the top 1-3 cm of soil, this value increased by 0.05 wt% during a fog event in soil not covered by vegetation and 0.1 to 1.0 wt% in soils within a plant's drip zone. Soil moisture at 10 cm depth did not change during the fog event (Figure 3-8). Increases in soil moisture were about the same during fog and dew events, and four successive dew events showed a cumulative increase up to around 2.0 wt% despite significant drying during the day. For comparison with fog and dew deposition described above, each wetting event observed gravimetrically corresponded to about 50 to 250 ml/m^2 (Figure 3-9). These soil samples were subsampled and composited for a grain size analysis. Soils from all three habitats – Dune (n=13), Riverbed (n=6), Gravel Plains (n=5) – were dominated by sand: 100%, 96%, and 96% of the <2 mm fraction by volume, respectively. Minor amounts of silt (2 to 50 μm) and clay (<2 μm) were found in Riverbed (3.2% silt, 0.5% clay) and Gravel Plains (3.1% silt, 0.7% clay).

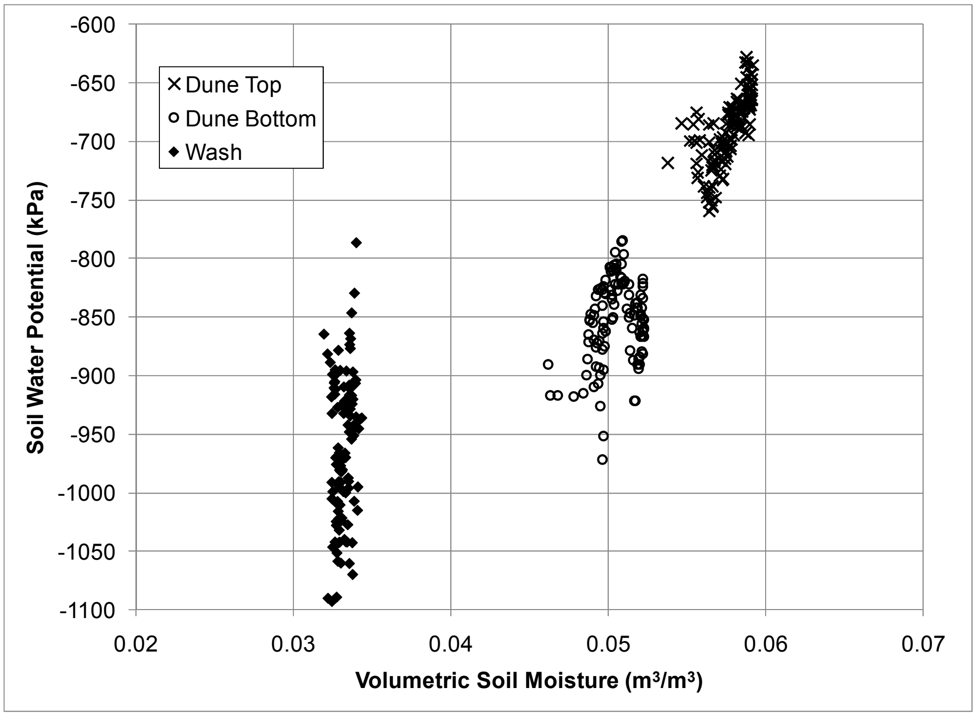

Figure 3-6: Soil moisture at the top and bottom of Gobabeb High Dune and in Welwitschia Wash. Note: Measurements taken July to October 2009 at 5-10 cm depth within the drip zone of common species in each location: *S. sabulicola* at Dune Top, *T. hereroensis* at Dune Bottom, *W. mirabilis* at Wash.

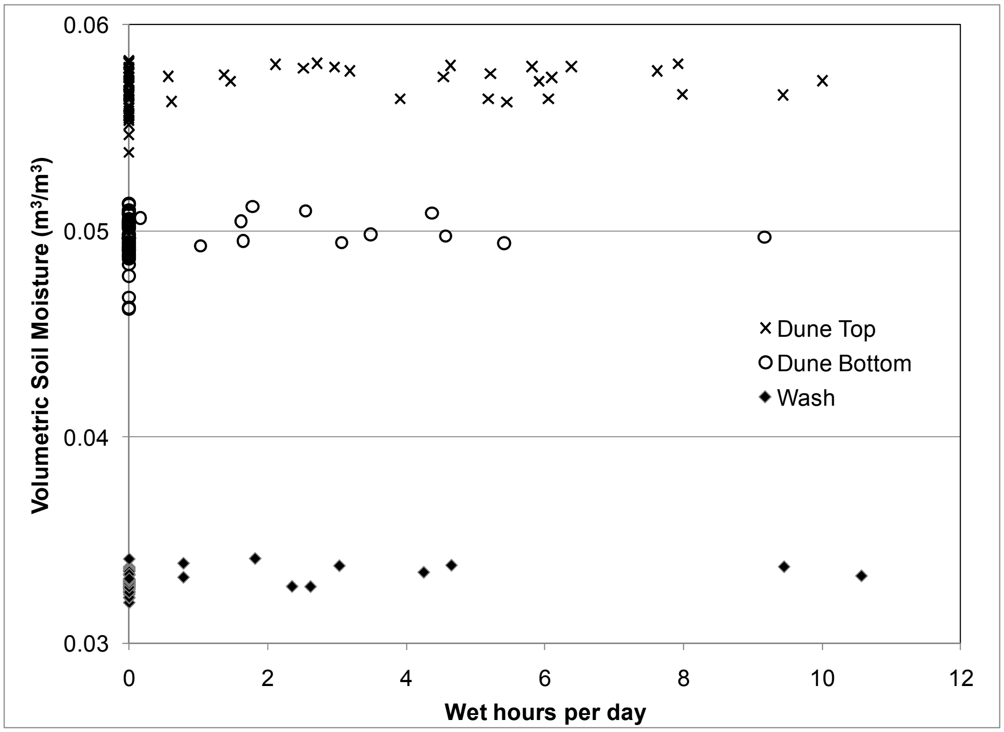

Figure 3-7: Soil moisture and hours of wetness at the top and bottom of Gobabeb High Dune and at Welwitschia Wash.

Note: Measurements taken July to September 2009. Soil moisture measurements as in Figure 3-6.

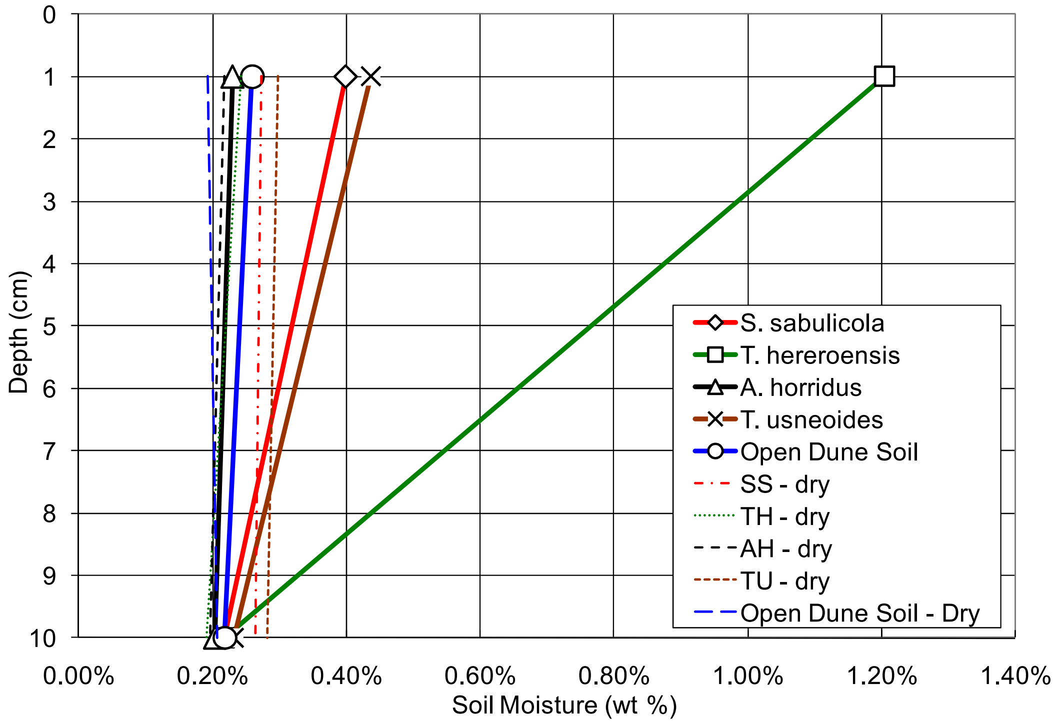

Figure 3-8: Soil moisture during (solid lines) and after (broken lines) a fog event at Gobabeb, 21 October 2007.

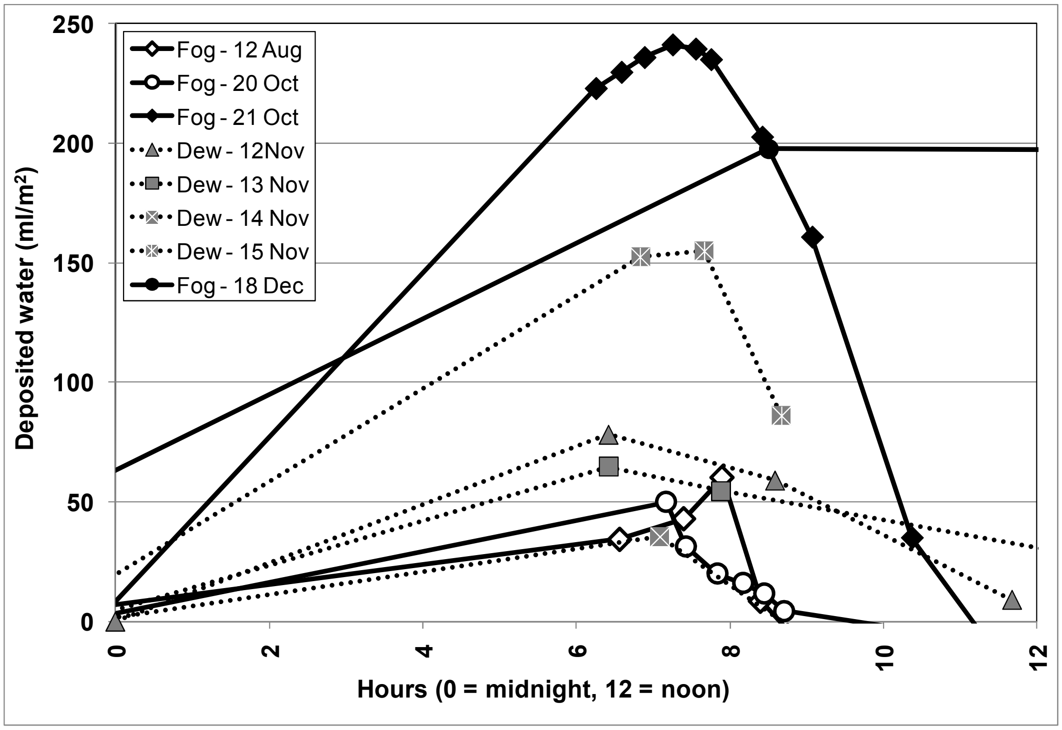

Figure 3-9: Deposition of water onto soil in the Gravel Plains at Gobabeb during several fog and dew events, August to December 2007.

Fog and relative humidity

For the period of July 2008 to June 2009, Leaf Wetness sensors along with direct observation indicate that there were 18 days with rain, 65 with fog, 117 with dew and 147 were dry (18 days with no data). Fog and rain days had an average RH of 61%, compared with 54% on days with dew and 41% on dry days. The RH at 8AM, when fog is typically still present during foggy days, was 88% for days with fog, 70% on rain days, 71% on dew days, and 53% on dry days. The relationship between daily and 8AM RH is significant ($R^2 = 0.8$), but exhibits a high degree of variability at the upper end, where fog events occur (Figure 3-10). The amount of fog or dew deposited during each event was weakly correlated ($R^2 = 0.25$ for dew, 0.06 for fog) with 8AM RH for events with RH > 90%, but did not show an overall correlation (Figure 3-11). This pattern suggests that a weak association exists between deposition amount and RH during a fog or dew event, but the association breaks down for events that ended before the RH reading was taken at 8AM.

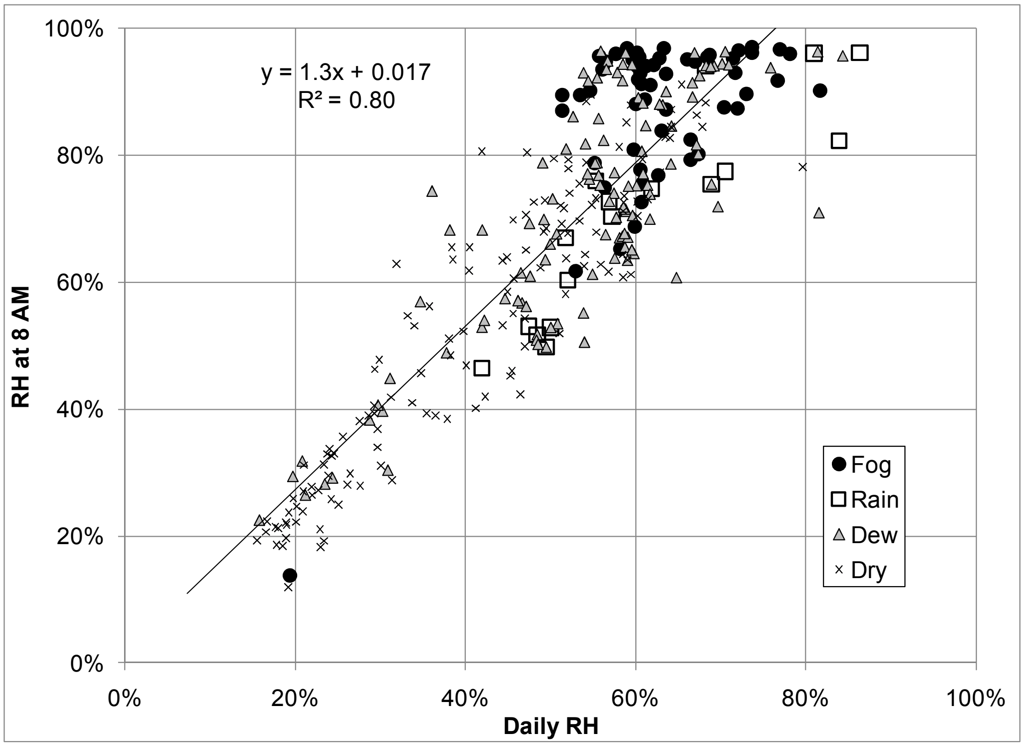

Figure 3-10: Relative humidity measured 30 cm above the sand surface at the western plinth of High Dune, 2km SW of Gobabeb (July 2008 to June 2009).

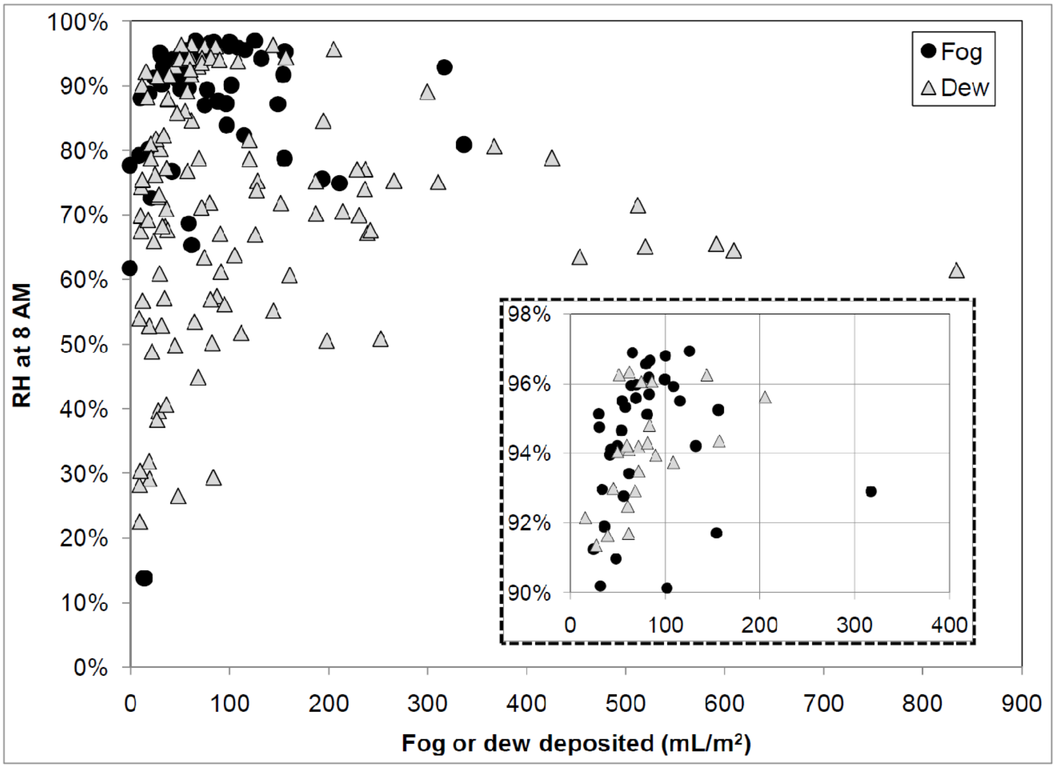

Figure 3-11: Relative humidity and deposition of fog and dew (July 2008 to June 2009).

Climate model data

For the 30-year composite data evaluated, there was a substantial difference between the two models. BCM2 showed very little variation in relative humidity from the control period (1961-1990) through all three future time periods (Figure 3-12). MIHR, in contrast, showed a decline of 1.5 to 3% in average annual relative humidity. The change is greater towards the south at Conception Bay, which is closer to the winter rainfall area in southern Namibia and western South Africa. Although this is still a small change, it warrants further investigation into the higher resolution regional downscaling data for the entire length of the Namib.

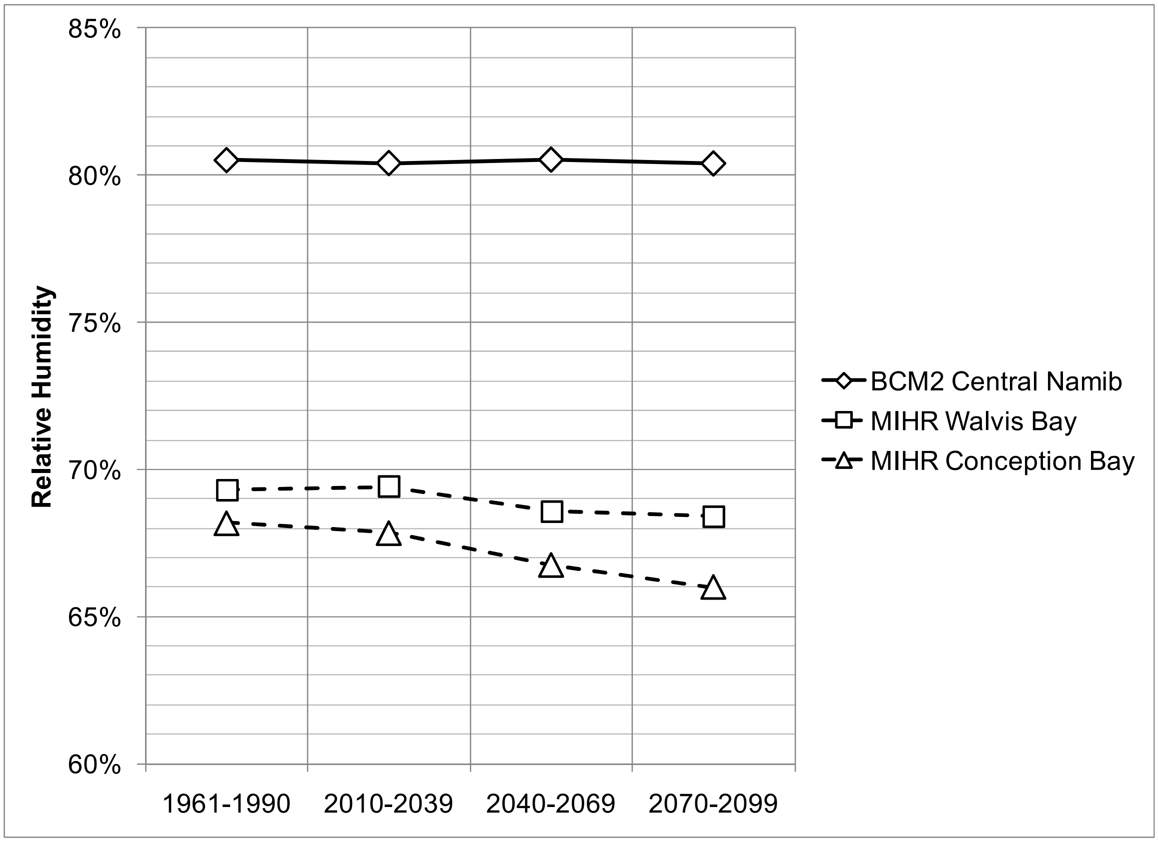

Figure 3-12: Global climate model 30-year composite relative humidity data for future and control periods.

3.4 Discussion

Rain, fog, dew and hours of wetness

Although the amount of fog deposited on plant surfaces is still highly uncertain, it is clear that dew is a significant contributor to the total non-rainfall moisture deposition in the Namib (Figure 3-3). The dew contribution more than doubles the total hours of wetness from about 750 hrs/year considering just fog and rain events to 1900 hrs/year. Many of these "dew" events may in fact be fog that was not observed due to data gaps and errors (Appendix C), but the distinction between fog and dew would not be significant for plants that absorb deposited water via leaves, like *T. hereroensis* (Seely *et al.*, 1977) given that the average fog and dew events deposited water at a similar rate (about 0.01 mm/hr) and lasted roughly the same amount of time (8 hrs). The concept of "Wetness Exposure" (with units of Volume*Time/Area) is introduced here (Table 3-1) as a way of integrating the deposition amounts over the duration of the wetting event. Wetness Exposure extends the traditional "Hours of Wetness" derived from LWS data, and could be an important variable for quantifying leaf water uptake. During the study period, average Wetness Exposure for each dew event (1.0 L*hr/m^2) was nearly double that of each fog event (0.6 L*hr/m^2), adding to the potential impact of dew on plants that take water up via their leaves.

The Atacama Desert provides an example of the potential importance of wetness duration. The Atacama is an analogous system to the Namib in terms of climatology, aridity, and the potential importance of fog as a water source (Walter and Breckle, 1986). A study of the occurrence of cyanobacteria identified the aridity gradient, defined by rainfall, as a controlling variable for the percentage of quartz rocks colonized by hypolithic cyanobacteria (Warren-Rhodes *et al*., 2006). In fact, if the duration of wetness is used to define the aridity gradient instead of rainfall totals, the relationship with colonization is striking, although a preliminary study near Gobabeb showed about twice the duration of wetness for the same level of colonization in the Atacama (Figure 3-13). This relationship is significant because hypolithic cyanobacteria simply need to be wetted in order to photosynthesize. Now, for vascular plants than can absorb water via wetted leaves or shallow roots, translocate it and store it for future use throughout a day or longer, the magnitude of the wetting event becomes a factor. This situation is where Wetness Exposure could become useful for describing moisture availability, and in turn for describing the occurrence of fog-dependent vascular plants.

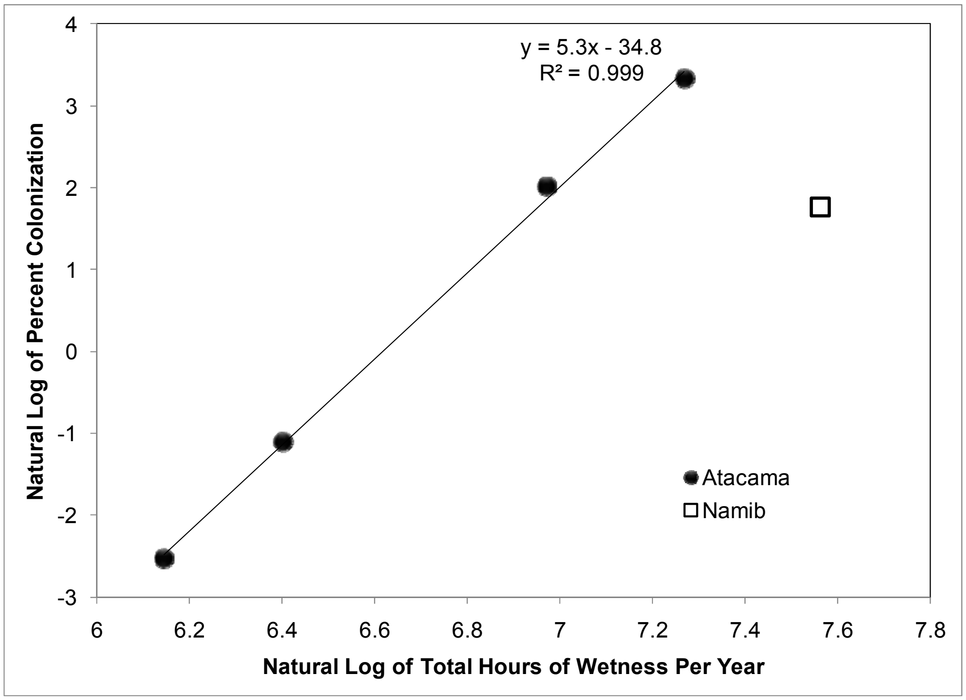

Figure 3-13: Hours of wetness (rain, fog and dew) and colonization of quartz stones by cyanobacteria in the Atacama Desert (after Warren-Rhodes *et al.* (2006) and Aiyambo (2007)).

Soil moisture

Surface soils can clearly be affected to the same degree during dew and fog events (Figure 3-9). Soils deeper than about 3 cm were not found to be affected by individual fog events based on continuous monitoring with dielectric probes. This type of probe may not be sensitive enough to pick up changes on this scale, and it is intriguing to note that the site with the most fog deposition had the highest 5-10 cm soil moisture (Figure 3-7). It should be noted that the three monitoring sites were within the drip zone of three different plants: *S. sabulicola* at the wettest site on High Dune, *T. hereroensis* at the drier base of High Dune, and *W. mirabilis* in the driest site, Welwitschia Wash. The same pattern between *S. sabulicola* and *T. hereroensis* was seen in the gravimetric soil moisture data as well (Figure 3-8). Extensive fog drip could account for the higher soil moisture in *S. sabulicola*, although vapor intrusion down to 5-10cm associated with the more frequent and longer wetting events experienced at the top of High Dune could also play a role. More sensitive probes should be tested in the soils for ongoing monitoring. The water potential probes (MPS-1, Decagon Devices, Inc.) appear to be more sensitive than the volumetric soil moisture probes (5TE, Decagon Devices, Inc.), but the 5TE probes have the advantage of native temperature correction. That is, the soil temperature is recorded in the same probe, so no post-processing has to be performed to correct for temperature dependence.

Fog, relative humidity and climate change

The most recent IPCC report suggests that the coast of Namibia will see at least 10% decline in rainfall (IPCC, 2007). Earlier models indicated a 0 to 20% decline in relative humidity, with the largest decreases in the summer months (Foster, 2001), which is consistent with the expected decline in rainfall. A large portion of the single grid cell evaluated here from the BCM2 model includes the entire fog zone over land and it also extends offshore. Regional downscaling efforts are designed to address these resolution issues (Jones *et al*., 2004) for determining locally important patterns, such as fog in the Namib. This effort is underway for southern Africa at the Climate Systems Analysis Group (CSAG) at the University of Cape Town, but the data have not been analyzed here.

If the climate predictions for RH are going to be useful in predicting changes in fog, there has to be a good relationship established between RH and fog occurrence. From the data presented here, daily RH values do not adequately separate foggy days from dry days. At least 3hr resolution data would be necessary, and a fog cutoff of about 90% RH seems appropriate based on the 8AM RH data (Figure 3-10). Other fog or cloud forest studies have suggested an 80% RH cutoff value, but this would include a large number of false positives. Ground-based fog monitoring from Leaf Wetness sensors and direct observation may provide a consistent predictor of fog day frequency. For example, if a 95% RH cutoff consistently predicts 50% of the fog days, then this will provide a useful link to both climate model output and remote sensing of RH. In addition, the relationship will likely be more significant if data are grouped by month or season than on an annual basis. That is, a different RH cutoff value could be used for each season leading to fewer errors. This relationship will have to be studied over several years of continuous measurements, or by going through high quality historical data at Gobabeb. In addition, in order to scale up to a GCM grid cell, RH and fog need to be consistently measured across the area covered by the grid cell. Towards this end, five mini-weather stations were left in the field and are being maintained by the Gobabeb Training and Research Centre. Also, the Standard Fog Collectors at Gobabeb were equipped in January 2010 with tipping buckets to automatically record the volume of fog water deposited, which will restore this measurement system to its previous high fidelity status.

3.5 Conclusions

The main findings of this study are (1) Leaf Wetness Sensors can provide information on amount of water deposited, (2) dew is a significant contributor of both hours of wetness and deposited water, (3) soil moisture below about 3 cm does not appear to be affected by fog or dew at the event scale, and (4) a preliminary look at GCM predictions for humidity in the Namib indicate a 0 to 3% decline in the next century. The initial evaluation of GCM data warrants further study of the vast accumulation of data made available by the IPCC and groups working on regional down-scaling. Connecting fog and dew deposition with GCM data is a necessary next step for making concrete predictions of future patterns in occult precipitation of the Namib and elsewhere. These connections, if the relationships among fog, dew and RH prove useful, could lead to expansion of the analysis to the entire Namib Desert. Such an analysis will allow for the evaluation of relationships among fog, dew and species distributions, which will help drive conservation priorities in the future.

References

Aiyambo, D., 2007. A baseline study of the microphytic soil crust in the Central Namib. Department of Nature Conservation. Polytechnic of Namibia, Windhoek.

Aravena, R., Suzuki, O., Pollastri, A., 1989. Coastal Fog and Its Relation to Groundwater in the Iv-Region of Northern Chile. Chemical Geology 79, 83-91.

Burgess, S.S.O., Dawson, T.E., 2004. The contribution of fog to the water relations of Sequoia sempervirens (D. Don): foliar uptake and prevention of dehydration. Plant Cell and Environment 27, 1023-1034.

Dawson, T.E., 1998. Fog in the redwood forest: ecosystem inputs and use by plants. Oecologia 117, 476-485.

Foster, P., 2001. The potential negative impacts of global climate change on tropical montane cloud forests. Earth-Science Reviews 55, 73-106.

Giannini, A., Biasutti, M., Held, I.M., Sobel, A.H., 2008. A global perspective on African climate. Climatic Change 90, 359-383.

Gut, S., 1988. Study of the moisture budget of the dunes of the central Namib Desert. Geographisches Institut der Universität Zürich, Zürich.

Hachfeld, B., Jurgens, N., 2000. Climate patterns and their impact on the vegetation in a fog driven desert: The Central Namib Desert in Namibia. Phytocoenologia 30, 567-589.

Henschel, J., Mtuleni, V., Gruntkowski, N., Seely, M., Shanyengana, S.E., 1998. NAMFOG: Namibian application of fog-collecting systems Desert Research Foundation of Namibia, Windhoek.

Henschel, J.R., Seely, M.K., 2008. Ecophysiology of atmospheric moisture in the Namib Desert. Atmospheric Research 87, 362-368.

Hildebrandt, A., Al Aufi, M., Amerjeed, M., Shammas, M., Eltahir, E.A.B., 2007. Ecohydrology of a seasonal cloud forest in Dhofar: 1. Field experiment. Water Resources Research 43, W10411.

Hulme, M., Doherty, R., Ngara, T., New, M., Lister, D., 2001. African climate change: 1900-2100. Climate Research 17, 145-168.

Ingraham, N.L., Mark, A.F., 2000. Isotopic assessment of the hydrologic importance of fog deposition on tall snow tussock grass on southern New Zealand uplands. Austral Ecology 25, 402-408.

Ingraham, N.L., Matthews, R.A., 1988. Fog-Drip as a Source of Groundwater Recharge in Northern Kenya. Water Resources Research 24, 1406-1410.

IPCC (Ed.), 2007. Climate change 2007 : The Physical Science Basis. IPCC Secretariat, Geneva.

Johnstone, J.A., Dawson, T.E., 2010. Climatic context and ecological implications of summer fog decline in the coast redwood region. Proceedings of the National Academy of Sciences of the United States of America 107, 4533-4538.

Jones, R., Noguer, M., Hassell, D., Hudson, D., Wilson, S., Jenkins, G., Mitchell, J., 2004. Generating high resolution climate change scenarios using PRECIS. Hadley Centre for Climate Prediction and Research, Exeter, UK.

Lancaster, J., Lancaster, N., Seely, M.K., 1984. Climate of the central Namib Desert. Madoqua 14, 5-61.

Louw, G., Seely, M., 1982. Ecology of desert organisms. Longman, New York.

MartinezMeza, E., Whitford, W.G., 1996. Stemflow, throughfall and channelization of stemflow by roots in three Chihuahuan desert shrubs. Journal of Arid Environments 32, 271-287.

Rech, J.A., Quade, J., Hart, W.S., 2003. Isotopic evidence for the source of Ca and S in soil gypsum, anhydrite and calcite in the Atacama Desert, Chile. Geochimica Et Cosmochimica Acta 67, 575-586.

Schemenauer, R.S., Cereceda, P., 1991. Fog-Water Collection in Arid Coastal Locations. Ambio 20, 303-308.

Seely, M.K., de Vos, M.P., Louw, G.N., 1977. Fog imbibition, satellite fauna and unusual leaf structure in a Namib Desert dune plant Trianthema hereroensis. South African Journal of Science 73, 169-172.

Shanyengana, E.S., Henschel, J.R., Seely, M.K., Sanderson, R.D., 2002. Exploring fog as a supplementary water source in Namibia. Atmospheric Research 64, 251-259.

Siesser, W.G., 1980. Late Miocene Origin of the Benguela Upswelling System off Northern Namibia. Science 208, 283-285.

Squeo, F.A., Aravena, R., Aguirre, E., Pollastri, A., Jorquera, C.B., Ehleringer, J.R., 2006. Groundwater dynamics in a coastal aquifer in north-central Chile: Implications for groundwater recharge in an arid ecosystem. Journal of Arid Environments 67, 240-254.

Still, C.J., Foster, P.N., Schneider, S.H., 1999. Simulating the effects of climate change on tropical montane cloud forests. Nature 398, 608-610.

Thomas, D.S.G., Knight, M., Wiggs, G.F.S., 2005. Remobilization of southern African desert dune systems by twenty-first century global warming. Nature 435, 1218-1221.

Walter, H., Breckle, S.W., 1986. Tropical and subtropical zonobiomes. Springer-Verlag, Berlin.

Warren-Rhodes, K.A., Rhodes, K.L., Pointing, S.B., Ewing, S.A., Lacap, D.C., Gomez-Silva, B., Amundson, R., Friedmann, E.I., McKay, C.P., 2006. Hypolithic cyanobacteria, dry limit of photosynthesis, and microbial ecology in the hyperarid Atacama Desert. Microbial Ecology 52, 389-398.

Weathers, K.C., 1999. The importance of cloud and fog in the maintenance of ecosystems. Trends in Ecology and Evolution 14, 214-215.

Weathers, K.C., Lovett, G.M., Likens, G.E., Caraco, N.F.M., 2000. Cloudwater inputs of nitrogen to forest ecosystems in southern Chile: Forms, fluxes, and sources. Ecosystems 3, 590-595.

Chapter 4 : Fog as a supplemental water source for plants in the Central Namib Desert

Abstract

The Namib Desert on the southwestern coast of Africa is hyper-arid in terms of rainfall, but experiences up to 100 days of fog each year. This fog is a more regular and potentially more plentiful source of water than the highly seasonal rainfall, which averages 20-80 mm/yr. Several studies have demonstrated fog use strategies of Namib biota, and the mechanism for fog uptake has been shown for three plants endemic to the Namib (*Stipagrostis sabulicola, Trianthema hereroensis, Arthraerua leubnitziae*). Although fog is not important for direct soil water recharge, uptake by leaves or very shallow roots of some plants can sequester fog deposited in the early morning before it is removed by evaporation. This study uses stable isotopes of water (fog, rain, groundwater, soil water, and plant water) to determine the amount of fog water used by ten common plant species in the Central Namib, notably including the enigmatic and very long-lived *Welwitschia mirabilis.* The greatest contribution of fog water to plant stem (xylem) water was found in the dune grass and shrub species (40%), followed by three shrubs of the gravel plains (5-20%). Riverbed trees, *W. mirabilis* and *Acanthosicyos horridus* (!nara) all had depleted stem water isotope values indicating a fairly consistent groundwater or deep soil water source. Fog utilization is minimal for *Zygophyllum stapffii* on the edges of the fog zone, and it is significantly correlated ($p < 0.02$) to plant size for *Z. stapffii* and *T. hereroensis*.

4.1 Introduction

Water in the Namib

The Namib Desert on the southwestern coast of Africa is hyperarid in terms of rainfall, but receives frequent coastal fog events that are thought to play a major role in the Namib ecosystem. Fog in the Namib most commonly occurs through advection of a low stratus cloud that forms over the cool Benguela Current that upwells along west coasts of South Africa, Namibia and southern Angola. When advected inland, this cloud intersects the land at elevations of 100-500 mamsl, which translates to 10-60km from the coast (Figure 2). Occasionally very low elevation fog occurs within 10 km of the coast. Radiation fog, which occurs much less frequently, results from warm moist air cooling rapidly at night in low-lying areas. Winter frontal systems from the southwest infrequntly bring light drizzle. Total rain accumulations range between 20 and 80 mm/yr, increasing to the east. Fog deposition, although operationally defined by the collection method, has been measured at 20-180 mm/yr within 60 km of the coast (Lancaster *et al*., 1984; Henschel *et al*., 1998; Hachfeld and Jurgens, 2000; Shanyengana *et al*., 2002). A simplified version of these patterns gives a sense of the overall atmospheric moisture regime active in the Namib, and the annual rainfall totals experienced during this study describe the typically dramatic interannual variability in rainfall (Figure 1-2).

Significant work has been done to show the utilization of fog water by Namib biota (Louw, 1972; Hamilton and Seely, 1976; Seely and Hamilton, 1976; Henschel and Seely, 2008), the general occurrence and characteristics of fog events (Lancaster *et al*., 1984; Pietruszka and Seely, 1985; Olivier, 1995; Henschel *et al*., 1998; Hachfeld and

Jurgens, 2000), as well as geochemical aspects of Namib ecosystem relating to fog deposition (Eckardt and Schemenauer, 1998; Goudie and Parker, 1998). However, several questions remain about the role of fog water in the ecohydrology and nutrient cycling of these ecosystems. In particular, the amount of fog water used by the unique plants of the Namib under natural conditions is virtually unknown. The central objective of this study is to estimate the relative utilization of fog water in several Namib plants.

Two early studies used tritiated water to demonstrate the ability, *in situ*, to take up fog water via surficial roots in a common dune grass, *Stipagrostis sabulicola* (Louw and Seely, 1980), and via leaves in a dune shrub, *Trianthema hereroensis* (Seely *et al*., 1977). Although infrequent and highly seasonal rainfall pulses increase soil moisture to much greater levels, fog events have been shown to increase soil moisture to a depth of 8 cm (Gut, 1988), supporting the surficial root uptake pathway for *S. sabulicola*. Investigators have also suggested that the long-lived and floristically enigmatic *Welwitschia mirabilis* absorbs fog water through its leaves (Bornman *et al*., 1973), but this pathway has not been proven and long-term observations link growth to rainfall rather than fog (Walter and Breckle, 1986; Henschel and Seely, 2000). Other studies have relied on correlating species distribution (*Zygophyllum stapffii, Arthraerua leubnitziae*) with fog occurrence (Hachfeld and Jurgens, 2000), or studying plant-scale water relations (Ebert, 2000; Loris, 2004).

The fog and rain deposition pattern affect the distribution of vegetation across the Namib, with large trees generally confined to the eastern edge of the desert and along ephemeral watercourses (Walter and Breckle, 1986; Burke, 2003; Curtis and

Mannheimer, 2005; Burke, 2006). Here the trees have access to the relatively shallow alluvial aquifers, which are recharged by seasonal floods that have high interannual variability and can be absent for several years (Jacobson *et al*., 1995; Lange, 2005). Common trees in the riverbeds include *Acacia erioloba*, *Faidherbia albida*, and *Tamarix usneoides*. The Kuiseb River marks the boundary between the great dune sea to the south and the gravel plains to the north. Perennial vegetation in the dunes is dominated by *S. sabulicola,* with *T. hereroensis* co-dominating towards the coast. And the gravel plains comprise various species of perennial shrubs (e.g., *A. leubnitziae, Z. stapffii, Calicorema capitata*) notably including the gymnosperm *W. mirabilis*.

Stable isotopes in fog studies

The stable isotopes of oxygen and hydrogen can be used in some systems to link the three aspects necessary for describing fog utilization occurrence, volume and uptake. Isotopes are measured as ratios of the heavy isotope to the light isotope ($^{18}O/^{16}O$, $^{2}H/^{1}H$), and reported relative to a standard in "per mil" (‰) notation by convention (Equation 4-1 gives the example of $\delta^{18}O$).

$$\delta^{18}O = (R_{sample}/R_{VSMOW} - 1) \times 1000 \qquad \text{(Equation 4-1)}$$

Where, R = the abundance ratio of ^{18}O to ^{16}O
VSMOW = Vienna Standard Mean Ocean Water, the international reference standard for water isotopes.

The movement of water in the environment leads to changes isotopic compositions due to fractionations that occur primarily during evaporation and condensation. Consistent variations in $\delta^{2}H$ and $\delta^{18}O$ in meteoric water globally were first reported more than 40 years ago (Craig, 1961), establishing the Global Meteoric Water Line (GMWL; Equation 4-2). Processes dominated by kinetic fractionation lead to deviations from the GMWL, as in evaporation from soil (Barnes and Allison, 1988) and evapotranspiration in leaves (Twining *et al*., 2006; Gat *et al*., 2007).

$$\delta^{2}H = 8 \times \delta^{18}O + 10 \qquad \text{(Equation 4-2)}$$

If the $\delta^{18}O$ and $\delta^{2}H$ values of the potential water sources for an ecosystem are significantly different, they can be used as end members in a mixing equation that describes their relative contribution to a given population of plant or soil water samples (White *et al*., 1985; Dawson and Ehleringer, 1991; Dawson *et al*., 2002). This situation is commonly the case for studying contributions from fog and rain because fog condenses from humid air at relatively low elevations, resulting in relatively little fractionation of stable isotopes. Whereas, rain is often depleted due to condensation at higher altitudes than fog, as well as rainout of the heavy isotopes from a given cloud as it moves across land (Ingraham and Mark, 2000).

For example, the California redwoods receive summer fog that is isotopically enriched relative to the winter rainfall by about 60 ‰ in $\delta^{2}H$. Water extracted from redwoods and undergrowth had $\delta^{2}H$ values between the fog and rain end-members, showing an annual contribution of up to 34% from fog (Dawson, 1998). Several other studies have been able to use the isotopic difference between fog and rain to determine the hydrologic importance of fog water in, for example, arid northern Kenya, grass fields of New Zealand, and the Atacama Desert of Chile (Ingraham and Matthews, 1988;

Aravena *et al*., 1989; Ingraham and Mark, 2000). No integrated isotopic study of plant water sources has been performed for the Namib, but sufficient isotopic discrimination between fog and rain in the Namib is suggested by separate studies of fog (Eckardt, 1996), rain (Rozanski *et al*., 1993) and groundwater (Schmitz, 2004).

4.2 Methods

Study site and plant species

Ten plant species were studied at several locations from 10 to 80 km from the coast in the Central Namib Desert, with most of the sampling near the permanent research station at Gobabeb (Figure 1-1). Gobabeb is situated at the confluence of the three main habitats of the Namib: dunes, ephemeral riverbed, and gravel plains. The plants to be sampled are representative of common plants in these three habitats (Table 1-2). Results from co-occurring species (e.g. *A. leubnitziae* and *Z. stapffii* in the gravel plains) will give insight into their relative fog utilization. Although *W. mirabilis* samples will only be taken from Hope Mine, it is hoped that comparisons with *Z. stapffii* in this area will help elucidate any connections with the fog gradient given that *Z. stapffii* occurs throughout the fog zone. Sampling and observations occurred from August 2007 to June 2009, including continuous measurements at Gobabeb's Permanent Weather Stations and at least six months of data from Mini Stations as described below (also see Appendix C).

Sampling and analysis

Fog samples were collected for each fog event at Gobabeb by the research station technicians during the 8am manual weather station duty from the Gobabeb SFC and stored at 4°C in 12 mL vacutainers sealed with Parafilm. Concomitant fog samples from X-harp collectors placed around Gobabeb and Swartbank were collected during field campaigns. Dew samples were also collected during field campaigns from the Gobabeb Standard Dew Collector ("SDC"), a $1 m^2$ teflon sheet sitting at 45° on a frame about 0.5 m off the ground. The SDC is checked for water and emptied every morning. Dew samples were collected on days when no fog was observed or collected in the vertical SFC. Rain water was collected opportunistically during field campaigns. Groundwater and surface water has been analyzed extensively for $\delta^{34}S$, $\delta^{2}H$ and $\delta^{18}O$ in previous studies (Eckardt, 1996; Schmitz, 2004), and the $\delta^{2}H$ and $\delta^{18}O$ values from groundwater were regionally shown to have a well-defined signal. Groundwater from Gobabeb was sampled periodically to confirm this robust signal.

Plants were sampled and stored according to the IAEA-MIBA (Moisture Isotopes in the Biosphere and Atmosphere) program protocol (Twining *et al*., 2006). Stem and leaf samples were stored in a glass vacutainers sealed with Parafilm, chilled in the field, and refrigerated in the laboratory. Due to long storage times (6-12 months) in the present study, the samples were stored frozen. For grass samples (*S. sabulicola*), a non-green piece of stalk was collected in lieu of stem material. In order to obtain an integrated water sample from the branchless *W. mirabilis,* a 5mm diameter core (Haglof increment borer) was taken from 12 individuals (Appendix B). Soils were collected and stored frozen in glass mason jars. Several soil profiles were collected in sand dunes from areas where the sand is solid enough to allow an auger to penetrate 0.5-1 m.

Soil and plant water was extracted by cryogenic vacuum distillation (West *et al*., 2006) and analyzed along with fog, rain, and groundwater for δ^2H and δ^{18}O using Laser-Absorption Spectroscopy at the University of Minnesota. This method is comparable in precision and accuracy to the traditional Isotope Ratio Mass Spectrometry, IRMS, (Wang *et al*., 2009) and can be performed with very little volume of sample (< 50 μL), which was important for some of the plant and soil samples in this study. Sulfur isotopes (δ^{34}S) in water and plant samples were analyzed by IRMS at the University of Virginia using Continuous Flow sample introduction with conversion of sample S to SO_2 in a Carlo Erba elemental analyzer coupled to an OPTIMA IRMS (Micromass, Manchester, UK). Sulfur in water samples was precipitated as $BaSO_4$ and the filtrate precipitated onto Whatman No. 1 Cellulose filters in the field.

Although stem water can give an authentic isotope signature of the source water (White *et al*., 1985), water involved in transpiration will become enriched along an evaporation line (Aravena *et al*., 1989; Shu *et al*., 2005; Twining *et al*., 2006; Gat *et al*., 2007). Leaf water involved in photosynthesis exchanges with xylem water in leaves and small branches, enriching the extracted branch water relative to the water source (Gat *et al*., 2007). In eastern Namibia, evaporation lines have been used to calculate the original water source for infiltrating soil water using Equation 3 (Kuells, 2000). Here, branch and leaf samples taken under similar moisture conditions at different times of the day (i.e. different transpiration rates) will be used to calculate evaporation lines for source water determination. The corresponding δ^2H and δ^{18}O values that fall on the meteoric water line will be calculated using Equation 4-3 for individual samples and this value will then be used to calculate the "Fog Contribution" from a linear interpolation between average groundwater and average fog, winter rainfall and dew (Equation 4-4).

$$\delta^{18}O_c = \frac{\delta^2 H_m - s_m \times \delta^{18}O_m - d_g}{s_g - s_m} \qquad \text{(Equation 4-3)}$$

With,
$\delta^{18}O_c$ = isotope value "corrected" to fall on the meteoric water line
d = intercept of the δ^2H vs. δ^{18}O relationship
s = slope of the δ^2H vs. δ^{18}O relationship
subscript m = measured
subscript g = meteoric water line

$$F_f = \frac{\delta^{18}O_c - \delta^{18}O_w}{\delta^{18}O_f - \delta^{18}O_w} \times 100 \qquad \text{(Equation 4-4)}$$

With,
F_f = contribution of water from fog, winter rainfall and dew
$\delta^{18}O_w$ = average isotope value of groundwater
$\delta^{18}O_f$ = average isotope value of fog, winter rainfall and dew

4.3 Results

Water and soil samples - δ^2H and δ^{18}O

Fog, dew and winter rainfall all had similar mean values of δ^{18}O and δ^2H (Figure 4-1: -1.3 to 0.4 ‰ and -1.6 to 2.7 ‰ for δ^{18}O an δ^2H, respectively), with unexpectedly large variability in fog (n=35, standard deviation of 1.4 and 6.9 ‰ for δ^{18}O and δ^2H, respectively). Gobabeb groundwater was the most depleted of all water samples. Both mean values and variability were consistent with 2004 samples from the same borehole (Schmitz, 2004), with δ^2H of -6.1 ‰ (n=20, σ=0.2) in 2004 and -6.0 ‰ in the present study (n=4, σ=0.5) and corresponding δ^{18}O of -38.3 ‰ (σ=4.1) and -39.6 (=6.2). Gobabeb groundwater is slightly depleted relative to the fresh groundwater at Homeb which is used for drinking water. Groundwater at Hope was highly brackish, with a value of 28 on the Practical Salinity Scale (PSS), compared with 0 at Gobabeb, 4 at Nara Valley, and 35 for seawater. Hope groundwater, at about 30 m depth, was also enriched relative to Gobabeb and Homeb groundwater, and consistent with 2004 values from a salt spring on the gravel plains (Schmitz, 2004). Nara Valley groundwater, at about 17 m depth, was opaque with a fine black sediment, potentially from biofouling. The water isotope values for this water fell to the left of the meteoric water line, a highly unusual deviation in water isotopes which could be caused by isotopic exchange with oxygen in minerals over long periods of time. This explanation would be consistent with the theory that the aquifer beneath Nara Valley being a paleochannel of the Kuiseb River (Lenz *et al*., 1995). Soil water from about 10 to100 cm was highly variable in δ^2H and δ^{18}O, and enriched in High Dune sand compared to gravel plains soils (Hope) at comparable depths. All High Dune soils were collected in winter 2008 after winter rainfall, and Hope soils were collected in winter and spring 2007 which saw no winter rainfall.

Plant samples - δ^2H and δ^{18}O

Stem water isotopes exhibited a large amount of variability among different species (Table 4-1), with dune plants being the most enriched (δ^2H 13.7 to 27.2 ‰), followed by gravel plains shrubs (δ^2H -17.9 to -13.4 ‰) and riverbed trees (δ^2H -55.3 to -

29.5 ‰). Stem water of *W. mirabilis* is most similar to that of *A. erioloba*, and it is statistically similar (95% confidence) to all of the riverbed trees as well as *A. horridus*. *Z. stapffii* has a water isotope signal that is distinct from both riverbed trees and dune plants, and it is most similar to *A. leubnitziae* and *C. capitata*. *A. leubnitziae* and *Z. stapffii* tend to occur together within about 40 km of the coast. *C. capitata* appears to replace *A. leubnitziae* in this niche further inland. The two species are of the same family (Amaranthaceae) and have very similar growth forms. For this reason and due to the low number of samples, *A. leubnitziae* and *C. capitata* are combined for statistical analyses. Stem water content (% of wet weight) ranges from 35 to 54% for the woody species and the one perennial grass; whereas, the stem succulent *A. horridus* was much higher at 74%.

Table 4-1: Stem water summary with mean isotope (δ^2H, δ^{18}O) and water content values.

Plant[1]	δ^{18}O	δ^2H	Water Content	n	Slope[2]	Fog Contribution[3]	Group[4]
S	10.9 (4.1)	13.7 (18.9)	48% (5)	20	2.0, 2.7, 2.3	41% (30)	A
T	17.4 (4.8)	27.2 (6.0)	54% (5)	16	2.0, 2.6, 2.1	37% (11)	A
CL	1.5 (2.6)	-13.4 (11.2)	43% (4)	5	2.5	18% (26)	AB
Z	1.3 (2.1)	-17.9 (11.0)	35% (11)	18	2.5	5% (24)	B
A	1.2 (3.8)	-29.5 (17.0)	40% (5)	6	2.5	-26% (33)	BC
W	0.0 (0.9)	-33.8 (6.6)	39% (6)	13	2.5	-31% (24)	C
F	-3.9 (1.9)	-51.3 (5.2)	51% (6)	4	2.5	-56% (3)	C
N	-1.3 (1.1)	-44.8 (5.5)	74% (4)	3	2.3, 2.6	-58% (9)	C
X	-5.6 (1.6)	-55.3 (11.2)	43% (3)	3	2.5	-55% (24)	C

Number in parentheses is 1 standard deviation

[1] – S = *S. sabulicola*, T = *T. hereroensis*, C = *C. capitata*, L = *A. leubnitziae* (combined with C for statistics, see text), Z = *Z. stapffii*, W = *W. mirabilis*, A = *A. erioloba*, F = *F. albida*, N = *A. horridus*, X = *T. usneoides*

[2] – Slopes are for linear relationships among stem or leaf water from different times of the day. Multiple values are given if enough data were available for each sampling event, and they correspond to: Summer 2007, Winter 2008 and Summer 2009 (not available for *A. horridus*), respectively.

[3] – From Equation 4-4; "Fog" = "Atlantic" (see text); negative values indicate a water source that is more depleted than Gobabeb groundwater.

[4] – Statistical grouping of Fog Contribution based on a fixed-effects ANOVA at 95% confidence

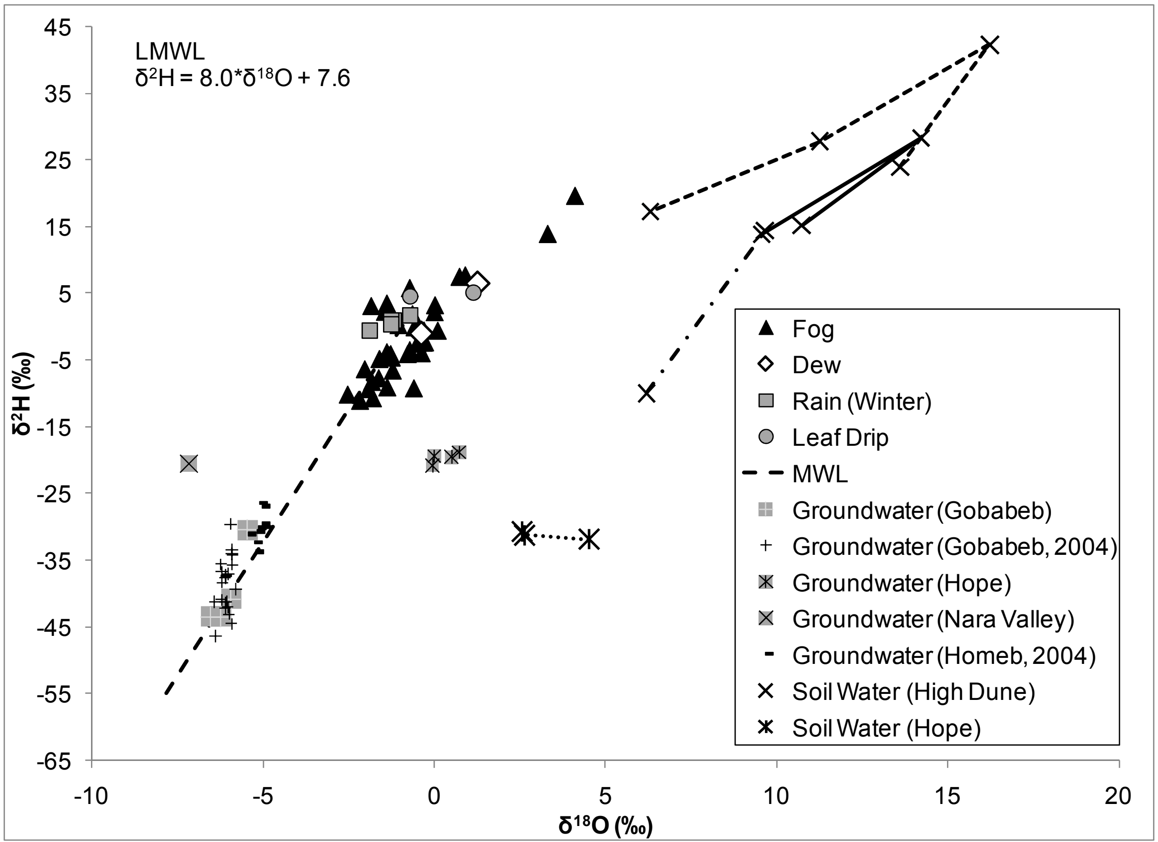

Figure 4-1: Isotope values (δ^2H, $\delta^{18}O$) for water and soil water samples.
Note: Gobabeb and Homeb groundwaters listed as 2004 are from Schmitz (2004). Soil waters were collected in winter (2008; depths of 12 to 72 cm) on High Dune 2km SW of Gobabeb and winter and spring (2007; depths of 20 to 100 cm) at Hope. Groundwaters at Gobabeb and Homeb are potable, whereas Hope is brackish (28 PSS) and Nara Valley contains fine black sediment indicative of biofouling.

Variability in the stem water isotopes of the riverbed trees is greatest in *A. erioloba* (Figure 4-2), but this mainly reflects the variety of individuals sampled. This variety includes large and small individuals in the riverbed and on both north and south banks of the Kuiseb, covering winter and summer sampling events. The *F. albida* data, while covering the same time periods, include samples from just one large individual, and thus have a standard deviation of less than one-third of that in the *A. erioloba* data (Table 4-1). Large variability in the dune grass *S. sabulicola* is expected due to the lack of woody tissue, and thus the interaction of water drawn up via the roots with that involved in transpiration along the grass blades and green stem. This is observed in the data, and appears to follow a similar pattern to the variability in stem water of *T. hereroensis*, the leaf succulent shrub growing in the same location. That is, the slopes of the evapotranspiration lines of both plants are lowest in the Summer 2007 samples, highest in Winter 2008, and intermediate in Summer 2009. There is not enough data to look for these patterns in the other species. Interestingly, the slopes of stem to leaf water in *T. hereroensis* (Figure 4-3) are consistently higher (2.5 to 3.2) than the corresponding slopes derived from stem water only (2.0 to 2.7). This indicates more enrichment in ^{2}H relative to the corresponding enrichment of ^{18}O in the leaf water compared to stem water.

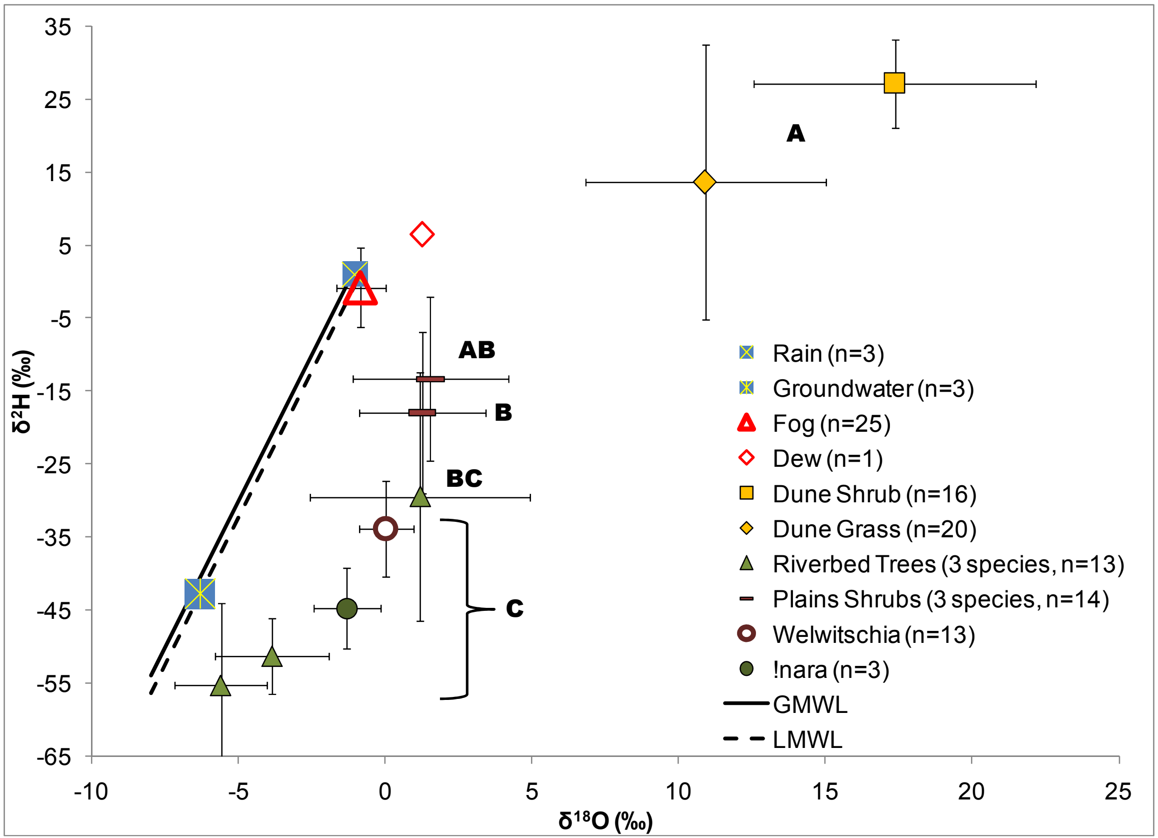

Figure 4-2: Average stem water isotope values ($\delta^{2}H$, $\delta^{18}O$) for each plant species.
Note: Species that share a letter cannot be distinguished statistically (95% confidence). Error bars indicate 1 standard deviation.

Using the available evapotranspiration lines for each species, average Fog Contribution to the stem water is shown to be highest in the dune plants at around 40% (+/- 1 standard deviation of 11% for *T. hereroensis* and 33% for *S. sabulicola*), followed by the gravel plains shrubs (20% +/- 26% for *C. capitata* and *A. leubnitziae*, 5% +/- 24% for *Z. stapffii*). All of the other species had evapotranspiration lines that intersected the meteoric water line below the Gobabeb groundwater signal. This is expressed as a negative Fog Contribution, but should be taken as simply a way of evaluating the isotopic value of their respective water sources by incorporating both δ^2H and δ^{18}O into one number. These depleted water sources cannot be distinguished statistically. However, if this group were to be divided into subgroups, *A. erioloba* (-26% +/- 33%) and *W. mirabilis* (-31% +/- 24%) plot together on the more enriched end, with *T. usneoides* (-55% +/- 24%), *F. albida* (-56% +/- 3%) and *A. horridus* (-58% +/- 9%) on the depleted end.

Sulfur isotopes

The δ^{34}S values of water samples ranged from about 10 ‰ in groundwater at Gobabeb to about 16 ‰ in fog water, with highly enriched values (16.5 ‰) found in the saline groundwater at Hope. Plants in the riverbed at Gobabeb had depleted values in the range of 8 to 12 ‰, whereas dune plants were much more enriched at 16 to 18 ‰. In the gravel plains, plants had intermediate values of 14 to 16 ‰ except for *W. mirabilis* at 10 ‰. At Gobabeb, where groundwater is quite depleted relative to fog, there is a significant positive correlation between Fog Contribution to stem water and the δ^{34}S of the stem material from which the water was extracted (Figure 4-4).

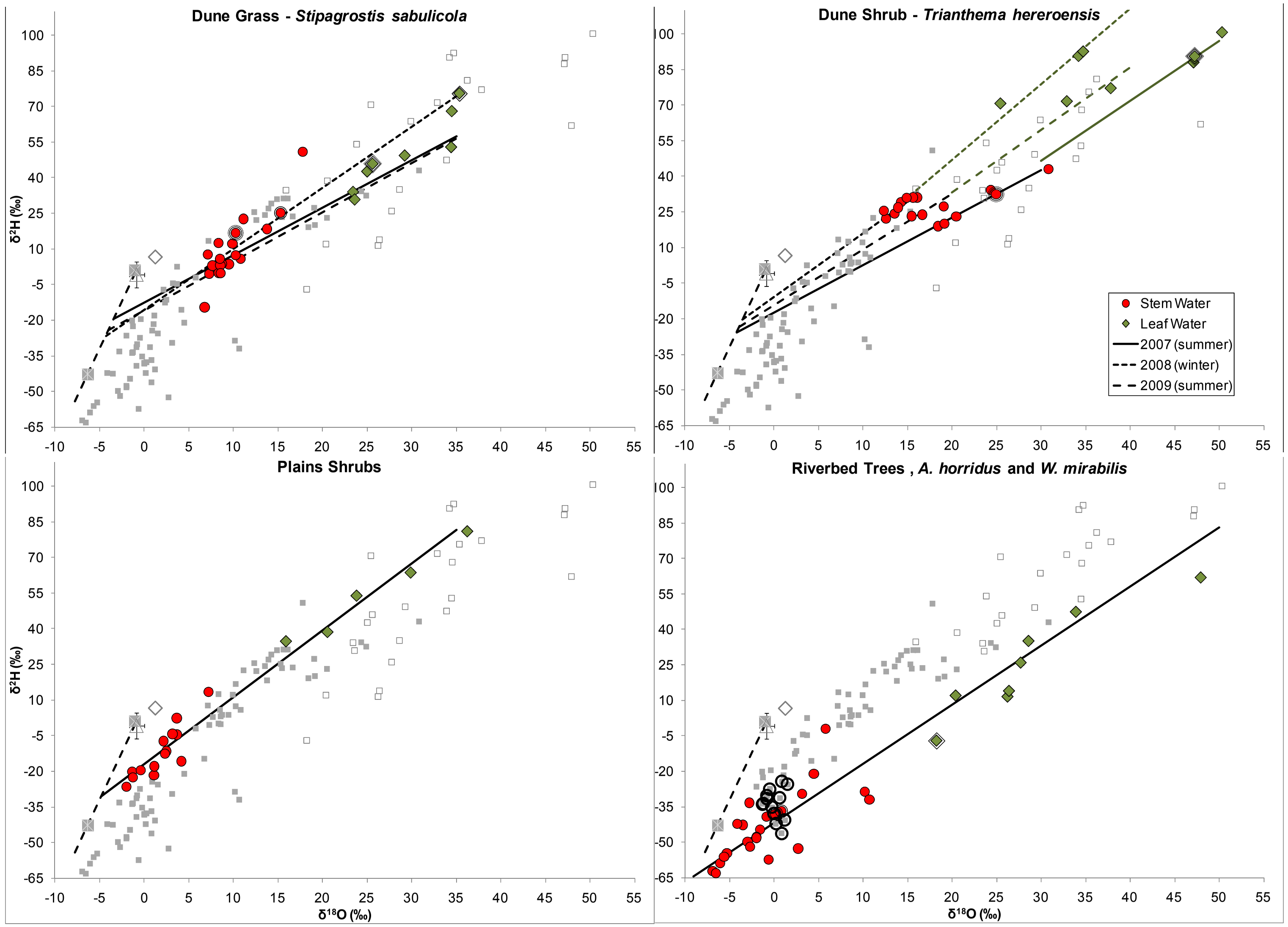

Figure 4-3: Plant stem and leaf water isotopes. Plains Shrubs *Z. stapffii* and *A. leubnitziae*; Riverbed Trees *A. erioloba*, *F. albida*, and *T. usneoides*.
Note: Water sources (see Figure 4-2) as well as all leaf (open squares) and stem (grey squares) shown in background.

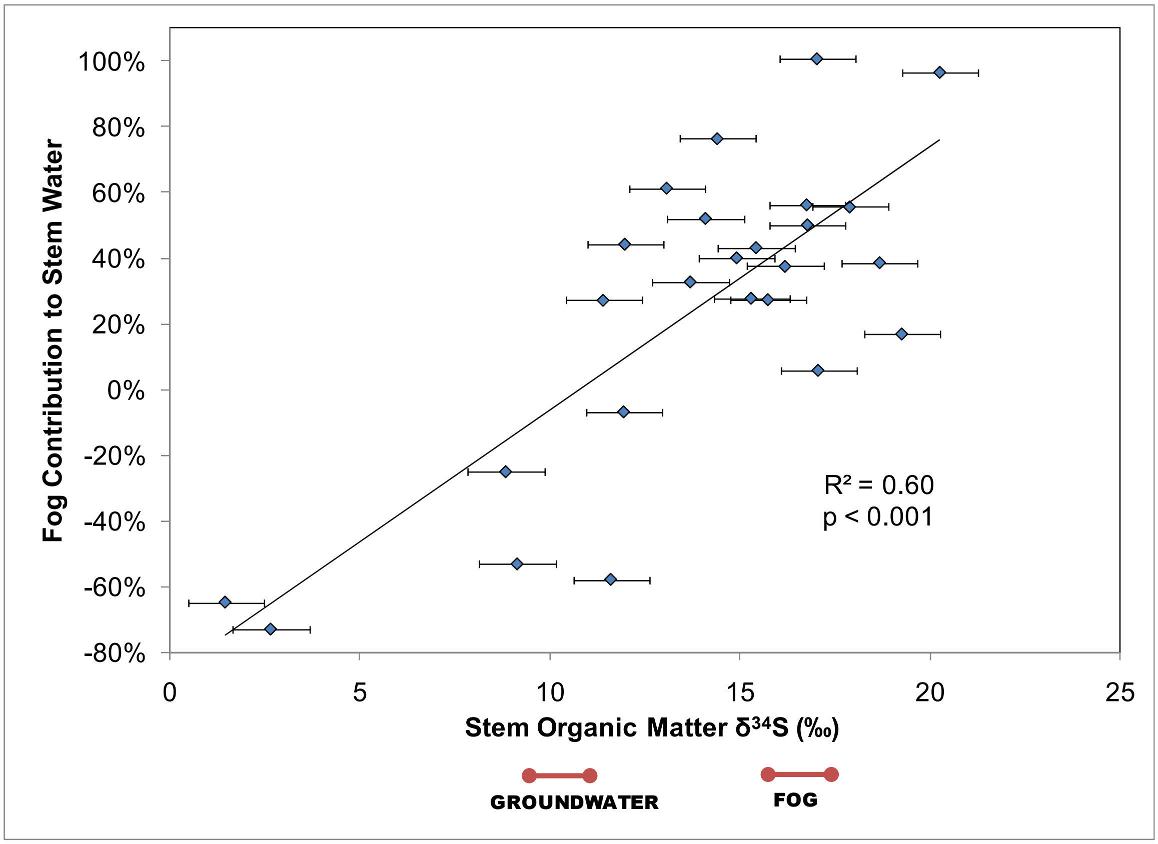

Figure 4-4: Fog Contribution and δ^{34}S of stem material for plants in the riverbed, dunes and gravel plains around Gobabeb, with the corresponding groundwater and fog δ^{34}S indicated.

4.4 Discussion

The statistical grouping of *W. mirabilis* and *A. horridus* with *A. erioloba* and the other riverbed trees (*F. albida* and *T. usneoides*) indicates that these species use the same water source. The water source is isotopically similar to the alluvial groundwater, which is consistent with *A. erioloba* being a known phreatophyte. This finding confirms the phreatophytic nature of *A. horridus*, which has long been thought to utilize groundwater (Sandelowsky, 1990; Klopatek and Stock, 1994; Hebeler *et al.*, 2004; Moser, 2004). However, the same conclusion cannot be drawn for *W. mirabilis* given its different hydrogeological setting (see Chapter 5) as well as the sulfur isotope results. The association of *A. horridus* and *F. albida* also supports the locally held belief that these species compete for the same water resources (Henschel *et al*., 2004; Ito, 2005). Further evidence for the groundwater connection in *A. horridus* comes from the observation of *A. horridus* die-offs in an area of the Kuiseb delta after a levy was built that diverted episodic flooding of the area, essentially eliminating groundwater recharge (Ito, 2005). Similarly, a drop of several meters in the Kuiseb alluvial aquifer water table in the 1970's and 1980's caused water stress in *F. albida* (Ward and Breen, 1983; DWA, 1987). The phreatophytic properties of some Acacias has long been discussed given their spatial association with groundwater (Meinzer, 1927). The extremely long roots (30 to 50 m) of *A. erioloba* (Leistner, 1986; Canadell *et al*., 1996), and observations of die-offs in a group of *A. erioloba* in Namibia after a drop in the water table (Dinter, 1921), indicate that this species is able to tap groundwater.

The "Fog Contribution" to stem water presented here includes negative values for the trees and deeply rooted shrubs. These values indicate a water source that is more depleted than that consistently found in the fresh groundwater (Figure 4-2). Such values have been seen in Kuiseb flood waters (Schmitz, 2004), which are isotopically variable covering the range of values required to explain the range in negative Fog Contribution values observed (e.g. δ^2H of -50 to -80 ‰ in one flood event). One explanation for depleted flood waters relative to groundwater is that the floods result from exceptional storms which have seen large fractionations due to intense rainfall prior to entering the watershed (Levin *et al*., 1980). The less variable groundwater signal is isotopically similar to summer rainfall, and reflects a longer-term integration of recharge. The signal is also consistent with more distal recharge in the upper portion of the watershed to the east of the Namib. Rainfall in this eastern portion of the Kuiseb basin would tend to be released from the cloud at an earlier stage in the rainout process, and would thus be less depleted than rain from the same cloud falling in the western portions of the watershed. The implication of this variable subsurface signal is that the Fog Contribution needs to be considered a minimum value as it uses groundwater as the subsurface end-member. It should be remembered that this end-member is consistent through time and reflects local summer rainfall (Rozanski *et al*., 1993).

It needs to be emphasized that the "Fog Contribution" discussed here is more appropriately termed the "Atlantic contribution" due to the isotopic similarity among fog, dew and winter rainfall which are all derived from Atlantic air masses. However, there was no winter rainfall at Gobabeb in 2007, so these samples should reflect only fog and dew contributions to the Atlantic end-member. Re-sampling the same *A. erioloba* and *F. albida* individuals showed only slightly higher Fog Contribution values in 2007 (-23% and -53%) relative to 2008 and 2009 (-41% and -57%). This is expected given the extensive roots and thus more consistent water source for these trees. The winter 2008 *Z. stapffii* samples at Gobabeb have a higher Fog Contribution than those in 2007 (31% vs 4%), suggesting that winter rainfall is a significant component of the Atlantic isotope signal in this species. For the dune plants, there is also an enrichment in the 2008 and 2009 samples, but the most significant pattern is in the slopes of the evapotranspiration lines. Both *S. sabulicola* and *T. hereroensis* have shallow slopes in 2007 (2.0, 2.0), steep slopes in 2008 (2.6 and 2.7), and intermediate slopes in 2009 (2.1, 2.3). A slope of 2.5 was found in the gravel plains and riverbed species with some variability. A study of Negev Desert plants found mean evaporation lines around 2.1-2.8 for several species including two from genera in the present study -- *Tamarix* and *Zygophyllum* (Gat *et al*., 2007). Evaporation line slopes are attributed to the water potential gradient along the soil-plant-air continuum which affects the diffusion of ^{2}H and ^{18}O and thus the relative fractionation factors (Zimmerman *et al*., 1967; Sofer and Gat, 1975; Shurbaji and Phillips, 1995). Lower slopes are found in drier soils (Barnes and Allison, 1988). Although soil moisture data is not available, the observed changes in slope are consistent with having drier soils in late 2007 followed by 82 mm of rain and thus wetter soils in winter 2008.

The highly enriched stem waters of *S. sabulicola* and *T. hereroensis* could be due, to some extent, to the translocation of leaf water which is enriched to a much greater degree (Figure 4-3). That is, some of the leaf water that has become enriched during the day is translocated from leaf to stem, and subsequently translocated back into the leaves for photosynthesis. Both species have been shown to be able to translocate water through all of their structures (i.e. roots, stems, leaves) in simulated fog wettings with tritiated water (Seely *et al*., 1977; Louw and Seely, 1980). When the dune sand is very dry, reversal of flow in the stems of these plants could potentially be caused by high relative humidity during the night or during fog events (Burgess and Dawson, 2004). The *T. hereroensis* stem and leaf waters tended to be more enriched than *S. sabulicola* although they appear to use approximately the same water mixture of water sources. This difference could indicate a higher degree of translocation in *T. hereroensis* than *S. sabulicola*. An alternative explanation to both the "Fog Contribution" and translocation is the utilization of highly enriched soil water in the dune deep enough to escape ongoing evaporation. Summer rainfall at Gobabeb dominates precipitation, and thus infiltration of soil water, on an annual volume basis. The soil water data presented here (Figure 4-1) is from a very limited soil water survey in June/July 2008 during an exceptionally wet winter, and thus is not taken as representative of the dune water available to the plants throughout the year. The conclusions drawn here about Fog Contributions are supported by the constancy of the stem water isotopes from 2007, a very dry year with no winter rainfall, through 2008 and 2009. Lastly, there is emerging evidence of compartmentation of water within leaves or grass stems, leading to sequential isotopic differences in the spatially separated, but connected reservoirs (Yakir, 1992; Gat *et al*., 2007). Micro-compartmentation of water in plant tissues is a challenging ongoing research area, and these two species could potentially be interesting candidates for field studies of this phenomenon.

Fog utilization was shown to decrease with the logarithm of plant size in the California redwoods ecosystem (Dawson, 1998). A similar pattern is seen here, with significant correlation between Fog Contribution to stem water and the natural log of canopy cover when all species are included (Figure 4-6). This relationship is primarily driven by the finding that trees tend to use more groundwater than shrubs and grasses of the dunes and gravel plains. However, there are similar patterns seen within four individual species. Significant intra-species correlations exist for *Z. stapffii* and *T.*

hereroensis – the two stem succulents sampled – and marginally significant correlations exist for *S. sabulicola* and *A. erioloba*, whereas, no intra-species correlation was found for *W. mirabilis* and *C. capitata/A. leubnitziae*. The implication is that as the four species with significant correlations grow larger, they are able to tap deeper into the subsurface, accessing the more isotopically depleted soil water or groundwater. For *W. mirabilis*, it is possible that exposed stem area is not a good measure of rooting depth, or that all of the plants sampled were already deeply rooted enough to obtain isotopically depleted soil water. The lack of a correlation in *C. capitata/A. leubnitziae* indicates that fog is important for both small and large plants, and potentially suggesting that these species do not develop extensive vertical root systems, implying the use of fog and shallow soil water to the same extent in small and large individuals. This interpretation is consistent with the confinement of the distribution of these species to the fog zone, as well as their co-occurrence with *Z. stapffii*. That is, these shrubs become established in the same habitats, often in the same rock crevice or shallow depression, likely due to the availability of transient shallow soil moisture and the occurrence of fog events. Then as they grow, in avoidance of the competetion for shallow soil water, *Z. stapffii* may be able to develop a deeper root system to survive, and *C. capitata/A. leubnitziae* continue to utilize fog uptake and storage in their stems and unique leaves through their entire life. Although excavations have shown similar root systems in these species (Kutschera *et al.*, 1997), *Z. stapffii* has been known to thrive in habitats with hardpad layers in the soil (Burke, 2003), indicating and ability to reach water despite these physical barriers . An extension of this work would be to examine the ability of *C. capitata/A. leubnitziae* to deliver fog water to the shallow soil, which is then used by *Z. stapffii*, potentially providing further explanation of their co-occurrence.

The only plant to be sampled at every location was *Z. stapffii*, and it exhibits a pattern of Fog Contribution to stem water with distance from the coast (Figure 4-5). Within 15 km of the coast there is very little fog deposition, and in this area *Z. stapffii* tends to occur in shallow wash areas leading to the depleted isotopic signal. Similarly depleted values are seen at Hope Mine on the inland edge of the fog zone. However, in the fog zone this shrub tends to grow on rocky outcrops, and these plants tend to have more enriched stem water values. In fact, the three individuals at Hope Mine with enriched stem water isotopes occur on the rocky slopes of the wash, and the two depleted individuals occur at a lower elevation in the middle of the sandy wash.

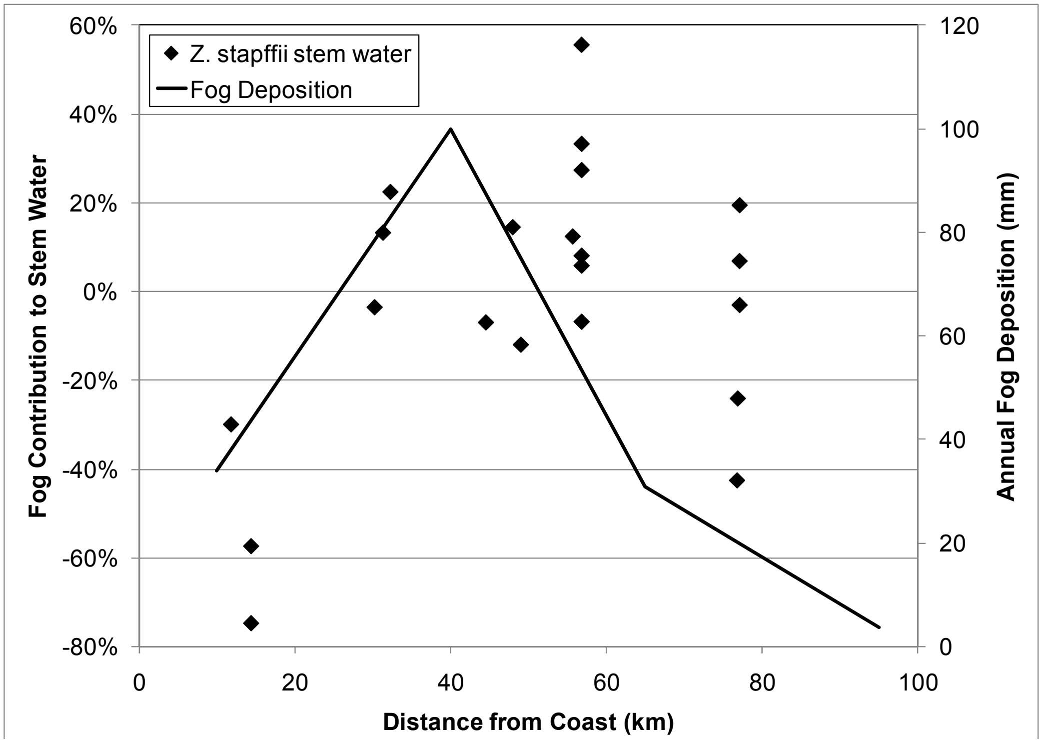

Figure 4-5: Fog Contribution and deposition vs distance from the coast for *Z. stapffii*.
Note: See Chapter 1 for discussion of the generalized fog deposition (Lancaster *et al*., 1984)

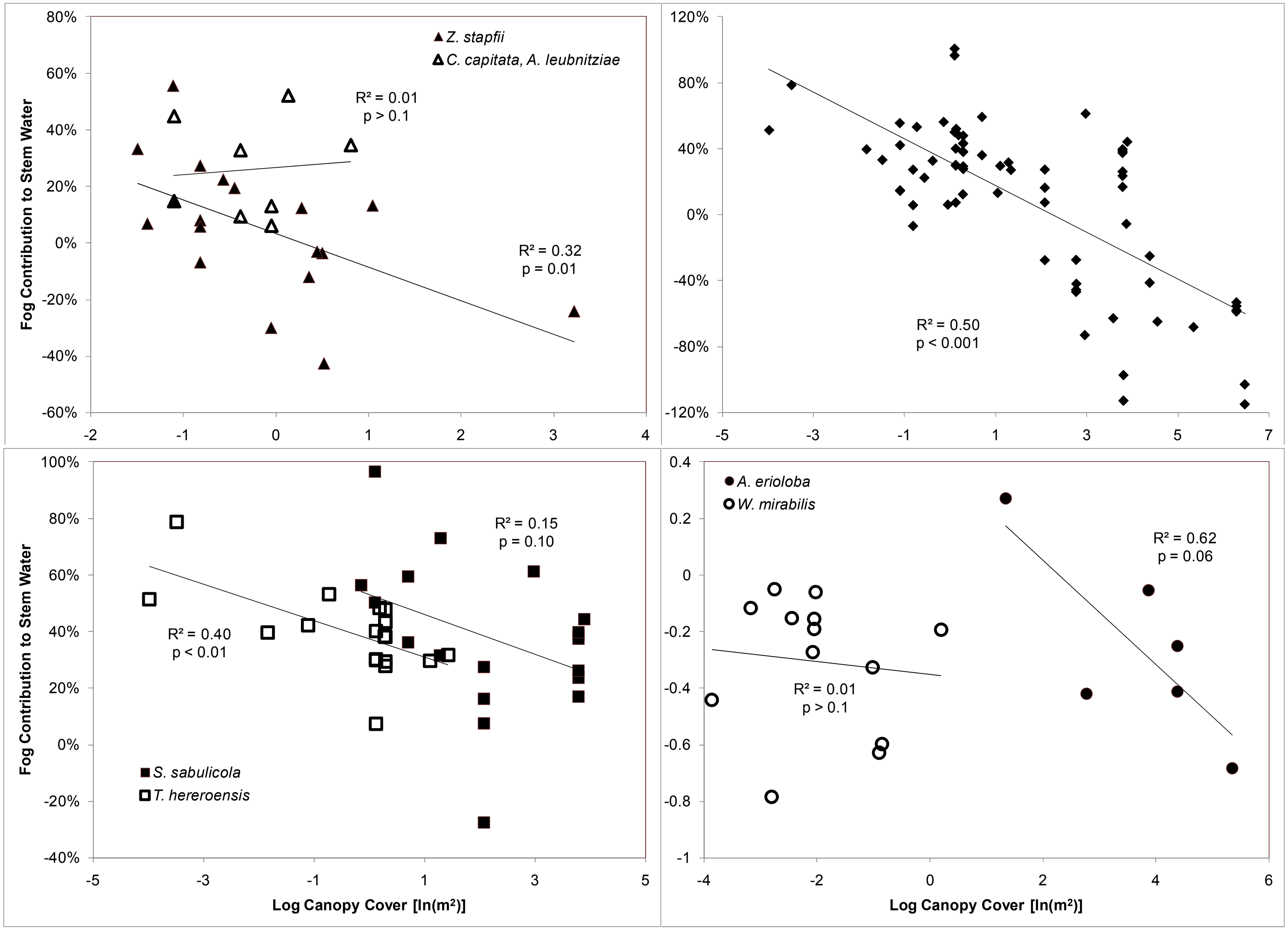

Figure 4-6: Fog Contribution vs plant size (canopy cover) for all plants (top right) and six individual species or groupings with sufficient data (Note: *W. mirabilis* size is the exposed stem area, not canopy cover, and is thus excluded from the top left "all plants" graph).

4.5 Conclusions

Water isotopes could not distinguish fog, dew and winter rainfall, but this can be achieved through a combination of sensor and manual observations (see Chapter 3). Fog – or winter rain, fog and dew – provided around 40% of the stem water in dune plants and 5-20% in shrubs of the gravel plains. In contrast, there is no indication of fog uptake in the riverbed trees, *A. horridus* or *W. mirabilis*. These results are consistent across two years of sampling including summer and winter conditions, and are corroborated by the positive correlation between Fog Contribution and the $\delta^{34}S$ of stem material. Significant relationships were found between fog utilization and plant size for the leaf succulents *Z. stapffii* and *T. hereroensis*, suggesting that deeper soil water becomes more important as the plants age. No such relationship was found in the shrubs that co-occur with *Z. stapffii*, and this finding can guide future research into the differential root development and water uptake strategies in these Namib endemics.

References

Aravena, R., Suzuki, O., Pollastri, A., 1989. Coastal Fog and Its Relation to Groundwater in the Iv-Region of Northern Chile. Chemical Geology 79, 83-91.

Barnes, C.J., Allison, G.B., 1988. Tracing of Water-Movement in the Unsaturated Zone Using Stable Isotopes of Hydrogen and Oxygen. Journal of Hydrology 100, 143-176.

Bornman, C.H., Botha, C.E.J., Nash, L.J., 1973. *Welwitschia mirabilis*: observations on movement of water and assimilates under föhn and fog conditions. Madoqua Series II 2, 25-31.

Burgess, S.S.O., Dawson, T.E., 2004. The contribution of fog to the water relations of Sequoia sempervirens (D. Don): foliar uptake and prevention of dehydration. Plant Cell and Environment 27, 1023-1034.

Burke, A., 2003. Wild flowers of the central Namib. Namibia Scientific Society, Windhoek.

Burke, A., 2006. Savanna trees in Namibia - Factors controlling their distribution at the arid end of the spectrum. Flora 201, 189-201.

Canadell, J., Jackson, R.B., Ehleringer, J.R., Mooney, H.A., Sala, O.E., Schulze, E.D., 1996. Maximum rooting depth of vegetation types at the global scale. Oecologia 108, 583-595.

Craig, H., 1961. Isotopic variations in meteoric waters. Science 133, 1702-1703.

Curtis, B., Mannheimer, C., 2005. Tree atlas of Namibia. National Botanical Research Institute, Ministry of Agriculture, Water and Forestry, Windhoek.

Dawson, T.E., 1998. Fog in the redwood forest: ecosystem inputs and use by plants. Oecologia 117, 476-485.

Dawson, T.E., Ehleringer, J.R., 1991. Streamside trees that do not use stream water. Nature 350, 335-337.

Dawson, T.E., Mambelli, S., Plamboeck, A.H., Templer, P.H., Tu, K.P., 2002. Stable isotopes in plant ecology. Annual Review of Ecology and Systematics 33, 507-559.

Dinter, K., 1921. Botanische Reisen in Deutsch-Sudwest-Afrika. Nov. Spec. Regn. Veg., Fedde Rep.

DWA, 1987. The Kuiseb Environment Project : an update of the hydrological, geohydrological, and plant ecological aspects. Water Quality Division (Research) : Hydrology Division : Geohydrology Division, Windhoek.

Ebert, O., 2000. Vergleichende Untersuchungen zum Wasserverbrauch von Sträuchern in der Namib-Wüste. Teaching Diploma. Universität Hohenheim Institut für Botanik, Stuttgart.

Eckardt, F., 1996. The distribution and origin of gypsum in the Central Namib Desert, Namibia. University of Oxford, Oxford.

Eckardt, F.D., Schemenauer, R.S., 1998. Fog water chemistry in the Namib Desert Namibia. Atmospheric Environment 32, 2595-2599.

Gat, J.R., Yakir, D., Goodfriend, G., Fritz, P., Trimborn, P., Lipp, J., Gev, I., Adar, E., Waisel, Y., 2007. Stable isotope composition of water in desert plants. Plant and Soil 298, 31-45.

Goudie, A.S., Parker, A.G., 1998. Experimental simulation of rapid rock block disintegration by sodium chloride in a foggy coastal desert. Journal of Arid Environments 40, 347-355.

Gut, S., 1988. Study of the moisture budget of the dunes of the central Namib Desert. Geographisches Institut der Universität Zürich, Zürich.

Hachfeld, B., Jurgens, N., 2000. Climate patterns and their impact on the vegetation in a fog driven desert: The Central Namib Desert in Namibia. Phytocoenologia 30, 567-589.

Hamilton, W.J., Seely, M.K., 1976. Fog basking by the Namib Desert beetle, *Onymacris unguicularis*. Nature 262, 284-285.

Hebeler, F., Botha, C., van Bel, A., 2004. Water, photosynthesis and transpiration of !nara. In: Henschel, J.R., Dausab, R., Moser, P., Pallett, J. (Eds.), !Nara: Fruit for development of the !Khuiseb Topnaar. Namibia Scientific Society, Windhoek, Namibia, pp. 93-106.

Henschel, J., Dausab, R., Moser, P., Pallett, J. (Eds.), 2004. !NARA: Fruit for development of the !Khuiseb Topnaar. Namibia Scientific Society, Windhoek.

Henschel, J., Mtuleni, V., Gruntkowski, N., Seely, M., Shanyengana, S.E., 1998. NAMFOG: Namibian application of fog-collecting systems Desert Research Foundation of Namibia, Windhoek.

Henschel, J.R., Seely, M.K., 2000. Long-term growth patterns of *Welwitschia mirabilis*, a long-lived plant of the Namib Desert (including a bibliography). Plant Ecology 150, 7-26.

Henschel, J.R., Seely, M.K., 2008. Ecophysiology of atmospheric moisture in the Namib Desert. Atmospheric Research 87, 362-368.

Ingraham, N.L., Mark, A.F., 2000. Isotopic assessment of the hydrologic importance of fog deposition on tall snow tussock grass on southern New Zealand uplands. Austral Ecology 25, 402-408.

Ingraham, N.L., Matthews, R.A., 1988. Fog-Drip as a Source of Groundwater Recharge in Northern Kenya. Water Resources Research 24, 1406-1410.

Ito, M., 2005. Changes in the distribution of the !nara plant that affect the life of the Topnaar people in the Lower Kuiseb River, Namib Desert. African Study Monographs Suppl.30, 65-75.

Jacobson, P.J., Jacobson, K.M., Seely, M., 1995. Ephemeral rivers and their catchments : sustaining people and development in western Namibia. Desert Research Foundation of Namibia, Windhoek.

Klopatek, J.M., Stock, W.D., 1994. Partitioning of nutrients in *Acanthosicyos-horridus*, a keystone endemic species in the Namib Desert. Journal of Arid Environments 26, 233-240.

Kuells, C., 2000. Groundwater of the North-Western Kalahari, Namibia: Estimation of Recharge and Quantification of the Flow Systems. Julius-Maximilian University of Würzburg, Würzburg, Germany.

Kutschera, L., Lichtenegger, E., Sobotik, M., Haas, D., 1997. Die Wurzel das neue Organ Ihre Bedeutung für das Leben von *Welwitschia mirabilis* und anderer Arten der Namib sowie von Arten angrenzender Gebiete mit Erklärung des geotropen Wachstums der Pflanzen. Eigenverlag: Pflanzensoziologisches Institut, Klagenfurt, Klagenfurt/Austria.

Lancaster, J., Lancaster, N., Seely, M.K., 1984. Climate of the central Namib Desert. Madoqua 14, 5-61.

Lange, J., 2005. Dynamics of transmission losses in a large and stream channel. Journal of Hydrology 306, 112-126.

Leistner, O.A., 1986. Southern Africa. In: Goodall, D.W., Perry, R.A. (Eds.), Arid-land ecosystems: structure, functioning and management. Cambridge University Press, New York, pp. 109-144.

Lenz, R., Grobbelaar, H., Djama, M., 1995. Reports on hydrogeological and isotope hydrological investigations. Bundesanstalt für Geowissenschaften und Rohstoffe. Federal Institute for Geosciences and Natural Resources, Hannover.

Levin, M., Gat, J.R., Issar, A., 1980. Precipitation, flood and groundwaters of the Negev Highlands: an isotopic study of desert hydrology., Arid Zone Hydrology: Investigations with isotope techniques. IAEA, Vienna, pp. 3-22.

Loris, K., 2004. Nebel als Wasserressource für den Strauch Arthraerua leubnitziae. In: Walter, H., Breckle, S.-W. (Eds.), Ökologie der Erde: Spezielle Ökologie der tropischen und subtropischen Zonen. Spektrum-Verlag, pp. 485-489.

Louw, G.N., 1972. The role of advective fog in the water economy of certain Namib Desert animals. Symposia of the Zoological Society of London 31, 297-314.

Louw, G.N., Seely, M.K., 1980. Exploitation of fog water by a perennial Namib dune grass, *Stipagrostis sabulicola*. South African Journal of Science 76, 38-39.

Meinzer, O.E., 1927. Plants as indicators of ground water. In: Survey, U.S.G. (Ed.), Reston, VA.

Moser, P., 2004. Root and shoot development of !nara seedlings. In: Henschel, J., Dausab, R., Moser, P., Pallett, J. (Eds.), !NARA: Fruit for development of the !Khuiseb Topnaar. Namibia Scientific Society, Windhoek, pp. 85-91.

Olivier, J., 1995. Spatial-Distribution of Fog in the Namib. Journal of Arid Environments 29, 129-138.

Pietruszka, R.D., Seely, M.K., 1985. Predictability of two moisture sources in the Namib Desert. South African Journal of Science 81, 682-685.

Rozanski, K., Araguasaraguas, L., Gonfiantini, R., 1993. Isotopic Patterns in Modern Global Precipitation. In: Swart, P.K., Lohmann, K.C., McKenzie, J., Savin, S. (Eds.), Climate Change in Continental Isotopic Records. American Geophysical Union, Washington, DC.

Sandelowsky, B.H., 1990. *Acanthosicyos horridus*, a multipurpose plant of the Namib Desert in southwestern Africa. In: Bates, D.M., Robinson, R.W., Jeffrey, C. (Eds.), Biology & Utilization of the Cucurbitaeceae. Cornell University Press, Ithaca & London, pp. 349-355.

Schmitz, A.U., 2004. Transmission losses and soil moisture dynamics in the alluvial fill of the Kuiseb river, Namibia. Albert-Ludwigs-Universität Freiburg i. Br., Freiburg i. Br.

Seely, M.K., de Vos, M.P., Louw, G.N., 1977. Fog imbibition, satellite fauna and unusual leaf structure in a Namib Desert dune plant *Trianthema hereroensis*. South African Journal of Science 73, 169-172.

Seely, M.K., Hamilton, W.J., 1976. Fog Catchment Sand Trenches Constructed by Tenebrionid Beetles, Lepidochora, from the Namib Desert. Science 193, 484-486.

Shanyengana, E.S., Henschel, J.R., Seely, M.K., Sanderson, R.D., 2002. Exploring fog as a supplementary water source in Namibia. Atmospheric Research 64, 251-259.

Shu, Y., Feng, X.H., Gazis, C., Anderson, D., Faiia, A.M., Tang, K.L., Etti, G.J., 2005. Relative humidity recorded in tree rings: A study along a precipitation gradient in the Olympic Mountains, Washington, USA. Geochimica Et Cosmochimica Acta 69, 791-799.

Shurbaji, A.R.M., Phillips, F.M., 1995. A Numerical-Model for the Movement of H2o, H-2 O-18, and (Hho)-H-2 in the Unsaturated Zone. Journal of Hydrology 171, 125-142.

Sofer, Z., Gat, J.R., 1975. Isotope Composition of Evaporating Brines - Effect of Isotopic Activity Ratio in Saline Solutions. Earth and Planetary Science Letters 26, 179-186.

Twining, J., Stone, D., Tadros, C., Henderson-Sellers, A., Williams, A., 2006. Moisture Isotopes in the Biosphere and Atmosphere (MIBA) in Australia: A priori estimates and preliminary observations of stable water isotopes in soil, plant and vapour for the Tumbarumba Field Campaign. Global and Planetary Change 51, 59-72.

Walter, H., Breckle, S.W., 1986. Tropical and subtropical zonobiomes. Springer-Verlag, Berlin.

Wang, L.X., Caylor, K.K., Dragoni, D., 2009. On the calibration of continuous, high-precision delta O-18 and delta H-2 measurements using an off-axis integrated cavity output spectrometer. Rapid Communications in Mass Spectrometry 23, 530-536.

Ward, J.D., Breen, C.M., 1983. Drought stress and the demise of *Acacia albida* along the lower Kuiseb River, central Namib Desert: preliminary findings. South African Journal of Science 79, 444-447.

West, A.G., Partrickson, S.J., Ehleringer, J.R., 2006. Water extraction times for plant and soil materials used in stable isotope analysis. Rapid Communications in Mass Spectrometry 20, 1317-1321.

White, J.W.C., Cook, E.R., Lawrence, J.R., Broecker, W.S., 1985. The D/H ratios of sap in trees: Implications for water sources and tree ring D/H ratios. Geochimica Et Cosmochimica Acta 49, 237-246.

Yakir, D., 1992. Water compartmentation in plant tissue: Isotopic evidence. In: Somero, G.N., Osmond, C.B., Bolis, C.L. (Eds.), Water and Life: Comparative analysis of water relationships at the organismic, cellular, and molecular levels. Springer-Verlag, New York, pp. 205-222.

Zimmerman, U., Ehhalt, D., Munnich, K.O., 1967. Soil-water movement and evapotranspiration: Changes in the isotopic composition of the water. In: IAEA (Ed.), Isotopes in hydrology; Proceedings of the symposium (1966: Vienna). International Atomic Energy Agency, Vienna, pp. 567-585.

Chapter 5 : Determining water sources of a *Welwitschia mirabilis* population within the context of increased mining operations in the Namib-Naukluft Park

Abstract

The coastal Namib Desert in southwestern Africa is hyperarid with respect to rainfall, but can receive up to 100 days of fog in a year, which is suspected to influence the water available for vegetation. With imminent increases in groundwater abstraction for new uranium and copper mines in the Namib, it is fundamental to assess the extent to which fog deposition can sustain this desert ecosystem. The southernmost community of *Welwitschia mirabilis*, a very long-lived and floristically enigmatic Namib endemic gymnosperm, lies in an area being explored for a new mine that would lower the water table significantly. Results from δ^2H and δ^{18}O analyses of *W. mirabilis* and nine other species common in the Central Namib suggest that this *W. mirabilis* population depends principally on deep soil water rather than fog as a water source. This finding is consistent with previous long-term observations of leaf growth, rainfall and fog deposition in an adjacent population. Water extracted from stem samples of 12 *W. mirabilis* individuals is highly depleted (δ^2H of -34 ‰ +/- 6.6) relative to coastal fog (-1.6 ‰ +/- 6.9), and lies on an apparent evaporation line (slope = 2.5) between soils (20-100 cm) and typical summer rainfall. The *W. mirabilis* values are statistically similar ($p<0.05$) to trees growing in the nearby ephemeral Kuiseb River ($n=16$), and distinct from known fog users of the dunes

(n=36) and gravel plains (n=14). Groundwater at the site does not appear to be a significant water source given that it is brackish, 20-40 m deep, and has an isotopic signature between that of *W. mirabilis* stem water and fog. Using $\delta^{34}S$ as additional water source tracer corroborates the deep soil water source given that *W. mirabilis* stem material (10 ‰) is depleted relative to Hope groundwater (17 ‰), soils (16 ‰) and fog (16 ‰), and it is similar to Kuiseb River groundwater (11 ‰).

5.1 Introduction

Welwitschia mirabilis (Gnetales: Welwitschiaceae) is a floristically unique and long-lived plant that is endemic to the coastal Namib Desert of southwestern Africa (Figure 5-1), and is listed in the Convention on International Trade in Endangered Species of Wild Fauna and Flora (CITES Appendix II). *W. mirabilis* has fascinated scientists for more than 150 years owing to its unusual morphology (Pearson, 1929; Rodin, 1953a; Bornman, 1972), longevity, reproductive strategies (Rodin, 1953b; Whitaker *et al*., 2008), photosynthetic pathways (Schulze *et al*., 1976; von Willert *et al*., 2005), as well as its overall ability to survive and remain perennially active in the hyperaridity and heat of the Namib Desert (Herppich *et al*., 1996; Henschel and Seely, 2000) despite having apparently non-xeromorphic characteristics (Bornman, 1972).

Welwitschia mirabilis has a low growth form with a thick stem up to a meter in diameter (Bornman, 1972) which is thought to be a stunted cotyledon (Rodin, 1953b). Two thick wide leaves grow from the bi-lobed stem and sprawl across the sand surrounding the stem. The leaves remain with the plant for its entire life, drying and

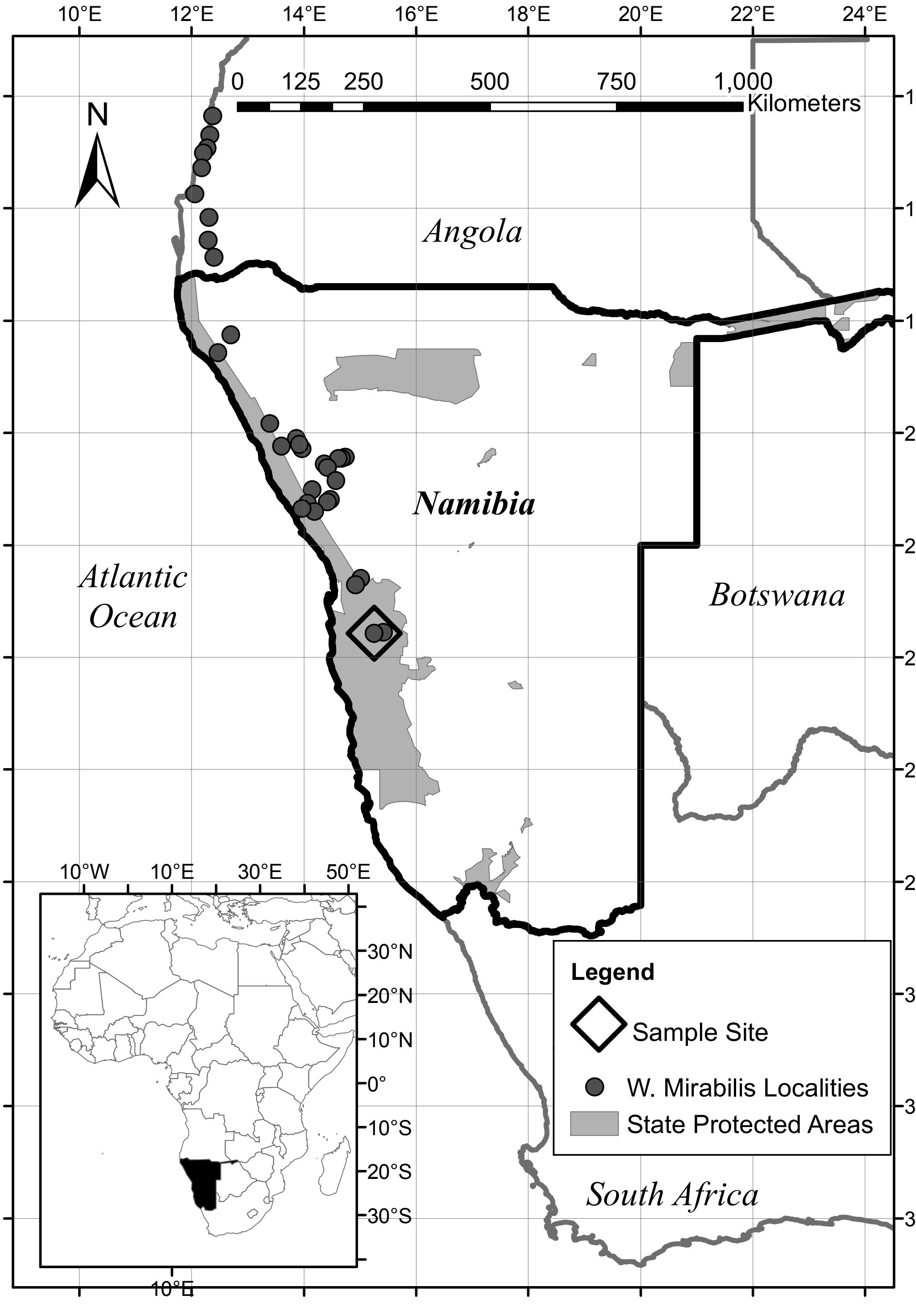

Figure 5-1: Study area with *W. mirabilis* distribution.
Note: All published locations of *W. mirabilis* populations are included (Taborda de Morais, 1958; Kers, 1967; Irish, 2008).

splitting at the ends. The green portion extends tens to hundreds of cm from the basal meristem. Medium-sized plants have been ^{14}C-aged at around 300 to 550 years (Herre, 1961; Vogel and Visser, 1981; Jurgens *et al.*, 1997), and one individual of unspecified size was determined to be 920 +/- 100 years old (Crane and Griffin, 1970). The leaves are considered to be the longest-lived in the plant kingdom because the original two leaves persist for the life of the plant (Bornman, 1977). Although, the green portion of each leaf is only years to decades old given that several centimeters are added from the basal meristem each year (Vogel and Visser, 1981; Walter and Breckle, 1986; von Willert and Wagner-Douglas, 1994; Henschel and Seely, 2000; Osborne and Gudde, 2001), and the ends become variably split and dried by winds and photodegradation.

It has long been suspected that water requirements of *W. mirabilis* are high owing to the large exposed leaves (Pearson, 1929). Water use in three contrasting central Namib habitats has been measured at 0.053 to 2.6 L/day (19 to 949 L/year), corresponding to leaf growth of 0.17 to 1.12 mm/day (von Willert and Wagner-Douglas, 1994). If these levels of water use are examined per unit leaf area they can be compared to estimates of mean annual rainfall and fog deposition (Table 5-1). With evaporation rates in the Namib of up to 1500 mm/year (Lancaster *et al.*, 1984) it is apparent that even a vast horizontal root system would have difficulty providing the several hundred liters of water per year needed to balance transpiration in *W. mirabilis.* The most complete *W. mirabilis* root excavation found lateral roots extending more than 15 m (Kutschera *et al.*, 1997). As an example, if the roots have a capture area of 50 m^2, 20 mm of rainfall and a recharge rate of 10% would yield only 100 L of water in the vadose zone near the roots.

It is tempting, then, to assume that the remaining water (about 250 L) comes from fog deposition. If fog is taken up at all, it would have to be channeled along the leaves to the meristem, reducing the effective capture area to about 2 m^2 for a given plant. Although fog deposition is operationally defined and continuous measurements are sparse, a value of 10 mm/year is a good first estimate for the Hope Mine area (see Chapter 3), which would provide a maximum of 20 L per plant each year.

Table 5-1:Growth and water use data for three *W. Mirabilis* populations relative to the Hope Mine population.

Location	Distance to coast (km)	Leaf growth (mm/yr)	Leaf area* (m^2)	Rainfall† (mm/yr)	Fog† (mm/yr)	Total wet deposition (mm/yr)	Transpired water‡ (mm/yr)
Welwitschia flats	45	305	0.651	25	60	85	513
Brandberg Junction	60	410	1.84	20	30	50	516
Brandberg	60	60	0.309	20	30	50	62
Hope Mine	75	§135	NA	30	10	40	NA

* – Upper side of leaves for representative specimens (von Willert and Wagner-Douglas, 1994)
† – Rainfall and fog were estimated from a relationship between precipitation and distance to the coast based on 9 long-term stations (Lancaster *et al*., 1984) and an intensive 1-year (1999-2000) study with 23 stations (Hachfeld and Jurgens, 2000). In these studies fog was collected using a wire structure above a rain gauge, and collected volume was compared to an adjacent rain gauge.
‡ – Volume of transpired water per unit leaf area, extrapolated from 5 months (November 1990 – March 1991) of data (von Willert and Wagner-Douglas, 1994)
§ – From a 14-year study of the adjacent “Welwitschia Wash” population (Henschel and Seely, 2000)
NA – Not available.

Observations of the potential for fog water availability in the Namib have been mostly qualitative, and have long led to the suggestion that *W. mirabilis* utilizes fog as a water source. In addition to the lack of rainfall, fog-dependence was suggested based on the apparent confinement of *W. mirabilis* to the fog-belt of the Namib (Rodin, 1953a). However, fog is apparently not necessary as some more mesic habitats on the Namib Desert margins also support abundant populations of *W. mirabilis* (Rodin, 1953a; Kers, 1967). This dichotomy has led to debate on fog use over the years. An early observation was that fog only wets the upper 4 cm of soil (Pearson, 1929), and that lateral roots of *W.*

mirabilis are no shallower than 20 cm. This shallow soil wetting from fog is consistent with measurements in the Namib dunes of 1 cm (Louw and Seely, 1982), 8 cm (Gut, 1988), and 1-3 cm in the present study (see Chapter 3). Thus, uptake of fog would have to happen through the leaves (Rodin, 1953a; Bornman, 1972). A study under artificial conditions showed that radioactively-labeled water pooled on a leaf could be taken up by the leaf and transported toward the stem (Bornman, 1977), but this has never been shown under natural conditions or beyond the leaf scale. In addition, saturating the stomata of any plant's leaves can temporarily reverse xylem flow in any plant depending on its water status and that of the soil (Burgess and Dawson, 2004). In addition, this experiment alone does not prove the ability to use natural foliar wetting as a water source given the apparent biophysical obstacles of wetting the stomatal guard cells and the thick waxy cuticle (Walter and Breckle, 1986).

A long-term study at the community level recently provided significant evidence to refute the fog-dependence hypothesis. The 14-year study of 21 individuals found an average growth rate of 0.37 mm/day – similar to earlier studies (Eller *et al*., 1983; von Willert and Wagner-Douglas, 1994). More importantly, this growth was highly seasonal and correlated with episodic rainfall. Annual growth also correlated with fluctuating annual rainfall, whereas fog deposition remained relatively stable over this time period (Henschel and Seely, 2000). This connection between *W. mirabilis* and rainfall was observed in two earlier expeditions with contrasting antecedent rainfall conditions. The same population of plants was visited twice – the end of an average rainy season (1907, 12.8mm) and the end of a poor rainy season (1909, 5.9mm). The second visit saw much degraded plant health and little reproductive activity (Pearson, 1909). The role of fog in germination and seedling development remains, however, poorly understood (Rodin, 1953b; Whitaker *et al*., 2008).

Namibia has great mineral wealth and is among the leading global producers of uranium and diamonds, with significant production of other metals including copper. The recent rise in prices has seen increased uranium exploration and mine development in Namibia, including within national parks. Namibia contributed 7.5%, 7.7%, and 9.1% of global uranium production during 2005, 2006 and 2007, respectively (Kwasny *et al*., 2007). Although there is currently a moratorium on issuing uranium prospecting licenses in Namibia, more than 60 licenses exist (Weidlich, 2008). Demands on local water sources and potential impacts by future mines are currently being evaluated; however, studies of ecosystem water requirements in the mining areas are difficult and expensive.

The Matchless amphibolite belt stretches northwest from central to north-east Namibia. This copper-zinc sulfide deposit is a significant source of metals regionally (Klemd *et al*., 1987), and like Namibia's uranium deposits, it has seen increased interest with the recent rise in copper price. The southernmost population of *W. mirabilis* lies in the southern tip of the Matchless deposit near Hope Mine. A new copper mine is being explored at this location. The mine would require dewatering of the unconfined aquifer, which could disrupt the water balance of the plants if they depended on groundwater.

Despite recent findings that relate *W. mirabilis* growth to rainfall and subsurface water availability (Henschel and Seely, 2000), the perception remains that this exceptional plant survives through the acquisition of water from fog (McGough *et al*., 2004; Curtis and Mannheimer, 2005; Mshigeni *et al*., 2005). The current study evaluates the hypothesis that the Hope Mine *W. mirabilis* population relies on fog as a water source through analysis of the stable isotope geochemistry of plant, soil and ground water, as well as water levels and watersheds around the community.

5.2 Methods

Site description

The Hope Mine site (E15.26° S23.57°) lies in the gravel plains of the Central Namib Desert about 10 km north of the ephemeral Kuiseb River. Shallow wash areas and low outcrops break the overall flat topography. Soils are patchy, coarse-grained, and shallow – 0 to 0.5 m deep in the middle of the wash areas, and are underlain by schist and amphibolites forming a fractured hardrock aquifer that contains brackish water in the saturated zone. *W. mirabilis* is the dominant perennial in the immediate vicinity, with a density of around 7.5 plants/ha (133 individuals over 0.177 km^2). This compares to around 50 plants/ha in the more narrow Welwitschia Wash (Henschel and Seely, 2000). Other plants include the perennial leaf-succulent *Zygophyllum stapffii*, and annual succulents and grasses. Trees, e.g. *Faidherbia albida*, *Acacia erioloba*, *Tamarix usneoides*, and *Acanthosicyos horridus* (!nara) occur in or near the Kuiseb River channel 10 km to the South with a few isolated *Acacia reficiens* individuals in the main wash area to the East of Hope Mine.

Using stable isotopes to determine water sources

Stable isotopes are here used to determine the sources of water used by *W. mirabilis*. The isotopic composition is generally expressed as ratios of the heavy isotope to the light isotope ($^{18}O/^{16}O$, $^{2}H/^{1}H$), and reported relative to a standard in "per mil" (‰) notation by convention. For example the $\delta^{18}O$ isotopic composition is expressed as:

$$\delta^{18}O = (R_{sample}/R_{VSMOW} - 1) \times 1000$$

Where, R = the abundance ratio of ^{18}O to ^{16}O
VSMOW = Vienna Standard Mean Ocean Water, the international reference standard for water isotopes.

The movement of water in the environment leads to changes isotopic compositions due to fractionations that occur primarily during evaporation and condensation. Consistent variations in $\delta^{2}H$ and $\delta^{18}O$ in meteoric water globally were first reported almost 50 years ago (Craig, 1961), establishing the Global Meteoric Water Line (GMWL) expressed as:

$$\delta^{2}H = 8 \times \delta^{18}O + 10$$

Processes dominated by kinetic fractionation lead to deviations from the GMWL, as in evaporation from soil (Barnes and Allison, 1988). If the $\delta^{18}O$ and $\delta^{2}H$ values of the potential water sources for an ecosystem are significantly different, they can be used as end-members in a mixing equation that describes the relative contributions to a given population of plant or soil waters (White *et al*., 1985; Dawson, 1998). This is the case for differentiating between fog and rain because fog condenses from humid air at relatively low elevations, resulting in relatively enriched isotope values. Rain is often depleted in the heavier isotope due to condensation at higher elevations than fog, as well as rainout from clouds as they move across land (Ingraham and Mark, 2000).

For example, the California redwoods receive summer fog that is isotopically enriched by about 60‰ in δ^2H relative to the winter rainfall. Water extracted from redwoods and undergrowth have δ^2H values between the fog and rain end-members, showing an annual contribution of 34% from fog (Dawson, 1998). This type of analysis is possible because water in non-photosynthetic parts of plants is not significantly different than its source water (White *et al*., 1985). Although soil water extraction and interpretation can be confounded by the presence of mineral bound water that is isotopically different from the water available for uptake by plant roots (Walker *et al*., 1994), soil water isotopes can still be useful in characterizing plant-available water (Corbin *et al*., 2005).

Sampling and analysis

Core samples (5mm diameter core, Haglof increment borer) of *W. mirabilis* stems from 12 individuals were collected in January and July 2009 along with adjacent soil (n=3) from depths of 20 cm, 50 cm, and 100 cm in July, and October 2007. Samples were stored in glass vacutainers sealed with Parafilm, chilled in the field, and refrigerated in the laboratory within 3 hours. To establish the context of stem water isotopes for various perennial plant forms across the Central Namib, 3 tree (*Acacia erioloba, Faidherbia albida, Tamarix usneoides*), 5 shrub (*Zygophyllum stapffii, Arthraerua leubnitziae, Calicorema capitata, Trianthema hereroensis, Acanthosycios horridus*) and 1 grass (*Stipagrostis sabulicola*) species were sampled at Hope and areas closer to the coast (see

Chapter 3). The samples were analyzed for δ^2H and δ^{18}O by Laser Absorption Spectroscopy (Wang *et al*., 2009) at the University of Minnesota following cryogenic vacuum extraction of soil and plant water (West *et al*., 2006). Replicate water samples (n=5), including three aliquots taken through the distillation procedure, had a standard deviation of 0.9 ‰ for δ^2H and 0.2 ‰ for δ^{18}O. Duplicates were also analyzed by the more traditional method of Isotope Ratio Mass Spectrometry, and mean values (n=2) deviated from the LAS results by -1.0 and +0.8 ‰ for δ^2H and δ^{18}O, respectively.

Depth to groundwater and watershed analysis

Current mine prospecting operations provided access to groundwater through several exploration boreholes drilled at an angle of about 50° from the ground surface towards the North. Water levels were measured using a conductivity meter in boreholes adjacent to and within the *W. mirabilis* population in October 2007 (n=10) and July 2008 (n=7). After correcting the measured groundwater elevation for the slant angle (obtained from the site geologist), the values were interpolated using linear universal kriging (Tonkin and Larson, 2002) to calculate a groundwater elevation surface covering a rectangular area of 3-6 ha that contains about 10% of the plant community. The groundwater elevation surface was then subtracted from the ground surface elevation (derived from GPS track points) to obtain depth-to-groundwater values.

Watersheds encompassing the *W. mirabilis* communities near Hope Mine and Welwitschia Wash were delineated based on topography using ArcGIS Spatial Analyst (ESRI, 2008). Ground surface elevation was derived from the Shuttle Radar Topography

Mission data (Farr *et al*., 2007). Watershed outlet grid cells were selected just downstream of the main Hope *W. mirabilis* community (“Hope West”), about halfway along the wash that includes the eastern Hope community, and about halfway along the Welwitschia Wash. Each watershed is then calculated by the software to include all grid cells (90 x 90 m each) that would contribute runoff to a selected outlet cell.

5.3 Results

Water extracted from stem samples of 12 *W. mirabilis* individuals is highly depleted (δ^2H of -34 ‰ +/- 6.6) relative to coastal fog (-1.6 ‰ +/- 6.9). Using and evaporation line typical of other gravel plains plants (slope = 2.5), the *W. mirabilis* stem water falls between soils (20-100 cm) and typical summer rainfall (Figures 4-1 and 4-2). The *W. mirabilis* values are statistically similar ($p<0.05$) to trees growing in the nearby ephemeral Kuiseb River (n=16), and distinct from known fog users of the dunes (n=36) and gravel plains (n=14). Groundwater at the site does not appear to be a significant water source given that it is brackish, 30-40 m deep, and has an isotopic signature between that of *W. mirabilis* and fog. Using δ^{34}S as additional water source tracer is consistent with a deep soil water source rather than groundwater or fog given that *W. mirabilis* stem material (10 ‰) is depleted relative to Hope groundwater (17 ‰), Hope soils (16 ‰) and fog (16 ‰), and it is similar to Kuiseb groundwater (11 ‰). Tree, shrub and grass species sampled near Gobabeb show a significant positive correlation between Fog Contribution to stem water and δ^{34}S (see Chapter 4).

Groundwater elevations ranged from 550 to 561 meters above mean sea level (MAMSL) in October 2007, and from 549 to 560 MAMSL in July 2008. The latter survey covered a smaller area, of about 3 ha compared to 6 ha in 2007. For the two boreholes that were measured in both surveys, levels were about 2 m lower in 2008. In both cases, groundwater elevation was found to be higher towards the southeast. Groundwater elevation gradients of around 70 and 80 m/km were found in 2007 and 2008, respectively. The depth to water was measured as 36 to 44 m in 2007. However, when the depth to water is calculated for a continuous rectangular area by subtracting interpolated groundwater elevations from ground surface elevations, the depth to water over the entire area ranges from 30 to 48 m (Figure 5-2). For the 19 plants in this area, depths range from 33 to 39 m with a mean of 35 m.

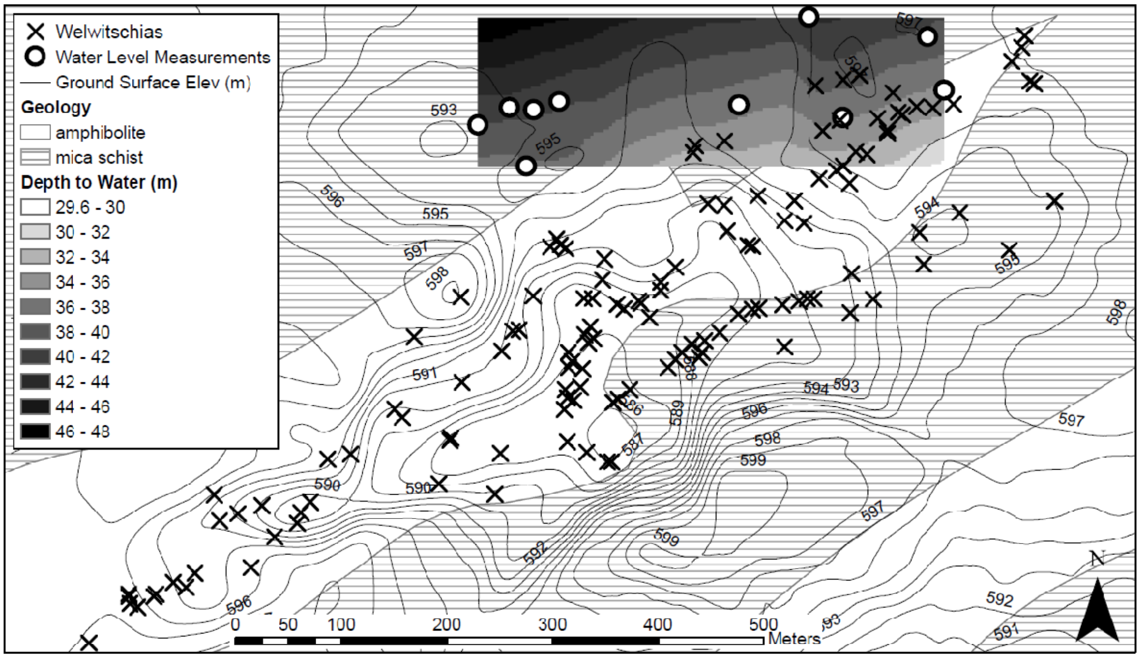

Figure 5-2: Geology, water levels, and *W. mirabilis* individuals at Hope Mine.

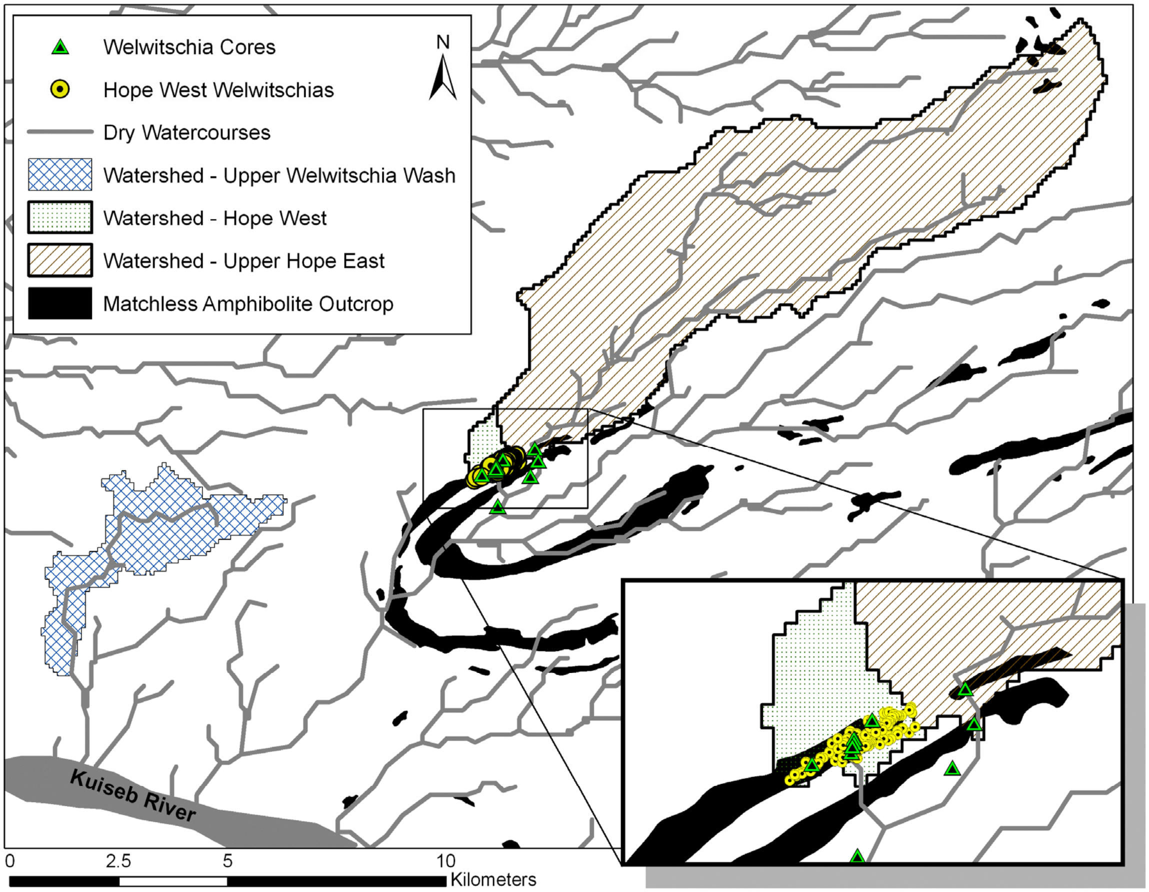

Figure 5-3: Watersheds and *W. mirabilis* near Hope Mine.
Note: Many additional *W. mirabilis* individuals exist East and South of the mapped community immediately adjacent to Hope Mine. The Welwitschia Wash watershed shows the contributing area upgradient of the mid-point in the community (*W. mirabilis* "F20" in Henschel and Seely 2000). Matchless Amphibolite is the stratigraphic target of mining operations, and its outcrop is taken from the electronic 1:250,000 Geological Map "Kuiseb 2314" (NGS, 2007).

The watershed encompassing most of the Hope West *W. mirabilis* community is quite small, at just 1.2 km^2, whereas the community just to the east is in the wash of a much more extensive watershed with a 48.2 km^2 area (Figure 5-3). The Welwitschia Wash watershed is on the small side with an 8.2 km^2 contributing area. The Hope East watershed takes a sharp turn to the left across alternating schist and amphibolite bands which form jagged steep hills. The wash drops 20 m in elevation quickly across these hills. The Hope East *W. mirabilis* community is confined to the edges of the wide sandy wash, whereas in Hope West the occurrence is more dense and associated with the outcropping of Matchless Amphibolite. This fractured metamorphic formation is the target of extensive copper mining operations stretching from Hope towards the northeast for hundreds of km.

5.4 Discussion

Desert plants are often adapted to make use of multiple water sources (shallow soil water, groundwater, fog/dew). Evaporation of precipitation during and after infiltration leads to a consistent fractionation in $\delta^{18}O$ and $\delta^{2}H$ that can be traced in soil water; one study of central Namib soils found a slope of 2.6 (Sofer, 1978), which is consistent with other desert soils (Liu *et al*., 1995) and plants (Gat *et al*., 2007). A similar slope of 2.5 was found for trees of the Kuiseb riverbed, which group statistically with *W. mirabilis*. This evaporation line intersects the GMWL in the vicinity of the Kuiseb groundwater, which is quite close to a long-term volume-weighted rainfall value from central Namibia (Rozanski *et al*., 1993).

All *W. mirabilis* in the area analyzed for groundwater levels occur where groundwater is less than 39m below ground surface (Figure 5-2). Although the water table had dropped from October 2007 to July 2008 by a couple of meters, the pattern of a shallower water table to the southeast is consistent between the two surveys. In addition, the bulk of the individuals in this population occur in the bottom of the wash, as indicated by the ground surface contours. This result suggests that *W. mirabilis* occurrence is associated with shallower groundwater. It has long been observed that *W. mirabilis* tends to occur in wash areas or on stream banks (Pearson, 1929; Rodin, 1953a; Kers, 1967;

Henschel and Seely, 2000). In the long-term observations described in the introduction, leaf growth rates were found to be higher on the edges of the main wash than in the middle (Henschel and Seely 2000). This pattern may be due to micro-environmental factors rather than water availability (Schulze *et al*., 1976; von Willert *et al*., 2005).

If this population of *W. mirabilis* is indeed accessing groundwater directly, the tap roots would have to reach depths of 30 to 39m. Although this would be an extremely deep root system, other species of plants from the nearby Kalahari Desert have been shown to reach depths of 40-68 m (Canadell *et al*., 1996). Another Namib endemic, *Acanthosicyos horridus* is phreatophytic with a tap root reported to reach depths of 15-40 m (Jurgens *et al*., 1997; Mshigeni *et al*., 2005), although excavations have shown depths of 2-5 m (Kutschera *et al*., 1997). Direct observations of *W. mirabilis* have shown that it can have an extensive lateral root system extending more than 15m. Tap roots are present, and have been directly observed in three incomplete excavations to depths of 1.6, 3.5 and ~5m (Bornman, 1972; Kutschera *et al*., 1997). Other qualitative explanations of *W. mirabilis* distribution have invoked a tap root, including the description of a Kaokoveld population in an area with groundwater around 22m belowground (Pearson, 1929; Rodin, 1953a). As noted above, the bulk of the *W. mirabilis* individuals in the Hope Mine population are in the wash area, where the ground surface is 5-10 m below the area of the groundwater surveys. Groundwater is likely to be even shallower here, which may indicate a typical tap root depth closer to 25 m. Although this depth would still require an exceptional energy investment by the plants, it has been shown that they can create lateral root networks of comparable lengths.

Table 5-2: Qualitative rainfall requirement estimation by watershed.

Watershed	Area (km^2)	Number of Plants[1]	Rainfall Requirement (mm)[2]
Welw Wash	**8.16**	**100**	**45**
Hope East	48.20	100	8
Hope West	1.16	150	473
Hope East + West	**49.35**	**250**	**18**

1 – Number of perennial plants (dominated by *W. mirabilis*) estimated from Whitaker (2006) for Hope West, Henschel and Seely (2000) for Welwitschia Wash, and personal observation in all locations.
2 – Based on 1 L of transpired water per plant per day (von Willert and Wagner-Douglas, 1994), and 10% recharge to the root zone of the plants as an example for watershed comparison.

The delineated watersheds (Figure 5-3) can be used to evaluate the hypothesis that local rainfall supplies enough water for the Hope *W. mirabilis* community. For comparison among the watersheds, a qualitative water requirement of 1 L/day for each plant can be assigned to the three *W. mirabilis* communities based on the number of perennial plants present (Table 5-2). Assuming 10% of the rainfall in each watershed reaches the collective root zones, around 470 mm/year of rainfall would be required to supply the dense *W. mirabilis* community in Hope West. In contrast, the Hope East and Welwitschia Wash watersheds could supply sufficient water to the root zones with 8 and 45 mm of annual rainfall, respectively, which is the same order of magnitude as measured annual rainfall in this area of 20 mm/yr. These first-order calculations are qualitative, but show that rainfall within the Hope West watershed is vastly insufficient for supporting the extant community. However, given the fact that the Hope West community occurs with the outcrop of Matchless Amphibolite and that the larger watershed feeding Hope East takes an orthogonal turn at the beginning of this outcrop, it is possible that the much larger Hope East watershed supplies water to the Hope West vadose zone during flooding events. That is, the fractures of Matchless Amphibolite and the Hope West plants that tap into these fractures, could be receiving quick flow originating in the Hope East watershed during flooding events. Further studies would be needed to show the hydrologic connection and to test the accuracy of the 10% recharge assumption, but this mechanism would explain the apparent water shortage in the Hope West watershed. This mechanism would also be consistent with the fact that Hope West and Hope East *W. mirabilis* stem water had very similar δ^2H and $\delta^{18}O$ values, suggesting a common water source.

5.5 Conclusions

The isotope data confirms that fog deposition does not appear to be a significant source of water for this *W. mirabilis* population. Rather, the stem water isotope values appear to be consistent with a water source that is isotopically similar to the water used by trees in the Kuiseb River. A first-order use of sulfur isotopes as a water tracer appears to corroborate a deep soil water source for this *W. mirabilis* population. The deep, brackish groundwater at Hope does not appear to be a significant water source, and shallow (20-100 cm) soil water cannot explain the isotope signature. The watershed extending 15 km to the Northeast would be able to supply enough water on an annual basis to support the *W. mirabilis* community in the vicinity of Hope Mine. All of this information points to a deep (~2-30 m) soil water source fed by local runoff. These findings are consistent with long-term observations correlating leaf growth with rainfall.

References

Barnes, C.J., Allison, G.B., 1988. Tracing of Water-Movement in the Unsaturated Zone Using Stable Isotopes of Hydrogen and Oxygen. Journal of Hydrology 100, 143-176.
Bornman, C.H., 1972. *Welwitschia Mirabilis* - Paradox of Namib Desert. Endeavour 31, 95-99.
Bornman, C.H., 1977. *Welwitschia mirabilis*: structural and functional anomalies. Madoqua 10, 21-31.

Burgess, S.S.O., Dawson, T.E., 2004. The contribution of fog to the water relations of Sequoia sempervirens (D. Don): foliar uptake and prevention of dehydration. Plant Cell and Environment 27, 1023-1034.

Canadell, J., Jackson, R.B., Ehleringer, J.R., Mooney, H.A., Sala, O.E., Schulze, E.D., 1996. Maximum rooting depth of vegetation types at the global scale. Oecologia 108, 583-595.

Corbin, J.D., Thomsen, M.A., Dawson, T.E., D'Antonio, C.M., 2005. Summer water use by California coastal prairie grasses: fog, drought, and community composition. Oecologia 145, 511-521.

Craig, H., 1961. Isotopic variations in meteoric waters. Science 133, 1702-1703.

Crane, H.R., Griffin, J.B., 1970. University of Michigan Radiocarbon Dates XIII. Radiocarbon 12, 161-180.

Curtis, B., Mannheimer, C., 2005. Tree atlas of Namibia. National Botanical Research Institute, Ministry of Agriculture, Water and Forestry, Windhoek.

Dawson, T.E., 1998. Fog in the redwood forest: ecosystem inputs and use by plants. Oecologia 117, 476-485.

Eller, B.M., Vonwillert, D.J., Brinckmann, E., Baasch, R., 1983. Ecophysiological studies on *Welwitschia mirabilis* in the Namib Desert. South African Journal of Botany 2, 209-223.

ESRI, 2008. ArcGIS 9.3 Spatial Analyst. ESRI, Redlands, CA.

Farr, T.G., Rosen, P.A., Caro, E., Crippen, R., Duren, R., Hensley, S., Kobrick, M., Paller, M., Rodriguez, E., Roth, L., Seal, D., Shaffer, S., Shimada, J., Umland, J., Werner, M., Oskin, M., Burbank, D., Alsdorf, D., 2007. The shuttle radar topography mission. Reviews of Geophysics 45, RG2004.

Gat, J.R., Yakir, D., Goodfriend, G., Fritz, P., Trimborn, P., Lipp, J., Gev, I., Adar, E., Waisel, Y., 2007. Stable isotope composition of water in desert plants. Plant and Soil 298, 31-45.

Gut, S., 1988. Study of the moisture budget of the dunes of the central Namib Desert. Geographisches Institut der Universität Zürich, Zürich.

Hachfeld, B., Jurgens, N., 2000. Climate patterns and their impact on the vegetation in a fog driven desert: The Central Namib Desert in Namibia. Phytocoenologia 30, 567-589.

Henschel, J.R., Seely, M.K., 2000. Long-term growth patterns of *Welwitschia mirabilis*, a long-lived plant of the Namib Desert (including a bibliography). Plant Ecology 150, 7-26.

Herppich, W.B., Flach, B.M.T., vonWillert, D.J., Herppich, M., 1996. Field investigations of photosynthetic activity, gas exchange and water potential at different leaf ages in *Welwitschia mirabilis* during a severe drought. Flora 191, 59-66.

Herre, H., 1961. The age of Welwitschia bainseii (Hook f.) Carr.: C14 Research. Journal of South African Botany 27, 139-140.

Ingraham, N.L., Mark, A.F., 2000. Isotopic assessment of the hydrologic importance of fog deposition on tall snow tussock grass on southern New Zealand uplands. Austral Ecology 25, 402-408.

Irish, J., 2008. Namibian Biodiversity Database. Namibian Ministry of Environment and Tourism.

Jurgens, N., Burke, A., Seely, M.K., Jacobson, K.M., 1997. Desert. In: Cowling, R.M., Richardson, D.M., Pierce, S.M. (Eds.), Vegetation of southern Africa. Cambridge University Press, Cambridge, pp. 189-214.

Kers, L.E., 1967. The distribution of *Welwitschia mirabilis* Hook f. Svensk botanisk tidskrift 61, 97-125.

Klemd, R., Maiden, K.J., Okrusch, M., 1987. The Matchless Copper-Deposit, South-West-Africa Namibia - a Deformed and Metamorphosed Massive Sulfide Deposit. Economic Geology 82, 587-599.

Kutschera, L., Lichtenegger, E., Sobotik, M., Haas, D., 1997. Die Wurzel das neue Organ Ihre Bedeutung für das Leben von *Welwitschia mirabilis* und anderer Arten der Namib sowie von Arten angrenzender Gebiete mit Erklärung des geotropen Wachstums der Pflanzen. Eigenverlag: Pflanzensoziologisches Institut, Klagenfurt, Klagenfurt/Austria.

Kwasny, R., Aul, F., Lohrey, K., 2007. Recent activities and trends in the uranium market. Atw-International Journal for Nuclear Power 52, 696-710.

Lancaster, J., Lancaster, N., Seely, M.K., 1984. Climate of the central Namib Desert. Madoqua 14, 5-61.

Liu, B.L., Phillips, F., Hoines, S., Campbell, A.R., Sharma, P., 1995. Water-Movement in Desert Soil Traced by Hydrogen and Oxygen Isotopes, Chloride, and Cl-36, Southern Arizona. Journal of Hydrology 168, 91-110.

Louw, G., Seely, M., 1982. Ecology of desert organisms. Longman, New York.

McGough, H.N., Groves, M., Mustard, M., Brodie, C., 2004. CITES and Succulents: An introduction to succulent plants covered by the Convention on International Trade in Endangered Species. Royal Botanic Gardens, Kew, London.

Mshigeni, K.E., Hangula, L., Mwandemele, O., 2005. Nostalgic reflections from a visit to the Namib desert in Namibia: A biological, ecological, and palaeontological wonderland. Discovery and Innovation 17, 1-7.

NGS, 2007. Kuiseb 2314. Namibian Geological Survey, Windoek.

Osborne, T.O., Gudde, E., 2001. Rapid growth of *Welwitschia mirabilis* following an episodic rainfall. Journal of the Namibian Scientific Society 42, 9-15.

Pearson, H.H.W., 1909. Percy Sladen Memorial Expedition in South-West Africa, 1908-9, I. Nature 81, 466-467.

Pearson, H.H.W., 1929. Gnetales. Cambridge University Press, Cambridge.

Rodin, R.J., 1953a. Distribution of *Welwitschia mirabilis*. American Journal of Botany 40, 280-285.

Rodin, R.J., 1953b. Seedling morphology of *Welwitschia*. American Journal of Botany 40, 371-378.

Rozanski, K., Araguasaraguas, L., Gonfiantini, R., 1993. Isotopic Patterns in Modern Global Precipitation. In: Swart, P.K., Lohmann, K.C., McKenzie, J., Savin, S. (Eds.), Climate Change in Continental Isotopic Records. American Geophysical Union, Washington, DC.

Schulze, E.-D., Ziegler, H., Stichler, W., 1976. Environmental control of crassulacean acid metabolism in *Welwitschia mirabilis* Hook. Fil. in its range of natural distribution in the Namib Desert. Oecologia 24, 323-334.

Sofer, Z., 1978. Isotopic composition of hydration water in gypsum. Geochimica Et Cosmochimica Acta 42, 1141-1149.

Taborda de Morais, A., 1958. Porque é notável a *Welwitschia mirabilis*. Boletim do Instituto de Angola 11, 53-66.

Tonkin, M.J., Larson, S.P., 2002. Kriging Water Levels with a Regional-Linear and Point-Logarithmic Drift. Ground Water 40, 185-193.

Vogel, J.C., Visser, E., 1981. Pretoria Radiocarbon-Dates 2. Radiocarbon 23, 43-80.

von Willert, D.J., Armbruster, N., Drees, T., Zaborowski, M., 2005. *Welwitschia mirabilis*: CAM or not CAM - what is the answer? Functional Plant Biology 32, 389-395.

von Willert, D.J., Wagner-Douglas, U., 1994. Water Relations, CO2 Exchange, Water-Use Efficiency and Growth of *Welwitschia mirabilis* Hook Fil in 3 Contrasting Habitats of the Namib Desert. Botanica Acta 107, 291-299.

Walker, G.R., Woods, P.H., Allison, G.B., 1994. Interlaboratory comparison of methods to determine the stable isotope composition of soil water. Chemical Geology 111, 297-306.

Walter, H., Breckle, S.W., 1986. Tropical and subtropical zonobiomes. Springer-Verlag, Berlin.

Wang, L.X., Caylor, K.K., Dragoni, D., 2009. On the calibration of continuous, high-precision delta O-18 and delta H-2 measurements using an off-axis integrated cavity output spectrometer. Rapid Communications in Mass Spectrometry 23, 530-536.

Weidlich, B., 2008. Govt grants 25-year uranium license to Canada's Forsys. The Namibian, Windhoek.

West, A.G., Partrickson, S.J., Ehleringer, J.R., 2006. Water extraction times for plant and soil materials used in stable isotope analysis. Rapid Communications in Mass Spectrometry 20, 1317-1321.

Whitaker, C., Berjak, P., Pammenter, N.W., 2008. Abnormal morphology of the embryo and seedling of *Welwitschia mirabilis*, and some observations on seed-associated fungi. South African Journal of Botany 74, 338-340.

Whitaker, C.R., 2006. Studies on the biology, fungal contamination, and conservation of seeds of *Welwitschia mirabilis* Hook fil., School of Biological and Conservation Sciences. University of Kwazulu-Natal, Durban, South Africa.

White, J.W.C., Cook, E.R., Lawrence, J.R., Broecker, W.S., 1985. The D/H ratios of sap in trees: Implications for water sources and tree ring D/H ratios. Geochimica Et Cosmochimica Acta 49, 237-246.

Chapter 6 : Environmental controls on C, N and S cycling in plants of the Namib Desert

Abstract

Nutrient cycles (C, N and S) in the Namib Desert are investigated through a survey of $\delta^{15}N$, $\delta^{13}C$ and $\delta^{34}S$ of plant material and soils along a fog gradient. The coastal Namib Desert in southwestern Africa is hyper-arid in terms of rainfall, but receives up to 100 days of fog each year. This climate regime leads to interesting water relations among the desert flora and fauna. Among many enigmatic characteristics, photosynthesis in *W. mirabilis* has puzzled researchers since the 1970's. Although it is predominantly a C3 plant, $\delta^{13}C$ ranges from -17.4 to -24.2 ‰ in natural habitats, and can be as enriched as -14.4 ‰ under artificial growing conditions. Recently the CAM pathway has been confirmed, but it is dominated by CAM-cycling rather than primary CAM fixation, and the driver for CAM utilization has not been identified. Literature values of $\delta^{13}C$ are re-plotted across a 150 km aridity gradient for comparison with new data from Hope Mine, showing a significant correlation that appears to be explained by rainfall ($R^2 = 0.25$, $p<0.001$). Within the Hope Mine community, there are significant positive relationships among stem size, N, $\delta^{13}C$ and $\delta^{15}N$. The responsible mechanism needs further investigation, but high levels of CAM-cycling and photorespiration along with recycling of N could explain the observed patterns. In addition, there appears to be a reversal of the trend between rainfall and $\delta^{15}N$ found in Kalahari C3 plants, as more depleted $\delta^{15}N$ values were found closer to the coast by.

6.1 Introduction

Namib Desert

The Namib Desert on the southwestern coast of Africa supports diverse flora and fauna while receiving extremely little water as rainfall. Although rainfall pulses are important for many biogeochemical processes in arid ecosystems (Seely, 1978; Jacobson and Jacobson, 1998; Huxman *et al*., 2004), many organisms in the Namib make use of the much more frequent fog and dew events to survive, and even thrive, between these pulses (see Chapter 4). Significant work has been done to describe the utilization of fog water by Namib biota (Louw, 1972; Hamilton and Seely, 1976; Seely and Hamilton, 1976; Loris, 2004; Henschel and Seely, 2008), the general occurrence and characteristics of fog events (Lancaster *et al*., 1984; Pietruszka and Seely, 1985; Olivier, 1995; Henschel *et al*., 1998; Hachfeld and Jurgens, 2000), as well as geochemical aspects of Namib ecosystem relating to fog deposition (Eckardt and Schemenauer, 1998; Goudie and Parker, 1998). However, several questions remain about the role of fog water in the nutrient supply and cycling in the Namib. The central objective of this study is to evaluate the effects of fog on C, N and S cycling in the Central Namib analyzing plant and soil samples from areas that receive different amounts of fog.

Photosynthetic pathways

There are three recognized pathways for photosynthesis: C3, C4 and CAM. The most common is C3, in which CO_2 is taken into the plant with the stomata open during the day and directly fixed via the enzyme ribulose diphosphate carboxylase (RuBP). The CAM and C4 pathways adapt this process by using a different enzyme, phosphoenolpyruvate carboxylase (PEPc), in the first step of CO_2 assimilation. CAM and C4 plants are then able to concentrate the CO_2 near RuBP using two distinct mechanisms: temporally through diurnal organic acid intermediaries in the case of CAM, and spatially through the presence of bundle-sheath cells or other specialized structures in the case of C4 (Keeley and Rundel, 2003). The CAM pathway is most common among succulent species, and is particularly adapted to arid environments because it allows the plant to close its stomata during the day, dramatically reducing water losses. Stomata in CAM plants are open during the night when CO_2 is brought into the mesophyll cells and converted to organic acids, predominantly malate (Kluge *et al.*, 1975). Since the original description of CAM photosynthesis, the indication has been that the CAM operates along with the more productive, less water-efficient C3 pathway under times of lower water stress (Osmond *et al.*, 1973).

Carbon isotopic values of plant material have been useful for identifying photosynthetic pathways in plants due to differences in isotopic discrimination due to (1) diffusion into the cell and (2) RuBP activity under the three pathways described above (Smith and Epstein, 1971; Osmond *et al.*, 1973; Griffiths, 1992; Keeley and Rundel, 2003). However, additional isotopic discrimination and various combinations of the three photosynthetic pathways must be considered when interpreting $\delta^{13}C$ for certain species depending on environmental conditions (Osmond, 1975; Ehleringer and Cooper, 1988; Warren and Adams, 2006). During periods of lowered water or temperature stress, many

CAM plants will utilize the more productive C3 pathway, indicated by differences in $\delta^{13}C$ for plants grown with imposed shorter or longer days (Lerman and Queiroz, 1974). Some plants also exhibit CAM-cycling where respiratory CO_2 is re-fixed into organic acids, and this variation also affects the resulting $\delta^{13}C$ in the plant material (Osmond *et al*., 1980; Griffiths, 1992). The most recent work on photosynthesis in *W. mirabilis* indicates that it utilizes the C3 pathway primarily, with a high degree of CAM-cycling and a small amount of primary CAM activity indicated by low levels of CO_2 uptake at night (von Willert *et al*., 2005), and this is consistent with less conclusive previous studies (Ting and Burk, 1983; Winter and Schramm, 1986; von Willert and Wagner-Douglas, 1994).

6.2 Methods

Plant and soil samples were collected along the precipitation gradient in the Central Namib. Sampling sites included dunes, gravel plains, and the ephemeral Kuiseb River at various distances from the coast: Rooibank (10 km), Swartbank (35 km), Gobabeb (56 km) and Hope (78 km). Plant species sampled include common trees of the Kuiseb (*Acacia erioloba*, *Faidherbia albida*, *Tamarix usneoides*), shrubs of the gravel plains (*Zygophyllum stapffii* , *Arthraerua leubnitziae* , *Calicorema capitata*), a shrub (*Trianthema hereroensis*) and grass (*Stipagrostis sabulicola*) of the dunes, as well as the Namib endemics *W. mirabilis* and *Acanthosicyos horridus*.

Microclimates at Hope were characterized by Leaf Wetness, Air Temperature, and relative humidity at three sites: central sandy wash (“Hope Wash”), the top of a rocky outcrop (“Hope Rocks”), and the rocky slope leading down to the wash (“Hope Slopes”). Leaf Wetness Sensors (Decagon Devices, Inc.) were placed on the tops of *W. mirabilis* leaves, and air temperature and relative humidity were determined at 30 cm above the ground surface – approximately the average height of the *W. mirabilis* canopy. Continuous measurements were made for 9 days in January 2009 and compared to concomitant measurements at the western base of High Dune near Gobabeb, 22 km to the west of Hope.

Plant and soil samples were dried (60°C), homogenized, weighed into tin capsules and converted to CO_2, N_2 and SO_2 for isotope analysis using a Carlo Erba elemental analyzer (EA) which is coupled to an OPTIMA stable isotope ratio mass spectrometer (Micromass, Manchester, UK). Carbon and nitrogen isotopes were determined with a single combustion using a dual furnace system composed of an oxidation furnace at $1020^{o}C$ and a reduction furnace at $650^{o}C$. Using the EA, the samples for sulfur were separately pyrolyzed at $1050^{o}C$ using a combination oxidation and reduction furnace system. The resulting gases are dried in a water trap ($MgClO_4$) and separated in a capillary column before flowing into the source of the mass spectrometer. The ratio of heavy to light isotope (e.g. $^{13}C/^{12}C$) in each sample is measured with respect to a reference peak of carbon dioxide, nitrogen or sulfur dioxide gases which have been calibrated against NBS 22, atmospheric N_2 and NBS 127, respectively. The stable isotopic ratio is reported as in Equation 1-1, using the following abundance ratios of the heavy to light isotopes: $^{13}C/^{12}C$, $^{15}N/^{14}N$ or $^{34}S/^{32}S$. The standard for carbon is the Peedee Belemnite limestone (PDB), for nitrogen the standard is atmospheric N_2 (Air) and for sulfur the standard is the Canyon Diablo Troilite (CDT) which are assigned values of 0.0‰ for $\delta^{13}C$, $\delta^{15}N$, and $\delta^{34}S$. For sulfur and carbon the isotope value is corrected for contribution from ^{18}O content. This correction involves multiplying by 1.09 for sulfur (Giesemann *et al*., 1994) after adjusting the value to an internal standard ($BaSO_4$). The reproducibility of the measurement is typically better than ±0.2‰ for these elements using the continuous flow interface on the OPTIMA.

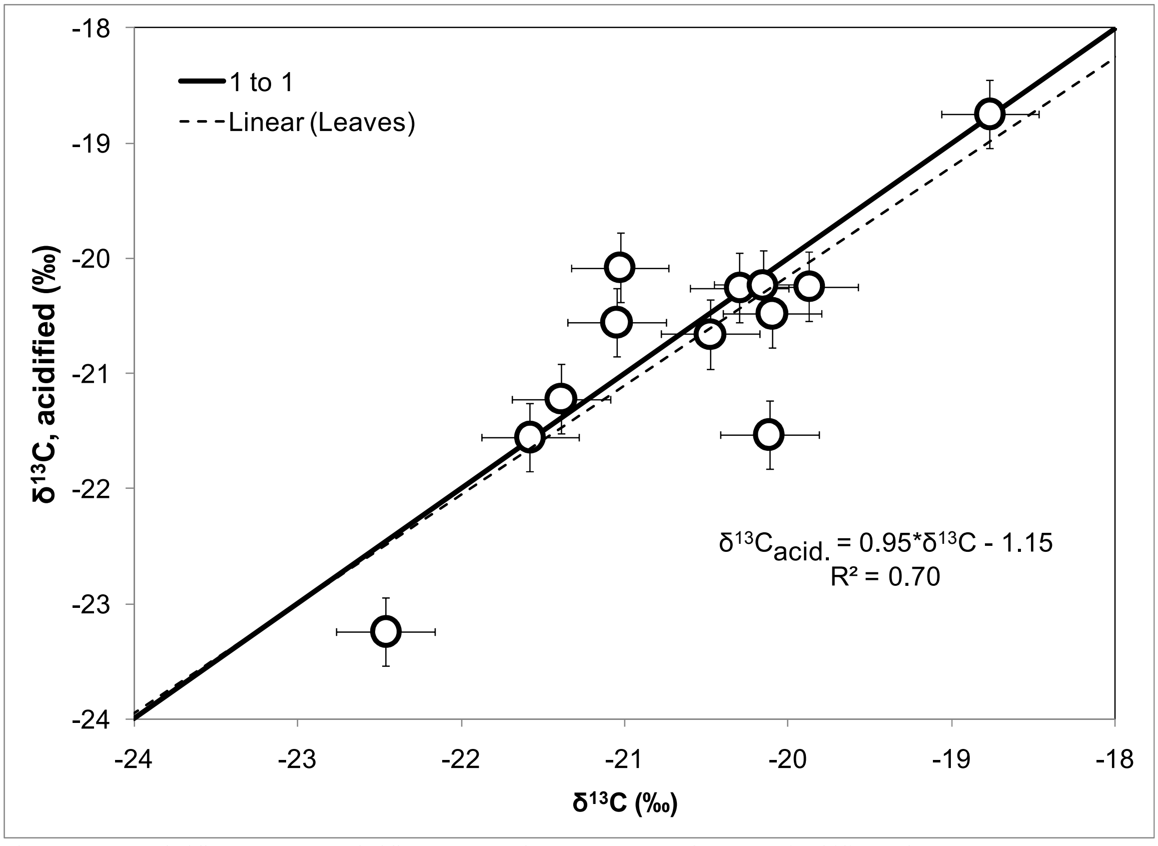

Figure 6-1: Acidified and un-acidified carbon isotope values for *W. mirabilis* leaf samples.

Previous studies have found a 0.5 ‰ enrichment in $\delta^{13}C$ after acidifying *W. mirabilis* leaves (von Willert *et al*., 2005). This observation was tested for leaves from 12 individuals, and no significant consistent change was seen in the acidified samples (Figure 6-1). Although no effect was seen in the 12 samples tested here, the enrichment due to carbonate removal found previously indicates that the presence of any carbonates would diminish the apparent CAM utilization in a given leaf.

6.3 Results

Microclimates of three locations at Hope indicate local variability in fog and dew deposition, which may help interpret the observed carbon and nitrogen isotope patterns. Three light fog events occurred at Gobabeb, and none at Hope during the 9 days of continuous measurements. Leaf Wetness, however, was experienced as dew deposition at Hope on four of the days (Figure 6-2). The dew wetness at Hope was the same order of magnitude as the first and third fog events, but no dew was experienced at Hope during the second Gobabeb fog event. Among the three sites at Hope, the highest elevation site at the top of a rock outcrop receieved much less deposition and shorter duration of wetting than the other two sites. This is likely due to higher or more consistent winds at this exposed site. Air temperature 30 cm above the soil surface was slightly lower at this site than in the middle of the wash. The wetting events and the nightly rise of relative humidity began sooner at Gobabeb than at Hope, which is consistent with a westerly (Atlantic) source of moisture being advected inland.

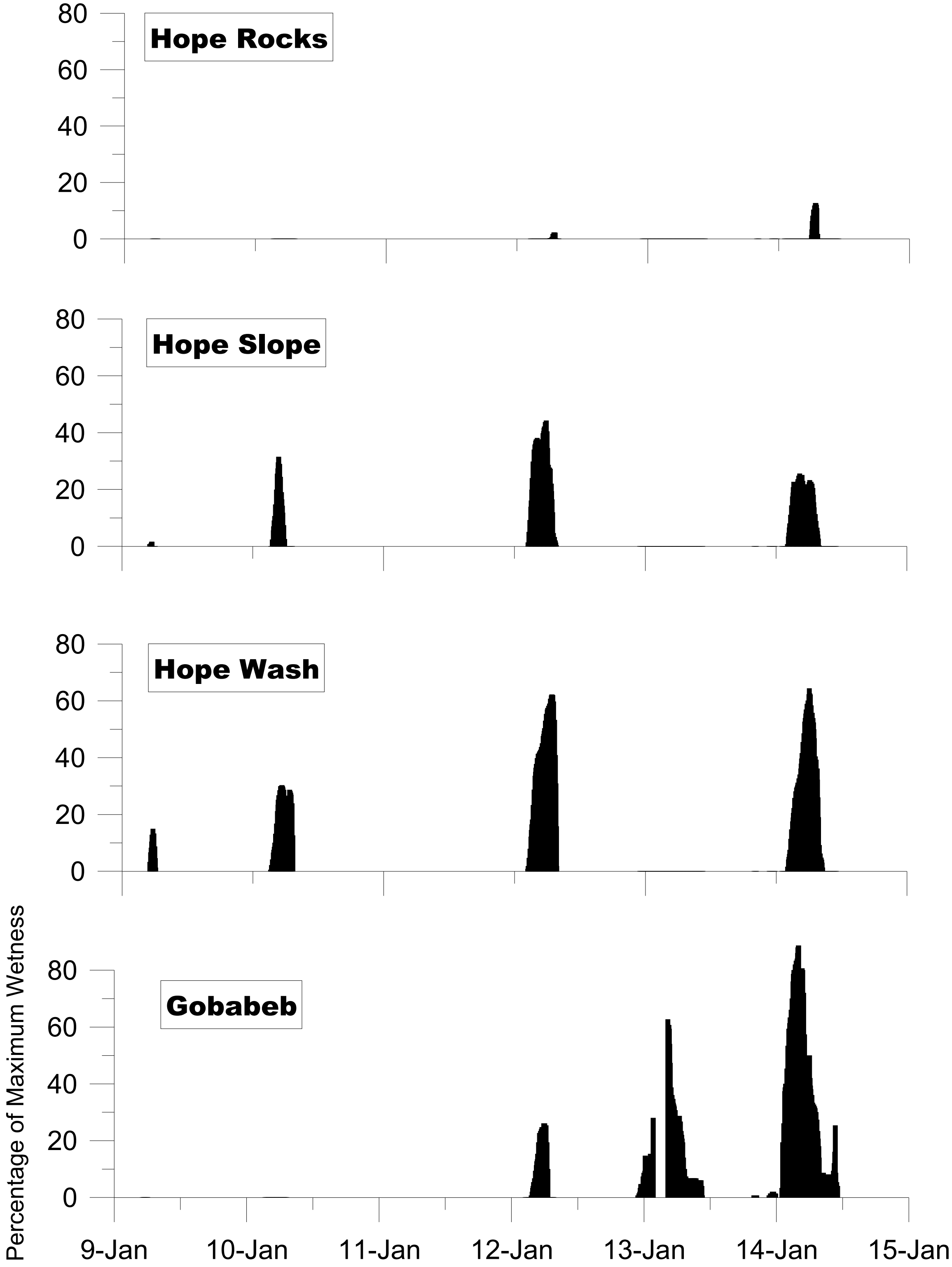

Figure 6-2: Leaf Wetness at Hope and Gobabeb in January 2009.

Note: Erratic values removed for Gobabeb 13 January between 1:20 AM and 4:20 AM

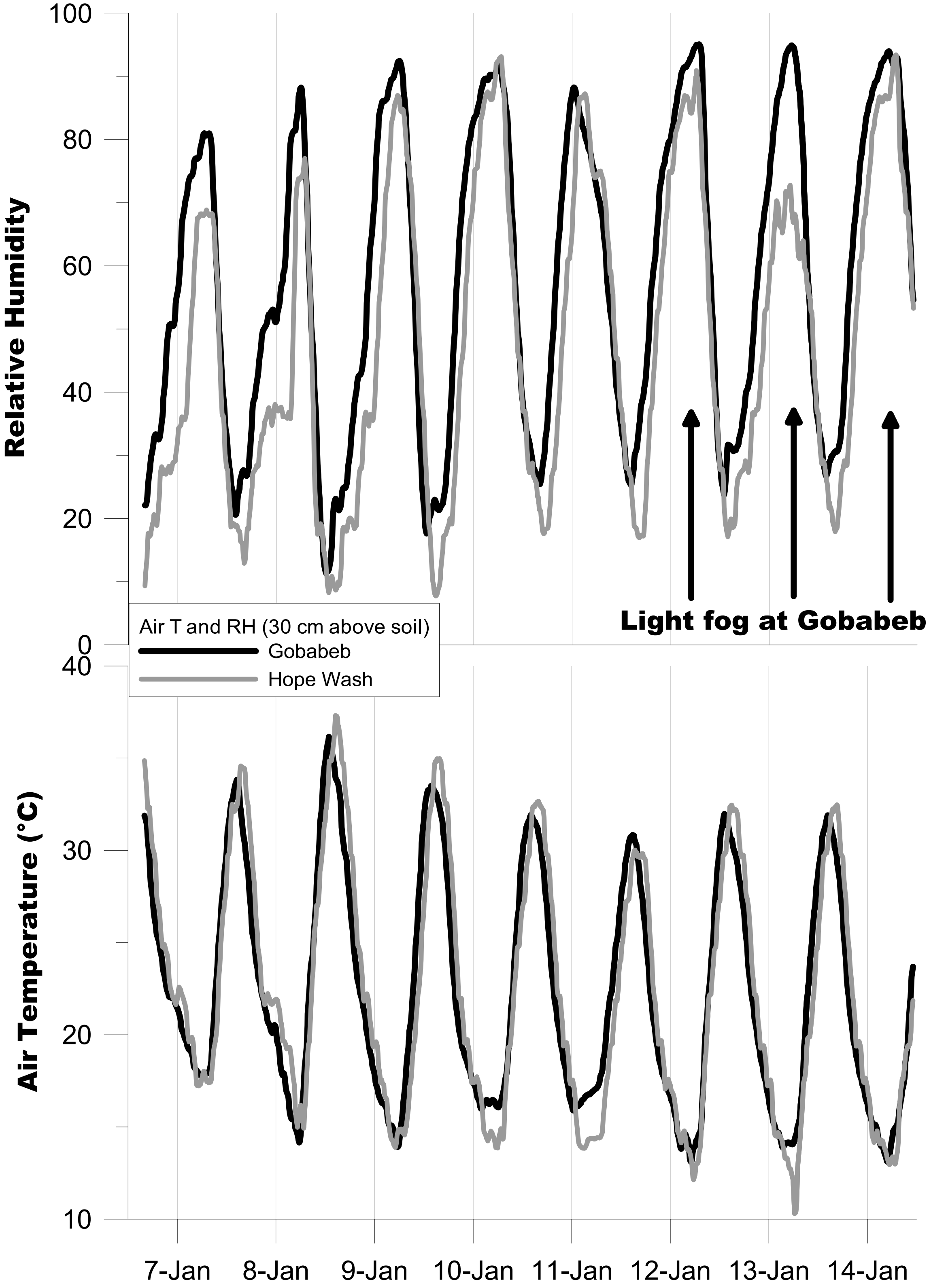

Figure 6-3: Air temperature and relative humidity at Hope and Gobabeb in January 2009.

Table 6-1: Carbon, nitrogen and sulfur for plant material (stem / leaf[1]) and associated soils.

Plant[2]	Water %	n	C %	N %	S %	δ^{13}C	δ^{15}N	δ^{34}S
S	48 / 46	23 / 8	45.4 / 44.2	0.6 / 1.3	0.07 / 0.13	-13.8 / -15.4	0.7 / 3.1	16.0 / 14.6
T	57 / 82	20 / 10	44.7 / 29.2	0.4 / 1.9	0.10 / 0.33	-13.3 / -11.3	4.5 / 6.2	15.4 / 14.1
N[1]	74 / 72	3 / 8	43.7 / 44.3	1.3 / 1.4	0.16 / 0.64	-22.7 / -23.6	10.4 / 6.6	14.6 / 14.0
Dune Soils		11	n.d.	n.d.	0.01	n.a.	n.a.	18.7
A	40 / 58	13 / 3	45.9 / 46.9	0.8 / 2.2	0.14 / n.a.	-28.8 / -30.0	5.4 / 4.0	11.5 / n.a.
F	53 / 60	9 / 4	44.5 / 46.0	0.8 / 2.1	0.28 / n.a.	-28.7 / -28.7	3.5 / 1.8	11.6 / 10.4
X	43 / 53	8 / 3	44.0 / 34.8	0.6 / 1.2	0.50 / 1.39	-26.0 / -23.2	7.6 / 9.9	5.2 / 11.2
Riverbed Soils		6	0.1	n.d.	0.01	n.a.	n.a.	9.5
W	39 / n.a.	12 / 32	42.0 / 38.7	0.9 / 1.4	0.07 / 0.11	-19.7 / -20.6**	5.9 / 1.9***	10.2 / 12.6
L	47 / 65	6 / 4	37.3 / 34.7	0.9 / 1.2	0.72 / 0.24	-22.5 / -21.6	4.1 / 8.0	15.9 / 16.4
C	41 / 55	3 / 2	43.4 / 41.1	0.9 / 1.8	0.10 / 0.12	-22.7 / -22.9	7.6 / 9.6	13.9 / 14.1
Z	36 / 89	20 / 5	40.2 / 13.8	0.5 / 0.5	0.12 / 6.1	-22.6 / -23.9	4.1 / 5.7	14.6 / 13.8
Gravel Plains Soils		9	0.6	0.06	0.03	n.a.	n.a.	15.2

n.a. – not analyzed, n.d. – not detected

* - stem and leaf samples (*W. mirabilis* was the only species evaluated) are significantly different at 95% confidence level (** 99%; *** 99.9%)

1 – "Leaf" material in *A. horridus* is simply younger succulent stem material

2 – Species represented: S = *Stipagrostis sabulicola,* T = *Trianthema hereroensis*, N = *Acanthosicyos horridus,* A = *Acacia erioloba*, F = *Faidherbia albida*, X = *Tamarix usneoides,* W = *Welwitschia mirabilis*, L = *Arthraerua leubnitziae*, C = *Calicorema capitata*, Z = *Zygophyllum stapffii*

The overall distribution of δ^{13}C for the three known C3 species in the study is somewhat bimodal (Figure 6-4), with the more enriched values found in *A. horridus*. The one highly enriched value (-17.8 ‰) was from a *T. hereroensis* leaf sample taken in Swartbank that also had an anomalously enriched δ^{15}N value of 15.8 ‰. The corresponding stem sample had values of -25.4 ‰ (δ^{13}C) and 12.3 ‰ (δ^{15}N). The only known C4 species sampled was *S. sabulicola*, which had highly enriched δ^{13}C values and relatively depleted δ^{15}N values (Figure 6-5). However, *T. hereroensis* showed even greater enrichment in δ^{13}C. No Krantz anatomy was found the leaves of *T. hereroensis*, suggesting that it is not C4 (Vogel and Seely, 1977), but the highly enriched δ^{13}C values indicate that it would have to make extremely efficient use of the CAM pathway (Keeley and Rundel, 2003). Interestingly, it has recently been found that Krantz anatomy is not required for the C4 pathway, and 20 species of the *Trianthema* genus have been shown to use C4 (Keeley and Rundel, 2003; Sage, 2005). In fact, *Trianthema* is one of the genera thought to represent an evolutionary origin of the C4 pathway (Sage, 2005) making the lack of Krantz anatomy and extremely enriched $\delta^{13}C$ values an interesting paradox that leaves the photosynthetic pathway uncertain. Thus, *T. hereroensis* is plotted with the "Unknown" group, and the possibility remains that it is either CAM or a non-Krantz C4. The other species with "Unknown" photosynthetic pathways (*Z. stapffii*, *C. capitata,* and *A. leubnitziae*) are all likely C3, potentially with CAM-cycling activity as will be discussed with respect to *W. mirabilis*.

Male *W. mirabilis* individuals were found to be significantly more enriched in ^{13}C than females (95% confidence, two-tailed t-test, assuming unequal variances) with respective mean values of -20.1 ‰ and -20.9 ‰ (Figure 6-6). Similarly, *W. mirabilis* stem material was enriched by 0.9 ‰ relative to leaf material (99% confidence). The $\delta^{15}N$ values in *W. mirabilis* leaves were also significantly depleted relative to stem material (99.9% confidence), and this was consistent among both male and female individuals (Figure 6-7). There was also a significant relationship between $\delta^{13}C$ and $\delta^{15}N$ for the *W. mirabilis* stem material. Leaf material did not follow a consistent trend, but did seem to form three groups on the $\delta^{15}N$ vs $\delta^{13}C$ plot. Notably, Group C was most enriched in $\delta^{13}C$ and also tended to occur on the rocky slopes of the study area, whereas Group B was grouped towards the center of the upper main wash area, overlapping with a few individuals from Groups A and C (Figure 6-8).

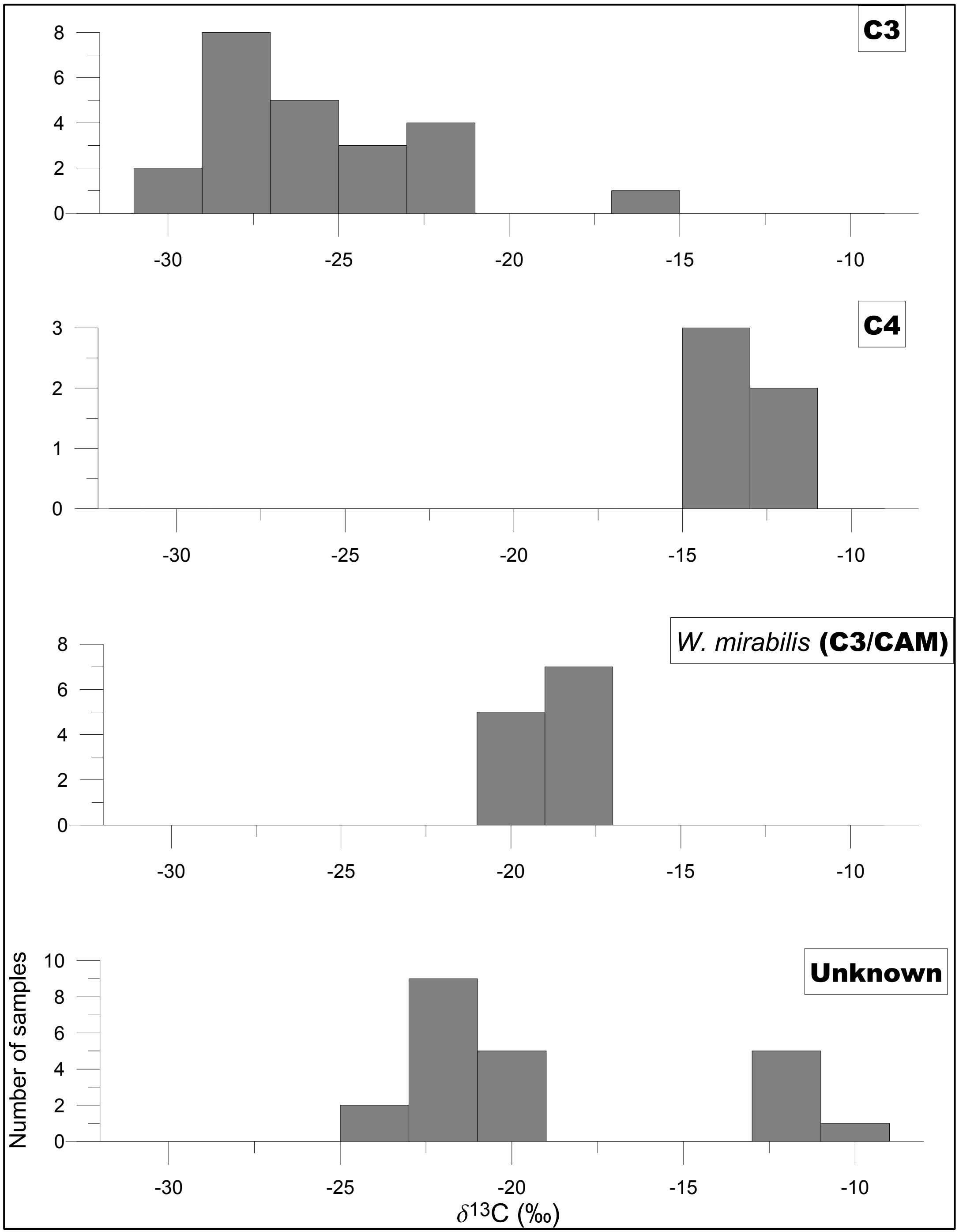

Figure 6-4: Distribution of δ^{13}C values for all plant samples.

Note: The C3 group includes *A. erioloba*, *F. albida*, *T. usneoides*; C4 includes *S. sabulicola*; C3/CAM includes *W. mirabilis*; and Unknown includes *Z. stapffii*, *C. capitata*, *A. leubnitziae*, and *T. hereroensis*.

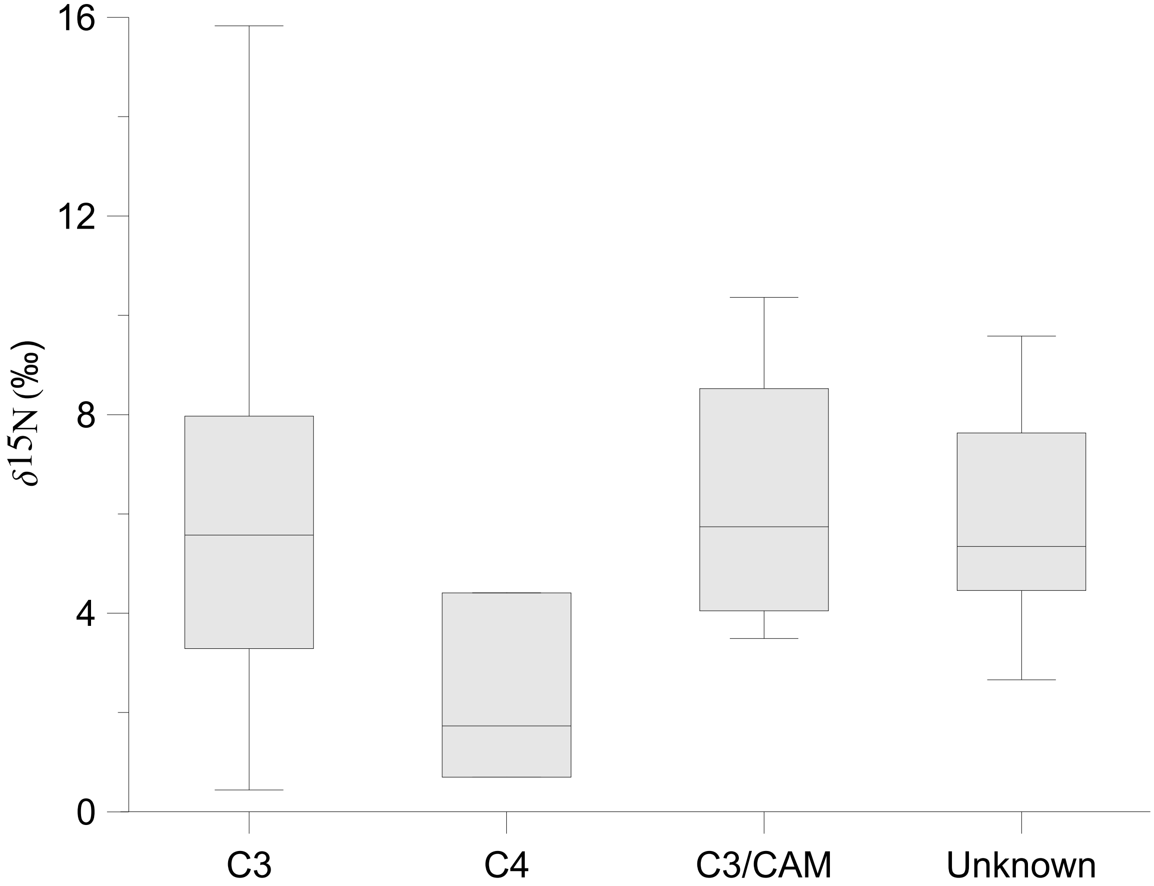

Figure 6-5: Distribution of δ^{15}N for all plant samples.
Note: Species groupings as in Figure 6-4.

Water content of stem material ranged fom 36 to 57 % for all species except the stem succulent *A. horridus* at 74%. Leaf material had higher water content in all species except *A. horridus* and *S. sabulicola*, which dropped slightly to 72 % and 46 % compared to 74 % and 48 %, respectively in stem material. “Leaf” and “Stem” material in these species refers to younger and older material, respectively, rather than herbaceous and woody as in the other species sampled. In both the stem succulent (*A. horridus*) and perennial grass (*S. sabulicola*), the “Stem” material is larger in diameter and somewhat differentiated relative to the “Leaf” material in that there is an outer layer of non-green tissue with variably green internal tissue. Leaf N content was highest in the Mimosaceae trees *A. erioloba* and *F. albida* at 2.2 and 2.1 % (dry weight basis), and ranged from 1.3 to 1.9 % in all dune and gravel plains species except *Z. stapffii* which had the lowest foliar N at 0.5 %. This value was low even for stem N content, which ranged from 0.5 to 0.9 % for all but *A. horridus* (1.3 %). The *A. horridus* values match well with the 1.2% reported previously (Klopatek and Stock, 1994). The C and S content of *Z. stapffii* were also anomalous: low for C at 13.8% and high for S at 6.1% relative to foliar ranges of 29-47% and 0.11-1.4% for C and S, respectively in the other species. The S content of leaves was higher than the corresponding stem material for all species except *A. leubnitziae*, in which stem material had three times the foliar concentration of S. Only marginally higher concentrations of S were found in the leaves of *W. mirabilis, S. sabulicola* and *C. capitata* relative to their stem material. *A. leubnitziae* had higher S concentrations in its stem than its leaves. And, in the remaining species foliar S was three to four times the stem concentration.

The $\delta^{34}S$ content of all dune and most gravel plains plants was fairly consistent around 14 to 16 ‰, and no significant difference was seen between stem and leaf values. Similar values were found in gravel plains soils, although a more enriched average value of 18.7 ‰ was found in the dune soils. The riverbed trees and *W. mirabilis* were much more depleted at 10.2 ‰, which reflects values seen in riverbed sediments (9.5 ‰) and alluvial groundwater (10.8 ‰). Groundwater directly beneath the *W. mirabilis* population was enriched at 16.5 ‰, as was groundwater of the interdune area at Nara Valley (14.9 ‰).

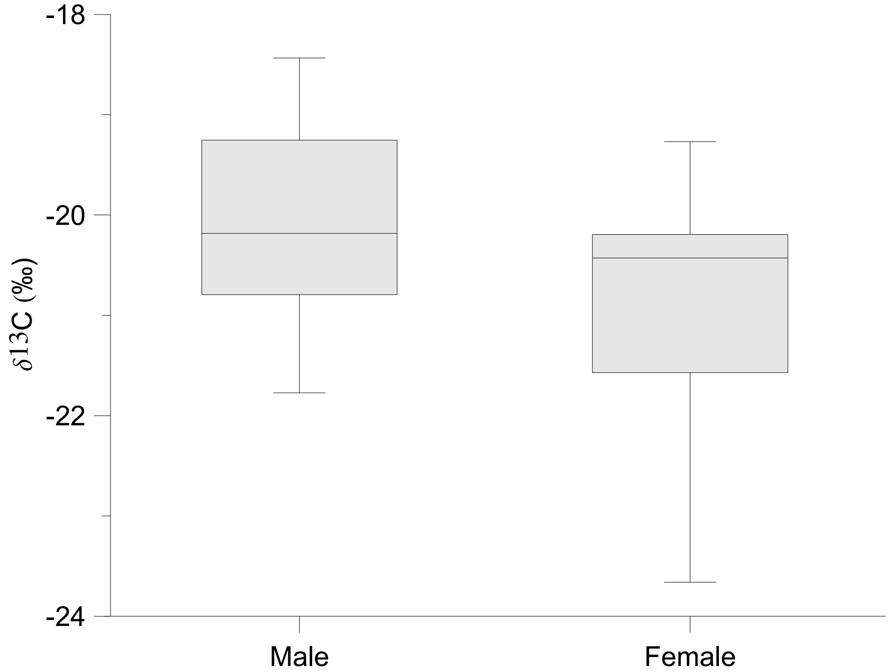

Figure 6-6: δ^{13}C values for all *W. mirabilis* male and female samples.
Note: Both leaf and stem samples are included.

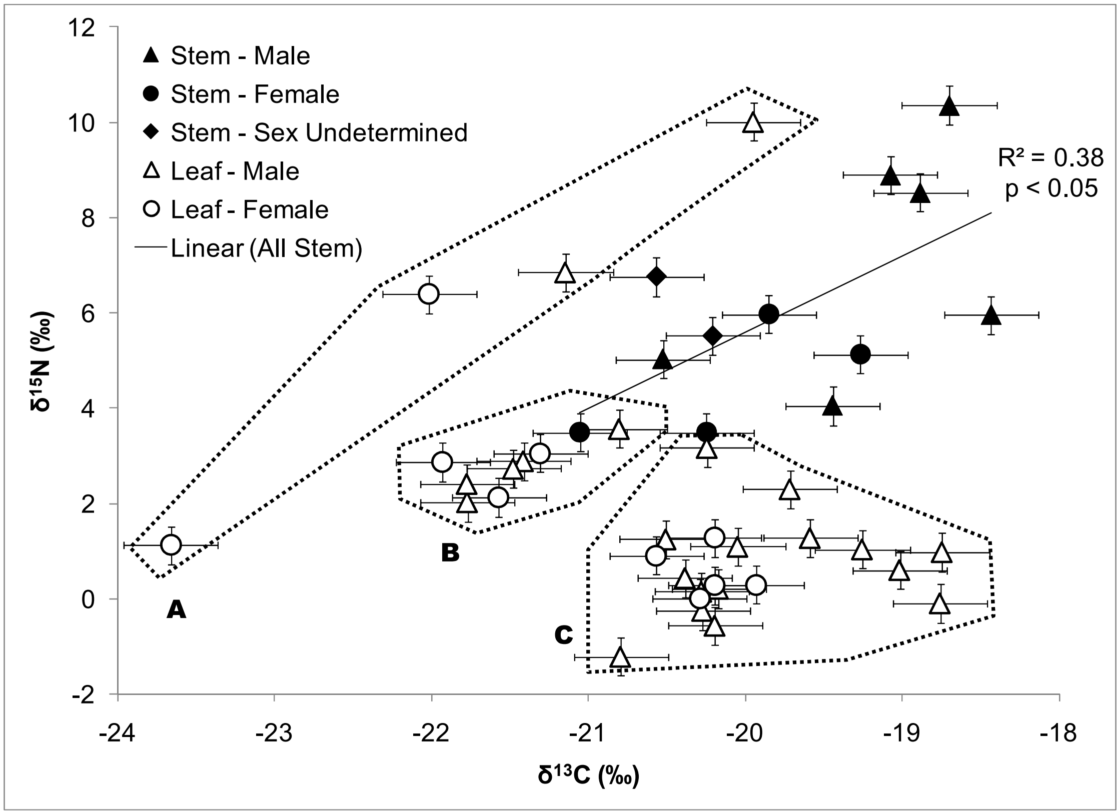

Figure 6-7: δ^{15}N and δ^{13}C for all *W. mirabilis* leaf (open symbols) and stem (filled symbols) samples.
Note: Male and female individuals are also identified where this information is available.

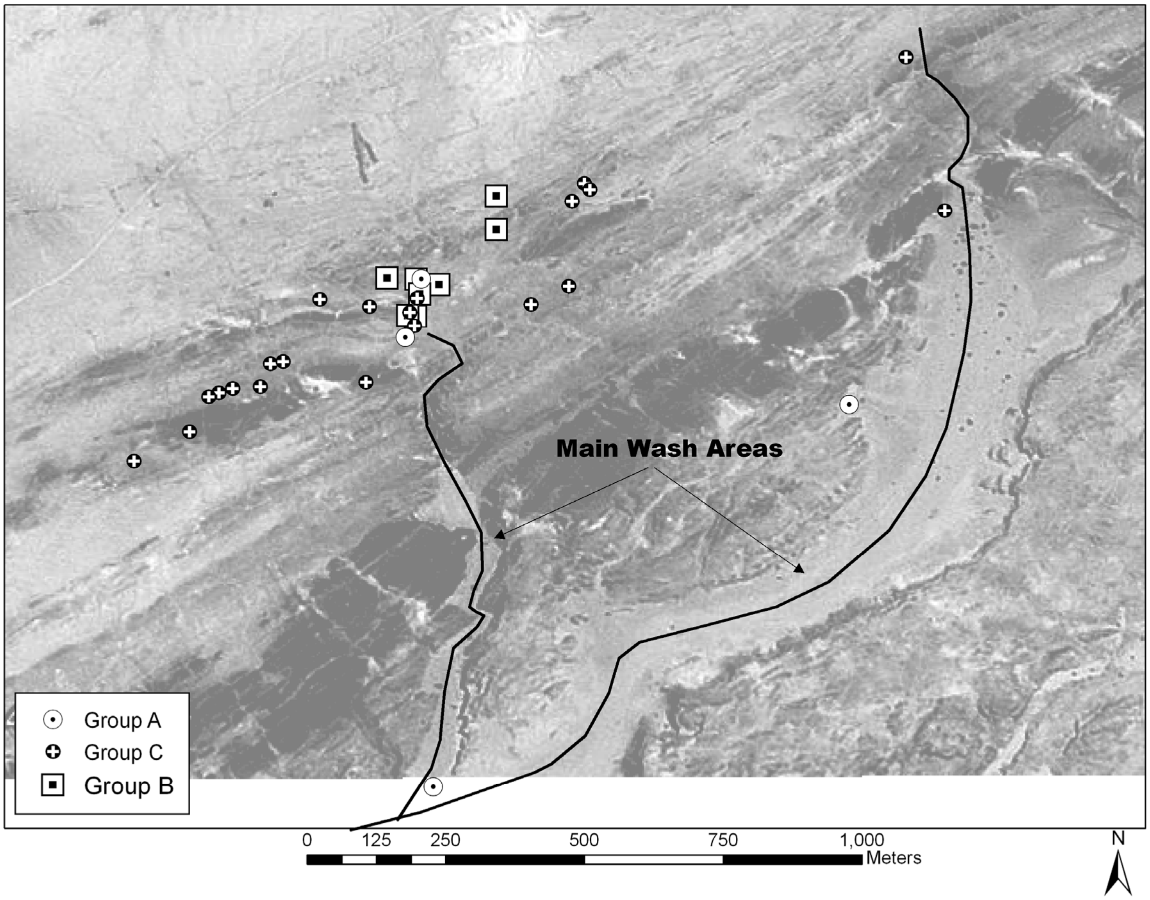

Figure 6-8: Aerial view of Hope Mine and the *W. mirabilis* leaf samples.
Note: Groups correspond to labels given in Figure 6-8.

6.4 Discussion

Plant water status and carbon cycling

One strategy for coping with very dry soils is to increase the solute concentration in the leaves, thereby creating a gradient in osmotic potential that promotes the movement of water from the stems to the leaves. This is suggested in the succulent plants studied here through the S concentration difference between stems and leaves. The ratio of leaf to stem S is 3, 4 and 50 in *T. hereroensis, A. horridus* and *Z. stapffii*, respectively.

A ratio of 2.8 was also seen in *T. usneoides*, a tree which is known to exude salts from its leaves leaving a grayish appearance. The S ratio in the two stem succulents *T. hereroensis* and *Z. stapffii* follows their respective ratios of leaf to stem water content: 1.6 and 2.5. However, *A. leubnitziae* has a leaf to stem water content ratio of 0.97 and an S content ratio of 0.34. This pattern is consistent with *A. leubnitziae* using osmotic potential to store water in its stem – a water-saving measure.

This osmotic regulation of water movement has also been suggested to help explain the use of CAM-cycling and the associated high organic acid content of *W. mirabilis* leaves, which was also found to be highly variable along a single leaf (von Willert *et al*., 2005). The high concentration of organic acids, e.g. malic acid, would not necessarily correlate with high foliar S concentrations. The leaf to stem S ratio in *W. mirabilis* was 1.6 – similar to trees and non-succulent shrubs. A better indication of the long-term impact of CAM or CAM-cycling activity is $\delta^{13}C$ of younger and older plant material. The $\delta^{13}C$ values in older material have been found to be enriched relative to younger material in CAM plants (Lerman and Queiroz, 1974). This pattern was observed here in *W. mirabilis*, with more enriched values in the woody stem relative to the leaves (Table 6-1). The leaves would have a maximum age on the order of decades compared to centuries for the stem material (Vogel and Visser, 1981; von Willert and Wagner-Douglas, 1994). This pattern could be due to changes in environmental conditions over time or to changes in the $\delta^{13}C$ of the material between the initial fixation of CO_2 in the leaves and the subsequent synthesis of structural organic compounds found in the stem. The latter is more likely due to the high levels of CAM-cycling activity and photorespiration (von Willert and Wagner-Douglas, 1994; von Willert *et al*., 2005), and the potential loss of ^{12}C during these processes (Griffiths, 1992; Warren and Adams, 2006). It should also be noted that the stem material of *W. mirabilis* has a highly unusual wood histology. The woody material contains both xylem and phloem produced by successive cambia, but also uniquely includes calcium oxalate crystals in the intercellular space. This last feature appears to be limited to just one other genera -- Ephedra (Carlquist and Gowans, 1995; Carlquist, 2007). These oxalate crystals could be related to the organic acids involved in CAM-cycling, and could thus contribute to the enriched δ^{13}C value of the stem material given preferential loss of ^{12}C during CAM-cycling.

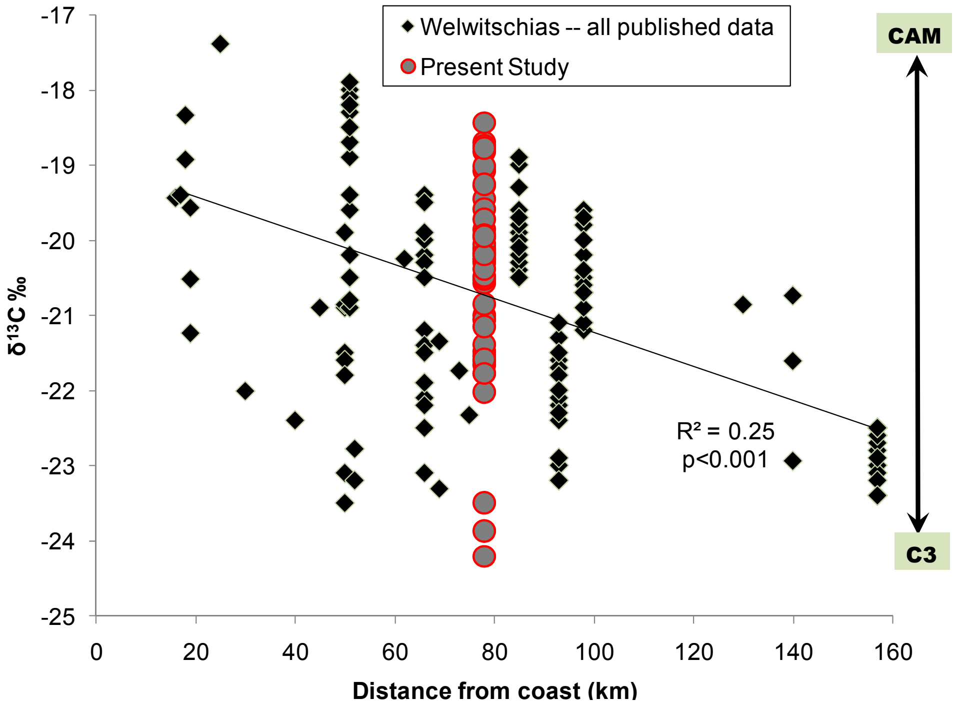

Figure 6-9: Carbon isotope values for *W. mirabilis* individuals with distance from the coast. Note: “All published data” are from four references (Schulze *et al*., 1976; Vogel and Seely, 1977; Vogel and Visser, 1981; von Willert *et al*., 2005). Data from Vogel and Visser (1981) and the present study (50 and 78 km from the coast, respectively) include both stem and leaf material, whereas the other data are all from leaf samples; original field notes from Schulze *et al*. (1976) were used to confirm distances; Data from von Willert *et al*. (2005) were generated randomly within the published minimum and maximum values for each site (51, 66, 85, 93, 98, and 157 km from the coast), and repeated realizations of the random values change the r^2 value by 0.04 but do not change the statistical significance of the overall trend.

The presence of more enriched $\delta^{13}C$ values in *W. mirabilis* closer to the coast has been suggested in two studies of leaf material across the Central Namib (Schulze *et al*., 1976; von Willert *et al*., 2005). The $\delta^{13}C$ values of the present study are consistent with these previous surveys, and together they form significant relationship when plotted with distance from the coast (Figure 6-9). To gain a rough estimate of how this relationship is explained by precipitation, corresponding rain and fog values were pulled from Figure 1-2 for each *W. mirabilis* location. The resulting correlations (Figure 6-10) were all statistically significant, but rain explained more of the variation in the data ($R^2 = 0.25$) than fog ($R^2 = 0.11$) or rain and fog combined ($R^2 = 0.21$). Rain still only explains 25% of the variability in the data, and an overall striking feature of the data is that $\delta^{13}C$ is highly variable at any given site. This variability is smallest (1 ‰) at the site with the highest rainfall, and greatest at the lower rainfall sites (3.5 ‰). The low rainfall sites are on average about 4 ‰ more enriched than the highest rainfall site, but this range in mean values is matched at individual sites within about 80 km of the coast, including the present study area at Hope Mine. Similar site-specific variability has been seen in C3 plants of the Sonoran Desert, with enrichment of about 2.5 ‰ in the more water-stressed rocky slope habitats attributed to both increased stomatal closure and decreased water-use efficiency relative to plants in the sandy wash areas (Ehleringer and Cooper, 1988). This pattern was broadly observed in the *W. mirabilis* population at Hope Mine, with many plants of the rocky slopes enriched by about 1.5 ‰ (Figure 6-7). A similar observation was made in the first survey of $\delta^{13}C$ in W. mirabilis across different habitats, where a 2 ‰ enrichment was seen in individuals located on hilltops relative to those in the valleys

(Schulze *et al.*, 1976). Differential CAM utilization is not necessary to explain such an enrichment (Winter and Schramm, 1986), but given the CAM functionality in *W. mirabilis*, it remains possible that the enrichment is due to a combination of stomatal control, CAM, CAM-cyling and photorespiration.

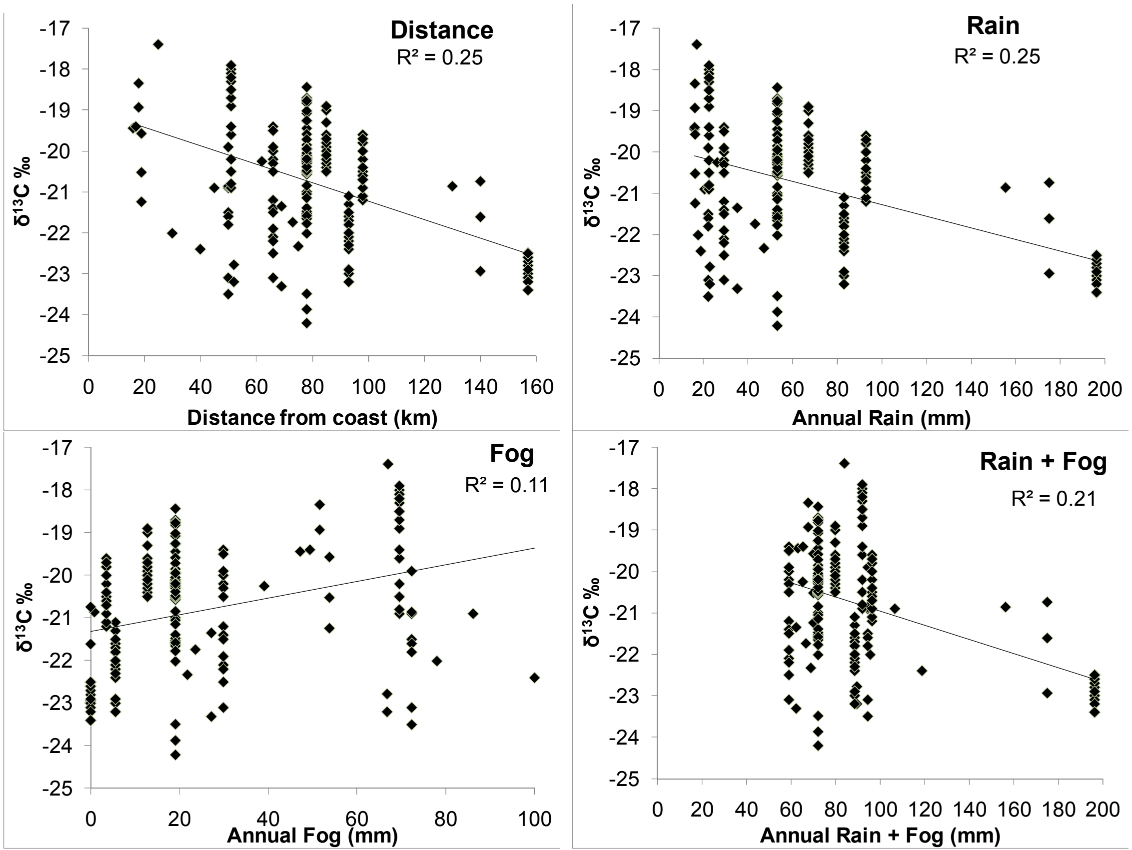

Figure 6-10: Correlations among δ^{13}C, distance from the coast and mean annual rain and fog. Note: Rain and fog data derived from linear interpolations among the data shown in Figure 1-2.

Precipitation and nitrogen cycling

A significant trend towards more enriched δ^{15}N values at lower rainfall sites was observed in C3 plants across the Kalahari, which covers much of southern Africa (Swap *et al.*, 2004). This matches the pattern seen in Australia (Schulze *et al.*, 1998; Schulze *et* *al*., 1999), but does not include any sites with less than 200 mm of annual rainfall. It is now possible to extend this sub-continental scale transect into the hyperarid Namib using data from literature (Schulze *et al*., 1991a) and the present study. Doing so reveals an apparent reversal of the trend, with more depleted values in the fog zone (Figure 6-11). There are many possible explanations for such a pattern, as discussed with respect to the original trend (Swap *et al*., 2004). Three possible contributing factors to different N-cycling in the Namib compared to the Kalahari are (1) coastal N deposition, (2) colonization of surface soils and rocks by N-fixing cyanobacterial crusts, and (3) frequent surface soil wetting. High productivity associated with the Benguela upwelling off of the Namibian coast leads to N releases from wetlands and seal colonies along the coast, which could be delivered to inland locations via fog or dry deposition with the prevailing SW winds. Although significant cyanobacterial crusts occur in the Kalahari (Aranibar *et al*., 2003), their presence is potentially more extensive in the fog zone of the Namib (Lange *et al*., 1991; Lange *et al*., 1994; Lalley *et al*., 2006). The frequent wetting of soil surfaces from fog and dew will likely increase the average rate of denitrification on an annual basis relative to the low rainfall sites in the Kalahari. Faster denitrification leads to less isotope discrimination. The N content of Namib soils (Table 6-1) is at the low end of the range of soils in the Kalahari (Wang *et al*., 2007a), which would tend to favor the third proposed mechanism – frequent soil wetting – which would promote the loss of N from the soil. Although each of the proposed mechanisms could be active in the ecosystem, frequent soil wetting appears to be most consistent with the fog occurrence, which makes this hyper-arid system look more like a 300 mm rainfall site in the Kalahari according to the trend of Swap *et al.* (2004).

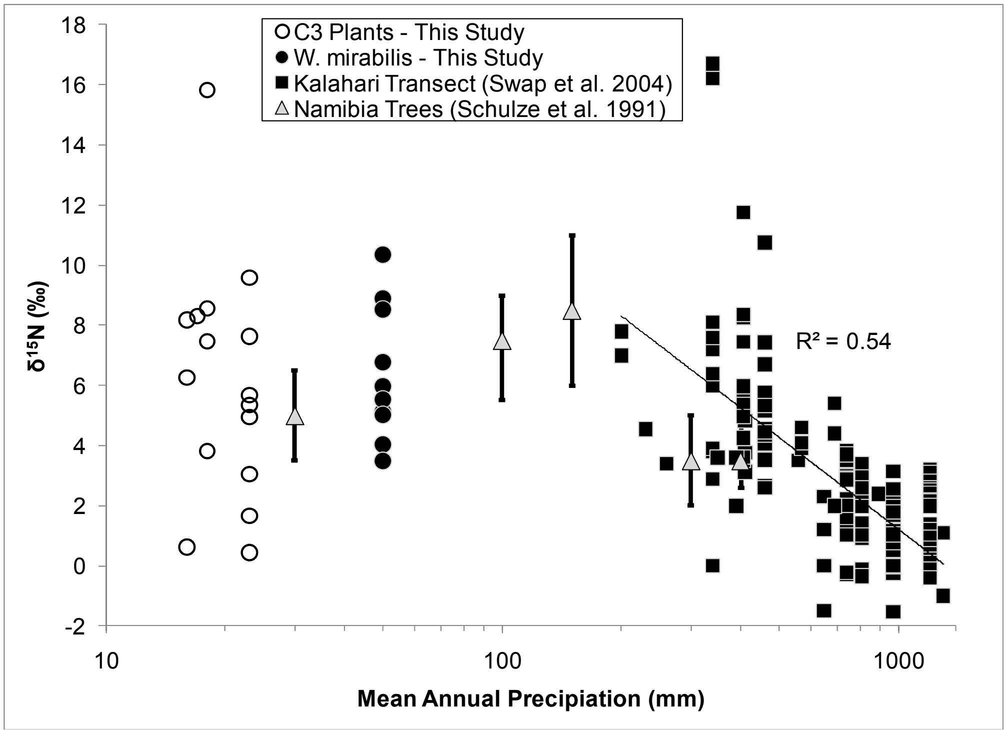

Figure 6-11: δ^{15}N for C3 plants across the Kalahari (Swap *et al.*, 2004), C3 trees across the Namib (Schulze *et al.*, 1991a), and C3/CAM plants in the present study.

Carbon and nitrogen in *W. mirabilis*

Five related correlations (Figure 6-12) indicate that enriched δ^{13}C values are associated with larger woody stems, enriched δ^{15}N and higher N concentration. As discussed above, enriched δ^{13}C values could be a result of (1) increased use of the CAM pathway for fixing atmospheric CO_2, (2) increased CAM-cycling and associated leakage of ^{12}C, and (3) preferential loss of ^{12}C during photorespiration. A similar pattern of enriched δ^{13}C associated with enriched δ^{15}N was seen in N-fixing Namib trees, but not in other trees (Schulze *et al.*, 1991a). Also similar to the *W. mirabilis* pattern, CAM species across the Namib tend to have enriched $\delta^{13}C$ with higher N content, although it is unclear whether such a correlation exists with $\delta^{15}N$ (Schulze *et al*., 1991b). The N relationship with $\delta^{15}N$ was not significant in the *W. mirabilis* stems (Figure 6-12), although this relationship has been commonly seen in other species (Wang *et al*., 2007b).

One interpretation of the association between N and $\delta^{13}C$ is that intrinsic Water Use Efficiency (WUE) increases with more N available for uptake. N-fixing plants have lower WUE (implied by depleted $\delta^{13}C$ values) if they fix more N than if they obtain it from the surrounding environment (Schulze *et al*., 1991a). Elsewhere, a positive relationship between foliar N and WUE was seen in C4 but not C3 plants (Sage and Pearcy, 1987). However, in a separate study a negative relationship between foliar N and WUE (implied by $\delta^{13}C$) was found for C3 but not C4 or CAM plants (Schmidt *et al*., 1993). Overall, the mechanism driving the relationship between $\delta^{13}C$ and N found in *W. mirabilis* is uncertain, but appears to be related to internal C and N cycling given the high levels of photorespiration and CAM-cycling as well as the associated $\delta^{15}N$ patterns.

Given the association between enriched $\delta^{15}N$ and lower rainfall in the Kalahari (Figure 6-11), it is tempting to explain the positive correlation between $\delta^{15}N$ and $\delta^{13}C$ in *W. mirabilis* as an extension of the precipitation gradient. This would imply that individuals that are more water-stressed, as indicated by more enriched $\delta^{13}C$, also take up N more enriched in ^{15}N. This could be explained by having isotopically distinct sources of N, with larger plants able to tap into N pools that are deeper in the subsurface and therefore less influenced by, e.g. denitrification occurring in shallower soils. The $\delta^{15}N$ of plant material has been used to show utilization of different N-pools in arid environments

(Page, 1995; Arndt *et al.*, 2004). However, this N-source explanation is not necessarily consistent with the strong positive correlations between $\delta^{15}N$, $\delta^{13}C$ and plant size. The $\delta^{15}N$ of various soil N pools would need to be determined to confirm this explanation. Also, discussed below, this N-source mechanism appears to be outperformed by more complex models of $\delta^{15}N$ fractionation in plants.

Nitrogen and carbon cycles are necessarily linked as most foliar N is involved in photosynthesis (Evans, 1989), and typically the simple relationship of lower stomatal conductance leading to higher WUE and lower photosynthetic nitrogen use efficiency is used to interpret $\delta^{13}C$ and N-status of plants (Warren and Adams, 2006). Thus, lower N content or higher C:N values correlated with more enriched $\delta^{13}C$ values is seen in many systems (Evans, 1989; Schmidt *et al.*, 1993; Li *et al.*, 2009). However, the reverse relationship is seen in the *W. mirabilis* stem samples, which is consistent with evidence that the typical relationship holds for C3 plants but not C4 or CAM (Schmidt *et al.*, 1993).

Alternative explanations of the C-N relationships in *W. mirabilis* could come from intraspecific differences in photosynthetic internal conductance, loss of ^{12}C during photorespiration or CAM-cycling, and loss of ^{14}N during uptake, assimilation, and recycling of N from older to younger material. Changes in internal conductance – i.e. conductance from the sub-stomatal cavity to the carboxylation site – can have a variable effect on $\delta^{13}C$ of the same order of magnitude as stomatal conductance (Warren and Adams, 2006). However, although internal conductance differences could alter $\delta^{13}C$ by up to 1.9 ‰ (Warren and Adams, 2006), it would not necessarily be expected to alter δ^{15}N as is seen here (Figure 6-12).

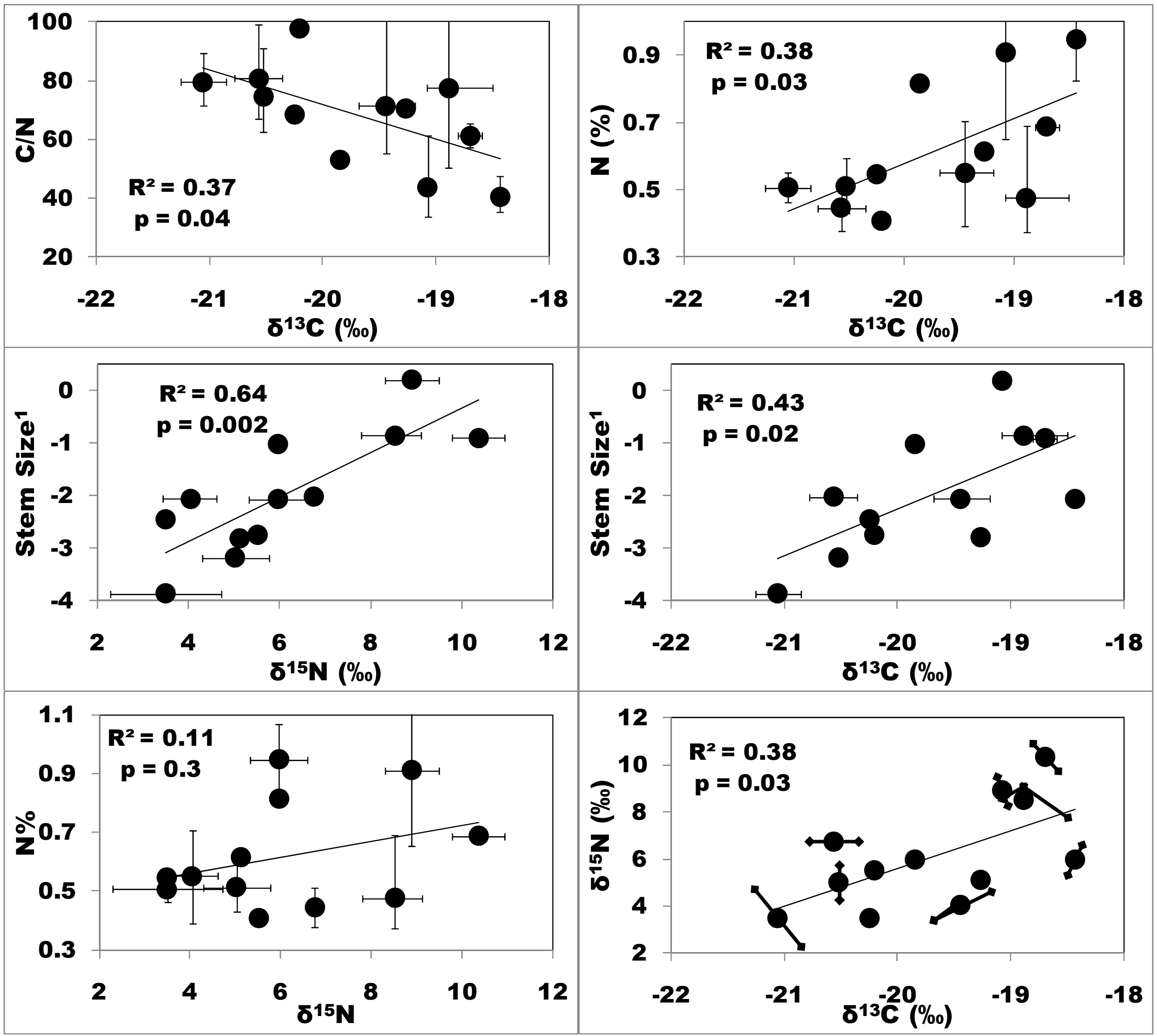

Figure 6-12: Correlations among δ^{13}C, δ^{15}N, C, N and plant size for *W. mirabilis* stem samples.
Note: Error bars show the minimum and maximum values from a given stem where multiple analyses (n=2 or 3) were performed along a core, except δ^{15}N vs δ^{13}C, in which paired samples for each stem are plotted to illustrate the lack of a consistent pattern across a stem.
1 – Natural log of exposed basal meristem when viewed from above. Although the exact mechanism causing this relationship remains uncertain as discussed in the text, the empirical inclusion of δ^{13}C in this general C-N-size relationship indicates that an overall contributing factor is the growth or metabolism of the plants. The use of log-transformations has a long history in helping to describe patterns in biological data (Barnes, 1952; Gingerich, 2000), including studies of plant size and nutrient distribution (Niklas *et al.*, 2005; Kerkhoff *et al.*, 2006). The log-transformation has a solid statistical foundation (Gaddum, 1945; Tukey, 1957; Box and Cox, 1964), and a recent critical review of its use concluded that geometric relationships are necessary in allometric studies (Kerkhoff and Enquist, 2009).

Photorespiration is high (40-80% of gross photosynthesis) in *W. mirabilis* (von Willert *et al*., 2005) compared with typical photosynthesis-limiting levels in C3 plants of 20-30% (Sage, 2005). CAM-cycling is a coping mechanism for the heat and temperature stress associated with photorespiration, and the two processes explain the continued leaf growth under a net negative CO_2 balance observed in some *W. mirabilis* individuals (von Willert and Wagner-Douglas, 1994). Loss of CO_2 or other compounds during photorespiration would enrich the $\delta^{13}C$ value of the remaining carbon. Similarly, CAM-cycling, or the re-fixation of CO_2 released via respiration, would preferentially fix ^{13}C (Griffiths, 1992), and even if this fractionation factor was small the process could have a cumulative effect over time in the remaining carbon. The photorespiration and CAM-cycling mechanisms are consistent with the association between larger, and presumably older, *W. mirabilis* individuals and more enriched $\delta^{13}C$ values.

The enrichment of ^{15}N in the *W. mirabilis* stem material is consistent with enrichment due to the recycling of N from older to younger tissues found in tree rings (Elhani *et al*., 2005), but this would tend to leave behind a lower N content in the enriched material, and the opposite was seen here. In addition, the enrichment seen here is greater in magnitude than found in tree rings, suggesting an additional mechanism, possibly related to CAM-cycling, but certainly related to plant size. The long-lived leaves of *W. mirabilis* could play a role in the stem $\delta^{15}N$ enrichment. That is, longer average residence time of N in the leaves could lead to preferential loss of ^{14}N as a result of CAM-cycling or the preferential partitioning of ^{15}N into organic compounds that are translocated to the stem. Although the longer life of leaves is a trait that conserves nutrients, it can also reduce Nitrogen Use Efficiency (Berendse and Aerts, 1987). Together with the overall slow growth and metabolism in *W. mirabilis* (von Willert and Wagner-Douglas, 1994; Henschel and Seely, 2000), these factors imply overall slow rates of biochemical reactions. Slower reactions allow for more isotope fractionation and in biosynthesis the heavier ^{15}N would be energetically more favorable than ^{14}N (Hoefs, 2005), leading to more enriched $\delta^{15}N$ values in compounds that are ultimately stored in the woody parts of the plant. Specifically, the assimilation of N into organic compounds by various enzymes (e.g. glutamate dehydrogenase, glutamine synthetase) in terrestrial organisms has been shown to lead to products more enriched in ^{15}N (Weiss *et al.*, 1988; Fogel and Cifuentes, 1993). Further, recycling of the organic N through photorespiration can lead to enriched $\delta^{15}N$ in proteins and depleted $\delta^{15}N$ in the remaining glutamate (Werner and Schmidt, 2002). The N residence time mechanism is supported by the observation of more enriched $\delta^{15}N$ in larger individuals.

The final $\delta^{15}N$ in stem material reflects an integration of source $\delta^{15}N$ and isotope fractionations during assimilation and subsequent cycling of N within the plant. Further studies of $\delta^{15}N$ in available N at different depths in the sub-surface could also help explain the enrichment, as this rooting-depth explanation has been shown to be important elsewhere for desert perennials (Handley *et al.*, 1994; Arndt *et al.*, 2004). Where this association has been observed elsewhere, higher N availability leading to higher rates of photosynthesis has been a suggested mechanism (Handley *et al.*, 1994). However, this N-source mechanism would not explain the positive correlation between $\delta^{15}N$ and $\delta^{13}C$, and more detailed models that incorporate all contributory factors are more consistently able to replicate observations (Robinson *et al*., 1998; Evans, 2001). Lastly, changes in atmospheric $\delta^{13}C$ over the life of the plants should be considered as a source of variation in stem $\delta^{13}C$ (McCarroll and Loader, 2004) given the possibility that the carbon was fixed hundreds of years ago in the larger individuals (see Chapter 5).

6.5 Conclusions

The inverse relationship between $\delta^{13}C$ in *W. mirabilis* and distance to the Namibian coast has been suggested for more than 30 years, and is shown here to be statistically significant after compiling all available $\delta^{13}C$ values. Using a first-order approximation of fog and rain deposition across the $\delta^{13}C$ gradient reveals that rainfall explains much more of the variability than fog or total precipitation. This finding implies a de-coupling of *W. mirabilis* physiology from fog occurrence, which is consistent with long-term growth observations of a population 70 km from the coast as well as stable water isotope findings in the present study (see Chapter 4).

The relationship between Mean Annual Rainfall and $\delta^{15}N$ of C3 plants across the Kalahari does not extend into the hyperarid Namib. There appears to be a trend towards more depleted $\delta^{15}N$ values closer to the coast from a peak in central Namibia. This finding indicates (1) additional inputs of N with depleted $\delta^{15}N$ in areas closer to the Namibian coast, (2) an overall more closed system with respect to N in the Namib, or (3) faster denitrification rates possibly related to frequent wetting of surface soil.

The brown, dried ends of *W. mirabilis* leaves, still attached to growing leaves, were found to be significantly depleted in both $\delta^{13}C$ and $\delta^{15}N$ relative to stem samples

(Table 6-1). In addition, samples taken from a single long-dead stem on display at the research station, although within the range of other stem samples, did not fall along the same C-N relationships shown in Figure 6-12. These observations indicate that changes in $\delta^{13}C$ and $\delta^{15}N$ after death of the tissue (still attached to the green leaf) could be due to resorption or degradation, and that it is important to incorporate this information into sampling strategies when studying *W. mirabilis*.

It remains unclear whether CAM-cycling and photorespiration can account for the enrichment in ^{15}N seen in *W. mirabilis* stem material. However, some indirect evidence is available. The $\delta^{13}C$ enriching processes of CAM-cycling and photorespiration have been clearly demonstrated as central to *W. mirabilis* physiology (Ting and Burk, 1983; Winter and Schramm, 1986; von Willert and Wagner-Douglas, 1994; von Willert *et al.*, 2005). These processes are the likely sources of $\delta^{13}C$ enrichment, and, in turn, are related to the $\delta^{15}N$ enrichment given the significant positive relationship between $\delta^{13}C$ and $\delta^{15}N$ observed in the stem samples. The isotopic enrichment is also positively correlated with the logarithm of stem size, which could provide an alternative explanation for enriched $\delta^{15}N$ values related to rooting depth with larger plants having access to isotopically distinct N sources.

References

Aranibar, J.N., Anderson, I.C., Ringrose, S., Macko, S.A., 2003. Importance of nitrogen fixation in soil crusts of southern African arid ecosystems: acetylene reduction and stable isotope studies. Journal of Arid Environments 54, 345-358.

Arndt, S.K., Kahmen, A., Arampatsis, C., Popp, M., Adams, M., 2004. Nitrogen fixation and metabolism by groundwater-dependent perennial plants in a hyperarid desert. Oecologia 141, 385-394.

Barnes, H., 1952. The Use of Transformations in Marine Biological Statistics. ICES J. Mar. Sci. 18, 61-71.

Berendse, F., Aerts, R., 1987. Nitrogen-Use-Efficiency: A biologically meaningful definition? Functional Ecology 1, 293-296.

Box, G.E.P., Cox, D.R., 1964. An analysis of transformations. Journal of the Royal Statistical Society. Series B (Methodological) 26, 211-252.

Carlquist, S., 2007. Successive cambia revisited: ontogeny, histology, diversity, and functional significance. Journal of the Torrey Botanical Society 134, 301-332.

Carlquist, S., Gowans, D.A., 1995. Secondary Growth and Wood Histology of *Welwitschia*. Botanical Journal of the Linnean Society 118, 107-121.

Eckardt, F.D., Schemenauer, R.S., 1998. Fog water chemistry in the Namib Desert Namibia. Atmospheric Environment 32, 2595-2599.

Ehleringer, J.R., Cooper, T.A., 1988. Correlations between Carbon Isotope Ratio and Microhabitat in Desert Plants. Oecologia 76, 562-566.

Elhani, S., Guehl, J.M., Nys, C., Picard, J.F., Dupouey, J.L., 2005. Impact of fertilization on tree-ring delta N-15 and delta C-13 in beech stands: a retrospective analysis. Tree Physiology 25, 1437-1446.

Evans, J.R., 1989. Photosynthesis and nitrogen relationships in leaves of C-3 plants. Oecologia 78, 9-19.

Evans, R.D., 2001. Physiological mechanisms influencing plant nitrogen isotope composition. Trends in Plant Science 6, 121-126.

Fogel, M.L., Cifuentes, L.A., 1993. Isotope Fractionation during Primary Production. In: Engel, M.H., Macko, S.A. (Eds.), Organic geochemistry : principles and applications. Plenum Press, New York, pp. 73-98.

Gaddum, J.H., 1945. Lognormal distributions. Nature 156, 463-466.

Giesemann, A., Jager, H.J., Norman, A.L., Krouse, H.P., Brand, W.A., 1994. Online sulfur isotope determination using an elemental analyzer coupled to a mass spectrometer. Analytical Chemistry 66, 2816-2819.

Gingerich, P.D., 2000. Arithmetic or geometric normality of biological variation: an empirical test of theory. Journal of Theoretical Biology 204, 201-221.

Goudie, A.S., Parker, A.G., 1998. Experimental simulation of rapid rock block disintegration by sodium chloride in a foggy coastal desert. Journal of Arid Environments 40, 347-355.

Griffiths, H., 1992. Carbon isotope discrimination and the integration of carbon assimilation pathways in terrestrial CAM plants. Plant Cell and Environment 15, 1051-1062.

Hachfeld, B., Jurgens, N., 2000. Climate patterns and their impact on the vegetation in a fog driven desert: The Central Namib Desert in Namibia. Phytocoenologia 30, 567-589.

Hamilton, W.J., Seely, M.K., 1976. Fog basking by the Namib Desert beetle, *Onymacris unguicularis*. Nature 262, 284-285.

Handley, L.L., Odee, D., Scrimgeour, C.M., 1994. d15N and d13C patterns in savanna vegetation: Dependence on water availability and disturbance. Functional Ecology 8, 306-314.

Henschel, J., Mtuleni, V., Gruntkowski, N., Seely, M., Shanyengana, S.E., 1998. NAMFOG: Namibian application of fog-collecting systems Desert Research Foundation of Namibia, Windhoek.

Henschel, J.R., Seely, M.K., 2000. Long-term growth patterns of *Welwitschia mirabilis*, a long-lived plant of the Namib Desert (including a bibliography). Plant Ecology 150, 7-26.

Henschel, J.R., Seely, M.K., 2008. Ecophysiology of atmospheric moisture in the Namib Desert. Atmospheric Research 87, 362-368.

Hoefs, J., 2005. Stable Isotope Geochemistry. Springer, New York.

Huxman, T.E., Snyder, K.A., Tissue, D., Leffler, A.J., Ogle, K., Pockman, W.T., Sandquist, D.R., Potts, D.L., Schwinning, S., 2004. Precipitation pulses and carbon fluxes in semiarid and arid ecosystems. Oecologia 141, 254-268.

Jacobson, K.M., Jacobson, P.J., 1998. Rainfall regulates decomposition of buried cellulose in the Namib Desert. Journal of Arid Environments 38, 571-583.

Keeley, J.E., Rundel, P.W., 2003. Evolution of CAM and C-4 carbon-concentrating mechanisms. International Journal of Plant Sciences 164, S55-S77.

Kerkhoff, A.J., Enquist, B.J., 2009. Multiplicative by nature: Why logarithmic transformation is necessary in allometry. Journal of Theoretical Biology 257, 519-521.

Kerkhoff, A.J., Fagan, W.F., Elser, J.J., Enquist, B.J., 2006. Phylogenetic and growth form variation in the scaling of nitrogen and phosphorus in the seed plants. American Naturalist 168, E103-E122.

Klopatek, J.M., Stock, W.D., 1994. Partitioning of nutrients in *Acanthosicyos-horridus*, a keystone endemic species in the Namib Desert. Journal of Arid Environments 26, 233-240.

Kluge, M., Bley, L., Schmid, R., 1975. Malate synthesis in crassulacean acid metabolism (CAM) via a double CO2 dark fixation? In: Marcelle, R. (Ed.), Enivronmental and biological control of photosynthesis. Dr. W. Junk b.v., The Hague.

Lalley, J.S., Viles, H.A., Copeman, N., Cowley, C., 2006. The influence of multi-scale environmental variables on the distribution of terricolous lichens in a fog desert. Journal of Vegetation Science 17, 831-838.

Lancaster, J., Lancaster, N., Seely, M.K., 1984. Climate of the central Namib Desert. Madoqua 14, 5-61.

Lange, O.L., Meyer, A., Ullmann, I., Zellner, H., 1991. Microclimate Conditions, Water-Content and Photosynthesis of Lichens in the Coastal Fog Zone of the Namib Desert - Measurements in the Fall. Flora 185, 233-266.

Lange, O.L., Meyer, A., Zellner, H., Heber, U., 1994. Photosynthesis and Water Relations of Lichen Soil Crusts - Field-Measurements in the Coastal Fog Zone of the Namib Desert. Functional Ecology 8, 253-264.

Lerman, J.C., Queiroz, O., 1974. Carbon fixation and isotope discrimination by a crassulacean plant - dependence on photoperiod. Science 183, 1207-1209.

Li, C.Y., Wu, C.C., Duan, B.L., Korpelainen, H., Luukkanen, O., 2009. Age-related nutrient content and carbon isotope composition in the leaves and branches of Quercus aquifolioides along an altitudinal gradient. Trees-Structure and Function 23, 1109-1121.

Loris, K., 2004. Nebel als Wasserressource für den Strauch Arthraerua leubnitziae. In: Walter, H., Breckle, S.-W. (Eds.), Ökologie der Erde: Spezielle Ökologie der tropischen und subtropischen Zonen. Spektrum-Verlag, pp. 485-489.

Louw, G.N., 1972. The role of advective fog in the water economy of certain Namib Desert animals. Symposia of the Zoological Society of London 31, 297-314.

McCarroll, D., Loader, N.J., 2004. Stable isotopes in tree rings. Quaternary Science Reviews 23, 771-801.

Niklas, K.J., Owens, T., Reich, P.B., Cobb, E.D., 2005. Nitrogen/phosphorus leaf stoichiometry and the scaling of plant growth. Ecology Letters 8, 636-642.

Olivier, J., 1995. Spatial-Distribution of Fog in the Namib. Journal of Arid Environments 29, 129-138.

Osmond, C.B., 1975. Environmental control of photosynthetic options in crassulacean plants. In: Marcelle, R. (Ed.), Environmental and biological control of photosynthesis. Dr. W. Junk b.v., The Hague, pp. 311-321.

Osmond, C.B., Allaway, W.G., Sutton, B.G., Troughto.Jh, Queiroz, O., Luttge, U., Winter, K., 1973. Carbon isotope discrimination in photosynthesis of CAM plants. Nature 246, 40-42.

Osmond, C.B., Winter, K., Powles, S.B., 1980. Adaptive significance of carbon dioxide cycling during photosynthesis in water-stressed plants. In: Turner, N.C., Kramer, P.J. (Eds.), Adaptation of plants to water and high temperature stress. John Wiley & Sons, New York, pp. 139-154.

Page, H.M., 1995. Variation in the natural abundance of N-15 in the halophyte, *Salicornia virginica*, associated with groundwater subsidies of nitrogen in a southern California salt-marsh. Oecologia 104, 181-188.

Pietruszka, R.D., Seely, M.K., 1985. Predictability of two moisture sources in the Namib Desert. South African Journal of Science 81, 682-685.

Robinson, D., Handley, L.L., Scrimgeour, C.M., 1998. A theory for N-15/N-14 fractionation in nitrate-grown vascular plants. Planta 205, 397-406.

Sage, R.F., 2005. Atmospheric CO2, environmental stress, and the evolution of C4 photosynthesis. In: Ehleringer, J., Cerling, T.E., Dearing, M.D. (Eds.), A history of atmospheric CO2 and it effects on plants, animals, and ecosystems. Springer, New York, pp. 185-213.

Sage, R.F., Pearcy, R.W., 1987. The nitrogen use efficiency of C3 and C4 plants II. Plant Physiology 84, 959-963.

Schmidt, G., Gebauer, G., Widmann, K., Ziegler, H., 1993. Influence of nitrogen supply and temperature on stable carbon-isotope ratios in plants of different photosynthetic pathways (C(3), C(4), CAM). Isotopenpraxis 29, 9-13.

Schulze, E.-D., Ziegler, H., Stichler, W., 1976. Environmental control of crassulacean acid metabolism in *Welwitschia mirabilis* Hook. Fil. in its range of natural distribution in the Namib Desert. Oecologia 24, 323-334.

Schulze, E.D., Farquhar, G.D., Miller, J.M., Schulze, W., Walker, B.H., Williams, R.J., 1999. Interpretation of increased foliar delta N-15 in woody species along a rainfall gradient in northern Australia. Australian Journal of Plant Physiology 26, 296-298.

Schulze, E.D., Gebauer, G., Ziegler, H., Lange, O.L., 1991a. Estimates of Nitrogen-Fixation by Trees on an Aridity Gradient in Namibia. Oecologia 88, 451-455.

Schulze, E.D., Lange, O.L., Ziegler, H., Gebauer, G., 1991b. Carbon and Nitrogen Isotope Ratios of Mistletoes Growing on Nitrogen and Non-Nitrogen Fixing Hosts and on Cam Plants in the Namib Desert Confirm Partial Heterotrophy. Oecologia 88, 457-462.

Schulze, E.D., Williams, R.J., Farquhar, G.D., Schulze, W., Langridge, J., Miller, J.M., Walker, B.H., 1998. Carbon and nitrogen isotope discrimination and nitrogen nutrition of trees along a rainfall gradient in northern Australia. Australian Journal of Plant Physiology 25, 413-425.

Seely, M.K., 1978. Grassland productivity: the desert end of the curve. South African Journal of Science 74, 295-297.

Seely, M.K., Hamilton, W.J., 1976. Fog Catchment Sand Trenches Constructed by Tenebrionid Beetles, Lepidochora, from the Namib Desert. Science 193, 484-486.

Smith, B.N., Epstein, S., 1971. Two categories of $^{13}C/^{12}C$ ratios for higher plants. Plant Physiology 47, 380-384.

Swap, R.J., Aranibar, J.N., Dowty, P.R., Gilhooly, W.P., Macko, S.A., 2004. Natural abundance of C-13 and N-15 in C-3 and C-4 vegetation of southern Africa: patterns and implications. Global Change Biology 10, 350-358.

Ting, I.P., Burk, J.H., 1983. Aspects of carbon metabolism in Welwitschia. Plant Science Letters 32, 279-285.

Tukey, J.W., 1957. On the comparative anatomy of transformations. The Annals of Mathematical Statistics 28, 602-632.

Vogel, J.C., Seely, M.K., 1977. Occurrence of C-4 plants in the central Namib Desert. Madoqua 10, 75-78.

Vogel, J.C., Visser, E., 1981. Pretoria Radiocarbon-Dates 2. Radiocarbon 23, 43-80.

von Willert, D.J., Armbruster, N., Drees, T., Zaborowski, M., 2005. *Welwitschia mirabilis*: CAM or not CAM - what is the answer? Functional Plant Biology 32, 389-395.

von Willert, D.J., Wagner-Douglas, U., 1994. Water Relations, CO2 Exchange, Water-Use Efficiency and Growth of *Welwitschia mirabilis* Hook Fil in 3 Contrasting Habitats of the Namib Desert. Botanica Acta 107, 291-299.

Wang, L., D'Odorico, P., Ringrose, S., Coetzee, S., Macka, S.A., 2007a. Biogeochemistry of Kalahari sands. Journal of Arid Environments 71, 259-279.

Wang, L.X., Okin, G.S., Wang, J., Epstein, H., Macko, S.A., 2007b. Predicting leaf and canopy N-15 compositions from reflectance spectra. Geophysical Research Letters 34, L02401.

Warren, C.R., Adams, M.A., 2006. Internal conductance does not scale with photosynthetic capacity: implications for carbon isotope discrimination and the economics of water and nitrogen use in photosynthesis. Plant Cell and Environment 29, 192-201.

Weiss, P.M., Chen, C.Y., Cleland, W.W., Cook, P.F., 1988. Use of primary deuterium and N-15 isotope effects to deduce the relative rates of steps in the mechanisms of alanine and glutamate-dehydrogenases. Biochemistry 27, 4814-4822.

Werner, R.A., Schmidt, H.L., 2002. The in vivo nitrogen isotope discrimination among organic plant compounds. Phytochemistry 61, 465-484.

Winter, K., Schramm, M.J., 1986. Analysis of Stomatal and Nonstomatal Components in the Environmental-Control of Co2 Exchange in Leaves of *Welwitschia Mirabilis*. Plant Physiology 82, 173-178.

Chapter 7 : Fog-aerosol interactions in the coastal Namib Desert

Abstract

The hyper-arid coastal Namib Desert in southern Africa is characterized by frequent morning fog, which is an important water supply for certain desert organisms. The fog is climatologically driven by both the cool upwelling Benguela Current and the general stability of the lower atmosphere at tropical latitudes. High dimethyl sulfide (DMS) concentrations associated with the productive upwelling zone suggest DMS as a major source of condensation nuclei for fog formation. However, the few available chemical analyses of fog water show a strong relationship between dissolved calcium and sulfur in the fog. A likely source of these ions is the gypsum ($CaSO_4$) crust common across the gravel plains of the Namib. The current study exploits the difference in sulfur isotopes between the gypsum crusts ($\delta^{34}S$ = 10 to 15 ‰) and that of marine sulfur ($\delta^{34}S_{seasalt}$ = 20‰, $\delta^{34}S_{DMS}$ = 18‰) to determine sources of sulfur in size-segregated aerosols collected before, during, and after a fog event in the Central Namib, 56 km from the coast. Values of $\delta^{34}S$ were significantly higher ($p < 0.02$) for the coarse fraction (1.5-7.6 μm) at 14.6 +/- 1.5 (1 S.E.) ‰ than for the fine fraction (0.5-1.0 μm) at 9.3 +/- 1.2 ‰ with no significant change as the winds shifted from fog-bearing (westerly) to hot and dry (easterly). Although these values are within the range found for local soils and

gypsum crusts, the strong easterly winds brought both higher sulfur and carbon, consistent with a contribution from continental biomass burning. Total sulfur concentrations were low (58 ng/m^3) compared to previous studies (94 to 335 ng/m^3).

7.1 Introduction

The Namib Desert on the southwestern coast of Africa is hyper-arid in terms of rainfall but experiences regular coastal fog events (Figure 1-2). The fog and hyperaridity is primarily caused by the overall stability of the atmosphere around the Tropic of Capricorn which is enhanced by the cold Benguela Current that upwells just offshore. This study investigates the fog-formation mechanism by looking at the relationship between aerosols and fog using stable isotopes of sulfur (δ^{34}S) to identify aerosol sources during and after fog events. The potential sources of sulfur are local gypsum crust, dimethyl sulfide (DMS) from the ocean, sea-salt, hydrogen sulfide from sulfate-reducing bacteria on the Namibian shelf, biomass burning (seasonal), fossil fuel burning, and other terrestrial materials that are mobilized from dry pans and riverbeds.

The Namib Desert is known as having some of the lowest background aerosol chemical concentrations in the world – e.g. Pb of 0.6 ng/m^3 (Bollhöfer and Rosman, 2000) and S of 200 ng/m^3 (Annegarn *et al.*, 1983). A recent global modeling effort lists the background S in <2.5 μm aerosols over Africa as 278 ng/m^3 (Liu *et al.*, 2009), which lies between the Namib value and that of a background sampling station in Zimbabwe – 452 ng/m^3 (Nyanganyura *et al.*, 2007).

Dust and fog both occur frequently in the Namib (Eckardt *et al.*, 2001). The chemical composition of fog indicates that particles of dust have contributed elements such as sulfur and calcium by dissolving into the water droplets that make up fog (Figure 1-6). The “Enrichment” of sulfur and calcium means that more of the element is present relative to chloride when compared to the composition of seawater. Seawater is the source of fog and rain water in the Namib. Dust that mixes with clouds in India has recently been shown to prevent the clouds from releasing rain (Rosenfeld *et al*. 2001). Dust can also help to “seed” clouds because water may condense out of the atmosphere onto the dust particles, depending on the type of dust (Noone *et al*. 2000). Dust may also suppress cloud formation on larger scales by helping to cool the sea surface (Lau and Kim 2007).

Previous studies of elemental concentrations in size-segregated Namib aerosols from the same study area found a biogenic marine signal in the fine fraction (<1 micron), whereas the coarse fraction (>1 micron) had a mixed inorganic marine (sea salt) and terrestrial signature (Annegarn *et al*., 1983). A more recent investigation of elemental concentrations in individual particles collected by aircraft below, within and above the marine stratus cloud bank off of the Namib found a sea-salt signature in most of the 0.3 to 2.0 μm fraction, and an “aged sea-salt” signature in the <0.3 μm fraction where Cl had been replaced by SO_4 (Posfai *et al*., 2003). A minority of the particles in the <0.3 μm fraction exhibits high K content relative to S and Ca, which was attributed to the inclusion of biomass burning particles, consistent with the dry-season timing of the sampling (13 September 2000). This biomass burning contribution was apparently not significant for aerosols collected in the summer (Annegarn *et al*., 1983). In these ground-based studies (collection occurred November 1976 to February 1977), S and Ca are present in much higher concentrations than K in both coarse and fine fractions. Similar patterns were seen in 3-hr samples collected over one week (30 October to 7 November 1978) in the Namib (Annegarn *et al*., 1979). Interestingly, this last study showed an increase in the relative amount of K at the onset of a "Berg Wind" event. These events involve dry air moving in from across the continent to the East often with high winds. The timing of this sampling at the end of the dry season coincides with biomass burning across southern Africa, a potential source for this increase in K which would be consistent with the more recent detailed particle composition study (Posfai *et al*., 2003). However, higher K relative to Ca and S was also found in the <0.3 μm fraction of dust generated from Namib soils (Eltayeb *et al*., 1993). This fine fraction K could be associated with either clay minerals or soil organic matter, but in either case would represent a local source that could help explain the observed patterns without the need for a contribution from biomass burning.

7.2 Methods

Aerosols were collected with a High Volume Cascade Impactor system (Turekian *et al*., 2001; Tisch Environmental Inc., 2004) at flow rates averaging about 1000 liters per minute (LPM). Glass Fiber filters on four impactor stages (7.6, 1.5, 1.0, and 0.5 μm) were used to collect aerosols for 11 hr sampling periods: "Day" (~7am to 6pm local time) and "Night" (~7pm to 6am). Flow rates were recorded continuously and calibrated with a NIST-traceable variable orifice calibration unit at the beginning and end of the sampling period. The aerodynamic diameter particle size cutoffs for each of stage vary up to 0.1

μm based on flow rate and atmospheric conditions. Flow rate and size cutoff calculations are given in Appendix A. Collection was performed at Gobabeb from 21 June to 2 July 2009 at 1.5 m above the ground in a location as far as possible from the daily activities of the research station (~500 m). Filters were pre-ashed at 550°C for 4 hours and no sulfur was detected in field or lab blanks of the slotted GF filters. The backing filter media contained a binder that retained a sulfur blank after ashing, and thus these results are not presented.

Additional aerosol samples were collected using a low flow cascade impactor (Sioutas, 2004) with four stages (2.5, 1.0, 0.5 and 0.25 μm) and a backing filter (Quartz Fiber). This collector was placed at a height of 4 m above the ground and ran at a flow rate of 9 LPM from 19 June to 2 July 2009, resulting in 4 sets of day and night samples. Separate sets of day and night collection stages were used for up to four days to increase sample mass. The same backing filter was used for all four days. However, due to insufficient mass collected on each individual stage, the two coarse and two fine fraction stages were combined for each $\delta^{34}S$ analysis. Analytical grade tin was used as the collection substrate on the impactor stages. The tin material can be directly introduced to the Elemental Analyzer system described below , and is expected to have comparable aerosol collection efficiencies as Glass Fiber substrates (Sioutas, 2004). Three Total Suspended Particulate samples (Glass Fiber) were also collected at 6-8 LPM for a few hours each, but no sulfur was detected in these samples.

Sulfur isotope values ($\delta^{34}S$) were determined using Isotope Ratio Mass Spectrometry (VG/Elementar Optima) on slotted, pre-ashed glass fiber filters.

Immediately following collection, glass fiber filters were folded in half to protect the collection surfaces, enclosed in pre-ashed aluminum foil, and kept frozen until analysis. The collection surface of each impaction stage comprised 10 strips of filter separated by slots. The mass loading on each strip was not determined, but they were visually similar. Even on heavily-loaded filters, the sample was concentrated along a thin line in the center (Figure 2-3). One day prior to analysis, a scalpel was used to scrape the sample from a representative selection of 3 to 7 strips.

The glass fiber filter samples contained very low levels of S, requiring correspondingly low-level standards and detailed post-processing of the data. This data processing was involved three steps after allowing the software (GV Instruments, 1995) to find the sample and reference peaks. First, the peak zero lines were adjusted to include as much of the sample peak as possible. Second, the peak definitions were adjusted for consistency among samples and standards. And third, the sensitivity of the isotope ratio to changes in peak definition was checked and categorized. Any change between 1 and 5 ‰ was flagged for a large error bar (+/- 2 ‰), 5 to 10 ‰ was flagged as "Trace" and anything greater was flagged as "Non-detect."

In addition to $\delta^{34}S$, elemental abundances of C and N were determined by TCD during $\delta^{34}S$ analyses. This information is accessible through the Optima software, although there is less separation between C and N peaks than during a typical C/N analysis which employs a lower temperature in the gas chromatograph. Given that there is a limited amount of sample for each aerosol filter, any C and N data available from a single $\delta^{34}S$ run is very useful. Orchard Leaves (NBS 1571) were used as a standard for C and N elemental composition, giving a consistent calibration for November and December 2009. If the original calculated mass was less than 10 ug for C and or 2 ug for N, the value was flagged as “Trace”. If no TCD peak was found, the sample was flagged as “Non-detect”. Finally, for many of the aerosol filters, only a portion of the full sample was analyzed as described above. The results for these aliquots were scaled up to the full sample size to give an estimate of the total C and N mass collected for each sampling period. Given this procedure and the low abundance of C and N in most of the aerosol samples, uncertainty is fairly high (+/- 10%)

7.3 Results

Generally, a wide range of sulfur isotope values was found both day and night, with overall average values of 10.1‰ (n = 22, sd = 5.3 ‰) and 11.1 ‰ (n=21, sd = 5.1 ‰) for Day and Night samples, respectively. The coarse fraction (1.5 and 7.6 µm stages) had significantly enriched δ^{34}S values relative to the fine fraction (Figure 7-6). Although the coarse fraction was statistically similar during the day and night sampling, fine fraction daytime aerosols were significantly depleted relative to fine fraction nighttime aerosols (Figure 7-7). The first three days of sampling saw two fog events (21 and 23 June) and one afternoon rain event (22 June) which came from the Atlantic (i.e. the same water source as the fog). From 24 June to 2 July a strong East Wind brought hot dry conditions. Mean air temperatures during the day and night were 23ºC and 14ºC, respectively. relative humidity averaged 34% during the day (58% for the first 3 days, 17% for the next 7), and 53% at night (83% for the first 4 nights, 27% for the next 4). The wind patterns are captured by 24hr back trajectories (Figure 7-5).

Table 7-1: Number of aerosol samples by stage for which sulfur mass and stable isotope ratio could be determined.

$\delta^{34}S$	S mass	High Volume				Low Flow		
		7.6	1.5	1.0	0.5	1.0, 2.5	0.25, 0.50	<0.25
Quantifiable (61)	Detect	2	13	9	11	0	0	0
	Trace	4	3	2	3	2	0	1
	Non-Detect	4	1	2	2	0	2	0
Unquantifiable	Non-Detect	10	3	7	4	4	4	3
Total Samples (96)		20	20	20	20	6	6	4

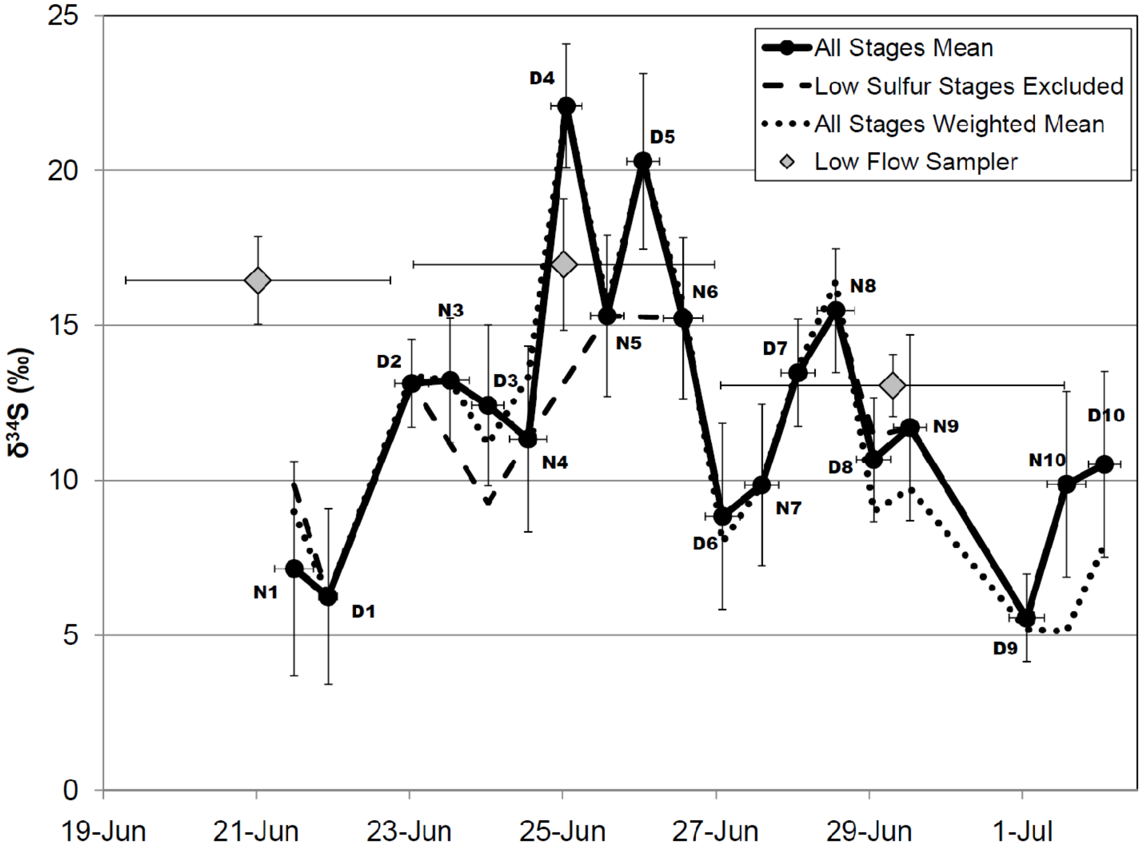

Figure 7-1: Average $\delta^{34}S$ values for each sampling event.

Table 7-2: Sulfur isotopes and general atmospheric conditions for aerosol samples.

Event	Mid Date/ Time	V	V_{max}	D	Conditions	δ^{34}S - Low Flow Sampler				
						1.0, 2.5 μm			0.25,0.50	<0.25
DA	6/21/2009 1:55				Clear/Fog[1]/Rain[2]	U			U	U
NA	6/21/2009 12:30				Rain/Fog/Fog	^{T}15.9			^{N}17.0	
DC	6/25/2009 0:57				Clear	U			U	U
NC	6/25/2009 12:20					^{T}12.2			^{N}21.7	
DD	6/29/2009 12:57				Clear/Windy	U			U	^{T}13.1
ND	6/30/2009 1:07					U			U	
						δ^{34}S - High Volume Sampler				
						7.6	1.5	1.0	0.5	<0.5
N1	6/21/2009 23:51	2.8	5.4	233	Clear	U	8.4	^{N}1.7	11.3	High S Blank
D1	6/22/2009 10:30	1.5	5.8	178	Rain	U	8.4	U	4.1	
N2	6/23/2009 0:45	2.5	6.3	236	Fog	U	U	U	U	
D2	6/23/2009 12:40	0.4	4.0	248	Fog	U	13.7	U	^{T}12.6	
N3	6/24/2009 0:44	3.1	8.9	245	Clear	U	U	^{N}13.2	U	
D3	6/24/2009 12:34	1.2	4.0	180		^{N}8.4	9.3	U	^{N}19.6	
N4	6/25/2009 1:08	2.6	9.8	147	Clear/Windy	13.6	13.8	14.9	^{T}3.0	
D4	6/25/2009 13:07	2.3	9.4	157		^{N}22.1	U	U	U	
N5	6/26/2009 1:54	3.1	10.7	171		^{T}14.8	15.9	15.2	U	
D5	6/26/2009 13:09	1.9	6.3	149		U	^{N}25.1	U	^{N}15.5	
N6	6/27/2009 1:43	2.1	8.0	171		U	24.4	6.3	15.0	
D6	6/27/2009 14:03	4.0	9.8	143		^{N}8.7	^{T}14.2	^{T}6.6	5.9	
N7	6/28/2009 2:20	4.9	12.5	89		U	^{T}6.8	^{T}8.1	^{T}14.7	
D7	6/28/2009 13:42	4.7	9.4	125		U	17.4	9.6	13.4	
N8	6/29/2009 1:34	2.0	6.7	140		^{T}12.3	17.7	14.1	17.8	
D8	6/29/2009 13:25	3.6	9.8	120		^{N}8.4	22.6	8.9	2.7	
N9	6/30/2009 0:47	3.7	11.6	130		^{T}14.8	17.9	9.8	4.3	
D9	7/1/2009 13:19	2.4	9.8	113		U	^{T}6.0	U	5.1	
N10	7/2/2009 1:50	4.1	9.8	164		^{T}20.9	6.8	9.3	2.5	
D10	7/2/2009 13:44	2.6	8.0	133		15.6	12.6	9.3	4.5	
Mean		3.2	9.1	158		14.0	14.2	9.8	9.5	
Standard Deviation		1.6	3.2	50		4.8	6.1	3.8	6.0	
Night Mean		2.6	7.9	154		15.3	14.0	10.3	9.8	
Day Mean		3.7	10.2	163		12.6	14.4	8.6	9.3	

V = mean of 30-minute average wind speed (m/s); V_{max} = maximum wind speed (m/s)
D = mean of 30-minute average wind direction (degrees, with North=0 and East=90)
1 – Fog events occurred on the nights of June 20-21 and 22-23
2 – Rain events occurred on the night of June 19-20 (short thunderstorm) and during the day on June 22 (light, advected from West)
N – Sample was Non-Detect for sulfur mass; T – Sample was Trace for sulfur mass

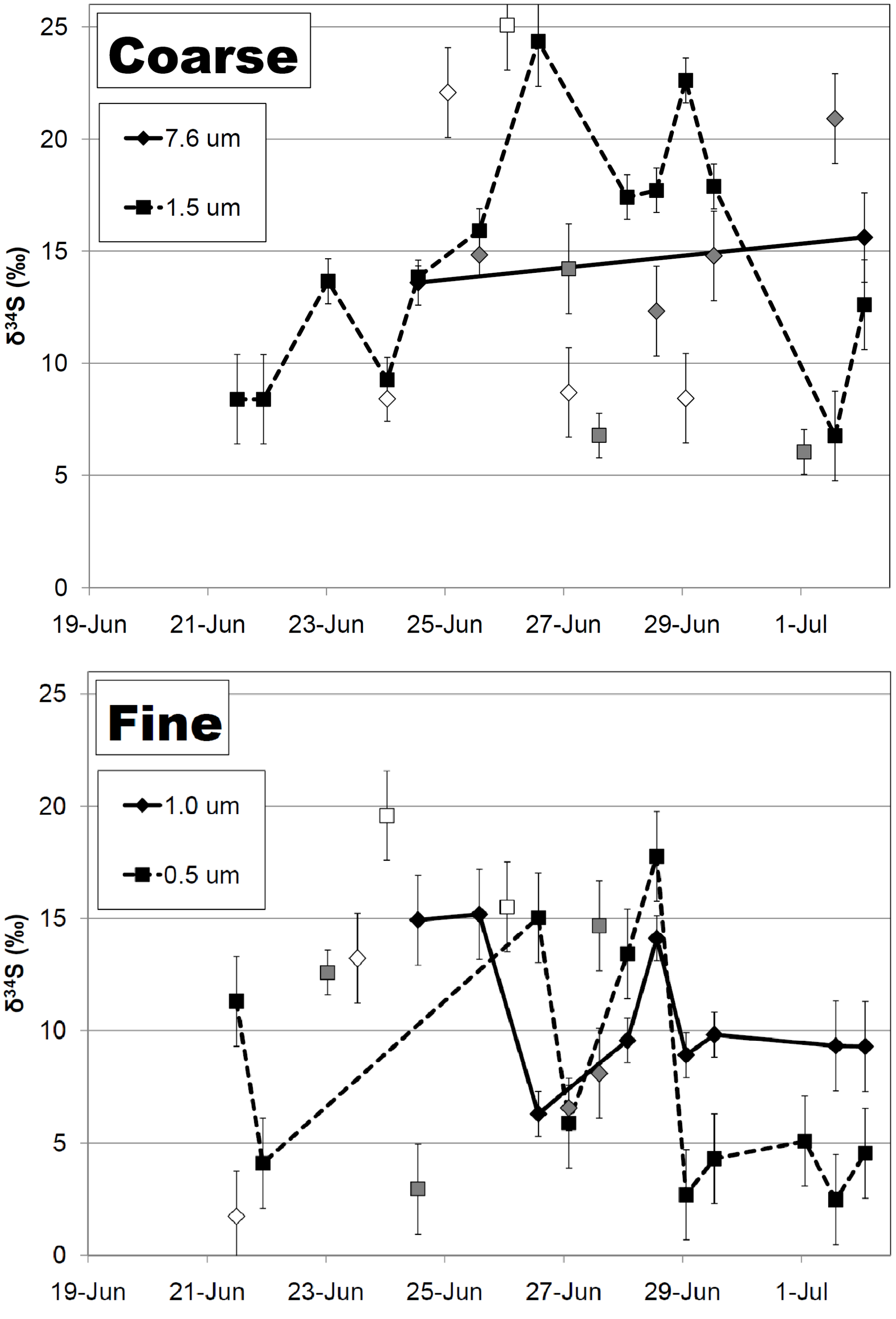

Figure 7-2: All quantifiable $\delta^{34}S$ values for the HV samples.
Note: Samples with detectable S mass have black symbols and are connected by lines, Trace S mass samples have grey symbols, and Non-Detect S mass samples have open symbols.

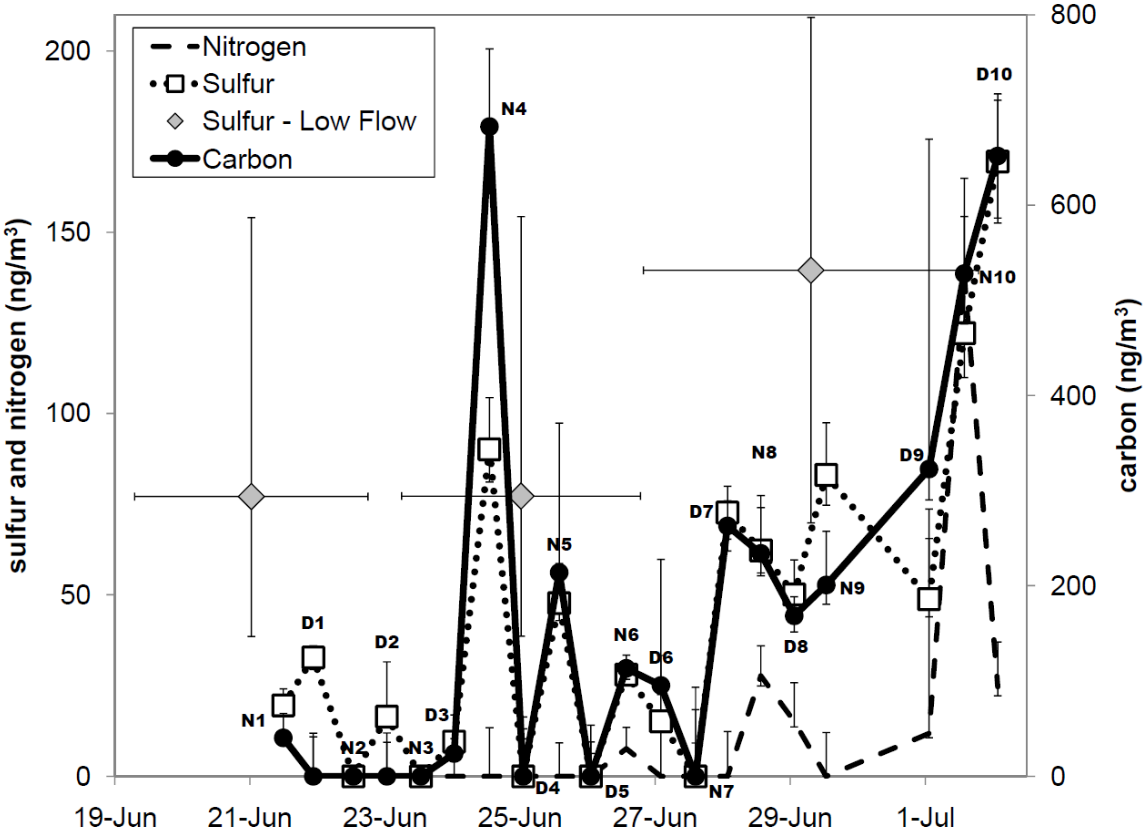

Figure 7-3: Average carbon, nitrogen and sulfur mass loadings for each sampling event.
Note: Symbols reflect the detected mass, and error bars incorporate both 10% analytical uncertainty and potential additional mass from Trace and Non-Detect collection stages at half of the trace or detection limit.

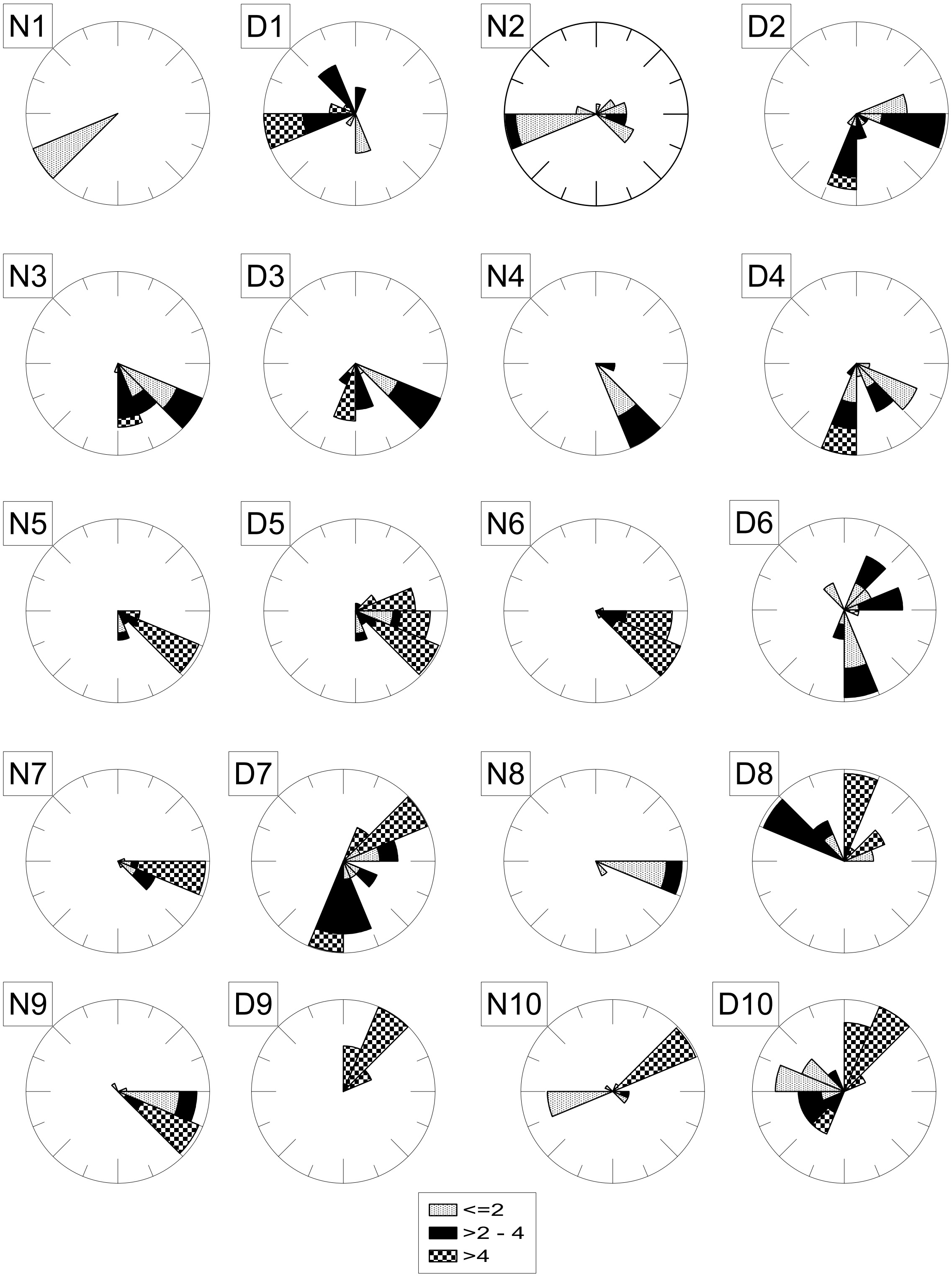

Figure 7-4: Wind direction and speed (m/s) diagrams for each High Volume aerosol sampling event.

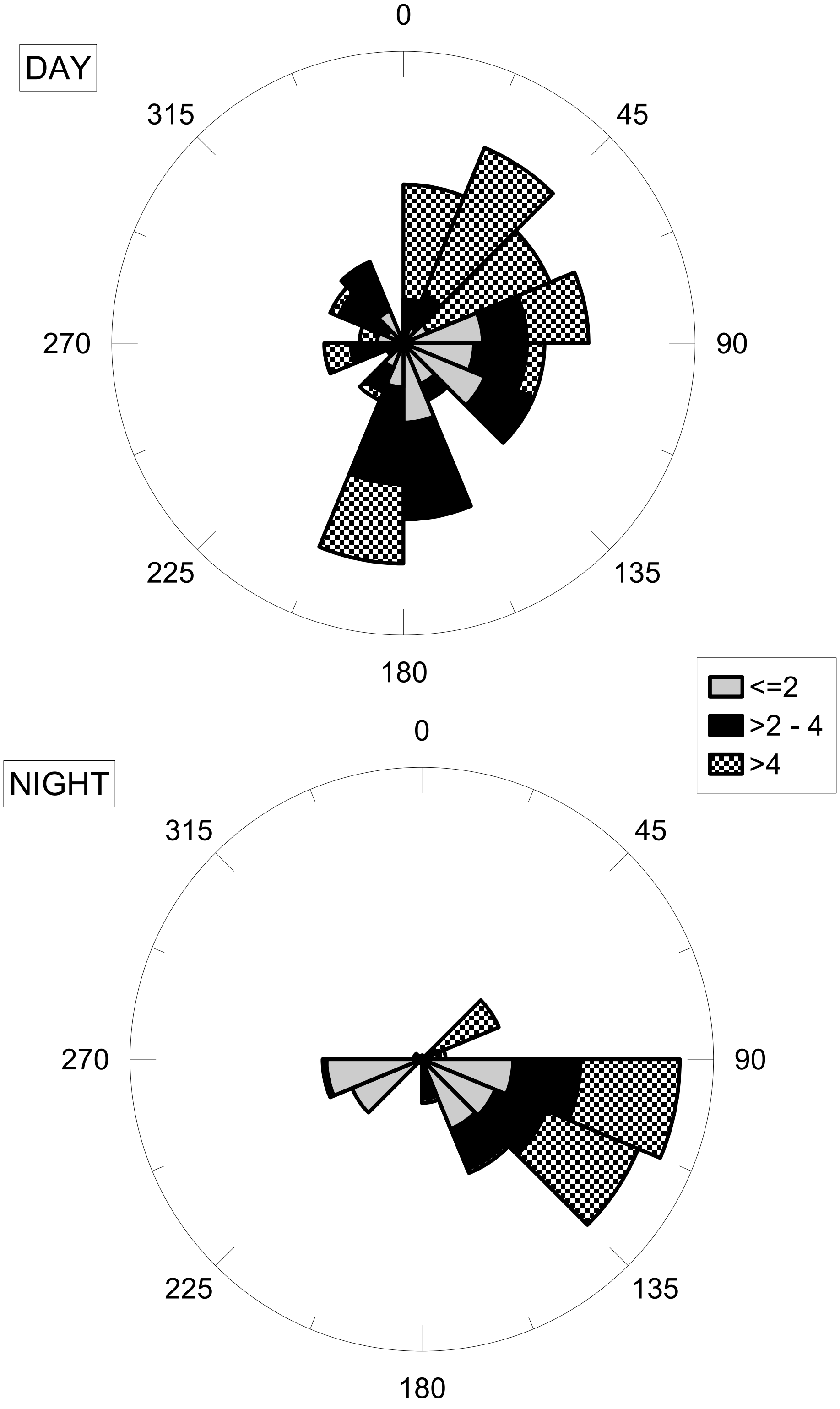

Figure 7-5: Wind direction and speed (m/s) for all night and day sampling periods.

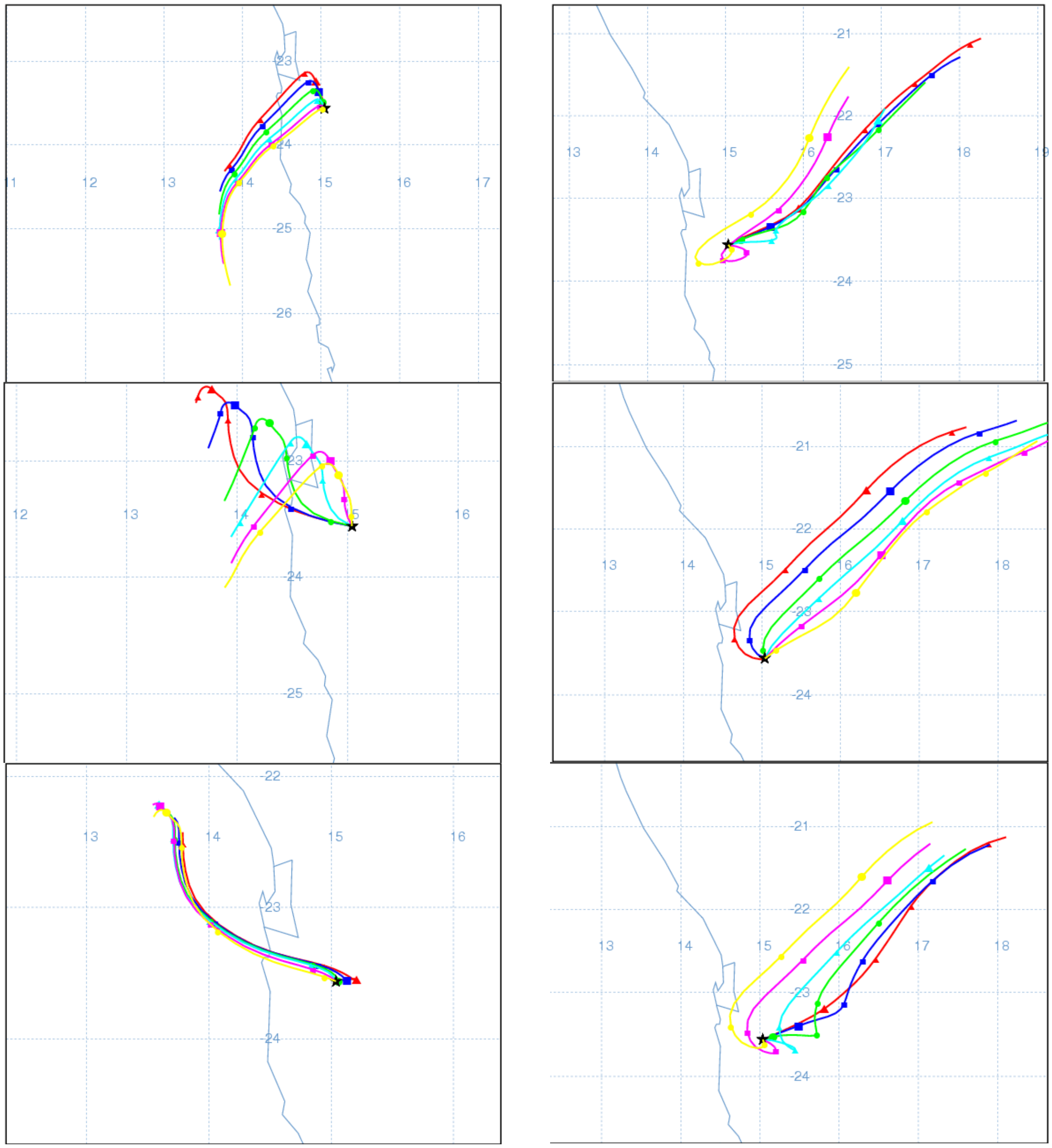

Figure 7-6: HYSPLIT model back-trajectories for representative sampling events .
Note: Six trajectories were modeled for each 10-hour sampling event (ie beginning, end, and at 2-hour intervals); each trajectory goes back 24hrs.
Events: left column, top to bottom: N1, D1, N2; right column, top to bottom: N8, D8, N9.

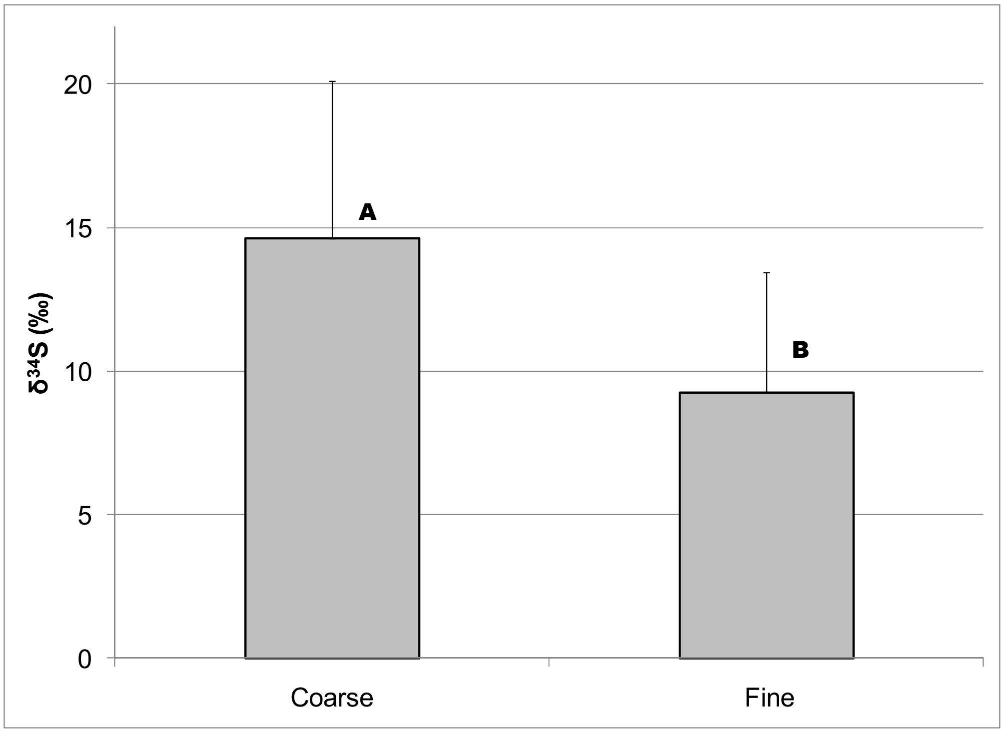

Figure 7-7: Statistical comparison of $\delta^{34}S$ for aerosol size fractions.

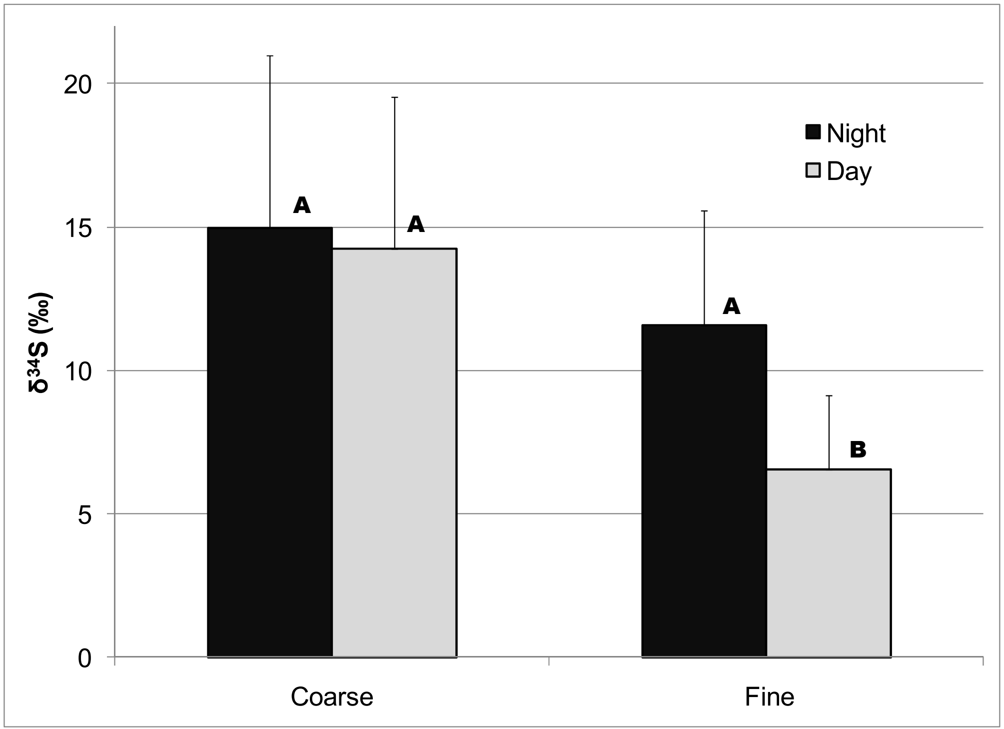

Figure 7-8: Statistical comparison of $\delta^{34}S$ for day and night aerosol samples.

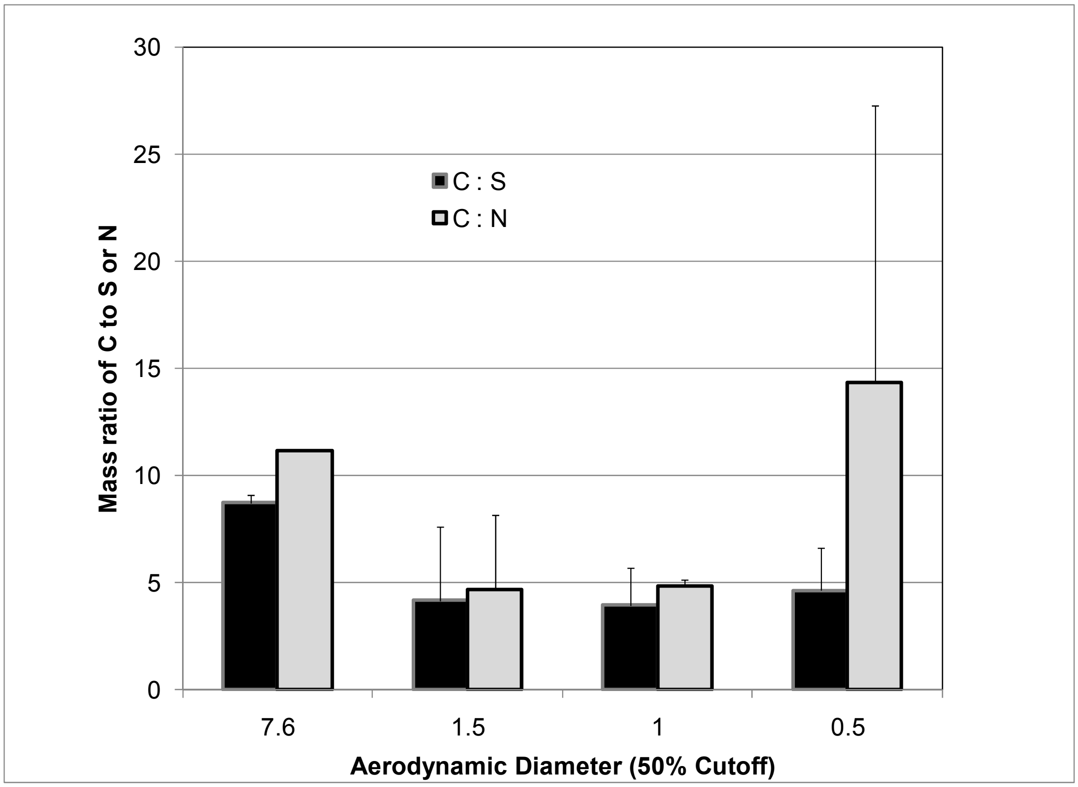

Figure 7-9: Carbon ratios (mass basis) with sulfur and nitrogen for various size fractions. Note: Samples with one of the two elements below detection are excluded. Error bars indicate the maximum value.

7.4 Discussion

Although the isotope results do not show a fog-associated shift from enriched marine to depleted terrestrial values over this period, two interesting patterns emerge. First, whereas the range of values covers several possible end-members -- sea-salt (20 ‰), DMS (18 ‰), gypsum (10-15 ‰), and other terrestrial (e.g. local precambrian sulfide-containing rocks at 1-10 ‰) – the bulk of the data fall within the gypsum range (Eckardt and Spiro, 1999). This, along with the relationship between Ca and S in Namib fog (Figure 1-6), is consistent with local dust as a source for S in the fog. Second, the fine fraction (0.5-1.0 µm) is significantly depleted relative to the coarse fraction (Figure 7-7), mainly due a highly depleted signal in the daytime fine fraction (Figure 7-8). This is most likely a result of consistently stronger daytime winds (Figure 7-4) bringing continental aerosols from further inland. The higher concentrations of aerosols in Day 7 to Day 10 resulted in a very consistent depleted δ^{34}S signal in the 0.5 µm fraction (Figure 7-2). Mixing of highly depleted H_2S with DMS could also produce the depleted values observed in the fine fraction. However, H_2S releases from the muddy Benguela sediments are intermittent (Dubecke and Bruchert, 2004; Emeis *et al*., 2004; Weeks *et al*., 2004; van der Plas *et al*., 2007), and thus an inconsistent source relative to DMS and gypsum (Eckardt and Spiro 1999).

Ratios of C:S in the aerosols ranged from 4 in the 0.5-1.5 µm fractions to 9 in the 7.6 µm fraction (Figure 7-9). These are somewhat lower than values from nearby soils of 7 in the Kuiseb Riverbed, 50 in the Gravel Plains, and 10 on Swartbank Berg (see Chapter 6). Another study of inselberg soils (Spitzkoppe, NE of Gobabeb) found C:S values of 150 to 300 (Burke, 2002). This comparison gives a first-order indication that Kuiseb River soils contribute substantially to the C and S in the aerosols, which is consistent with the δ^{34}S results (see Chapter 6). Kuiseb soils had depleted δ^{34}S (9.5 ‰) relative to soils of the gravel plains (15 ‰) and dunes (19 ‰).

7.5 Conclusion

No distinctive marine signal was found in 0.5 to 7.6 µm aerosols on foggy days compared to East Wind days. It remains possible that the marine signal seen in previous studies existed in the ultra-fine (<0.5 μm) fraction, which was not included in this analysis due to a high S blank in the backing filter media. This would also help explain the relatively low total S concentrations found here (53 ng/m^3), although corresponding total from the 0.5 to 4.0 μm fraction in the 1976 study ((Annegarn *et al.*, 1983) was still around 3 times higher (144 ng/m^3).

Local gypsum likely dominates the aerosol sulfur with additions from more depleted terrestrial sources apparent during East Wind and additions from more enriched marine sources variably important for the larger size fractions. Further investigation of the collected aerosols, specifically for elemental concentrations of K and Ca, could lead to more concrete conclusions about the relative importance of biomass burning, local riverbed soils, and gypsum crusts for the terrestrial δ^{34}S values reported here.

References

Annegarn, H., Van Grieken, R.E., Winchester, J.W., Sellschop, J.P.F., Von Blottnitz, F., 1979. Background aerosol concentrations for the Namib-Atlantic interface. International Conference on Air Pollution. CSIR, Pretoria.

Annegarn, H.J., van Grieken, R.E., Bibby, D.M., von Blottnitz, F., 1983. Background aerosol composition in the Namib Desert, South West Africa (Namibia). Atmospheric Environment 17, 2045-2053.

Bollhöfer, A., Rosman, K.J.R., 2000. Isotopic source signatures for atmospheric lead: The Southern Hemisphere. Geochimica Et Cosmochimica Acta 64, 3251-3262.

Burke, A., 2002. Properties of soil pockets on arid Nama Karoo inselbergs - the effect of geology and derived landforms. Journal of Arid Environments 50, 219-234.

Dubecke, A., Bruchert, V., 2004. Organic sulfur in Namibian shelf sediments - rates and processes. Geochimica Et Cosmochimica Acta 68, A349-A349.

Eckardt, F.D., Spiro, B., 1999. The origin of sulphur in gypsum and dissolved sulphate in the Central Namib Desert, Namibia. Sedimentary Geology 123, 255-273.

Eckardt, F.D., Washington, R., Wilkinson, J., 2001. The origin of dust on the West Coast of Southern Africa. Palaeoecology of Africa and the Surrounding Islands 27, 207-219.

Eltayeb, M.A.H., Vangrieken, R.E., Maenhaut, W., Annegarn, H.J., 1993. Aerosol Soil Fractionation for Namib Desert Samples. Atmospheric Environment Part a-General Topics 27, 669-678.

Emeis, K.C., Bruchert, V., Currie, B., Endler, R., Ferdelman, T., Kiessling, A., Leipe, T., Noli-Peard, K., Struck, U., Vogt, T., 2004. Shallow gas in shelf sediments of the Namibian coastal upwelling ecosystem. Continental Shelf Research 24, 627-642.

GV Instruments, 1995. Optima EA 1.4. Manchester, UK.

Liu, J.F., Mauzerall, D.L., Horowitz, L.W., Ginoux, P., Fiore, A.M., 2009. Evaluating inter-continental transport of fine aerosols: (1) Methodology, global aerosol distribution and optical depth. Atmospheric Environment 43, 4327-4338.

Nyanganyura, D., Maenhaut, W., Mathuthua, M., Makarau, A., Meixner, F.X., 2007. The chemical composition of tropospheric aerosols and their contributing sources to a continental background site in northern Zimbabwe from 1994 to 2000. Atmospheric Environment 41, 2644-2659.

Posfai, M., Simonics, R., Li, J., Hobbs, P.V., Buseck, P.R., 2003. Individual aerosol particles from biomass burning in southern Africa: 1. Compositions and size distributions of carbonaceous particles. Journal of Geophysical Research-Atmospheres 108, 8483.

Sioutas, C., 2004. Development of New Generation Personal Monitors for Fine Particulate Matter (PM) and its Metal Content. Research Report. NUATRC.

Tisch Environmental Inc., 2004. Series 230 High Volume Cascade Impactors Multi-Stage Particulate Size Fractionator: Operations Manual. Village of Cleves, OH.

Turekian, V.C., Macko, S.A., Keene, W.C., 2001. Application of stable sulfur isotopes to differentiate sources of size-resolved particulate sulfate in polluted marine air at Bermuda during spring. Geophysical Research Letters 28, 1491-1494.

van der Plas, A.K., Monteiro, P.M.S., Pascall, A., 2007. Cross-shelf biogeochemical characteristics of sediments in the central Benguela and their relationship to overlying water column hypoxia. African Journal of Marine Science 29, 37-47.

Weeks, S.J., Currie, B., Bakun, A., Peard, K.R., 2004. Hydrogen sulphide eruptions in the Atlantic Ocean off southern Africa: implications of a new view based on SeaWiFS satellite imagery. Deep-Sea Research Part I-Oceanographic Research Papers 51, 153-172.

Chapter 8 : Synthesis

Water is a limiting resource in Namibia. Thus, balancing the water requirements of both the people and the ecosystems in which they live is critical for Namibia's long term prosperity. The availability of water has governed the general population distribution around the country. Competition for water resources is becoming an even more important national issue with population and mining activities increasing, and as the society continues to grow its industrial and agricultural output. Such growth is good for Namibians, and it can be even more beneficial if done in a way that conserves water in support of the natural ecosystem. The ecosystem provides various services as well as being an integral part of the tourism industry, one of the most important sectors of the Namibian economy. Balancing growth and conservation is exceptionally difficult and depends largely on the priorities of the Namibian people for determining conservation targets. The weighing of conflicting priorities requires an understanding of the potential impacts of resource use on the natural environment. This is a practical motivation behind the research presented here on water use by plants in the Namib Desert.

The Namib is inhabited by flora and fauna that have adapted to highly stressed conditions (Louw and Seely, 1982; Henschel and Seely, 2008). Understanding these adaptations can help determine the physiological boundaries within which ecosystems can thrive and continue to provide services in support of human life: e.g. clean water, clean air, habitat, food (Rockstrom *et al*., 2009). As southern Africa faces drier conditions in the coming decades, these xeromorphic adaptations will help determine which types of plants can be used to stabilize soils or even used in cultivation. For example, the !nara melon (*Acanthosicyos horridus*) has been an important food for the Topnaar people of the Kuiseb River for centuries (Henschel *et al*., 2004), and its oil and seeds are now marketed in the cities as part of a sustainable small-scale agriculture initiative. The !nara is very limited in its distribution, and understanding its water use strategies will be key to its potential cultivation.

Adjacent to areas where the food-producing !nara plants grow are vast gravel plains that support very little biomass (Seely, 1978), but notably include microorganisms that are linked to the origins of photosynthesis – cyanobacteria. Accurately describing the soil surface wetting in the gravel plains will help understand their colonization patterns and the limit to the amount of moisture needed for photosynthesis. This is exciting from a scientific point of view, and could help parameterize the search for life on other planets (Warren-Rhodes *et al*., 2006).

The gravel plains are also home to the very long-lived primitive gymnosperm *Welwitschia mirabilis*, which has fascinated scientists for almost 150 years (Darwin, 1861; Hooker, 1863; Bower, 1880; Pearson, 1909; Rodin, 1953; Schulze *et al*., 1976; Henschel and Seely, 2000; von Willert *et al*., 2005). This unusual plant is among the most well-known aspects of the Namib, and thus contributes to the influx of tourists to Namibia. Based on its extant distribution, globally confined to the central and northern portions of the Namib, there appears to be a link between *W. mirabilis* and fog occurrence. Although fog and dew may play a role during germination and overall N-cycling, long-term observations of growth in adult plants suggest a decoupling of *W. mirabilis* physiology from fog. The present study provides new information on *W.*

mirabilis water sources using natural stable isotope abundances in a multiple tracer approach.

8.1 Main findings – water sources

Fog cannot be distinguished isotopically from dew or winter rain, so “Fog Contribution” in the following discussion should be considered “Atlantic Contribution.” Five plant species were found to have isotopically enriched water in their stems (grouped by relative Fog Contribution): *Stipagrostis sabulicola* and *Trianthema hereroensis* > *Arthraerua leubnitziae* and *Calicorema capitata* > *Zygophyllum stapffii*. The quantification of fog utilization is uncertain and would have to be followed closely through several additional seasons to ensure accuracy, but the evidence here allows relative fog use to be described as shown above corresponding to Fog Contributions of around 40 %, 15% and 5% in the three groups. Dune plants showed the greatest contribution from fog, and the water source appeared to be consistent among several contrasting antecedent moisture conditions during the study period of October 2007 to July 2009. The Fog Contribution findings are corroborated by δ^{34}S values of the stem material, which is enriched in the plants that exhibited Fog Contributions in their stem water, suggesting delivery of marine S with the uptake of fog water.

The leaf succulent *Z. stapffii* showed maximum Fog Contribution 30 to 60 km from the coast, with minimal contribution outside of this range either closer or further from the coast. In the middle, foggy, zone *A. leubnitziae* co-occurs with *Z. stapffii*, and it had fairly constant, slightly larger, Fog Contributions. Thus the ability of *Z. stapffii* to extend its distribution further inland than *A. leubnitziae* could be related to being able to tap deeper soil water suggesting different root systems in these two shrubs. They tend to occur side by side in the fog zone, and thus having different rooting depths would be consistent with their ability to coexist in the same niche. However, single plant excavations of both species indicate that they have similar root systems (Kutschera *et al*., 1997).

Trees growing the riverbed (*A. erioloba*, *F. albida*, *T. usneoides*), *W. mirabilis* and *A. horridus* all had isotopically similar stem water ($p<0.05$), indicative of a common water source. The water source for Kuiseb River trees is fairly clear given that their distribution in the Namib is essentially confined to the ephemeral riverbed or nearby washes. Here the alluvial aquifer contains fresh water within 10 m of the ground surface and is recharged by flood waters every year or two. The distribution of *A. horridus* is also associated with the Kuiseb River, with certain communities extending to the base of the large dunes to the south of the river. In contrast, *W. mirabilis* occurs far from this constant freshwater source, and yet it has isotopically similar stem water to the riverbed trees. The most likely explanation for this is a deep soil water source (>2 m) where local summer rain has infiltrated and accumulated in the vadose zone above the brackish groundwater. This explanation is consistent with the few soil waters analyzed (0.2-1m), which showed evaporative enrichment relative to *W. mirabilis* stem water. It is also consistent with previous observations of *W. mirabilis* tap roots reaching several meters belowground (Bornman, 1972; Kutschera *et al*., 1997).

8.2 Main findings – fog occurrence

The use of Leaf Wetness Sensors to determine the amount of fog and dew deposited in addition to the duration of wetness, is a new approach developed here in conjunction with Decagon Devices, Inc. that has the potential to be a very valuable tool in describing aridity gradients for biota and processes that depend on these occult water sources. Using these sensors, it was shown that annual dew deposition volumes are on the same order of magnitude as fog. Fog and dew volumes at Gobabeb exceeded rainfall in 2007, a dry year, and they were still about a third of annual rainfall in the relatively wet period from July 2008 to June 2009.

There is a relationship between fog occurrence and daily average relative humidity, and extending the analysis of this relationship could allow for the use of daily RH as a proxy for fog. If such a proxy is shown to be statistically valid, readily available output from Global Climate Models can be used to determine the future patterns of fog under different emissions and climate forcing scenarios. A broad first look at climate model predictions for relative humidity in the Namib show no change in one model and a 1.5 to 3% decline in relative humidity using a second model. The decline in the second model appears to be related to the overall declines in rainfall predicted for the winter rainfall region in South Africa.

The connection between fog and dust suggested by Namib fog chemistry in a previous study is consistent with the $\delta^{34}S$ values of size-segregated aerosols found here. These $\delta^{34}S$ values covered the range of values seen in local soils including gypsum crusts The fine fraction showed a consistently depleted $\delta^{34}S$ signal during East Wind events, which could be explained by either a local source (e.g. ephemeral riverbed sediments) or more distal continental sources potentially associated with biomass burning. Additional analyses of the K and Ca composition of the collected aerosols may allow for discrimination between gypsum and biomass burning sources.

8.3 Main findings – biogeochemical cycling

The occurrence of more enriched $\delta^{13}C$ values in *W. mirabilis* communities closer to the coast was shown to be statistically significant after compilation of all available data. Further, rainfall appears to explain more of the variability in the data than fog or the total precipitation. This finding adds to the growing weight of scientific evidence decoupling *W. mirabilis* physiology from fog deposition, and is consistent with the water isotope findings summarized above. The range in community-averaged $\delta^{13}C$ values across the gradient (4 ‰) is matched by the range in values seen within a single *W. mirabilis* community. This intra-community variability suggests that microenvironmental stressors or highly variable access to subsurface water is contributing to fractionation of ^{13}C during or after photosynthesis. Primary fixation via the CAM pathway would need to be invoked to explain variable fractionation during photosynthesis. Post-photosynthesis fractionation would involve CAM-cycling and photorespiration, both of which occur at very high levels in *W. mirabilis*, whereas levels of primary CAM fixation are very low.

Significant relationships among stem material $\delta^{13}C$, $\delta^{15}N$ and plant size were found in the *W. mirabilis* community at Hope Mine. There was a significant positive correlation between N content and $\delta^{13}C$, but not $\delta^{15}N$. The $\delta^{15}N$ of stem material is the result of source $\delta^{15}N$ and fractionations during and after assimilation. However, the association between enriched $\delta^{15}N$, larger stem size and enriched $\delta^{13}C$ suggests a connection between photorespiration, CAM-cycling and internal N recycling. The enrichment of $\delta^{15}N$ with plant size would also be consistent with difference in rooting depth giving larger plants access to an isotopically distinct N pool in the subsurface. If the N-source mechanism controls $\delta^{15}N$, then a second mechanism, most likely related to CAM-cycling, would have to be invoked to explain the $\delta^{13}C$ enrichment.

Nitrogen cycling in the Namib does not follow the same trend with precipitation seen across the Kalahari. There appears to be a reversal of the Kalahari $\delta^{15}N$-precipitation trend, with more depleted $\delta^{15}N$ values in C3 plants closer to the coast. This depletion could indicate additional N sources, faster denitrification due to frequent soil wetting, or a generally less open system with respect to N in the Namib relative to central Namibia and the driest parts of the Kalahari.

8.4 Conclusions

This study confirms that fog plays a significant role in water and nutrient cycles for certain parts of the Namib ecosystem. Fog, or Atlantic moisture more generally, is a water source for four shrubs and a perennial dune grass, but not *W. mirabilis* or *A. horridus*. Fog and dew occurrence and semi-quantitative deposition volumes can be continuously monitored using Leaf Wetness Sensors, although direct observation is required to distinguish between the two forms. There does appear to be an influence of fog on N cycling, with depleted $\delta^{15}N$ values closer to the coast. However, the water and carbon cycles of *W. mirabilis* appear to be somewhat decoupled from the occurrence of fog.

Hypothesis 1 – Fog is a significant water source – is supported given the Fog Contribution to five species endemic to the fog zone.

Hypothesis 2 – Fog uptake increases with fog deposition – needs further evaluation given the complexities of estimating fog deposition for all locations, and monitoring is ongoing with the instrumentation installed during the present study. However, the data do suggest increased fog utilization by *Z. stapffii* in the 30-60 km zone, which appears to confirm Hypothesis 2 with respect to this species.

Hypothesis 3 – *Welwitschia mirabilis* CAM usage is a function of water availability – is supported after including data from previous studies across the entire aridity gradient. However, the diurnal organic acid production appears to be due to CAM-cycling in response to a lack of rainfall and high photorespiration levels, rather than primary fixation of carbon at night via the CAM pathway.

Hypothesis 4 – N-cycling does not follow the Kalahari trend – is supported as there appears to be a depletion of δ^{15}N closer to the coast.

Hypothesis 5 – fog influences S-cycling – is supported, but could only be evaluated at Gobabeb where the groundwater δ^{34}S endmember was significantly different from fog.

References

Bornman, C.H., 1972. Welwitschia Mirabilis - Paradox of Namib Desert. Endeavour 31, 95-99.
Bower, F.O., 1880. The germination of Welwitschia mirabilis. Nature 22, 590-591.
Darwin, C.R., 1861. Letter 3346 -- Darwin C. R. to Hooker J. D. 18 Dec 1861. Darwin Correspondence Project. University of Cambridge, Cambridge.

Henschel, J., Dausab, R., Moser, P., Pallett, J. (Eds.), 2004. !NARA: Fruit for development of the !Khuiseb Topnaar. Namibia Scientific Society, Windhoek.

Henschel, J.R., Seely, M.K., 2000. Long-term growth patterns of Welwitschia mirabilis, a long-lived plant of the Namib Desert (including a bibliography). Plant Ecology 150, 7-26.

Henschel, J.R., Seely, M.K., 2008. Ecophysiology of atmospheric moisture in the Namib Desert. Atmospheric Research 87, 362-368.

Hooker, J.D., 1863. On Welwitschia, a new Genus of Gnetaceae. Transactions of the Linnean Society of London 24, 1-47.

Kutschera, L., Lichtenegger, E., Sobotik, M., Haas, D., 1997. Die Wurzel das neue Organ Ihre Bedeutung für das Leben von Welwitschia mirabilis und anderer Arten der Namib sowie von Arten angrenzender Gebiete mit Erklärung des geotropen Wachstums der Pflanzen. Eigenverlag: Pflanzensoziologisches Institut, Klagenfurt, Klagenfurt/Austria.

Louw, G., Seely, M., 1982. Ecology of desert organisms. Longman, New York.

Pearson, H.H.W., 1909. Percy Sladen Memorial Expedition in South-West Africa, 1908-9, II. Nature 81, 499-500.

Rockstrom, J., Steffen, W., Noone, K., Persson, A., Chapin, F.S., Lambin, E.F., Lenton, T.M., Scheffer, M., Folke, C., Schellnhuber, H.J., Nykvist, B., de Wit, C.A., Hughes, T., van der Leeuw, S., Rodhe, H., Sorlin, S., Snyder, P.K., Costanza, R., Svedin, U., Falkenmark, M., Karlberg, L., Corell, R.W., Fabry, V.J., Hansen, J., Walker, B., Liverman, D., Richardson, K., Crutzen, P., Foley, J.A., 2009. A safe operating space for humanity. Nature 461, 472-475.

Rodin, R.J., 1953. Distribution of Welwitschia mirabilis. American Journal of Botany 40, 280-285.

Schulze, E.-D., Ziegler, H., Stichler, W., 1976. Environmental control of crassulacean acid metabolism in Welwitschia mirabilis Hook. Fil. in its range of natural distribution in the Namib Desert. Oecologia 24, 323-334.

Seely, M.K., 1978. Grassland productivity: the desert end of the curve. South African Journal of Science 74, 295-297.

von Willert, D.J., Armbruster, N., Drees, T., Zaborowski, M., 2005. Welwitschia mirabilis: CAM or not CAM - what is the answer? Functional Plant Biology 32, 389-395.

Warren-Rhodes, K.A., Rhodes, K.L., Pointing, S.B., Ewing, S.A., Lacap, D.C., Gomez-Silva, B., Amundson, R., Friedmann, E.I., McKay, C.P., 2006. Hypolithic cyanobacteria, dry limit of photosynthesis, and microbial ecology in the hyperarid Atacama Desert. Microbial Ecology 52, 389-398.

Appendix A: Aerosol sampling calculations

Calibration of flow rates for the High Volume Air Sampler was performed using a "Slack-Tube Manometer" and a variable flow calibration orifice on the first and last day of sampling following established procedures (Tisch Environmental Inc., 2004b). Five readings of manometer fluid displacement were taken corresponding to five different flow rates from about 20 cfm to 60 cfm. These fluid displacements were converted to actual flow rates using Equation A-1. A nominal flow rate corresponding to each fluid displacement reading was taken from the continuous flow chart recorder, and adjusted to ambient atmospheric conditions through Equation A-2. Then, I_c was plotted against Q_{std} to obtain the calibration Equation A-3. The slope and intercept of Equation A-3 were adjusted linearly from the first to the last day of sampling to give flow rates for each sampling period (Table 1). Note that barometric pressures should be the actual measured pressures at the sampling elevation, not a "Sea-Level Pressure." Pressures listed as "Sea-Level" can be corrected by subtracting 0.1 inches of Hg for every 100 ft of elevation above sea level, and this was the case for pressure measurements the main Gobabeb weather station. Finally, the aerodynamic diameter of the 50% cutoff point for each collection stage of the Cascade Impactor is calculated according to Equation A-4, with parameter values are given in Table 2 (Marple and Liu, 1974; Tisch Environmental Inc., 2004a).

$$Q_{std} = \frac{1}{m} \times \left(\sqrt{F \times \frac{P_a}{760} \times \frac{298}{T_a}} - b \right) \tag{A-1}$$

With,
Q_{std} = actual flow rate (m^3/min)
F = Slack-Tube Manometer fluid displacement (in)
P_a = ambient barometric pressure during calibration (mm Hg)
T_a = ambient air temperature during calibration (K)
m = "Qstandard slope of orifice" (Tisch Environmental Inc., 2009)
b = "Qstandard intercept of orifice" (Tisch Environmental Inc., 2009)

$$I_c = I \times \sqrt{\frac{P_a}{760} \times \frac{298}{T_a}} \tag{A-2}$$

With,
I_c = continuous flow chart recorder values corrected to ambient T and P (cfm)
I = continuous flow chart recorder values (cfm)

$$Q_{avg} = \frac{1}{m_{samp}} \times \left(I_{avg} \times \sqrt{\frac{P_{avg}}{760} \times \frac{298}{T_{avg}}} - b_{samp} \right) \tag{A-3}$$

With,
I_{avg} = average continuous flow chart value for the sampling period (cfm)
Q_{avg} = average actual flow for the sampling period (m^3/min)
m_{samp} = slope of least squares regression for I_c vs Q_{std}
b_{samp} = intercept of least squares regression for I_c vs Q_{std}
P_{avg} = average barometric pressure during sampling period (mm Hg)
T_{avg} = average air temperature during sampling period (K)

$$D_{p50} = \sqrt{S_t} \times w \times \sqrt{\frac{9 \times \eta \times L}{C \times P_p \times Q_{ps}}} \tag{A-4}$$

With,
D_{p50} = aerodynamic diameter of ideal spherical aerosol at 50% collection efficiency
S_t = Stoke's Number (unitless)
w = Width of each slot (cm)
η = gas viscosity (g/cm/s)
L = length of each slot (cm)
P_p = particle mass density (g/cm^3)
C = Cunningham slip correction
Q_{ps} = flow rate per slot (cm^3/s)

Table A-1: Flow rate calculation parameters and Cascade Impactor aerodynamic diameter cutoffs for all high volume sampling periods. See Equations 3 and 4 for an explanation of variables.

Date		m_{samp}	b_{samp}	I_{avg}	Q_{avg}	T_{avg}	P_{avg}	Collection Mode	1	2	3	4	5
									Stages, D_{p50}				
6/20/2009	Day	43.483	-23.160	50	58.8	293	726	TSP[1]					
	Night	43.627	-23.371	50	59.5	284	729	TSP					
6/21/2009	Day	43.770	-23.581	42	52.8	289	731	TSP					
	Night	43.914	-23.792	22	37.0	283	733	Cascade	7.5	3.1	1.5	1.0	0.5
6/22/2009	Day	44.058	-24.003	22	36.8	288	731	Cascade	7.5	3.1	1.5	1.0	0.5
	Night	44.202	-24.214	22	37.0	284	733	Cascade	7.5	3.1	1.5	1.0	0.5
6/23/2009	Day	44.345	-24.424	22	36.9	290	734	Cascade	7.5	3.1	1.5	1.0	0.5
	Night	44.489	-24.635	22	37.1	283	733	Cascade	7.5	3.1	1.5	1.0	0.5
6/24/2009	Day	44.633	-24.846	22	36.9	291	731	Cascade	7.5	3.1	1.5	1.0	0.5
	Night	44.777	-25.057	22	37.2	284	731	Cascade	7.5	3.1	1.5	1.0	0.5
6/25/2009	Day	44.920	-25.267	22	36.9	295	730	Cascade	7.5	3.1	1.5	1.0	0.5
	Night	45.064	-25.478	22	37.1	289	730	Cascade	7.5	3.1	1.5	1.0	0.5
6/26/2009	Day	45.208	-25.689	21	36.0	301	729	Cascade	7.6	3.2	1.5	1.0	0.5
	Night	45.351	-25.899	22	37.1	292	729	Cascade	7.5	3.1	1.5	1.0	0.5
6/27/2009	Day	45.495	-26.110	21	36.1	302	728	Cascade	7.6	3.2	1.5	1.0	0.5
	Night	45.639	-26.321	21	36.5	291	728	Cascade	7.6	3.1	1.5	1.0	0.5
6/28/2009	Day	45.783	-26.532	20	35.5	301	727	Cascade	7.7	3.2	1.6	1.0	0.5
	Night	45.926	-26.742	21	36.6	291	729	Cascade	7.6	3.1	1.5	1.0	0.5
6/29/2009	Day	46.070	-26.953	21	36.4	300	728	Cascade	7.6	3.1	1.5	1.0	0.5
	Night	46.214	-27.164	22	37.4	290	729	Cascade	7.5	3.1	1.5	1.0	0.5
6/30/2009	Sampler out of use for motor replacement												
7/1/2009	Day	46.358	-27.375	20	35.7	301	729	Cascade	7.7	3.2	1.6	1.0	0.5
	Night	46.501	-27.585	21	36.8	291	730	Cascade	7.6	3.1	1.5	1.0	0.5
7/2/2009	Day	46.645	-27.796	20	35.8	299	730	Cascade	7.7	3.2	1.6	1.0	0.5
Cascade Impactor Mean					**36.6**				**7.6**	**3.1**	**1.5**	**1.0**	**0.5**

1 – Total Suspended Particulates (Cascade Impactor stages removed)

Table A-2: Parameters for an example calculation of aerodynamic diameter 50% cutoff values using Equation 4.

Variable		Units	Stage1	Stage2	Stage3	Stage4	Stage5
D_{p50}	particle size at 50% collection efficiency for spherical particles	microns	7.6	3.1	1.5	1.0	0.5
S_t	stoke's number	unitless	0.36	0.34	0.27	0.48	0.48
w	slot width	cm	0.396	0.163	0.0914	0.0457	0.0254
η	gas viscosity	g/cm.s	1.80E-04	1.80E-04	1.80E-04	1.80E-04	1.80E-04
L	slot length	cm	12.28	12.40	12.40	12.40	12.40
P_p	particle mass density	g/cm^3	1	1	1	1	1
C	cunningham slip correction	unitless	1.02	1.06	1.11	1.17	1.33
Q_{avg}	flow rate	cfm[1]	36.5	36.5	36.5	36.5	36.5
	number of slots	unitless	9	10	10	10	10
Q_{ps}	flow rate per slot	cm^3/s	1914	1723	1723	1723	1723

1 – Cubic feet per minute

References

Marple, V.A., Liu, B.Y.H., 1974. Characteristics of laminar jet impactors. Environmental Science & Technology 8, 648-654.

Tisch Environmental Inc., 2004a. Series 230 High Volume Cascade Impactors Multi-Stage Particulate Size Fractionator: Operations Manual. Village of Cleves, OH.

Tisch Environmental Inc., 2004b. TE-5000 Total Suspended Particulate High Volume Air Sampler: Operations Manual. Village of Cleves, OH.

Tisch Environmental Inc., 2009. Orifice transfer standard certification worksheet TE-5028A. Village of Cleves, OH.

Appendix B: Welwitschia cores

Cores from the woody stems of 12 Welwitschia mirabilis individuals near Old Hope Mine in the Namib-Naukluft Park were taken in January and July 2009 with an increment borer. The individuals comprise 8 from the rocky and sandy (wash) areas immediately adjacent to Old Hope Mine and 4 from the larger wash downstream to the east. There are 4 female plants, 6 male, and 2 of unknown sex. Individuals sampled in January were thriving in July, and the health of all 12 will be monitored periodically. An additional set of samples was taken from a dead Welwitschia stem (W28) on display at Gobabeb Training and Research Centre. Details about each individual are displayed in Table B-2 along with photos indicating where subsamples were taken from each core (e.g., position "1" on Site "W35" refers to the subsample "W35-1"). These subsample ID's correspond to analytical data listed in Table B-1. Cores are shown with the deepest portion to the left and the shallowest (closest to the edge of the plant where the core was initiated) to the right of the photo, except for W28 which is a vertical section. The scale beneath each core is in increments of 1 cm. "Stem Dimension" gives the length of perpendicular axes of the nominally oval-shaped stem as viewed from above.

The research and export permits associated with the samples of this protected species (CITES Appendix II) were issued from the Namibian Ministry of Environment and Tourism (Research and Collecting Permit Numbers 1190/2007, 1312/2008; Export Permit Numbers 73440, 63540) and a Material Transfer Agreement was signed with the Namibian National Botanical Research Institute on 16 January 2009.

Table B-1: *W. mirabilis* core analytical data.

Site	Sample	^{14}C Years BP	Calibrated Years BP[1]	δ^{13}C	δ^{15}N	C (%)	N (%)	Water (%)
W1	A1			-19.2	4.6	39.4	0.7	44.2
	A2			-19.7	3.4	40.0	0.4	38.9
	B1			-19.5	4.1	38.8	0.6	40.8
W2	1			-18.4	6.6	37.9	1.1	40.8
	2			-18.5	5.3	39.1	0.8	39.5
W4	1			-20.9	2.3	41.2	0.5	42.3
	2			-21.3	4.7	39.4	0.6	42.8
W24	1			-19.3	5.1	43.4	0.6	27.0
W28	1	135 +/- 25	0 - 145 (78%) 220 - 260 (18%)	-20.0	6.7	40.8	1.8	
	2	80 +/- 25	20 - 75 (53%) 140 - 110 (30%)	-19.6	6.9	39.2	1.5	
	3	165 +/- 40	0 - 155 (61%) 205 - 280 (29%)	-18.9	4.8	40.9	1.4	
	4	135 +/- 25	0 - 145 (78%) 220 - 260 (18%)	-18.9	6.0	41.0	1.2	
	5	110 +/- 25	0 - 75 (48%) 80 - 145 (35%) 225 - 255 (13%)	-19.5	4.7	41.4	1.0	
W29	M[2]			-19.9	6.0	43.1	0.8	38.2
	1							38.7
	2							37.7
W30	1			-19.0	8.3	39.4	0.7	44.2
	2			-19.1	9.5	40.0	1.2	37.2
W31	1			-18.9	9.1	38.8	0.4	25.4
	2			-18.5	7.8	39.2	0.7	42.7
	3			-18.9	8.7	38.9	0.6	40.4
W32	1			-18.6	9.8	43.9	0.7	51.1
	2			-18.8	10.9	40.3	0.7	31.2
W34	M			-20.2	5.5	39.7	0.4	46.3
	1							52.6
	2							39.9
W35	1			-20.4	6.7	37.5	0.5	53.8
	2			-20.8	6.8	34.4	0.4	53.8
W36	1			-20.2	3.5	37.5	0.5	37.8
W37	1			-20.5	5.8	37.2	0.6	53.2
	2			-20.5	4.3	39.0	0.4	45.4
P1		480 +/- 45	1402-1509 (86%)	-23.1				
P2		920 +/- 100	983-1300 (95%)					
P3		260 +/- 70	1498-1600 (18%) 1608-1818 (63%)	-19.9				
P4,P5		550 +/- 50	1383-1463 (86%)					

1 – The calibrated date ranges (Years BP = years before 1950) are listed along with the percentage of the original ^{14}C age range that intersects the corresponding portion of the calibration curve (Figure B-1). Calculations were performed by the program OxCal (Ramsey, 2009) using the latest calibration curve for the southern hemisphere(McCormac *et al*., 2004).

2 – "M" refers to a mixture of multiple subsamples

P1 to P5 are from previous studies, with dates recalibrated here (Herre, 1961; Crane and Griffin, 1970; Vogel and Visser, 1981; Jurgens *et al*., 1997)

Table B-2: Location, dimensions, habitat and sampling details on cored *W. mirabilis* individuals.
Note: Coordinates are given in decimal degrees, WGS84 datum.

Site ID	W1
Plant ID	023MHM
Sex	Male
Stem dimensions	64 x 20 cm
Core length	12.5, 5.8 cm
Sample time	13:00, 16:30
Sample date	14 Jan, 30 June 2009
Latitude	-23.569830
Longitude	15.259960
Elevation	595 m
Habitat	Shallow sandy soil on plateau

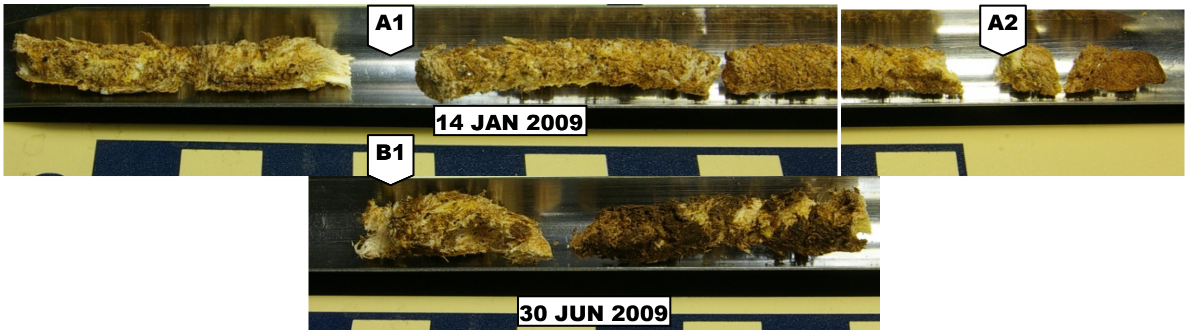

Site ID	W2
Plant ID	063MHM
Sex	Male
Stem dimensions	60 x 21 cm
Core length	9 cm
Sample time	14:00
Sample date	14 Jan 2009
Latitude	-23.571420
Longitude	15.258720
Elevation	591 m
Habitat	Middle of west wash, sandy soils

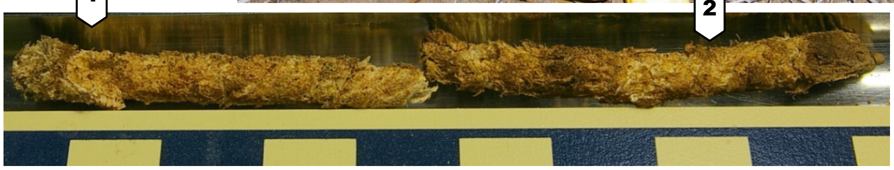

Site ID	W4
Plant ID	083FHM
Sex	Female
Stem dimensions	35 x 6 cm
Core length	13.5 cm
Sample time	14:35
Sample date	14 Jan 2009
Latitude	-23.572130
Longitude	15.258480
Elevation	586 m
Habitat	Middle of west wash, sandy soils

Site ID	W24
Plant ID	00FFHM
Sex	Female
Stem dimensions	39 x 19 cm
Core length	5.5 cm
Sample time	11:00
Sample date	14 Jan 2009
Latitude	-23.572960
Longitude	15.255680
Elevation	592 m
Habitat	Rocky slope with very thin to no soil

Site ID	W28
Plant ID	Dead Stem
Sex	Unknown
Stem dimensions	40 x 20 cm
Core length	14 cm
Sample time	12:00
Sample date	20 Dec 2007
Latitude	Unknown
Longitude	Unknown
Elevation	Unknown
Habitat	Unknown

Site ID	W29
Plant ID	008FHM
Sex	Female
Stem dimensions	90 x 40 cm
Core length	9 cm
Sample time	12:30
Sample date	14 Jan 2009
Latitude	-23.571180
Longitude	15.258740
Elevation	592 m
Habitat	Middle of west wash, sandy soils

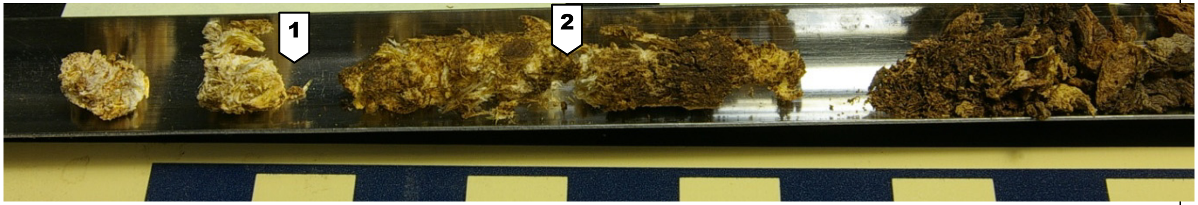

Site ID	W30
Plant ID	009MHM
Sex	Male
Stem dimensions	143 x 85 cm
Core length	9 cm
Sample time	12:30
Sample date	14 Jan 2009
Latitude	-23.571180
Longitude	15.258660
Elevation	592 m
Habitat	Middle of west wash, sandy soils

Site ID	W31
Plant ID	001MEW
Sex	Male
Stem dimensions	89 x 48 cm
Core length	12 cm
Sample time	15:00
Sample date	14 Jan 2009
Latitude	-23.579411
Longitude	15.258932
Elevation	567 m
Habitat	Middle of east wash, sandy soils

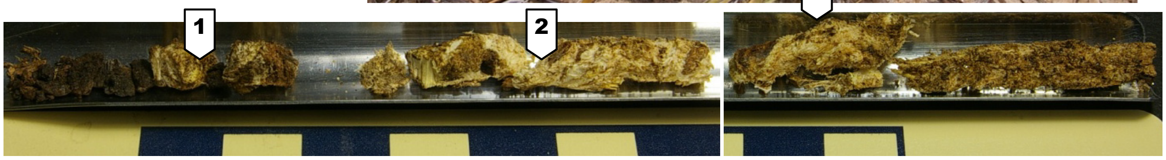

Site ID	W32
Plant ID	002MEW
Sex	Male
Stem dimensions	135 x 30 cm
Core length	20 cm
Sample time	15:30
Sample date	14 Jan 2009
Latitude	-23.573219
Longitude	15.265679
Elevation	578 m
Habitat	Middle of east wash, sandy soils

Site ID	W34
Plant ID	UW1
Sex	Unknown
Stem dimensions	40 x 16 cm
Core length	10.5 cm
Sample time	15:30
Sample date	2 July 2009
Latitude	-23.567582
Longitude	15.266599
Elevation	591 m
Habitat	Middle of upper east wash, sandy soils

Site ID	W35
Plant ID	UW20
Sex	Unknown
Stem dimensions	55 x 24 cm
Core length	9 cm
Sample time	16:00
Sample date	2 July 2009
Latitude	-23.57008
Longitude	15.26723
Elevation	581 m
Habitat	Middle of east wash, sandy soils

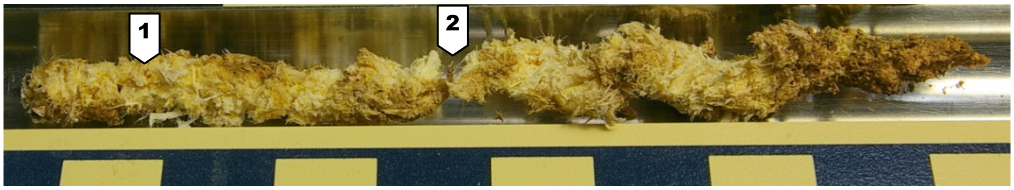

Site ID	W36
Plant ID	072FHM
Sex	Female
Stem dimensions	48 x 18 cm
Core length	4.5 cm
Sample time	16:30
Sample date	2 July 2009
Latitude	-23.571490
Longitude	15.258670
Elevation	591 m
Habitat	Middle of west wash, sandy soils

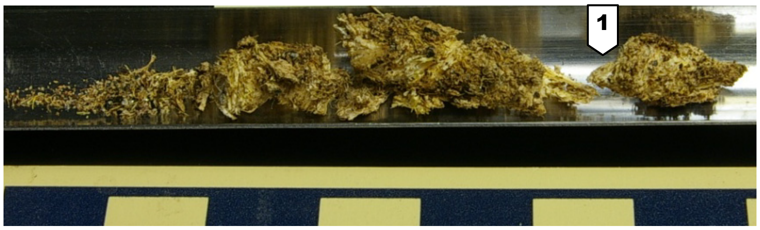

Site ID	W37
Plant ID	013MHM
Sex	Male
Stem dimensions	26 x 16 cm
Core length	7.5 cm
Sample time	17:00
Sample date	2 July 2009
Latitude	-23.571720
Longitude	15.258550
Elevation	591 m
Habitat	Middle of west wash, sandy soils

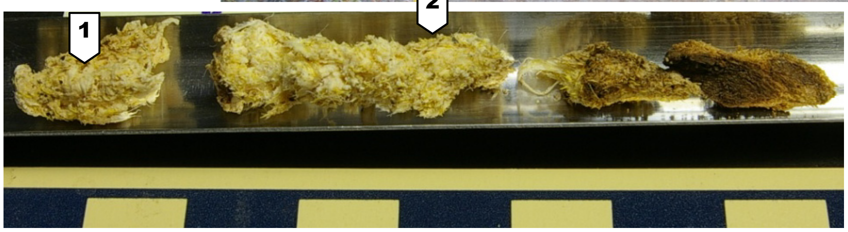

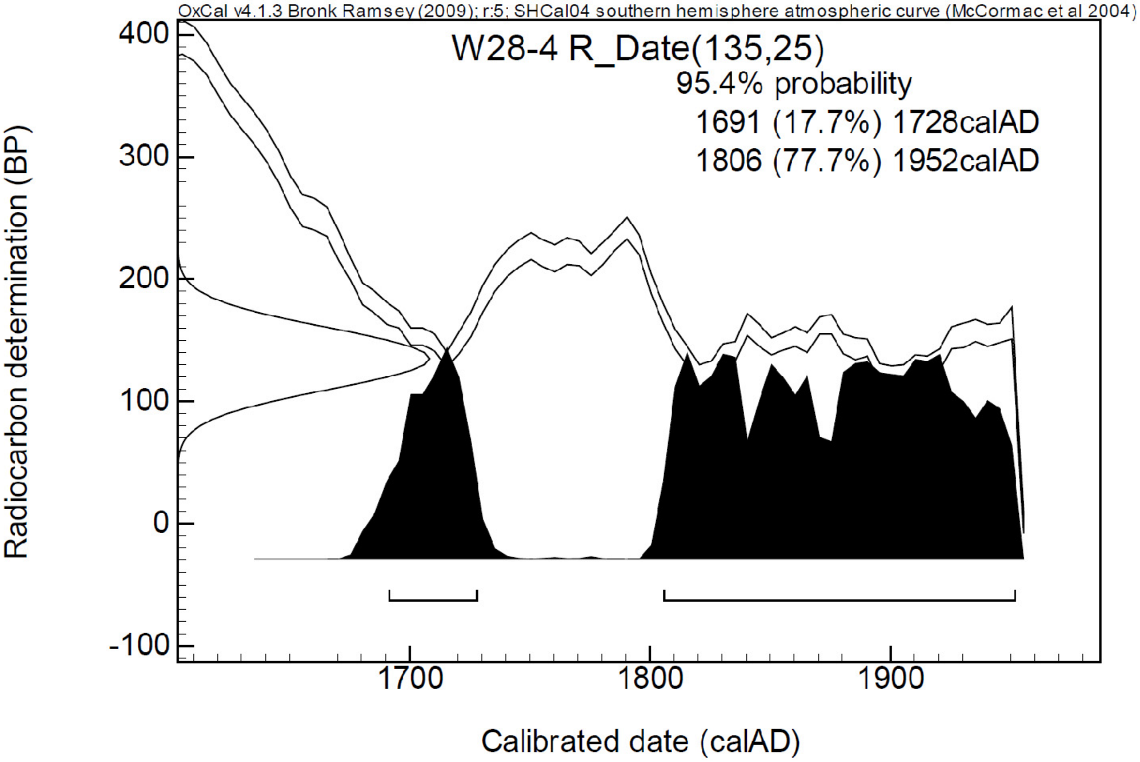

Figure B-1: Output from the OxCal program for sample W28-4 showing the original ^{14}C age range on the vertical axis and the calibrated ranges on the horizontal axis.

References

Crane, H.R., Griffin, J.B., 1970. University of Michigan Radiocarbon Dates XIII. Radiocarbon 12, 161-180.

Herre, H., 1961. The age of Welwitschia bainseii (Hook f.) Carr.: C14 Research. Journal of South African Botany 27, 139-140.

Jurgens, N., Burke, A., Seely, M.K., Jacobson, K.M., 1997. Desert. In: Cowling, R.M., Richardson, D.M., Pierce, S.M. (Eds.), Vegetation of southern Africa. Cambridge University Press, Cambridge, pp. 189-214.

McCormac, F.G., Hogg, A.G., Blackwell, P.G., Buck, C.E., Higham, T.F.G., Reimer, P.J., 2004. SHcal04 southern hemisphere calibration, 0-11.0 Cal KYR BP. Radiocarbon 46, 1087-1092.

Ramsey, C.B., 2009. OxCal. University of Oxford, Oxford, http://c14.arch.ox.ac.uk.

Vogel, J.C., Visser, E., 1981. Pretoria Radiocarbon-Dates 2. Radiocarbon 23, 43-80.

Appendix C: Data availability

Table C-1: Data availability for weather stations and sampling locations during the study period.

Station	2007												2008												2009												2010	
	J	F	M	A	M	J	J	A	S	O	N	D	J	F	M	A	M	J	J	A	S	O	N	D	J	F	M	A	M	J	J	A	S	O	N	D	J	F
Weather Stations																																						
GBB Auto	f	f	f	f	f	f	f	f	f	f	f	f	f	f	p	f	f	p	p	f	f	f	f	f			p	f	f	f	f	f	f	f	f	f		
GBB Manual	f	f ▨	f	f ▨	f ▨	f	f	f ▨	f	f ▨	f ▨	f ▨	f	f	f	f	f	f ▨	f ▨	f	f	f	f	f	f ▨	f	f	f	f	f ▨	f ▨	f	f	f	f	f		
GBB Fog[1]	f	f	f	f	f	f	f	f	f	f	f	f							f	f	f	f	f		f	f	f		f	f		f	f	f	f	f		p
High Dune West Low																		p	p	p	f	f	f	f	f	f	f	f	f	f	f	f	f	p				
High Dune West High																		p	f	f	f	f	f	f	p													
High Dune East High																		p	f	f	f	f	f	f	p					p	f	f	f	p				
Kuiseb																		p	f	f	f	f	f	f	p													
Kommabes																																						
Rooibank																																						
Welwitschia Wash																															p	f	f	p				
Hope																									p													
Sampling - water																																						
GBB fog										x	x	x	x						x	x	x	x	x	x	x	x	x		x	x								
GBB rain																				x										x								
GBB groundwater											x	x							x											x								
Hope groundwater				x						x																				x								
Nara Valley groundwater																															x							
Sampling – aerosols																																						
GBB aerosols																														x	x							
Sampling – plants and soils																																						
GBB										x	x	x						x	x						x					x	x							
Hope				x						x									x						x					x	x							
Swartbank											x	x							x						x													
Rooibank											x	x													x						x							
Swakop												x													x					x	x							

f – full coverage; x – partial coverage; blank – no data; x – samples collected; grey – author present for observations at Gobabeb

1 – Fog data were provided by Gobabeb for all months in 2007, 2008 and 2009, but several months were rejected here. No fog was reported by Gobabeb during the rejected months, but fog was either observed by the author or collected by Gobabeb technicians. For this reason, a tipping bucket and data logger were installed in January 2010 to monitor the fog volumes on a continuous basis.